NTNU
Norwegian University of
Science and Technology

Investigations on the Applicability of Membrane Introduction as a Sampling Technique for Oil in Air and Water with Flame Ionization Detector (FID) and Mass Spectrometry (MS) Detection

Terese Trefjord

Environmental Toxicology and Chemistry
Submission date: February 2012
Supervisor: Rudolf Schmid, IKJ
Co-supervisor: Morten Martinsen, IKJ
                           Christian Collin-Hansen, Statoil

Norwegian University of Science and Technology
Department of Chemistry

Preface

The work with this master thesis has been carried out at the Department of Chemistry at the Norwegian University of Science and Technology (NTNU), in the period autumn 2009 to winter 2012. This master thesis should originally deal with analyses by MIMS only, but due to instrumental problems and delivery delays analyses by MIFID was included. Due to these delays and the time limitations of the master thesis work, all of the planed tests could not be performed. Also, only two oil samples were analyzed by water MIMS, within the given time limit.

First of all I would like to thank Rudolf Schmid for all experimental help, feedback on the thesis and for sacrificing some of his Christmas holiday for closure on the experimental work. A great thank to Morten Martinsen for contribution with MIMS analyses, and also for experimental help and feedback on the thesis.

I would also like to thank Chris Gill, Erik Krogh and Nicholas Davey from the Applied Environmental Research Laboratories (AERL) at the Vancouver Island University (VIU) and Christian Collin-Hansen from Statoil for their hospitality, and making the trip to Canada (Leismer and Nanaimo) both interesting and inspirational. I would also like to thank Christian, as well as Alf G. Melbye from SINTEF for providing of oil samples.

I am also grateful to all my fellow students for all the discussions, coffee breaks and moments we have shared both here at NTNU and the University Centre in Svalbard (UNIS). A special thanks to Eva Kristin Aakre for proofreading.

Finally I would like to thank my family and friends for all encouragement during my period of study, and especially Erik Einarsen Sellæg how always brightens my day.

Trondheim, 6th of February 2012

Terese Trefjord

Abstract

During a membrane introduction (MI) analysis the analytes are separated from the bulk matrix (e.g. air or water) by a semi-permeable membrane and transported to the detector by a carrier gas (usually helium). The most commonly used detector for MI-analyses is the mass spectrometer, resulting in membrane introduction mass spectrometry (MIMS). The main advantages of MIMS are short response times, high sensitivity, simplicity and elimination of sample preparation and pre-separation. Membrane introduction analyses are suitable for detection of volatile organic compounds (VOCs) and semi volatile organic compounds (SVOCs).

In this project the applicability of MIMS and membrane introduction flame ionization detector (MIFID) for oil analyses were tested. Investigations of 12 different oil samples from light crude oils to heavy oils were performed by MIFID and MIMS for both water and air (only two oil samples were analyzed by water MIMS).

For the oil in air analyses good response were achieved, and information about response times and half-times could be obtained within a reasonable period of time. The water analyses however showed some limitations. Even after long analysis times (up to 1200 minutes) useful information on response time were rarely obtained, and no half-times for depletion could be measured. Pre-equilibration of the oil samples seems to be necessary to enable reasonably fast MI analyses of water samples (approximately) equilibrated with the oil, allowing an estimation of oil concentrations in water.

For the MIMS analyses spectral information are obtained, providing an indication of the content of the oil samples, as well as information about how the abundance of different ions change throughout the analyses due to weathering.

Best results were obtained by the lighter oil samples, due to higher amounts of compounds favorable for MI-detection. Analysis times obtained were slightly shorter for MIFID analyses, as compared to MIMS analyses.

Sammendrag

Under en membranintroduksjon (MI) analyse blir analyttene separert fra prøvematerialet (f.eks. luft eller vann) ved hjelp av en semipermeabel membran og deretter fraktet til detektoren av en transportørgass (vanligvis helium). Den vanligst detektoren for MI-analyser er et massespektrometer, som resulterer i membranintroduksjon massespektrometri (MIMS). De viktigst fordelene til MIMS er kort responstid, høy sensitivitet, enkelhet og eliminering av prøvepreparering og forhåndsseparasjon. Membranintroduksjon er best egnet for analyser av flyktige organiske forbindelser (VOCs) og semi-flyktige organiske forbindelser (SVOCs).

I dette prosjektet ble anvendbarheten av MIMS og membranintroduksjon flammeionisasjonsdetektor (MIFID) for oljeanalyser testet. 12 ulike oljeprøver, fra lette råoljer til tunge oljer, ble undersøkt ved hjelp av MIFID og MIMS. Analysene ble utført både i vann og i luft (bare to oljeprøver ble analysert med vann-MIMS).

For olje i vann analysene ble god respons oppnådd, samt at informasjon om responstider og halveringstider ble tilgjengelig innenfor fornuftige analysetider. Vannanalysene på sin side hadde visse begrensninger. Selv etter lange analysetider (opptil 1200 minutter) ble brukbar informasjon om responstider sjeldent oppnådd, og halveringstider kunne ikke måles i det hele tatt. En forhånds-likevekt innstilling av oljeprøvene kan være nødvendig for å oppnå raskere analyser, da av vannprøver som er i (tilnærmet) likevekt med oljen. Dette vil tillate anslag av oljekonsentrasjoner i vann.

For MIMS analysene ble informasjon om masse spekteret oppnådd, noe som gir en indikasjon på innholdet i oljeprøvene. Masse spektrene gir også informasjon om hvordan konsentrasjonen av ulike ioner forandrer seg i løpet av analysetiden som et resultat av forvitring.

På grunn av høyere innhold av forbindelser som egner seg for MI-analyser for de lette oljeprøvene, ble de beste resultatene ble oppnådd ved analyser av disse prøvene. Analysene som ble utført med MIFID hadde noe kortere analysetid sammenlignet med MIMS analysene.

V

List of contents

1. Introduction

Improvements in mass spectrometry (MS) have revolutionized many fields of biology and chemistry during the last decades. Environmental chemistry is a field in which MS still increases in importance, both for laboratory-based analyses and, lately, for continuous, real-time analyses in the field. Compared to the traditional approach of taking samples at distinct time-points and bringing them back to the laboratory for analysis, continuous monitoring has clear advantages, especially if remote, unattended monitoring is becoming an option. New MS instruments are now introduced to the market, which are robust, easily transportable and capable of identifying and quantifying contaminants present even in very low concentrations (Etzkorn, Davey et al. 2009; Davey, Krogh et al. 2011).

Membrane introduction mass spectrometry (MIMS) is one such highly promising MS technique, capable of monitoring several contaminants simultaneously and in "real time" in different environmental media, such as air, water and soil. It is applicable for measuring and monitoring volatile (VOC) and semi-volatile organic compounds (SVOC). It may also have a potential as qualitative analytical method, e.g. for fingerprinting complex samples, such as oil, by a simple batch-analysis. Recent review articles describe theory and practice of the MIMS technique, including a number of environmental and process control applications (Johnson, Cooks et al. 2000; Kotiaho, Cisper et al. 2002; Ojeda, Rojas et al. 2007).

The advantage of MIMS, as compared to analyses on more conventional systems, is its ability to monitor samples continuously by direct contact of the sample with the membrane. This eliminates sample preparation and pre-separation by for instance extraction and chromato-graphy, respectively (Davey, Krogh et al. 2011).

Another possible combination of membrane introduction is with a flame ionization detector (MIFID). This is a detection system that should be applicable as an unselective detector for detection and quantification of organic compounds.

In this project the applicability of MIMS and MIFID for analyses of oil in water and air are investigated, to test the potential for application of MIMS and MIFID for oil related environmental problems.

1.1 Abbreviations

A list of the most frequently used abbreviations in this text is given in Table 1.1.

Table 1.1: The most frequently used abbreviations in this text

Abbreviations	Full name	Comments
CI	Chemical Ionization	
DCM	Dichloromethane	Solvent, formula: CH_2Cl_2
DIMP	Direct Insertion Membrane Probe	
EI	Electron Ionization	
FID	Flame Ionization Detector	
GC	Gas Chromatography	
HFM	Hollow Fiber Membrane	
i.d.	Inner diameter	
MIFID	Membrane Introduction Flame Ionization Detector	
MIMS	Membrane Introduction Mass Spectrometry	
MS	Mass Spectrometry	
MS/MS	Tandem Mass Spectrometry	
o.d.	Outer diameter	
PDMS	Polydimethylsiloxane	Membrane material
SAGD	Steam Assisted Gravity Drainage	Exploration method
SVOC	Semi-Volatile Organic Compound	
VOC	Volatile Organic Compound	

2. Theory

This section will mainly focus on the applications and theory of membrane introduction methods, mainly membrane introduction mass spectrometry, as well as the background of oil chemistry and the use of mass spectrometry.

2.1 Membrane Introduction Mass Spectrometry

Membrane introduction mass spectrometry (MIMS), also called membrane inlet mass spectrometry or just membrane mass spectrometry, takes the membranes ability to separate the analytes from the matrix, and a mass spectrometer for analyzing of the components. The main advantages of MIMS are short response times, high sensitivity, simplicity and no sample pretreatment. These factors leads to the possibilities for on-line analysis (Johnson, Cooks et al. 2000). Measurements by MIMS can also be cost effective compared to other mass spectrometric methods (Cisper, Gill et al. 1995). MIMS is best suited for analyses of volatile organic compounds (VOCs) and semi volatile organic compounds (SVOCs). Some analytical characteristics of MIMS can be found in Table 2.1 (adopted from Srinivasan et al. 1997).

Table 2.1: Analytical characteristics of MIMS (Srinivasan, Johnson et al. 1997)

Characteristics	Representative values
Response times ($t_{10\%-90\%}$)	10-120 s
Detection limits	ppb levels
Linear dynamic range	Several orders of magnitude
Quantitative accuracy	($\pm5\%$) with external standards
Matrix effects	Small, except in some CI
Molecular weight range	<500 Da
Specificity	High (when used with tandem mass spectrometry or derivatization)

2.1.1 Early history of MIMS

MIMS was first introduced in 1963, by Hoch and Kok, in use for photochemical analysis. They followed the reaction kinetics of oxygen and carbon dioxide, dissolved in a liquid phase, during the process of photosynthesis (Hoch and Kok 1963). Following this experiment more photochemical analysis were tested, and later also physiological analysis of blood and urine were carried out (Srinivasan, Johnson et al. 1997). Calvo et al. used a permeable membrane to perform biological analysis where they followed kinetic reactions during a α-chymotrypsin catalyzed transesterification (Calvo, Weisenberger et al. 1981; Calvo, Weisenberger et al. 1983). Degn and Kristensen took advantages of MIMS in the field of biology. They looked at hydration of carbon dioxide, and measured CO_2 transients (Degn and Kristensen 1986). Fermentation monitoring has developed to be an important application for MIMS, and was first tested by Reuss et al., who measured dissolved gases and volatile compounds (Reuss, Piehl et al. 1975). Hayward et al. used MIMS for online-monitoring of fermentation products from the Klebsiella oxytoca microorganism (Hayward, Riederer et al. 1991). Lately MIMS has been used as an application for environmental monitoring, where air, water and soil has been a crucial focus (Kotiaho, Cisper et al. 2002).

2.1.2 The MIMS-principle

During a MIMS analysis the analyte is introduced to the mass spectrometer through a membrane. For hydrophobic membranes this process is called pervaporation (Srinivasan, Johnson et al. 1997). Pervaporation is the process where analytes are transferred from the matrix to the vapor phase. This process are consisting of three main steps: I) the analytes gets adsorbed to the surface of the membrane, II) permeation through the membrane and III) desorption from the membrane to the vacuum or gaseous carrier stream (Johnson, Cooks et al. 2000). The parameters which influence these steps are the molecular properties of the analytes and the material of the membrane. Fick`s diffusion equations can be used to describe the permeation process (Kotiaho 1991).

$$I_m(x,t) = -AD\left[\frac{\partial C_m(x,t)}{\partial x^2}\right]$$

(2.1)

$$\partial C_m \frac{(x,t)}{\partial t} = D\left[\frac{\partial^2 C_m(x,t)}{\partial x^2}\right]$$
(2.2)

where $I_m(x,t)$ is the analyte flow inside the membrane (mol/s), A is the membrane surface area (cm^2), D is the diffusion constant (cm^2/s), $C_m(x,t)$ is the concentration inside the membrane (mol/cm^3), x is the membrane thickness (cm), and t is time (s).

Equation 2.1 describes the rate of the analyte flow in the membrane, while equation 2.2 describes how the concentration changes with time.

The temperature of the membrane can also affect the permeation rate (Kotiaho 1991). The membrane temperature will also affect the diffusion constant and the distribution ratio. The diffusion constant increases with increasing temperature, while the analyte concentration inside the membrane will decrease. An increase in temperature will also lead to shorter response times (Kotiaho and Lauritsen 2002). The response time (the time the signal uses to increase from 10 to 90 % of the maximum signal) can be described by equation 2.3 (Kotiaho and Lauritsen 2002).

$$t_{10-90\%} = 0,237 \times \frac{x^2}{D}$$
(2.3)

where x is the membrane thickness (cm) and D is the diffusion constant (cm^2/s)

As can be seen from equation 2.3 the response time increases with increasing membrane thickness, and decreases proportionally with the diffusion constant.

For hydrophilic membranes the transportation process of analytes through the membrane to the mass spectrometer is called diffusion (Kasthurikrishnan, Cooks et al. 1996). During diffusion the analytes gets absorbed to the membrane surface, and then diffuses through the membrane by binding to specific functional groups on the side chains of the membrane material (Xu, Patrick et al. 1995; Creaser, Lamarca et al. 2001). Examples of these functional groups are sulfonic acid for Nafion membranes (Creaser, Lamarca et al. 2001) and alkylamine for cellulose membranes (Xu, Patrick et al. 1995).

During a conventional MIMS analysis the membrane usually separates the analytes from the bulk matrix, but not individual analytes from each other (Xu, Patrick et al. 1995).

Figure 2.1 shows a MIMS configuration for a hydrophobic membrane interface.
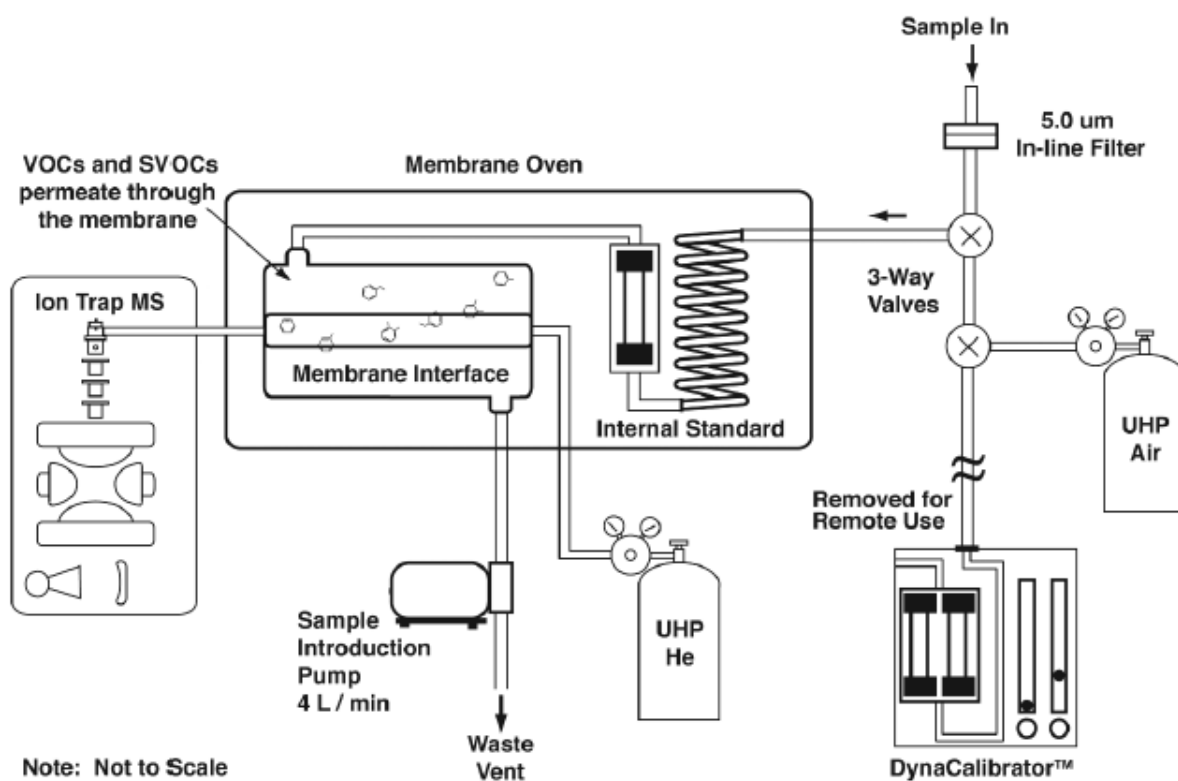
Figure 2.1: A schematic presentation of a MIMS system (Etzkorn, Davey et al. 2009). A more detailed presentation of the membrane interface is given in Figure 2.3.

2.1.3 Introduction systems

Several different introduction systems have been used in MIMS analysis (Srinivasan, Johnson et al. 1997). Some of the most common systems can be seen in Figure 2.2.
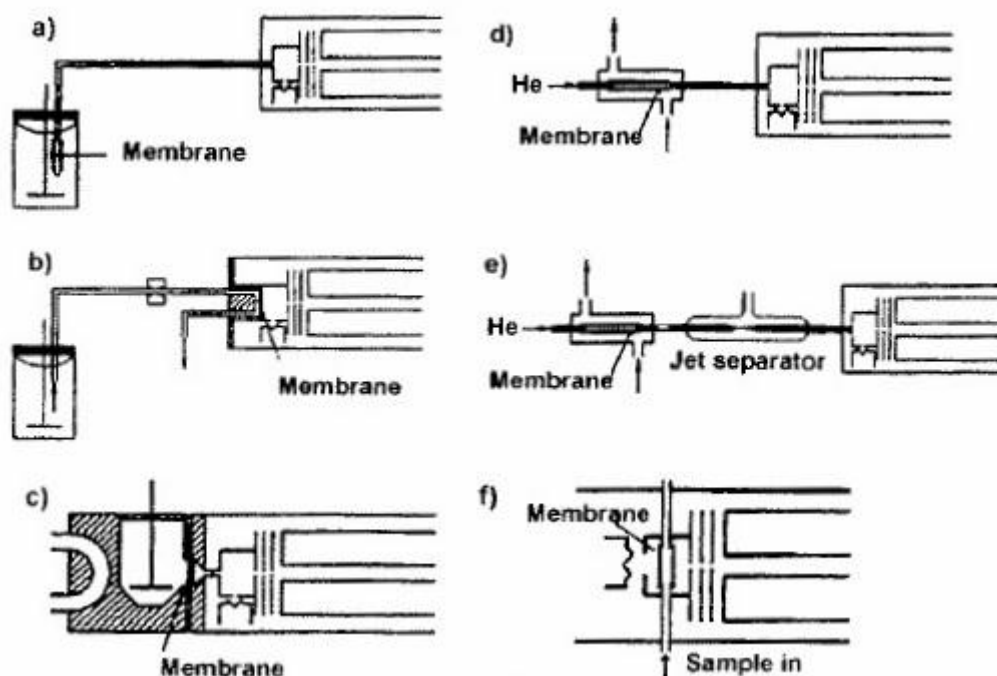

Figure 2.2: Examples on different introduction systems: a) membrane probe, b) direct insertion membrane probe, c) measuring cell, d) helium purge introduction, e) two stage introduction and f) membrane introduction using stimulated desorption (Kotiaho and Lauritsen 2002).

The membrane probe consists of a probe where one end is connected to the mass spectrometer while there is a membrane placed at the other end. This introduction system can only be used for analysis of gases and volatile organic compounds with boiling points less than 100 °C (Kotiaho and Lauritsen 2002).

The direct insertion membrane probe (DIMP) systems are constructed such that the membrane is placed directly into the ion source (Johnson, Cooks et al. 2000). Two different DIMP systems have been constructed, capillary direct insertion membrane probe (C-DIMP) and sheet direct insertion membrane probe (S-DIMP) (Srinivasan, Johnson et al. 1997). In this

setup condensation along the connection tube is eliminated, and compounds with boiling points up to 200 °C can be analyzed.

In the measuring cell the membrane makes up a part of one wall in a measuring cell which is placed right by the mass spectrometer. The compounds that can be measured with the DIMP system can also be measured with this system.

In the helium-purge introduction the sample is introduced on the outside of the membrane, while there is a constant flow of helium on the inside. The helium gas transports the permeated molecules to the mass spectrometer. Due to minimal effects of condensation, this introduction system can measure almost the same compounds as the DIMP system. The helium purge through the system results in shorter response times (Slivon, Bauer et al. 1991). A more detailed view of this introduction system is shown in Figure 2.3. This introduction system is also called flow over introduction (Davey, Krogh et al. 2011). Flow-through introduction has also been developed, where the sample is introduced on the inside of the membrane and is transported to the mass spectrometer by a carrier gas from the outside of the membrane (Kotiaho 1991).
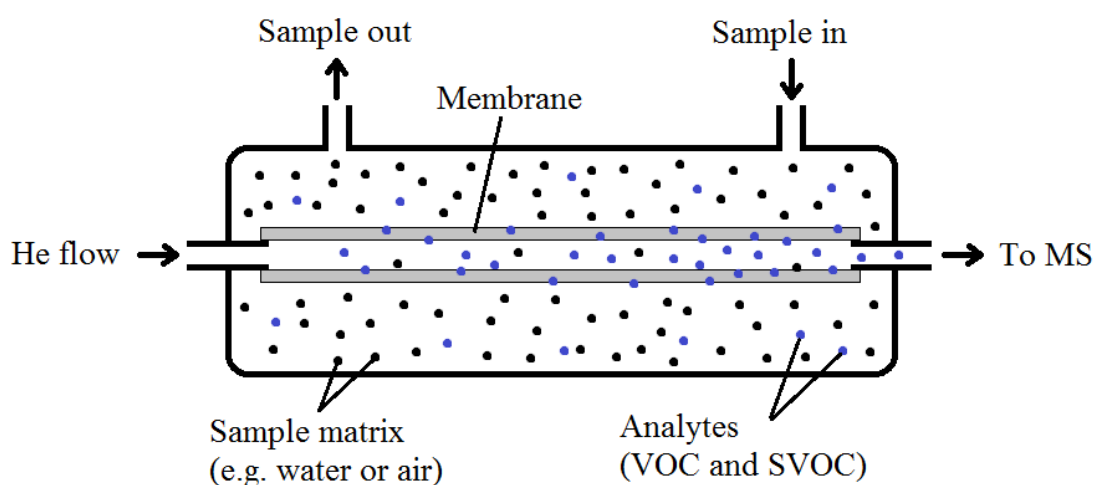
Figure 2.3: A schematic presentation of the helium-purge membrane introduction.

The two stage introduction combines an introduction system with another device for either concentrating or separation, which can be placed before or after the membrane. The example shown in Figure 2.2e) is the membrane/jet separator system (Srinivasan, Johnson et al. 1997) which combines a helium-purge membrane introduction with a jet separator. The jet separator

contributes to removal of the helium and water before the permeated compounds are transported to the mass spectrometer. Two stage introduction leads to analyte enrichment which results in lower detection limits.

The introduction systems mentioned above can only measure compounds with boiling points up to 200 °C. Compounds with higher boiling points will not evaporate from the membrane. To enable the detection of less volatile compounds, membrane introduction with stimulated desorption can be used. An example is the trap-and-release system. In this system the compounds diffuses through the membrane and is evaporated from the membrane by a rapid heating of the membrane (Kotiaho and Lauritsen 2002). Another system that uses a similar system is the single-sided membrane system (SS-MIMS). In this setup the analytes does not permeate through the membrane, but is absorbed and desorbed at the same side. The most volatile compounds will desorb from the membrane relatively fast, while the less volatile compounds is depending on a quick heating of the membrane surface to desorb (Riter, Takats et al. 2001).

Another overview of different introduction systems is given in Figure 2.4.
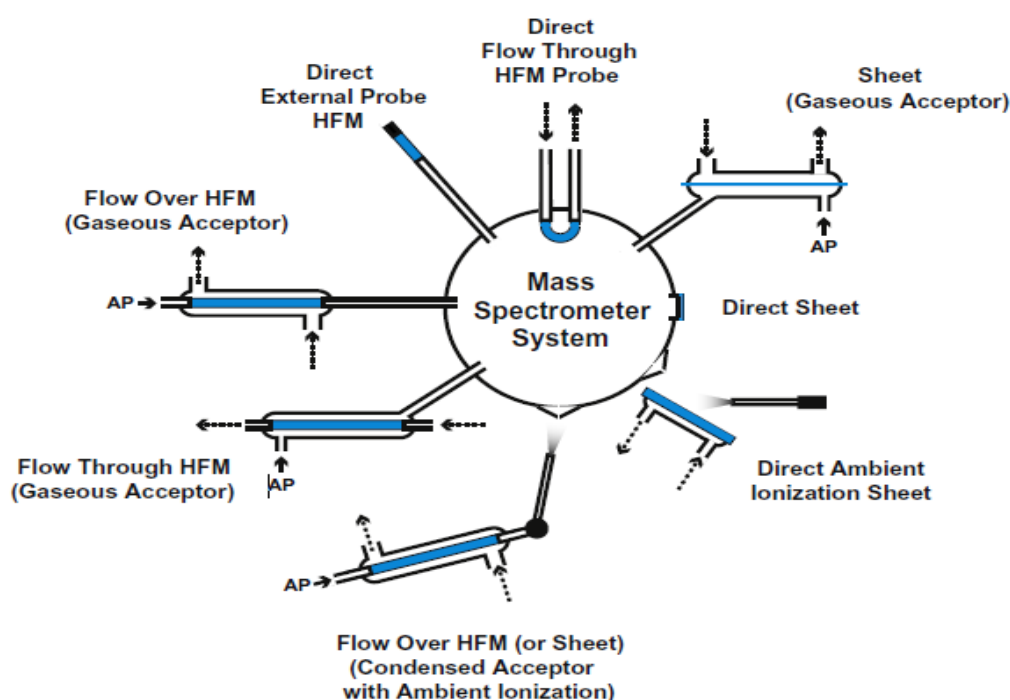
Figure 2.4: Different interface configurations for MIMS analyses. Dashed arrows show the sample flow path. HFM = hollow fiber membrane. AP = acceptor phase (Davey, Krogh et al. 2011)

2.1.4 The membrane

A great number of different membrane materials can be used, depending on the character of the target compounds. There are two main membrane groups; hollow fiber membrane (HFMs) and sheet membranes. Hollow fiber membranes can be used in introduction systems like membrane probes and flow through/over systems while sheet membranes can be used in DIMP and flow through systems. Sheet membranes can be varied in a greater extent considering choice of both materials and thicknesses. The most common membrane material in use is silicone polymer, usually polydimethylsiloxane (PDMS) which is a hollow fiber membrane (Davey, Krogh et al. 2011). PDMS membranes are non-porous, hydrophobic and are semi-permeable to non-polar organic compounds (Kotiaho and Lauritsen 2002).

The size and thickness of the membrane is crucial for the analyte flow. A maximum flow is obtained with thin and large membranes. The thickness of the membranes varies for different experiments, but the two most common thicknesses are 0.508 mm inner diameter (i.d.) and 0.940 mm outer diameter (o.d.) (e.g. Cisper, Gill et al. 1995 and Creba, Ferguson et al. 2006) or 0.305 mm i.d. and 0.635 mm o.d. (e.g. Ketola, Virkki et al. 1997 and Slivon, Bauer et al. 1991). There have also been performed experiments with ultra-thin membranes.

Kasthurikrishnan et al. used membranes in the range of 10 to 50 µm for analysis of volatile compounds in solution. For analyses with an organic phase (reversed phase) the ultra-thin membranes showed improved response times compared to the thicker membranes. However, an improvement in the sensitivity was not observed (Kasthurikrishnan, Cooks et al. 1996). Thin membranes are practical for chemical and petrochemical on-line process monitoring (Srinivasan, Johnson et al. 1997).

Hydrophilic membranes are used as a reversed phase. The most common materials for these analysis are cellulose (Xu, Patrick et al. 1995; Janfelt, Frandsen et al. 2006) and nafion (Creaser, Lamarca et al. 2001). When hydrophilic membranes are used the method is often called affinity MIMS. These membranes contribute to an improved selectivity by adsorbing analytes with particular functional groups (Xu, Patrick et al. 1995).

Experiments with membranes made up by liquids have also been tested. Liquid membranes have the advantages that they easily can be adjusted with respect to membrane thickness. Johnson et al. tested the suitability for MIMS analysis of volatile organic compounds for four liquids of low vapor pressure. From this work it is shown that liquids such as polyphenyl

ether, alkylated cyclopentane and silicone oil are suitable as semi-permeable membranes (Johnson, Koch et al. 1997).

To enable the possibilities for detection of compounds that are not detected by conventional MIMS, Creba et al. modified a PDMS membrane to include enzymes. This membrane was used to analyze esters of low volatility and hydrophilic character. Enzyme membranes can be used to increase the selectivity of the system with the help of specific interactions between enzyme and substrate (Creba, Weissfloch et al. 2007).

The best suited membranes for normal-phase environmental analyses are, concluded after experiments on membrane materials for water analysis by Maden et al., silicon, latex, polyethylene and polyurethane (Maden and Hayward 1996).

2.2 Applications of MIMS

2.2.1 Environmental applications

As mentioned earlier the technique of MIMS has lately been used in several different environmental applications, especially for air and water analysis.

2.2.1.1 Air analysis

Analysis of compounds from air has become an important aspect in environmental monitoring, and MIMS allows for measurements of volatile organic compounds in air samples in the low $\mu g/m^3$ range (Kotiaho and Lauritsen 2002).

Ketola et al. optimized a MIMS system for air analysis by studying different factors such as membrane thickness, temperature and flow rate. The achieved response times were three to six times better with the thinner PDMS membrane (25 µm compared to 100 mm). Similar response effects due to membrane thickness were also obtained in water analysis, carried out by Dongré et al. (Dongré and Hayward 1996). From the experiment with ultra-thin membranes mentioned earlier, the results with the thin hydrophobic membranes did not show an improvement compared to normal size membranes, just for the hydrophilic membranes (Kasthurikrishnan, Cooks et al. 1996). This can result from differences in the membrane

materials (Ketola, Ojala et al. 1997). Both the response factor and response times were better with a higher flow rate. To get the best results, as high flow rates as possible are ideal, and the value of this experiment was 1500 ml min^{-1}. However, a flow rate of 400-500 ml was selected so that the system would not be under too much pressure, while keeping the response and response times relatively close to the optimal values. An increase in the temperature lead to a decrease in the response times up to 110 °C where the curve leveled out. Up to 140-160 °C the response curve had a weak decrease, leading from a decrease in permeabilities for organic compounds in air with increasing temperatures. They concluded with an optimal temperature around 80 °C, when considering both response and response times (Ketola, Ojala et al. 1997).

Riter et al. used a long membrane to allow for high surface analysis of VOCs and SVOCs with low detection limits (ppt). Compared to similar analysis of water samples, matrix interactions and poor response and fall times were minimized when using air as the sample matrix (Riter, Takáts et al. 2001).

Analysis of volatile organic sulfur compounds (VOSCs) in air samples was done by Ketola et al. Detection limits in the low µg/m^3 were obtained and identification of individual compounds in a mixture were achieved by comparison to a reference library. The effect of humidity levels on the response was also investigated, and they concluded that high humidity would saturate the membrane and decrease the permeation of target compounds (Ketola, Mansikka et al. 1997).

2.2.1.2 Water analysis

MIMS analyses of water samples often have detection limits in the parts-per-billion range (Ketola, Virkki et al. 1997; Alberici, Sparrapan et al. 2001). By combining the MIMS system with a cyrotrap, making a CT-MIMS system, Mendes et al. increased the signal intensity, hence the sensitivity, by a factor of 100 compared to a conventional MIMS system. This system makes it possible to detect VOCs at the low parts-per-trillion level (Mendes, Pimpim et al. 1996). Bauer et al. was able to detect toluene and *trans*-1,2-dichloroethene at parts-per-quadrillion level by using long ionization times to concentrate analyte ions and eliminate other ions (Bauer, Amy et al. 1995).

Wong et al. studied the effect of two different membranes, a non-porous silicone membrane and a microporous polytetrafluoroethylene (PTFE) membrane, for SVOC and VOC analysis in water. During this work it was achieved quite similar performance on the tested membranes concerning detection limits and linearity (Wong 1995).

Ketola et al. tested three different methods, MIMS, purge-and-trap gas chromatography-mass spectrometry (P&T) and static headspace gas chromatography (HSGC), for VOC analyses in water samples. The summarization of the results can be seen in Table 2.2, adopted from their paper.

Table 2.2: Characteristics of the three analytical methods (Ketola, Virkki et al. 1997)

Characteristics	MIMS	P&T	HSGC
Detection limits (μg l^{-1})	< 1	< 1	1-10
Linear dynamic range	10^4	10^2	10^6
Repeatability (%)	1-11	2-13	1-8
Analysis time (min)	5-10	35-45	35-45
On-line monitoring capability	Very good	Fair	Fair
Identification capability	Good	Very good	Good[a]
Simplicity of instrumentation	Good	Fair	Very good

[a] Flame ionization detector used

As can be seen from Table 2.2 MIMS has the advantages of low detection limits, shorter analysis times compared to the other methods and also the possibility of on-line monitoring. Compared to P&T and HSGC, MIMS is less efficient to identify individual compounds (Ketola, Virkki et al. 1997). A method to overcome the difficulties of individual compound determination in mixtures can be achieved by combining the MIMS system with a gas chromatograph (GC). This setup takes the advantages of separation by GC, and the on-line ability of MIMS. Chang and Her used this method for monitoring of trihalomethanes (THMs) in chlorinated drinking water (Chang and Her 2000). Another way to avoid identification difficulties is the use of tandem mass spectrometry (Kotiaho and Lauritsen 2002), described in

section 2.3.4. Mathematical approaches have also been used to solve this problem. Ketola et al. developed a method called a nonlinear asymmetric error function-based least mean square (NALMS) based on the assumption that *"the intensity of any mass-to-charge ratio (m/z) is a linear function of the concentration of the chemical compounds contributing to that particular m/z"* (Ketola, Ojala et al. 1999).

Another advantage for use of MIMS in environmental analyses, is that many of the MIMS setups can easily be used for both air and water analysis without any modifications (Ketola, Ojala et al. 1997). Cisper et al. demonstrated this feature, also including a soil sample, which can be seen in Figure 2.5. They used a MIMS system with a hollow fiber silicone membrane coupled to an ion trap spectrometer. The sampling was done be moving the inlet from one sample to the next. The system was not optimized to yield optimal response for the different materials, it was just a demonstration for VOCs analysis in different sample matrix (Cisper, Gill et al. 1995).
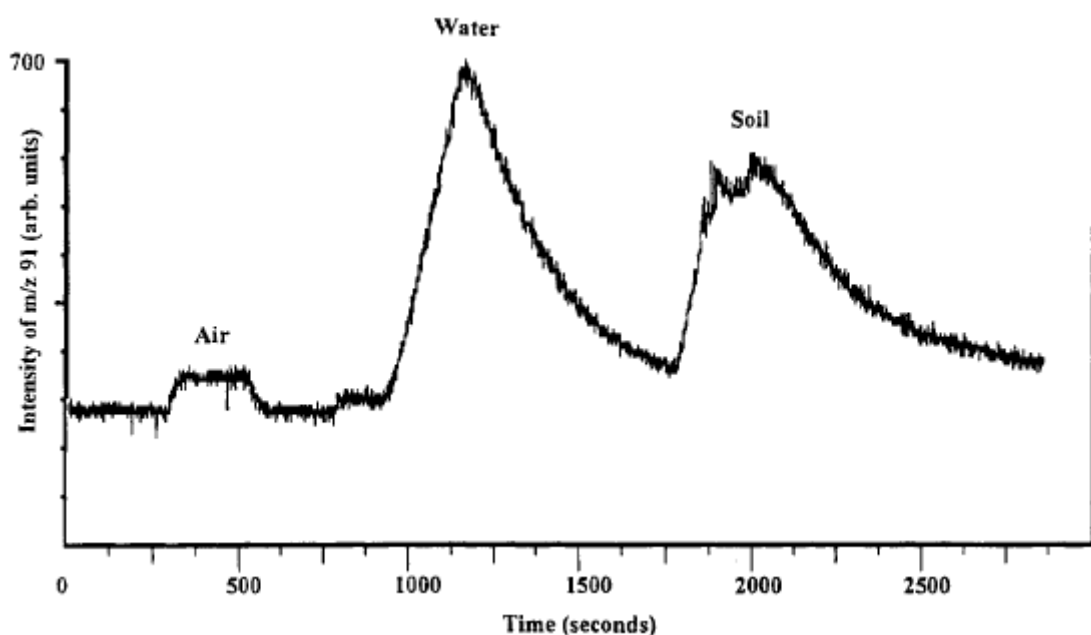
Figure 2.5: Demonstration of the versatility of a MIMS setup. Presented are the signal (*m/z* 91 and 92) for toluene (1 ppb) in air, water and soil samples (Cisper, Gill et al. 1995).

2.2.1.3 Soil analysis

Publications where soil is used as the sampling matrix is much more limited compared to air and water analysis. Kostiainen et al. developed a method called purge-and-membrane mass spectrometry (PAM MS) for analysis of VOCs in both air and soil samples. The analysis time for the analytes had a longer duration compared to the internal standard, fluorotoluene. The reason for this is that the VOCs are more strongly bound to the soil. Parameters such as sensitivity, reproducibility and linearity that were achieved were good, indicating that soil is a promising sample material for MIMS analysis (Kostiainen, Kotiaho et al. 1998). Sheppard et al. used MIMS for continuous monitoring of gas concentrations in core soil samples as an impact of sludge applications (Sheppard, Gray et al. 2005).

2.2.1.4 On-line analysis

The possibilities for on-line analysis are one of the greatest advantages of MIMS. Short response times is one of the factors that makes on-line monitoring possible (Ketola, Mansikka et al. 1997; Ketola, Ojala et al. 1997), and thus rapid changes in the environment can be monitored. Advantages of on-line analysis are reduced environmental pollution, less energy and material consumption (Kotiaho, Cisper et al. 2002). The technique is also used in the field by several industries, but is not always reported in publications in journals (Janfelt, Frandsen et al. 2006).

2.2.2 Other MIMS experiments

MIMS analysis are an important application in biological monitoring, especially for bioreactor monitoring and fermentation processes (Johnson, Cooks et al. 2000). Srinivasan et al. monitored the production of methanol, and also lactic acid and glycerol, during a glucose fermentation process. The measurements was successfully done on-line with feedback control by a MIMS system constructed by a DIMP introduction, a silicone membrane, a jet separator and an ion trap mass spectrometer (Srinivasan, Kasthurikrishnan et al. 1995). Thompson et al. preformed an on-line monitoring of isoprene, a biogenic volatile organic compound (BVOC), emission from potato plants during mechanical wounding and heat stress. By the use of a

tandem mass spectrometry (MS/MS) MIMS system, they were able to follow the production of isoprene at part-per-billion levels (Thompson, Etzkorn et al. 2008).

Creba et al. preformed a MIMS experiment with a heated interface for measurements of VOCs in both water and air analysis. The system was set up with a nickel-chromium resistive heating wire through the membrane, and the interface was heated to 120 °C. See Figure 2.6 for the heated interface setup. The result of this experiment is an increase in sensitivity and a decrease in response times (Creba, Ferguson et al. 2006).
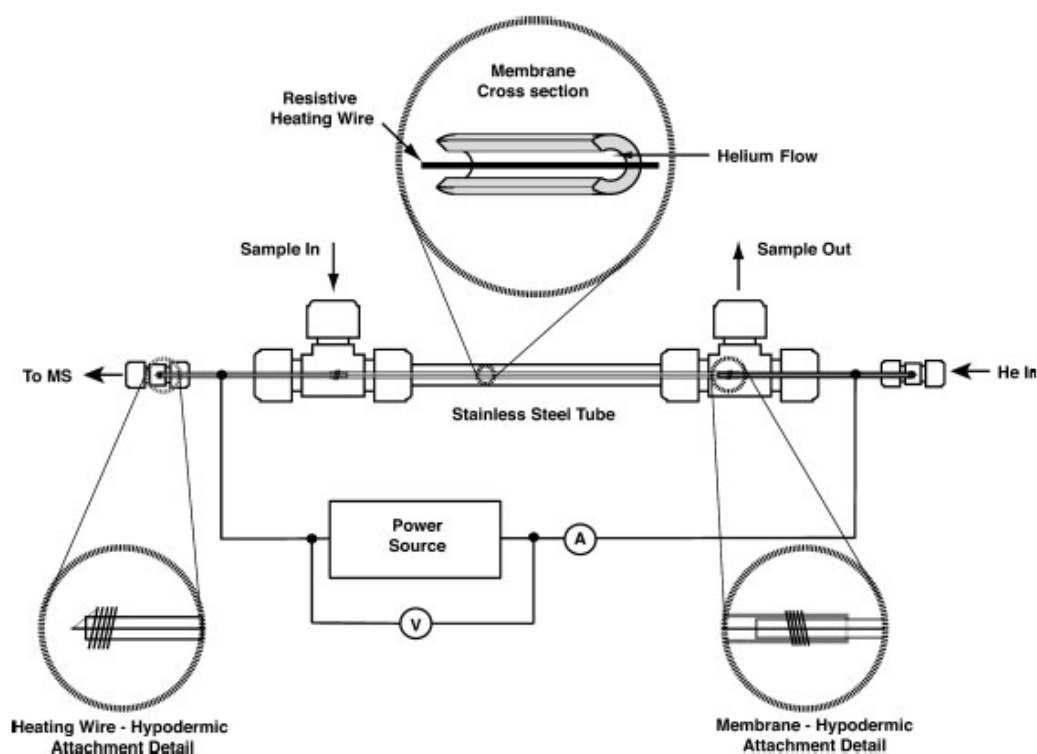
Figure 2.6: A schematic view of a heated MIMS system. The system is constructed with a resistive heating wire inside a PDMS hollow fiber membrane (Creba, Ferguson et al. 2006).

To ease the field of on-site analysis, miniaturization of the MIMS system has been carried out. Janfelt et al. constructed a mini-MIMS for detection of contaminants in organic samples, both aqueous and liquid. The total weight of the mini-MIMS was no more than 12 kilograms. The mini-MIMS can take advantages of a higher pressure compared to standard MIMS systems, and has thus a more controlled permeation to hydrophilic organic compounds when using a cellulose membrane (Janfelt, Frandsen et al. 2006).

Miniaturization has also been carried out with respect to the introduction system. Trushina et al. (1998) used a microMIMS interface to enable measurements of total NO from plasma samples. A 3 cm long membrane of polysilane was connected to fused silica capillary and placed in PEEK tubing. The system was well suited for analysis of small molecules in biological sample materials (Trushina, Clarke et al. 1998).

2.3 Mass spectrometry

The principle of mass spectrometry is based on ionization and detection. The compound is ionized and afterwards the ions are separated and detected according to their mass-to-charge (*m/z*) ratio (Silverstein, Webster et al. 2005). The *m/z* ratio is calculated from the ions mass number, m, and the ions elementary charge, z, resulting in a dimensionless *m/z*.

As can be seen from Figure 2.7 a mass spectrometer is built up by three main components, an ion source, a mass analyzer and a detector.
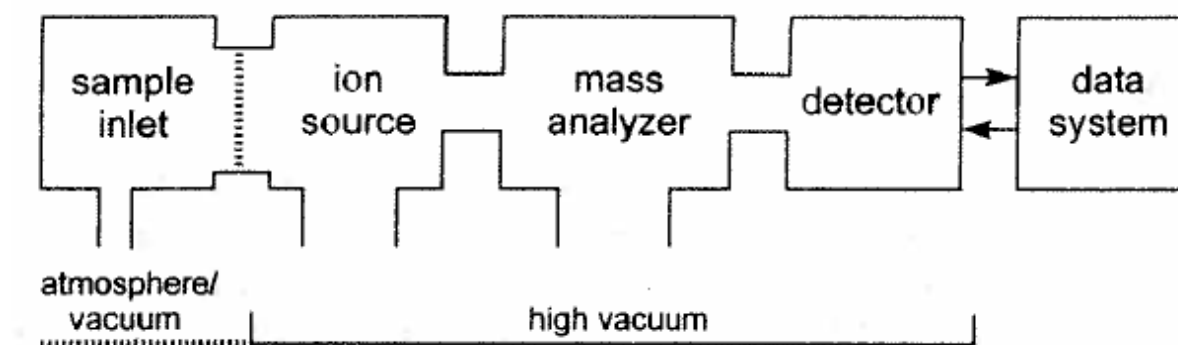
Figure 2.7: A schematic presentation of a typical mass spectrometer (Gross 2004).

2.3.1 Mass spectrum

The data information from the mass spectrometer is represented as a mass spectrum. The mass spectrum is a two-dimensional chart of signal intensity versus *m/z*. The y-axis is composed of relative abundance, where the highest peak gets assigned 100 %. The rest of the peaks are measured as percentage of the largest peak, which is called the base peak. The x-axis is based on neutral loss. Therefor the distance between two peaks is similar to the difference in the *m/z*

ratio between the two peaks. The difference from a higher peak to a lower peak is the value of the molecular weight lost to produce a lower fragment (Gross 2004). A mass spectrum can give information about molecular weights and chemical structures, especially in the case of tandem mass spectrometry (Ouyang and Cooks 2009).

2.3.2 Ionization methods

The mass analyzer can only analyze charged species; ions most commonly produced from either atoms or molecules. The ion source has the job to produce these ions, and this process can be performed by several different ionization methods.

Electron ionization (EI) is the most common ionization method used in mass spectrometry, especially in organic analysis. In EI the neutral gets bombarded with electrons too create molecular ion, M^+. EI is used for the analysis of low to medium polarity, non-ionic organic compounds with molecular weight up to 1000. The neutral has to be transported to the gas phase before the ionization, which is achieved by the introduction system. The gas phase has usually a pressure around 10^{-4} Pa. Under this condition the gas phase may be regarded as highly diluted.

Chemical ionization (CI) uses the advantages of less energy than the EI process, producing a less complex spectrum due to less fragmentation. CI is usually used when there is an easily detected molecular ion. During the process of CI fragments are produced by collision with ions from a reagent gas.

Other ionization methods are field ionization, plasma and glow discharge fast atom bombardment (FAB), laser ionization (LIMS), matrix-assisted laser desorption ionization (MALDI), electrospray ionization (ESI), plasma-desorption ionization (PD), resonance ionization (RIMS), secondary ionization (SIMS), spark source, thermal ionization (TIMS) (Gross 2004).

2.3.3 Mass analyzer

Several different mass analyzers can be used for MIMS analysis, but the most common ones are ion traps, time-off-flight (TOF) and linear quadrupole mass analyzers (Johnson, Cooks et al. 2000).

The linear quadrupole is a dynamic instrument constructed of four parallel rod electrodes, each positioned in the corner of a square. A schematic view of a linear quadrupole is presented in Figure 2.8. The rods opposite of each other have the same potential. It is the change of this potential on the two rod pairs that leads to the separation of the ions, depending on the ions charge and size (March and Todd 2005). Compared to other mass analyzers, quadrupole analyzers can operate under higher pressure, especially for miniaturized systems (Ketola, Kiuru et al. 2003).
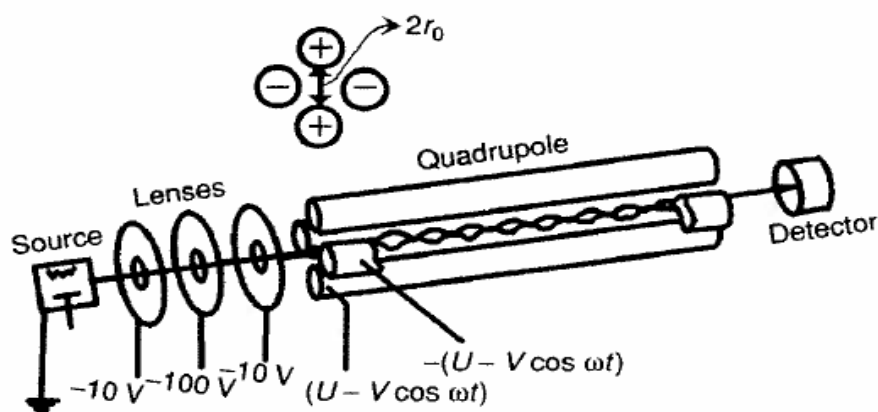
Figure 2.8: A linear quadrupole mass analyzer with a ion source, focusing lenses, quadrupole cylindrical rods and a detector (Hoffmann and Stroobant 2007).

The mass analyzer used for this project is a quadrupole ion trap (QIT). A schematic view of the quadrupole ion trap is given in Figure 2.9. The quadrupole ion trap consist of a ring electrode and two hyperbolic electrodes, making up the end caps (Gross 2004). These electrodes create a three dimensional quadrupole field, which can store ions. Ions of different masses are stored together in the trap, and ions of given masses are transported to the detector, e.g. by applying certain frequencies along the z-axis (Hoffmann and Stroobant 2007). An

advantage of the quadrupole ion trap, as compared to the linear quadrupole, is the possibility for tandem mass spectrometry, described in more detail in the next section.
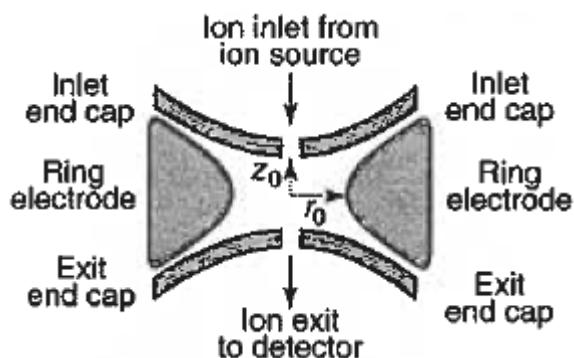
Figure 2.9: Schematic view of a quadrupole ion trap (QIT) (Hoffmann and Stroobant 2007)

2.3.4 Tandem Mass Spectrometry

Tandem mass spectrometry (MS/MS) is a technique where the ions are mass analyzed at least two times. The first MS stage isolates a precursor ion that is fragmented, usually by collision, to product ions and neutral fragments. The product ions is then analyzed by the second stage MS (Hoffmann and Stroobant 2007). MS/MS may enhance the determination of molecules in mixtures by these characteristic secondary fragment ions (Shukla and Futrell 2000). There are also possibilities for multistage MS analysis, e.g. MS^3, MS^4 (generally abbreviated as MS^n) (Gross 2004). MS/MS analysis has great sensitivity, specificity and is also time efficient (McLafferty 1980).

In relation to MIMS analysis the use of tandem mass spectrometry (MS/MS) increases the selectivity. MS/MS makes the identification of individual compounds much easier, and on-line monitoring of several different compounds in a complex mixture possible (Thompson, Etzkorn et al. 2008).

2.4 Flame Ionization Detector

One of the most common detectors for chromatographic analysis is the flame ionization detector (FID), presented in Figure 2.10. The compounds are burned in an air/hydrogen flame to produce charged particles (Skoog 2004). The FID detector takes advantages of the principle that the concentration of charged particles in the gas is proportional to the electrical conductivity in the gas phase. The response is also proportional to the amount of carbon atoms (Torkil 1999). The FID detector gives good response for organic compounds and other compounds which are easily flammable (Greibrokk, Lundanes et al. 2005). The FID detector has advantages such as high sensitivity, great linear response, little influence of noise and it is robust and user friendly. One disadvantage of this detector is its destructive character by destroying the sample during the combustion (Skoog 2004).
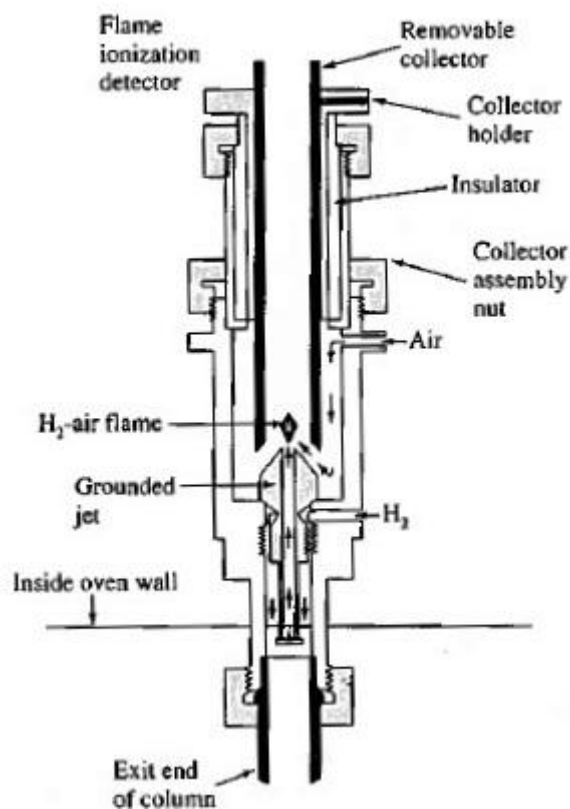
Figure 2.10: A schematic view of a typical flame ionization detector (Skoog 2004)

2.4.1 Membrane Introduction Flame Ionization Detector

A FID detector can also be used in combination with a membrane introduction, resulting in a membrane introduction flame ionization detector (MIFID) system. Devlin et al. preformed a membrane introduction flame ionization/electron capture detection (MIFID/ECD) analysis of VOCs and volatile organic halides (VOXs) in water. They obtained real-time measurements at sub parts-per-billion levels. Compared to a MIMS system, a MIFID system will have lower selectivity but comparable sensitivity. A MIFID system is not dependent on the same vacuum requirements as MIMS systems, but has the capabilities of on-line measurements (Devlin, Amaral et al. 2008).

The FID signal profiles give information about the total signal for the whole sample, and not individual masses as can be obtained by MIMS, thus disabling the possibilities for individual compound identification.

2.5 Petroleum

In the modern society petroleum is a very important product, and is used both as raw materials and fuel. Petroleum provides about 40 % of humans' energy consumption, and the other percentages are mainly covered by coal and natural gas. In nature, more precisely in sedimentary rock deposits, petroleum exists as gases, liquids, semisolids and solids (Speight 2007).

2.5.1 Petroleum chemistry

Petroleum is far from a homogenous material, it consist of a highly complex mixture of thousands of chemical compounds. The elements that makes up these compounds are carbon, hydrogen, nitrogen, oxygen, sulphur and metals, listed from highest percentage to lowest (Speight 2007). The most common metals found in petroleum are vanadium, nickel, iron, zinc, mercury, boron, sodium, potassium, calcium and magnesium, but there has been found around thirty metals in total (Simanzhenkov and Idem 2003). The main compound groups found in petroleum are hydrocarbons and nonhydrocarbons (Speight 2001).

Figure 2.11 shows an overview of the different petroleum compound groups and some compound examples.
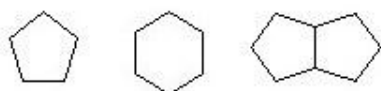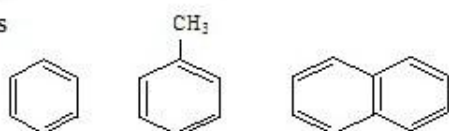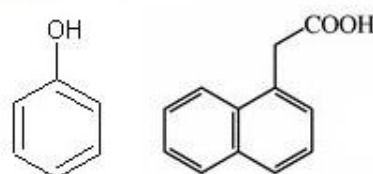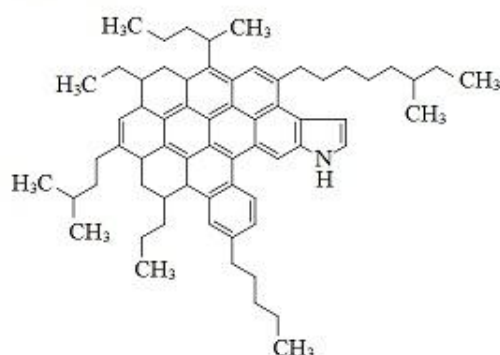
Figure 2.11: An overview of the main compound groups in petroleum, with under groups and some examples of compounds representing each group.

The biggest compound group is the hydrocarbons, which consists of paraffins (n-alkanes and iso-alkanes), naphthenes and aromatics. The hydrocarbons are composed of hydrogen and oxygen, and consist of a broad range of compounds from small molecules to large and complex molecules.

Paraffins are saturated alkane chains which are either straight-chained (n-alkanes) or branched-chained (iso-alkanes). The amount of straight-chained paraffins in oil varies from small percentages in naphthenic and asphaltic oil and up to 20-50 % in paraffinic oils. Paraffins with branched chains usually appears in the heavier oil fractions (Simanzhenkov and Idem 2003). Waxes are an important sub-group of paraffins, and consist of compounds

containing more than 20 carbon atoms. Increasing boiling point of the oil fraction leads to decreasing amounts of paraffins.

Naphthenes are a group of saturated hydrocarbons in ring structures, which can have paraffinic side chains. The most common naphthenes are cycloalkanes consisting of five- or six-carbon rings; these are the most thermodynamically stable ring structures. Naphthenes are often the most abundant group in crude oils, covering up to 60 % of the hydrocarbons.

Aromatics consist of compounds with aromatic ring structures. They can have paraffinic or naphthenic side chains, or both, giving a large number of isomers. The amount of aromatics in petroleum increases with increasing boiling point of the fraction (Speight 2007).

The other group, nonhydrocarbons, consists of resins and asphaltenes. They are organic compounds containing small amounts of oxygen, nitrogen, sulphur or trace metals (e.g. nickel and vanadium), and can be either saturated or aromatic. The presence of these atoms brings a polar character to the compounds (Wang and Stout 2007). The nonhydrocarbons mainly occur in the higher boiling range fractions (Speight 2007), making them unsuitable for MIMS analysis due to high volatility.

The divisions between the different groups are highly variable from oil to oil. On this basis different oils have distinct physical and chemical properties depending on their exact composition. The composition of each oil is dependent on the age and location of the oil, geological condition (Lin and Tjeerdema 2008) and the depth of the reservoirs (Speight 2007).

Petroleum is often described as "conventional" or "heavy", depending on boiling ranges. Conventional crude oils have a large content of volatile compounds having low boiling points, whereas heavy crude oils have bigger fractions of high boiling compounds. Conventional crude oils have a big portion of hydrocarbons (paraffins, naphthenes and aromatics), and are classified by having viscosities below 100 cP (Wang and Stout 2007).

The most important physical properties of oils are boiling point, pour point, density, viscosity and flash point.

With respect to membrane introduction analysis the most interesting oil compounds are the most volatile compounds, e.g. small hydrocarbons.

2.5.2 Weathering

When oil is spilled either on land or at sea, the oil will undergo several different weathering processes. These weathering processes can be chemical, physical or biological. Figure 2.12 gives an overview of different oil weathering processes at sea. The most important processes affecting the chemical composition are evaporation and dissolution. The different processes will also affect the rate of each other, e.g. spreading will lead to an increase in evaporation and dissolution (Wang and Stout 2007).
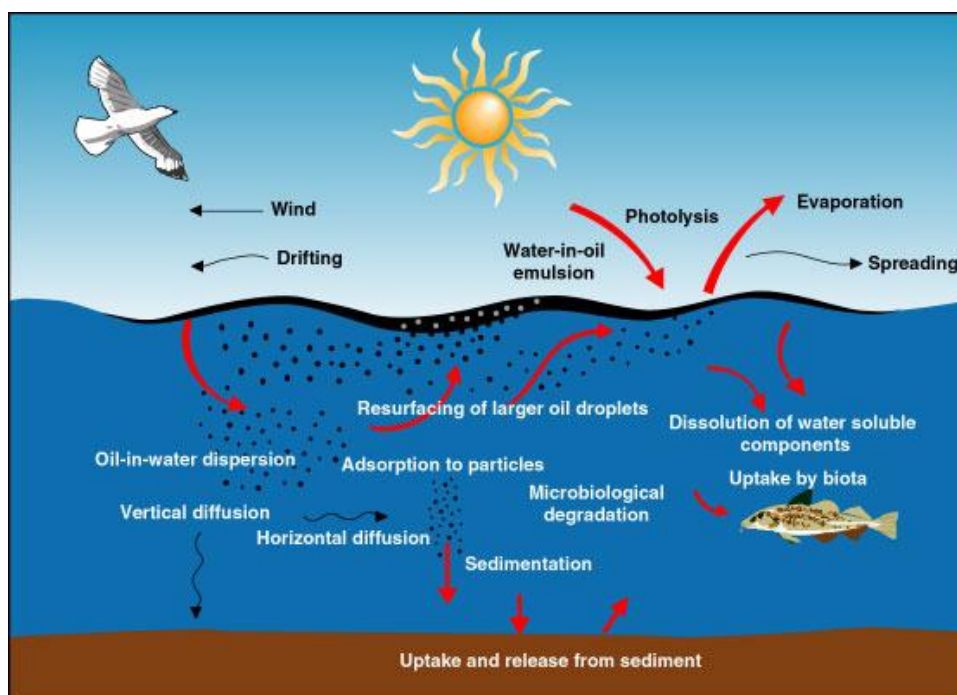
Figure 2.12: An overview of the most important oil weathering processes that occur after an oil spill at sea (Daling and Brandvik 2009).

Weathering of oils is expected to have a significant influence on analysis results obtainable by MIMS or MIFID.

2.6 Statistics

The average of a data set can be calculated from equation 2.4, where n is the number of data values.

$$\bar{X} = \frac{1}{n} \sum_{i=1}^{n} X_i$$
(2.4)

Standard deviation (s) is a measure of the deviation from the mean value, and can be calculated from equation 2.5.

$$s = \sqrt{\frac{1}{n-1} \sum_{i=1}^{n} (X_i - \bar{X})^2}$$
(2.5)

The relative standard deviation (RSD) gives information about how big or small the variation between parallels are (Løvås 2004). RSD can be calculated from equation 2.6, given in percentages.

$$RSD = \frac{\text{Standard deviation of array X}}{\text{Average of array X}} \times 100\%$$
(2.6)

3. Materials and methods

3.1 Chemicals

All water used in the analyses was clean. The water purifying system that was used was Elix S from Millipore.

To make standard solutions methanol, toluene (Merck, p.a. quality) and n-heptane (J.T.Baker, analytical grade) were used.

For washing of the components for the interface methanol and dichloromethane (analytical grades) were used, while acetone was used for cleaning of the glassware. The flask used for the water analyses was cleaned with soap, acetone and clean water, and dried overnight between each analysis.

3.1.1 Petroleum

12 different petroleum samples were investigated in this project, listed in Table 3.1.

Ten of the oils are from different oil fields in the North Sea, one is from the Athabasca area in Alberta, Canada, and one is from the Campos Basin area in Brazil.

Petroleum samples were tested by a membrane introduction flame ionization detector (MIFID), both for water and air analysis. The same air analysis was also carried out with membrane introduction mass spectrometry (MIMS), and also two oil samples were analyzed by water MIMS. The MIMS analysis however, had shorter analysis times than the MIFID analysis.

Table 3.1: Information about the petroleum samples used in this project (Collin-Hansen 2011; Melbye 2011; Statoil 2011)

Name	Characteristics
Falk	Light crude oil, asphaltic, small amounts of waxes, North Sea
SAGD [a]	Heavy crude oil, Alberta
Peregrino JOB 0391	Brazilian crude oil
Mariner Maureen	North Sea crude oil
Bressay JOB0081-0001	North Sea crude oil
Heidrun Tilje	Medium density, low sulphur, high TAN [b], North Sea crude oil
Troll B 2005-0722	North Sea crude oil, topped to 150 °C
Balder Blend 2010-0159	North Sea crude oil, topped to 200 °C
Norne Blend 2009-0549	Medium density, low sulphur, waxy, North Sea crude oil, topped to 200 °C
Oseberg Blend 2011-0355	Light crude oil, low sulphur, North Sea, fresh
Unspecified 1	North Sea crude oil, fresh
Unspecified 2	North Sea crude oil, fresh

[a] SAGD (Steam Assisted Gravity Drainage) is an exploration method for tar sand. This SAGD sample was extracted with naphtha for removal of water before the lightest compounds was removed by a heating process.

[b] TAN (Total Acid Number) is the amount of KOH (mg) that is necessary to neutralize the acid in one gram of oil.

3.2 Building of the interface

The interface used in this project is constructed as a flow-over introduction system.

An approximately 11 centimeters long piece of the polydimethylsiloxane hollow fiber membrane (Dow-Corning, 0.508 mm i.d. x 0.940 mm o.d., Helix Medical) was placed in a beaker with hexane overnight. The next day it was dried in an empty desiccator, with several evacuate/vent cycles. The tubing was stored wrapped in aluminum foil. These procedures prevent easy accumulation of dust on the membrane.

All the metal parts were first washed sequentially in two beakers of dichloromethane (DCM), for 15 minutes periods. Afterwards they were dried and then washed in the same way with methanol. (The liquids in the second beaker of each solvent can be saved and used in the first beaker for later washing procedures.)

The washed and dried parts were then assembled (Figure 3.1). Approximately 0.5 cm of each side of the membrane were threaded on thin stainless steel capillary tubing (hypodermic needle stock, 21 Gauge, cut to 6 cm length, Hamilton, VWR International, Oslo) secured with thin copper wires, leaving 10 cm of membrane between these two. Two 1/4" stainless steel Tees (1/4" Tee Union, Swagelok, SVAFAS Stavanger, Norway) were connected to a 1/4" stainless steel tube (10 cm, 4.6 mm i.d.) The membrane was installed inside the tube by fixing the hypodermic tubing in the Tees with appropriate 1/4" reducing ferrules. (The 1/4" connections at right angels are available for passing the sample medium along the outside of the membrane.)
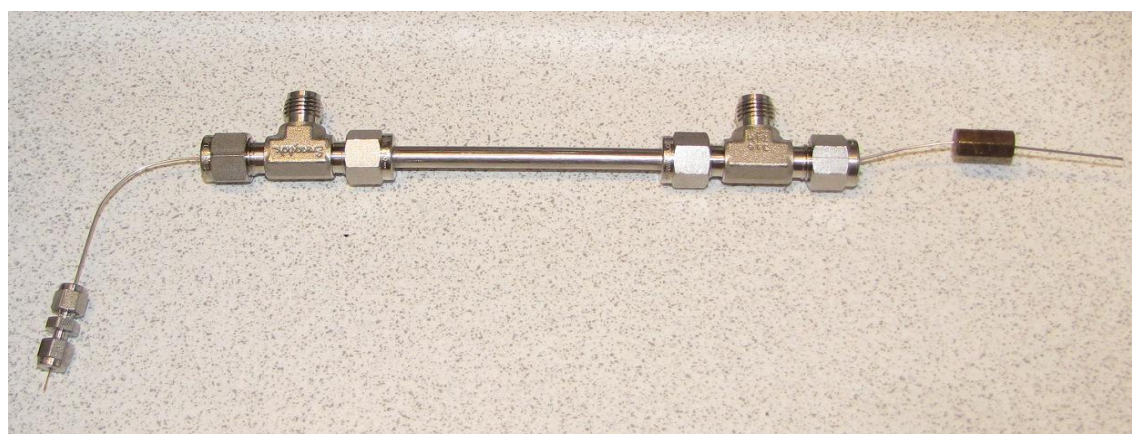
Figure 3.1: A partly installed membrane interface. A more detailed schematic presentation of such an introduction system is given in Figure 2.3.

3.3 MIFID petroleum analysis

3.3.1 Equipment for the MIFID-analyses

The different pieces of equipment used for the MIFID analyses are listed in Table 3.2.

Table 3.2: Equipment used in the MIFID analyses

Equipment	Model
GC	Shimadzu GC-2010 Gas Chromatograph (with split/splitless injector and FID detector, controlled by GC-Solution software (Version 2.30.00, Shimadzu)
Hydrogen flow restrictor column	GC column (DB-5, 30 m x 0.32 mm i.d.)
Peristaltic pump	Masterflex L/S Easy-Load II with pump head (Masterflex, Model 77200-62) and pump tubing (approximately 20 cm of Masterflex Tygon LFL tubing, HV-06249-24, 6.4 mm i.d.)
Water bath	Büchi Heating Bath B-490
Air pump	VWR Vacuum gas pump, Type: PM20405-86
Gas flow meter	Aalborg model P single flow tube meter (KIT-T1T-TA-A)
Transfer tubing	1/4" Teflon tubing connected by short pieces of 1/4" Viton tubing

3.3.2 Optimization of the MIFID-system

Some of the MIFID system parameters were optimized using mixtures of toluene or n-heptane in water or air as a test analyte. The different parameters and settings that were tested are listed in Table 3.3.

Table 3.3: Parameters and tested settings for the optimization

Parameter	Tested settings
Water flow (mL/min)	60, 90, 140, 210 and 250
Water bath/Interface temperature (°C)	30, 40, 50 and 60
MI-hydrogen flow (mL/min)	5.0, 10.1 and 20.1
FID-Hydrogen flow (mL/min)	20, 30 and 40
FID-Airflow (mL/min)	350 and 400
FID-Makeup gas flow (mL/min)	With and without
	20, 30, 40 and 50

All water analyses were done by introducing 1 µL of toluene solution (methanol:toluene 90:10) to 1.20 liters of recirculating water. After equilibration different parameters were tested, and clean water was pumped through the system between analyses of different settings to bring the signal to zero. The tested MI-hydrogen flow, 5.0 mL/min, 10.1 mL/min and 20.1 mL/min, were obtained with restrictor column inlet pressures of 70 kPa, 119 kPa and 193 kPa, respectively, as calculated by the GC software.

To reduce the testing time, testing of the different FID-gas velocities was done with air MIFID samples. Samples of either toluene (methanol:toluene 90:10) or n-heptane (methanol:n-heptane 90:10) were prepared by collecting 1 µL of the vapor right above the liquid level in flasks containing the respective liquids.

The values of the different parameters chosen after the optimization are listed in Table 3.4.

Table 3.4: Operative settings for the MIFID-analyses

Parameter	Setting
Water bath temperature (°C)	40
Water flow (mL/min)	250
GC settings:	
Column temperature (°C)	40
Injector temperature (°C)	40
Detector temperature (°C)	250
Column flow (H_2) (mL/min)	10.1
H_2 flow (mL/min)	30
Makeup flow (mL/min)	40
Air flow (mL/min)	350

3.3.3 Oil in water analysis

3.3.3.1 Experimental setup

The system for water analysis can be seen in Figure 3.2 and Figure 3.3. It was used a closed system with recirculation of water. A 1 liter three-necked flask was placed in a water bath at 40 °C (± 1 °C) (Figure 3.2 C). Clean water was pumped from the bottom of the flask to the interface through Teflon tubing (Figure 3.2 B). The interface (Figure 3.2 D) was fixed inside the oven of a gas chromatograph by 30 cm long 1/4" stainless steel tubing used to connect the interface Tees with the Teflon tubing transporting water (or air) to and from the interface across the top of the GC oven. The hypodermic tubing pieces were connected to the hydrogen gas flow provided from the injector through a standard GC column (DB-5, 30 m x 0.32 mm i.d.) by a 1/16" union and appropriate reducing ferrules. After passing the membrane the hydrogen was transferred to the FID through a short piece of deactivated fused silica (30 cm,

0.32 mm i.d.), connected to the interface by another 1/16" union. The FID detector operated at the given gas flows and a temperature of 250 °C. The gas flow and water flow run in opposite directions through the interface. The Teflon tubing transporting the water or air to and from the outside ends of the stainless steel tubing are not isolated. Water returns from the MIFID to the flask through the peristaltic pump, regulating the water flow to approximately 250 mL/min. The volume of the tubing system is about 0.05 liters and the total volume of the flask is about 1.15 liters, resulting in a total water volume of approximately 1.20 liters.

Figure 3.2: Overview of the MIFID system for water analysis. A) An overview of the whole setup. A flask with water is placed in a water bath and connected to the MI in a GC oven by Teflon tubing. B) The top of the GC: The tube to the right introduces the sample to the membrane, and the tube to the left returns the samples to the flask. The tubing to the far right is used to introduce clean air/water via the 3-way Ball valve in the back. C) Oil sample spread on a piece of aluminum foil in the flask. D) Inside view of the GC oven: The sample flow is introduced from right to left, in the horizontal metal tubing, while the hydrogen gas in the membrane tubing inside the interface flows from left to right.
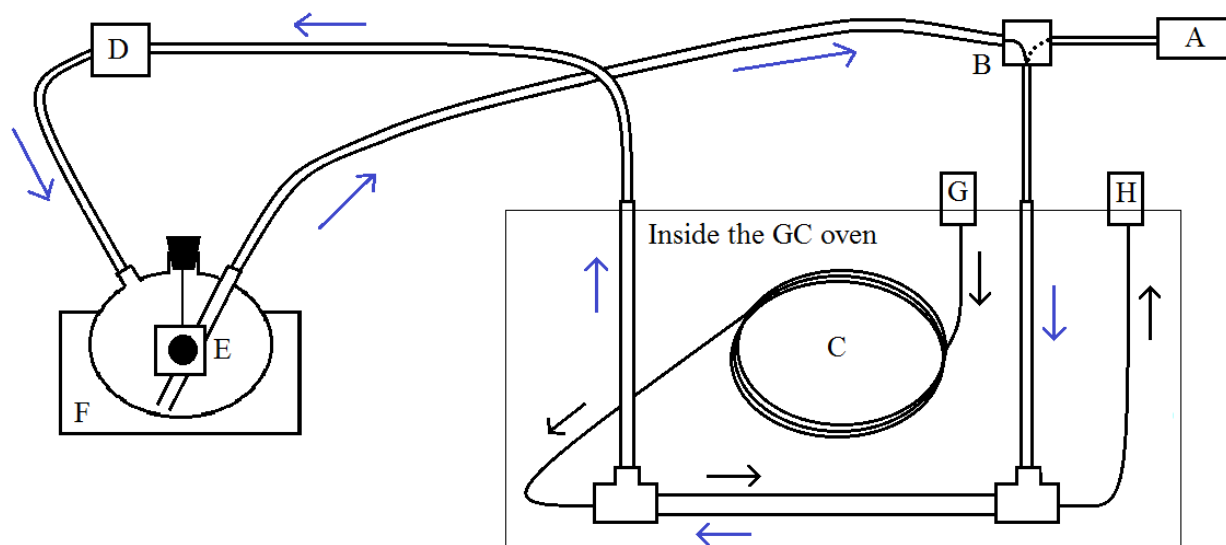
Figure 3.3: Schematic presentation of the MIFID setup for water analysis. A = Clean water reservoir or charcoal filter, B = Three-way ball valve (Whitey SS 43GXS4, Swagelok, SVAFAS Stavanger, Norway) (set to recirculate water in flask E in this picture), C = Gas flow restrictor/GC column, D = Peristaltic pump, E = Flask with the oil sample, F = Water bath, G = Split/splitless injector and H = FI detector. The blue arrows show the path for recirculation of the oil sample, while the black arrows show the direction of the carrier gas.

3.3.3.2 Individual oil analyses

Individual analyses of the 12 oil samples, listed in Table 3.5, were performed. The oil samples (approximately 10 mg) were spread out on a thick aluminum foil (1 cm x 1 cm) which was connected to a thin copper wire. For each analysis the foil with the oil sample was placed in the center of the flask, which was sealed by a cork stopper covered in aluminum foil (Figure 3.2 C). The minimum analysis time for each sample was 600 minutes.

Table 3.5: Samples for the oil in water analysis; origin and amount applied to a thick aluminum foil (before transport to the MIFID system)

Sample name	Weight (mg)	Analysis time (min)
Oseberg Blend	9.7	600
Troll B	10.2	600
Unspecified 1	10.1	600
Balder Blend	10.3	600
Unspecified 2	10.1	1170
Norne Blend	10.9	900
Falk	10.5	1200
SAGD	10.9	900
Peregrino	9.9	960
Mariner Maureen	10.4	960
Heidrun Tilje	10.0	960
Bressay	10.3	900

3.3.3.3 Oil dissolution speed test

A test was also done to look at how the concentration of water soluble oil components in a closed, recirculating MIFID system changed over time. The setup for this test was similar to the one described above, except that two flasks were connected to the interface, one with a volume of 0.60 liters and the other with a volume of 1.20 liters. These flasks were switched into the MIFID flow alternating. A schematic view of the setup can be seen in Figure 3.4. The 1.20 liters flask was filled with clean water only, while the 0.60 liters flask was filled with clean water and an oil sample (5.4 mg Oseberg Blend). The analysis was started with circulation of clean water to obtain a reference point (baseline at zero), before switching to circulation of the oil sample. After maximal signal was achieved a switch back to clean water was performed to get the signal back to approximately zero. This switch was done by

loosening the Teflon tube transporting the oil sample from the flask (flask E in Figure 3.4) from the two-way ball valve. The water in this tube was poured back to the flask, and some air was pumped into the system. When air passed the peristaltic pump and the second two-way ball valve, the pump was turned off. The Teflon tube was reconnected and both two-way ball valves were positioned to recirculating of the clean water. The peristaltic pump was turned on again, and recirculation of the clean water started. When the signal had returned to the reference point a switch back to the oil sample was performed to obtain a new measurement of the oil-exposed water. This switch was done in the same way as the one mentioned above, except that it was the Teflon tube (from flask F in Figure 3.4) transporting clean water that was loosened. These steps were repeated, and the total analysis time was 1570 minutes. The duration for circulating of the oil sample was held fairly constant, while the periods of circulating clean water were more variable.
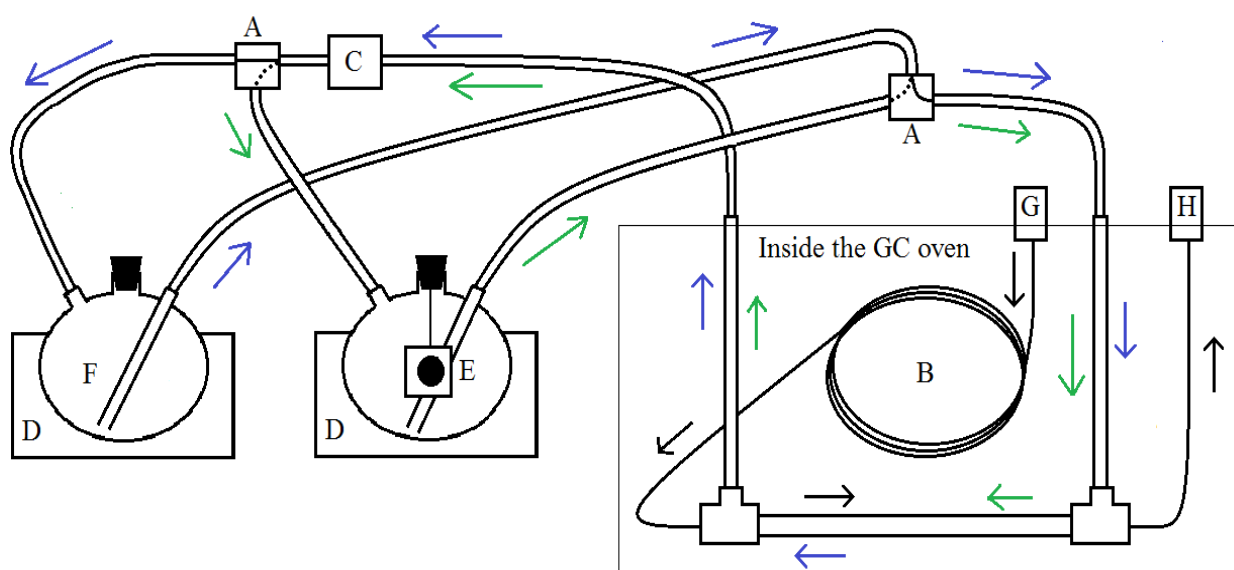
Figure 3.4: Schematic presentation of the two flask system for MIFID water analysis. A = Three-way ball valves (Whitey SS 43GXS4, Swagelok, SVAFAS Stavanger, Norway) (set to recirculation of flask F in this picture), B = Gas flow restrictor/GC column, C = Peristaltic pump, D = Water bath, E = Flask with the oil sample, F = Flask with clean water only, G = Split/splitless injector and H = FI detector. The green arrows follow the path for recirculation of the oil sample, the blue arrows follow the path for the circulation of clean water and the black arrows follow the direction for the carrier gas.

3.3.3.4 Cleaning of the interface between analyses

Between each analysis the system was cleaned by pumping clean air and clean water through the system. A conditioning was also performed by heating the interface (GC oven) to 60 °C and the detector to 320 °C when pumping air for approximately 20 minutes. As the system was getting dirtier after several runs, a conditioning up to 90 °C for the interface for 30 minutes was required.

3.3.4 Oil in air analysis

3.3.4.1 Experimental setup

The system for air analysis can be seen in Figure 3.5 and Figure 3.6. To ensure purity of the air pumped through the system a charcoal filter (Merck; granulated "pellets" 1-4 mm in diameter in a glass tube, 4x12 cm) is placed at the end of the air inlet tube. An air pump coupled to a rotameter pumps the air though the system at a velocity of approximately 80 L/min. The same interface used for the water analysis is used, except that the inlet is connected to a glass tube containing the oil sample (Figure 3.3 A). This glass tube (ca. 60 mL, 2.5 cm x 12.5 cm) is constructed with two side tubes connected to the air flow path, making it an air flow-through system. The gas supplies and the FI detector operated under the same conditions as for the water analysis.
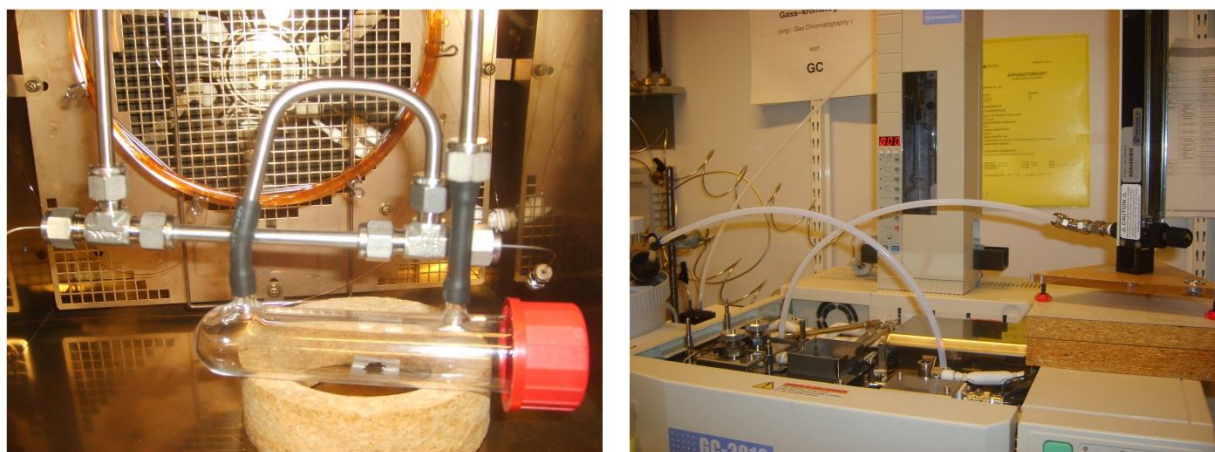
Figure 3.5: Overview of the MIFID system for air analysis. A) Inside the GC oven: The oil sample placed on aluminum foil is placed inside a glass tube, which is connected to the membrane interface. B) The top of the GC: Clean air is introduced to the system by the Teflon tube going from the charcoal filter to the left down on the right, and pumped out of the interface on the left side by a pump connected to the rotameter visible on the right in the picture.
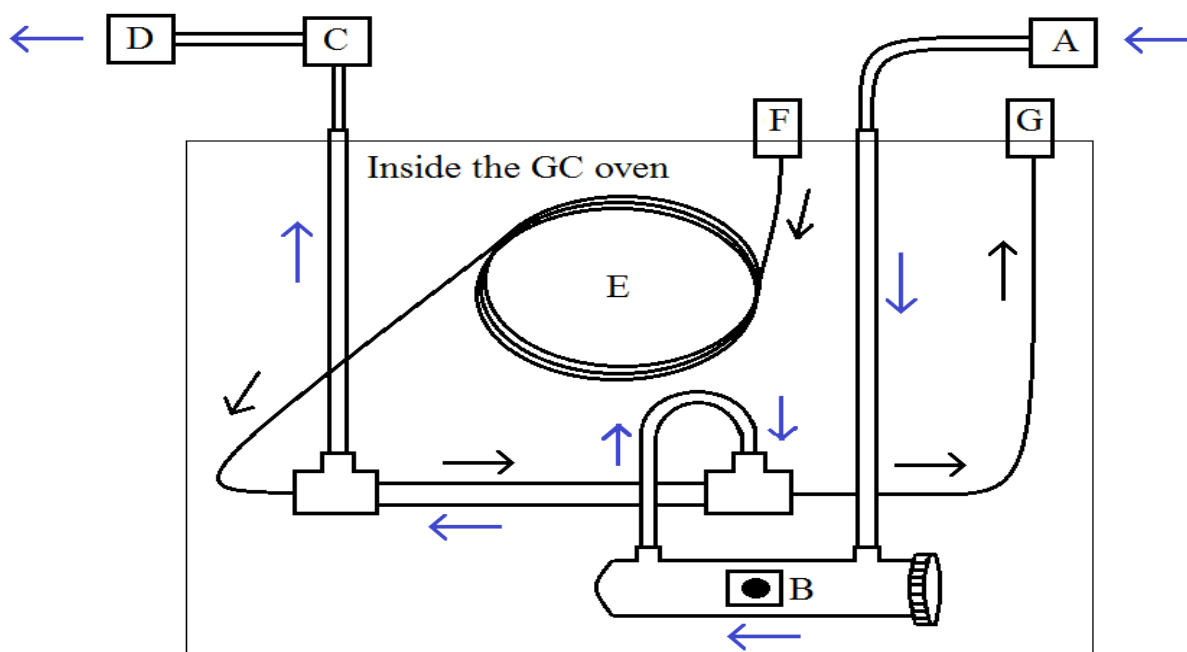
Figure 3.6: Schematic presentation of the setup for MIFID air analysis. A = Charcoal filter, B = Glass tube with the oil sample, C = Rotameter, D = Pump, E = Gas flow restrictor/GC column, F = Split/splitless injector and G = FI detector. The blue arrows follow the direction of the air flow, while the black arrows follow the direction of the carrier gas.

3.3.4.2 Individual oil analyses

As for the water analysis, the oil samples are spread out on a thick aluminum foil (1 cm x 1 cm). The foil with the oil sample is placed in the middle of the glass tube, which is sealed by a screw cap. A total of 12 oil samples were analyzes, listed in Table 3.6. The analysis time for the oil samples was from 90 minutes up to 180 minutes, depending on the character of the oil sample.

Table 3.6: Samples for the oil in air analysis; origin and amount applied to a thick aluminum foil (before transport to the MIFID system)

Sample name	Weight (mg)	Analysis time (min)
Oseberg Blend	10.1	180
Troll B	10.4	120
Unspecified 1	9.6	90
Balder Blend	10.4	120
Unspecified 2	10.0	90
Norne Blend	9.9	110
Falk	10.1	150
SAGD	9.6	180
Peregrino	10.6	150
Mariner Maureen	10.1	150
Heidrun Tilje	9.9	150
Bressay	10.4	150

3.3.4.3 Repeatability test

To test the repeatability of the MIFID system, a series of three parallels of Oseberg Blend (10.0 mg, 10.2 mg and 10.0 mg) were analyzed. Theses analyses were similar to the previous air analyses, except that the samples were prepared as close as possible to the system. This was done to ensure minimum weathering or contamination of the oil samples. Preparing of the samples too close to the inlet of the MIFID may contribute to signal interference.

3.3.4.4 Cleaning of the interface between analyses

Between each analysis clean air was pumped through the system, and a conditioning was performed by heating the interface to 80 °C and the detector to 320 °C for approximately 30 minutes.

3.4 MIMS petroleum analysis

3.4.1 Oil in air analysis

Individual analysis of 12 oil samples, listed in Table 3.7, was performed with air MIMS analysis. The setup for these analyses was similar to the air MIFID analyses (see Figure 3.6), except that a MS detector was used. The GC used for these experiments was a Thermo Scientific Trace GC Ultra (with split/splitless injector) installed with a TG-SQC column (30 m x 0.25 mm i.d., film: 0.25 µm). The mass spectrometer detector is a Thermo Scientific ITQ 1100 Ion Trap, controlled by Xcalibur, Version 2.1 and ITQ 1100, Version 2.1.0. A Jet-separator (SGE Scientific, MJSC/HP5890) was installed inside the GC oven between the membrane interface and the mass spectrometer transfer tube. The carrier gas used for the MIMS analyses was helium and not hydrogen as used for the MIFID analyses.

Table 3.7: Samples for the oil in air analysis; origin and amount applied to a thick aluminum foil (before transport to the MIMS system)

Sample name	Weight (mg)	Analysis time (min)
Oseberg Blend	10.0	22
Troll B	10.0	35
Unspecified 1	13.5	26
Balder Blend	10.0	24
Unspecified 2	10.0	41
Norne Blend	10.0	26
Falk	14.0	30
SAGD	9.0	27
Peregrino	13.5	28
Mariner Maureen	10.0	52
Heidrun Tilje	10.0	29
Bressay	15.6	50

3.4.2 Oil in water analysis

Two oils (Oseberg Blend and SAGD) were analyzed by water MIMS. The setup for these analyses was similar to the water MIFID analyses, see Figure 3.3, and the same instruments as for the air MIMS analyses were used. Analyses of a toluene solution (3% toluene in methanol) and n-heptane were also performed by water MIMS.

Samples, amounts and analysis times are given in Table 3.8.

Table 3.8: Samples for the oil in water analysis; origin and amount applied to a thick aluminum foil (before transport to the MIMS system)

Sample	Amount	Analysis time (min)
Oseberg Blend 1	8.4 mg	200
Oseberg Blend 2	8.5 mg	200
SAGD	11.7 mg	200
Toluene (3 %)	1.3 μL	120
n-Heptane	0.35 μL	110
n-Heptane	1.0 μL	40

4. Results and discussion

4.1 Test analyses and optimization of the MIFID-system

4.1.1 Test analyses

During test analyses toluene and n-heptane in solutions with methanol were analyzed. The reason for choosing methanol as a solvent is good to fair solubility of the chosen test analytes, as well as the polar character of methanol making it unfavorable for absorption into the membrane. Analyses of methanol only were performed to determine how much methanol would contribute to the total signal of the given solutions. FID signal profiles for methanol are given in Figure 4.1.
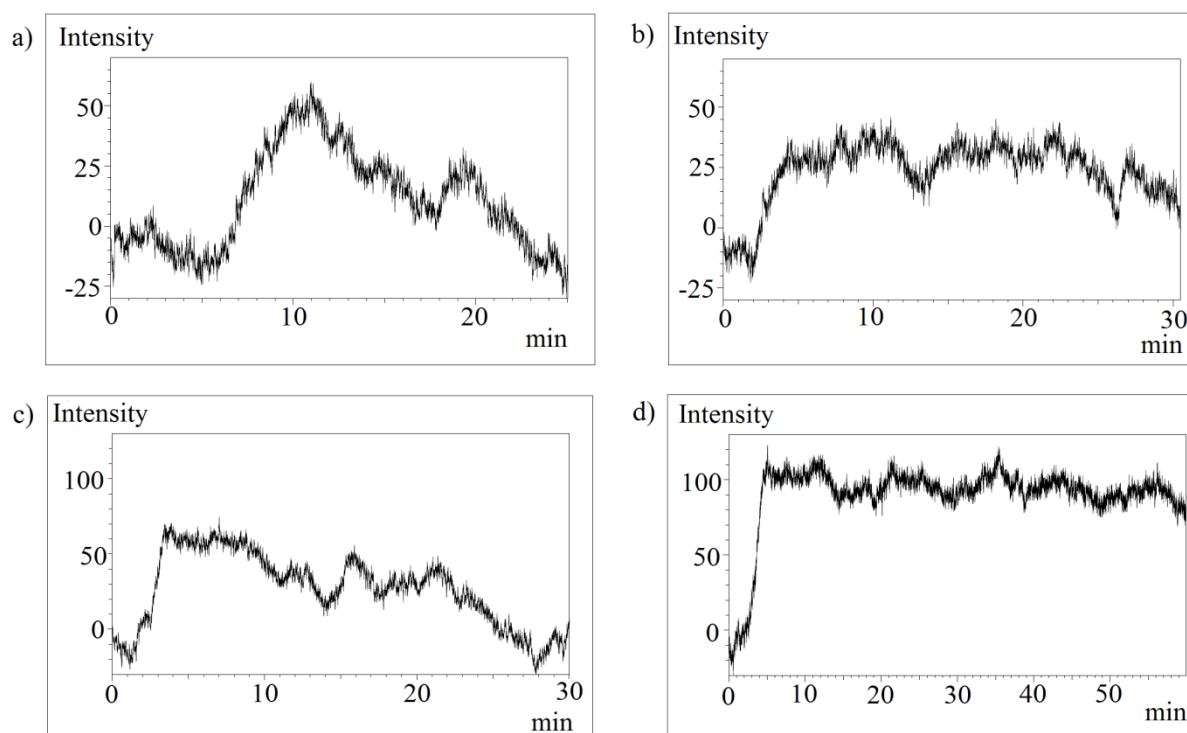
Figure 4.1: Preliminary tests: MIFID analyses of methanol in water (1.25 L) (non-optimized MIFID). a) and b) results from injection of 1.0 µL pure methanol after 5 and 2 minutes, respectively, c) and d) results from injections of 2.0 µL pure methanol after 2 minutes

 As can be seen from Figure 4.1 signal from injection of methanol is noticeable. However, the signal intensities measured for methanol was far lower than signals obtained with toluene:methanol and lower than n-heptane:methanol solutions (0.1 ppm). Based on these observations signal from methanol are considered as an acceptable background signal that could be controlled.

Preparation of petroleum samples in solution with methanol was attempted. Dissolution of the petroleum samples was supposed to be carried out by ultra sound. However, satisfying dissolution of the oil samples was not achieved, and application of an oil sample film on thick aluminum foil was chosen as a better method.

The toluene and n-heptane test analyses performed was an attempt to obtain some semi quantitative information from injections of known concentrations of the given samples. However, analyses of n-heptane proved to be very difficult. FID signal profiles for n-heptane analyses are given in appendix C.1. These profiles shows very uneven and strange behavior with an unexpectedly low response (as compared to similar concentrations of toluene) for the analyses of n-heptane, and thus no useful information was obtained.

4.1.2 Optimization

Some of the MIFID system parameters were optimized using toluene or n-heptane in water or air as a test analyte. Data for the optimization are summarized in appendix F.1, while FID signal profiles can be found in appendix C.2.

The water flow through the system was tested at several different velocities, from 60 up to 250 mL/min. The response time decreased with increasing water flow, while the response increased. Based on these factors, a water flow of 250 mL/min was used in the experiments.

The temperature of the water bath and the interface was tested at 30, 40, 50 and 60 °C. The response increased with increasing temperature, but an increase in temperature also resulted in increased noise. Considering both response and noise, a temperature of 40 °C was selected.

Concerning MI-hydrogen flow, three different hydrogen flows were tested; 5.0 mL/min, 10.1 mL/min and 20.1 mL/min, respectively. By increasing the column flow from 5.0 mL/min to 10.1 mL/min the response time was more than one and a half minutes shorter, while the response increased with approximately six percent. Increasing the column flow from 10.1 mL/min to 20.1 mL/min contributed to a slight decrease in the response time and also a slight decrease in the response. A column flow of 10.1 mL/min was selected for the experiments.

Optimization of the detector was done by testing for different gas flows for the makeup gas, the hydrogen gas and the air. A doubling of the response was observed with makeup gas, in comparison to analyses without makeup gas. To reduce the testing time, testing of the different gas velocities was done with air MIFID samples. Hydrogen flows of 20, 30 and 40 mL/min, respectively, were tested. The highest response was achieved at 30 mL/min, and this flow was selected for the experiments. Air flows were tested at 350 mL/min and 400 mL/min. 400 mL/min was chosen for the air flow due to higher response compared to 350 mL/min. Makeup gas flows of 20, 30, 40 and 50 mL/min were tested. Velocities up to 40 mL/min were first investigated by analyzing toluene samples, and resulted in increasing response with increasing velocity. Afterwards the response of toluene and n-heptane was tested at 40 mL/min and 50 mL/min. For n-heptane the response increased with increasing makeup gas flow, while it decreased for toluene. Based on these experiments a makeup gas flow of 40 mL/min was selected.

Compared to the settings for the test analyses, the parameters that were changed after the optimization were the hydrogen flow through the membrane interface and the makeup gas flow. The different setting before and after optimization are summarized in Table 4.1. During the optimization unnecessary length of the tubing system was removed, reducing the overall water volume from 1.25 L to 1.20 L, as well as the surface area for potential adsorption of analytes.

Table 4.1: Parameter setting before and after optimization of the MIFID-system

Parameter	Setting before optimization	Setting after optimization
Water bath temperature (°C)	40	40
Water flow (mL/min)	250	250
GC settings:		
Column temperature (°C)	40	40
Injector temperature (°C)	40	40
Detector temperature (°C)	250	250
Column flow (H_2) (mL/min)	5.0	10.1
H_2 flow (mL/min)	30	30
Makeup flow (mL/min)	30	40
Air flow (mL/min)	350	350

FID signal profiles for toluene before and after optimization are given in Figure 4.2 and Figure 4.3, respectively.
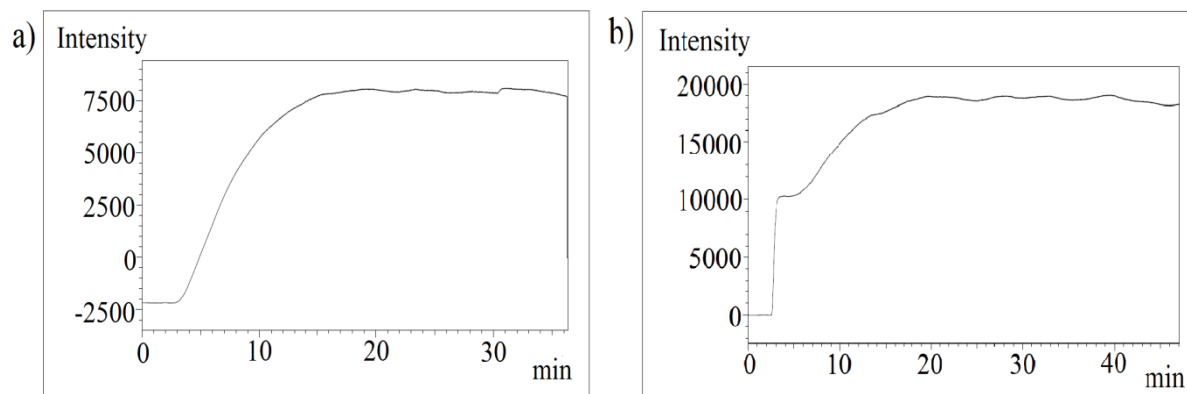
Figure 4.2: Preliminary tests: MIFID analyses of toluene in water (1.25 L) (non-optimized MIFID). a) Result from injection of 0.5 µL toluene (10 % toluene in methanol) after 2 minutes. b) Result from injection of 1.0 µL toluene (10 % toluene in methanol) after 2 minutes.
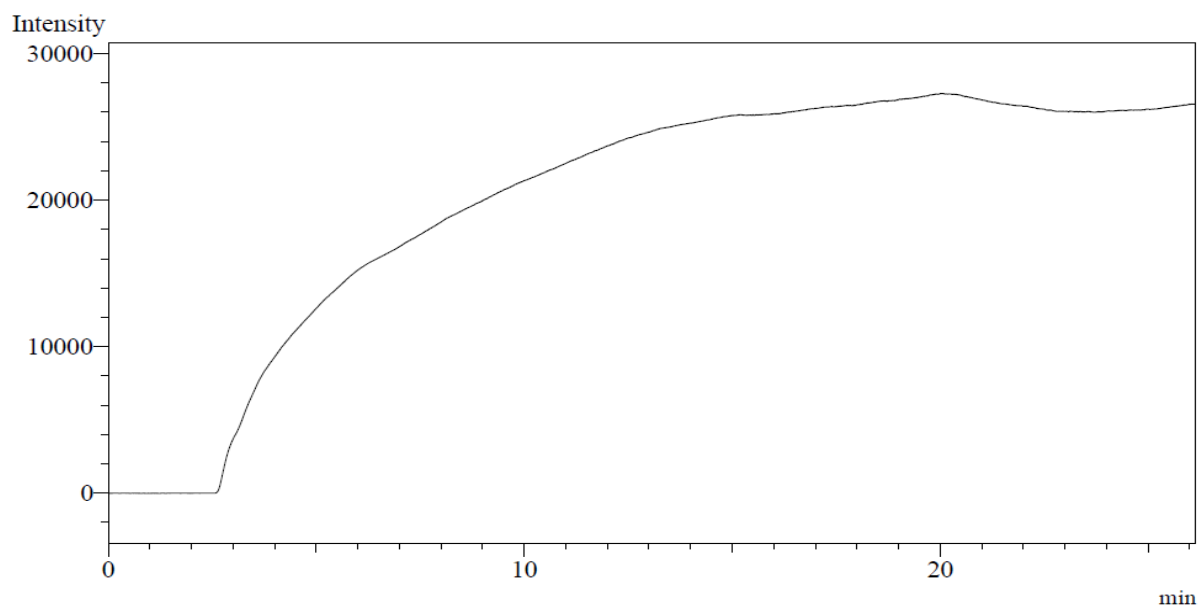
Figure 4.3: Preliminary test: MIFID analysis of toluene in water (1.20 L) (optimized MIFID). Result from injection of 1.0 µL toluene (10 % toluene in methanol) after 2 minutes.

47

From the FID signal profiles for toluene it can be concluded that optimization of the system leads to an increase in signal intensities, and hence better sensitivity. These results indicate that optimization of different parameters before an analysis can improve the results, and thus may be worth the use of time.

These results have some uncertainties due to low numbers of parallels, especially for the tests performed with water MIFID where only one analysis of each setting was carried out. More parallels should be performed for more reliable results. However, an improvement with respect to the signal was obtained as a result of successful optimization.

4.2 Oil in water analysis using MIFID

4.2.1 Individual oil analyses

Presented below are two examples of FID signal profiles from the oil in water analysis by MIFID. Figure 4.4 shows a relatively light oil (Oseberg Blend), while Figure 4.5 shows an oil of a more heavy character (SAGD). The FID signal profiles for the remaining oil in water analysis are summarized in Figure 4.6 and full size versions are presented in appendix C.3.
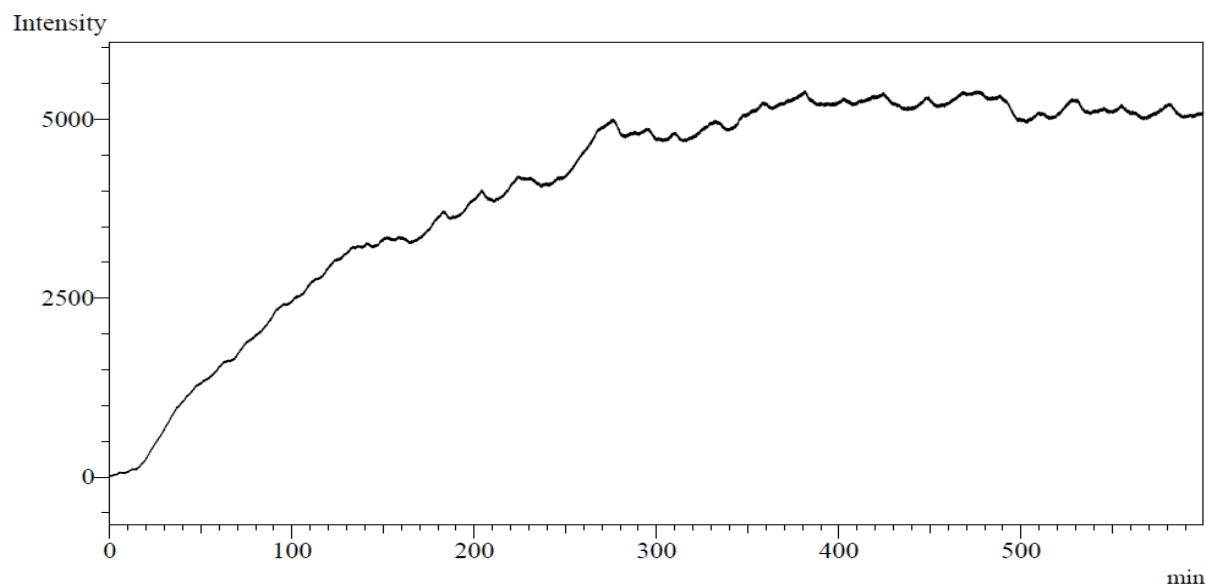
Figure 4.4: Oil in water MIFID analysis: Oseberg Blend (9.7 mg) in 1.20 L of recirculating water
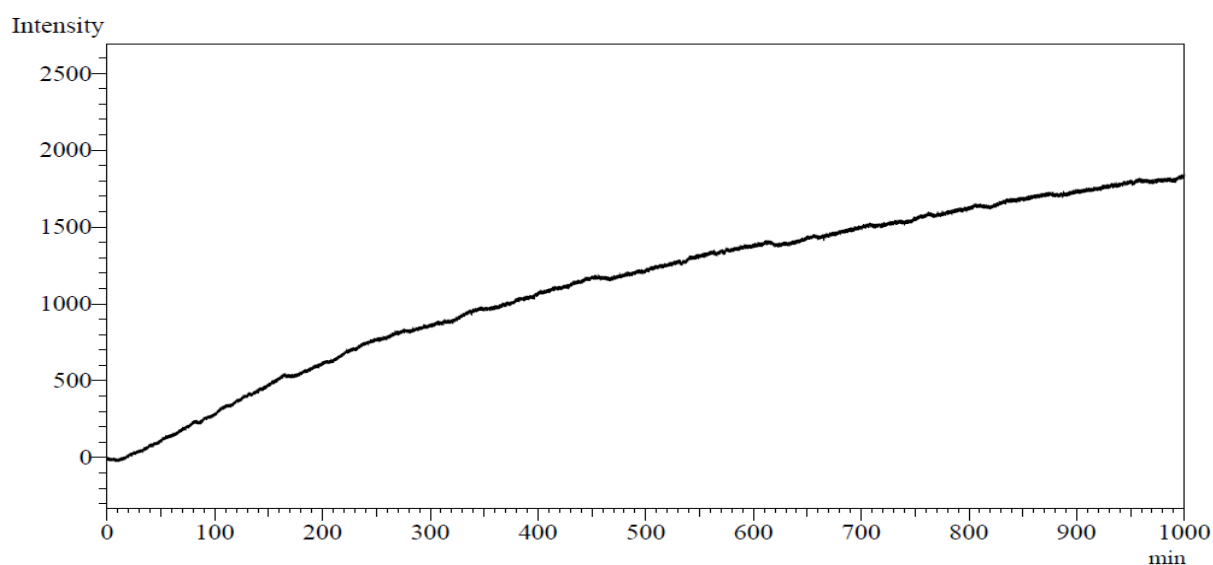
Figure 4.5: Oil in water MIFID analysis: SAGD (10.9 mg) in 1.20 L of recirculating water
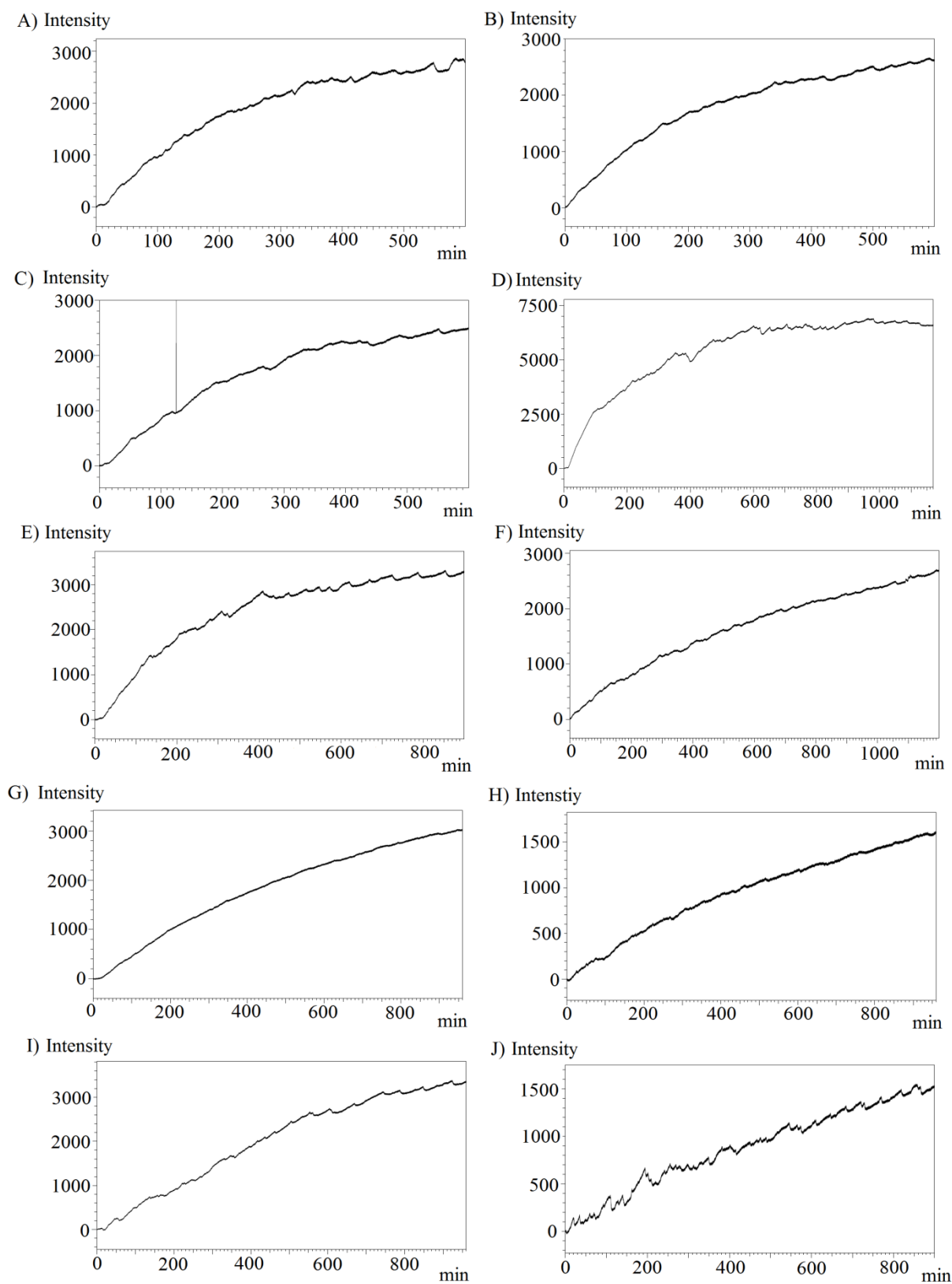
Figure 4.6: Oil in water MIFID analyses. A) Troll B, B) Unspecified 1, C) Balder Blend, D) Unspecified 2, E) Norne Blend, F) Falk Blend, G) Peregrino, H) Mariner Maureen, I) Heidrun Tilje and J) Bressay

50

As can be seen from these FID signal profiles, measurement of oil in water by MIFID is not a satisfactory method. The analysis times required to obtain information are very long. This is especially the situation for the heaviest oils; the signal is still increasing at the end of the analysis, even after 1200 minutes. For the lighter oils the signal intensities flattens after some time, enabling measurement of maximum response and response times.

The signal intensities are rater low and analytical noise becomes visible, e.g. signal-to-noise ratios (in Figure 4.4 and Figure 4.5) are estimated to approximately 10 and 40 for Oseberg Blend and SAGD, respectively. The signal-to-noise ratio is better for SAGD, even though this analysis has lower signal compared to the Oseberg Blend analysis. For the SAGD analysis mostly high frequency noise is observed, while low frequency noise with peak heights for several minutes is more prominent for the Oseberg Blend analysis. As can be seen from Figure 4.6 the degree of noise varies to a great extent between the different analyses, for unknown reasons.

Table 4.2 gives the different signal intensities after a fixed 600 minutes and at the end of the analyses (varying times) for the different oils and response times for two of the lighters oils. For the heaviest oils it is not possible to calculate the response time, since the signal is still increasing at the end of the analyses. This is also the situation for most of the lighter oils. Satisfying indications of achievement of maximum signal intensities are only observed for two oil samples (Oseberg Blend and Unspecified 2), and thus response times are calculated for these analyses only.

Table 4.2: Signal intensities and response times for the oil in water MIFID analyses

	Signal intensity after given time		Response time [c] (min)
	Time [a] (min)	Signal intensity [b] (μV)	
Oseberg Blend	600	4950	238.5
Troll B	600	2800	
Unspecified 1	600	2550	
Balder Blend	600	2350	
Unspecified 2	600	6250	518.0
	1170	6550	
Norne Blend	600	2950	
	900	3250	
Falk	600	1700	
	1200	2600	
SAGD	600	1400	
	900	1850	
Peregrino	600	2300	
	960	3000	
Mariner Maureen	600	1200	
	960	1600	
Heidrun Tilje	600	2750	
	960	3350	
Bressay	600	1150	
	900	1550	

[a] Duration time from start of the data acquisition, not from insertion of the sample.

[b] Signal intensities after 600 minutes are presented for all oil samples, and also at the end for analyses with analysis times exceeding 600 minutes.

[c] Time used for the signal to increase from 10 to 90 % of the maximum signal.

The fact that the signal is slowly increasing over long time periods, results from a slow dissolution of water soluble oil components from the oil samples, or from a slow transfer of the dissolved oil compounds from the flask to (and through) the membrane. Although inert materials were chosen for tubing and interface (Teflon, stainless steel and Viton), adsorption to tubing and interface parts could slow down oil component transfer to the membrane. Also, different compounds use different amounts of time to diffuse through the membrane.

To obtain some more information about the dissolution patterns for oil samples, the analysis in the next section was performed.

4.2.2 Attempt of oil dissolution speed test by MIFID

FID signal profile for the dissolution speed test is given in Figure 4.7. From this profile the maximum intensity is reached after approximately 1160 minutes with a value about 20 000 µV. However, during several hours no FID signal was recorded, and the true maximum intensity may be in this interval, which lasted 670 minutes.
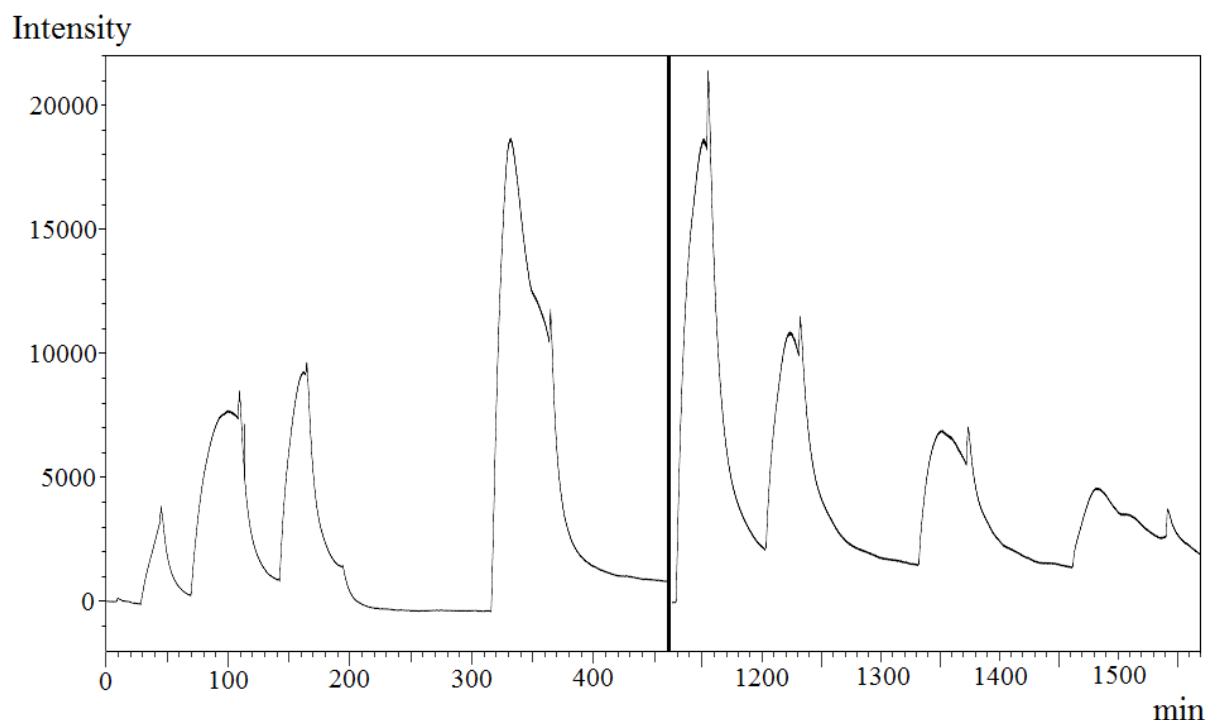
Figure 4.7: Alternating analysis of oil in water and pure water by MIFID. A sample of Oseberg (5.4 mg) was spread out on a thick aluminum foil which was placed in the center of a flask with 0.60 L of clean water. During the MIFID analyses this flask was connected to the MIFID alternating with another flask containing 1.20 L of clean water. This figure is a combination of two sequential recording periods during the analysis. The period from approximately 460 minutes to 1130 minutes of the analysis was not recorded.

The FID signal profile indicates an exponential decrease after the maximum value is reached. Why the signal has such a rapid decrease at the end is not sure. However, several different processes contribute. The long duration of the experiment may contribute to depletion of a significant part of the MI detectable compounds, and thus a decreasing signal at the detector,

although only during a minor part of this time chemicals are actually removed by the membrane interface. Another cause for the rapid decrease may be photo oxidation. The two recording periods are carried out at daytime, while the period not recorded was during nighttime. At the second recording period a part of the oil sample may thus have been affected by photo oxidation, as no protection against daylight was used. The photo oxidized products may be less favorable for MI-detection compared to the original compounds (e.g. due to a more polar character), and thus a lower signal is observed. As the time has elapsed during the analysis, the importance of microbial decomposition may also increase. Microbial decomposition may result in reduction of the MI-detectable compounds for the same reason as photo oxidation. By adding a suitable biocide and protecting the flask containing the oil sample from light exposure these effects may be reduced.

Compared to the "normal" oil in water analysis of Oseberg Blend, higher signal intensities are achieved in this analysis. The water volume and amount of oil used are different in the two analyses, but the relationships between these two factors are relatively similar, 8.1 mg/L and 9.0 mg/L for the dissolution speed test and the "normal" oil in water analysis, respectively. Longer saturation periods with no loss of substance through the membrane resulted in higher concentration of detectable chemicals in the short analysis periods.

4.3 Oil in air analysis using MIFID

4.3.1 Individual oil analyses

Presented below are two examples of FID signal profiles from the oil in air analysis by MIFID. Figure 4.8 shows a relatively light oil (Oseberg Blend), while Figure 4.9 shows an oil of a more heavy character (SAGD). The FID signal profiles for the remaining oil in air analysis are summarized in Figure 4.10 and full size versions are presented in appendix C.4.
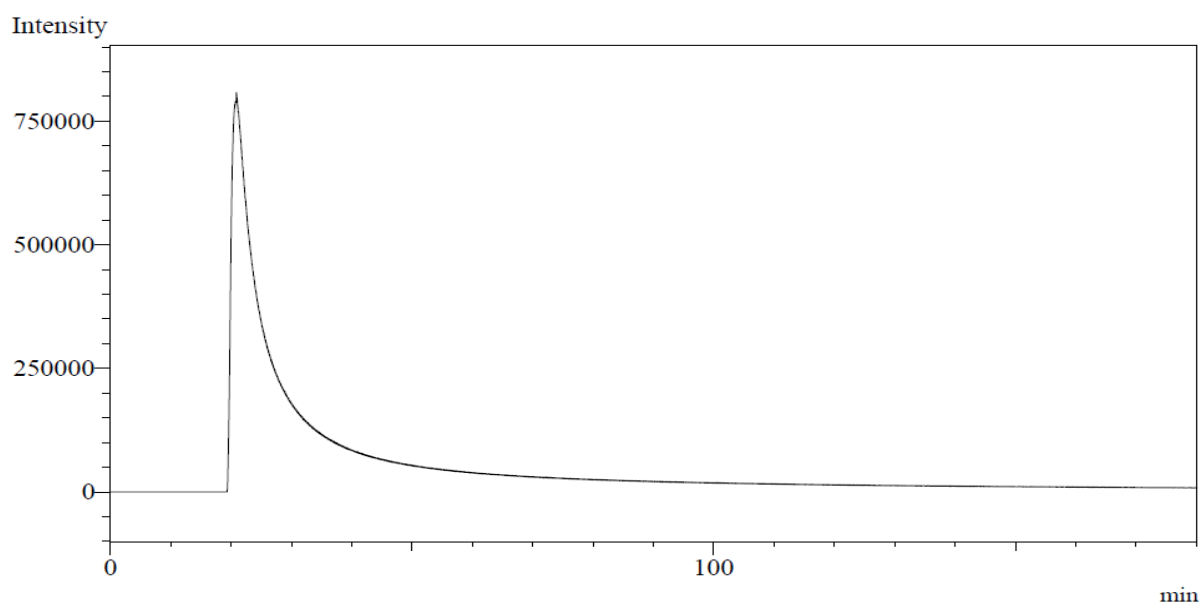
Figure 4.8: Oil in air MIFID analysis: Oseberg Blend (10.1 mg)
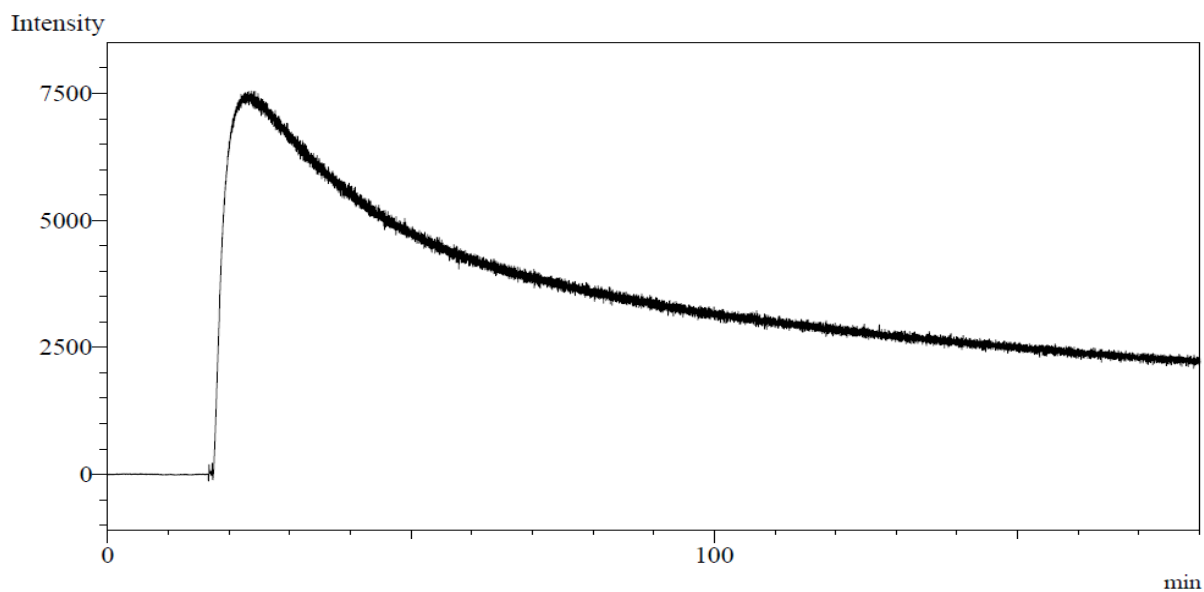
Figure 4.9: Oil in air MIFID analysis: SAGD (9.6 mg)
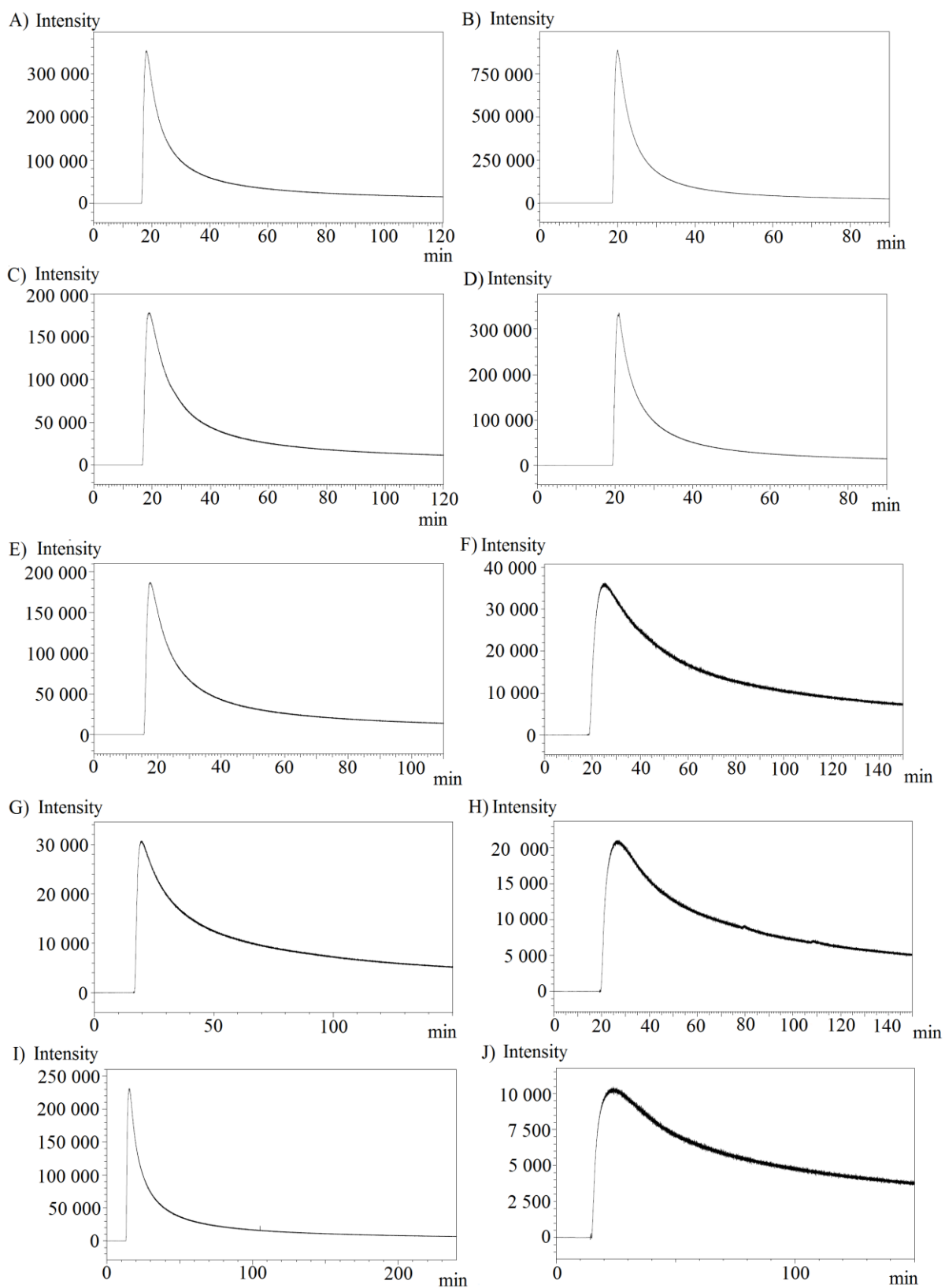
Figure 4.10: Oil in air MIFID analyses. A) Troll B, B) Unspecified 1, C) Balder Blend, D) Unspecified 2, E) Norne Blend, F) Falk Blend, G) Peregrino, H) Mariner Maureen, I) Heidrun Tilje and J) Bressay

Analysis of oil in air by MIFID is a much better analysis technique compared to the MIFID oil in water analysis. Response times, maximum signal intensities and also half-times can be obtained after reasonable analysis times. The maximum signal intensities, response times and half-times are given in Table 4.3.

Table 4.3: Maximum signal intensities, response times and half-times for the oil in air MIFID analyses

	Max. Signal Intensity (µV)	Response time [a] (min)	Half-time [b] (min)
Oseberg Blend	808 000	1.0	3.4
Troll B	354 000	1.1	5.0
Unspecified 1	888 000	0.7	3.4
Balder Blend	179 000	1.4	7.7
Unspecified 2	336 000	0.8	4.0
Norne Blend	188 000	0.8	7.2
Falk	36 500	3.7	30.0
SAGD	7 550	2.7	49.5
Peregrino	30 700	1.4	19.5
Mariner Maureen	21 100	3.4	36.0
Heidrun Tilje	231 000	0.9	7.2
Bressay	10 500	4.5	61.0

[a] Time used for the signal to increase from 10 to 90 % of the maximum signal

[b] Time used for the signal to decrease from the maximum signal to 50 % of the maximum signal

As can be seen from the FID signal profiles the rise and fall times for the lighter oils are relatively short. Due to high amount of volatile compounds, large amounts of the samples will evaporate in the beginning of the analyses and be lost, due to the non-recirculating arrangement of the oil in air analyses.

For the more heavy oils the maximum signal intensities are reached after short times, but the rates of decrease are much lower compared to the lighter oils. The signal peaks are not as steep and high as for the lighter oils, and thus the lower intensities are more visible due to scale on the y-axis. E.g. the signal intensity at the end of the analysis for Oseberg Blend, one of lightest oils, is approximately 12 000 µV. However, this value contributes to approximately

1.50 % of the maximum signal intensity only, compared to the remaining 34 % at the end for the SAGD analysis. This feature is described in more detail later.

The signal for the SAGD analysis is the lowest of all analyses. The SAGD sample is a heavy crude oil produced from tar sand (bitumen), which is highly viscous. This oil sample has also been through a heating process for removal of the lightest compounds, resulting in small amounts of volatile compounds, and thus fewer compounds with favorable properties for transfer through the membrane.

To compare how the signal profiles of the different oils behave after the maximum signal intensities are passed, signal intensities as a function of analysis time for each oil sample are converted to percentages of the maximum signal intensity for the respective oil (Figure 4.11). This figure indicates a division of the different oils in two groups, with similar decrement patterns. The lines (Bressay, SAGD, Mariner Maureen, Falk and Peregrino) in the upper part of the graph represent "the heavy oils", while the lines (Norne Blend, Balder Blend, Heidrun Tilje, Troll B, Unspecified 2, Unspecified 1 and Oseberg Blend) in the lower part represent "the lighter oils".
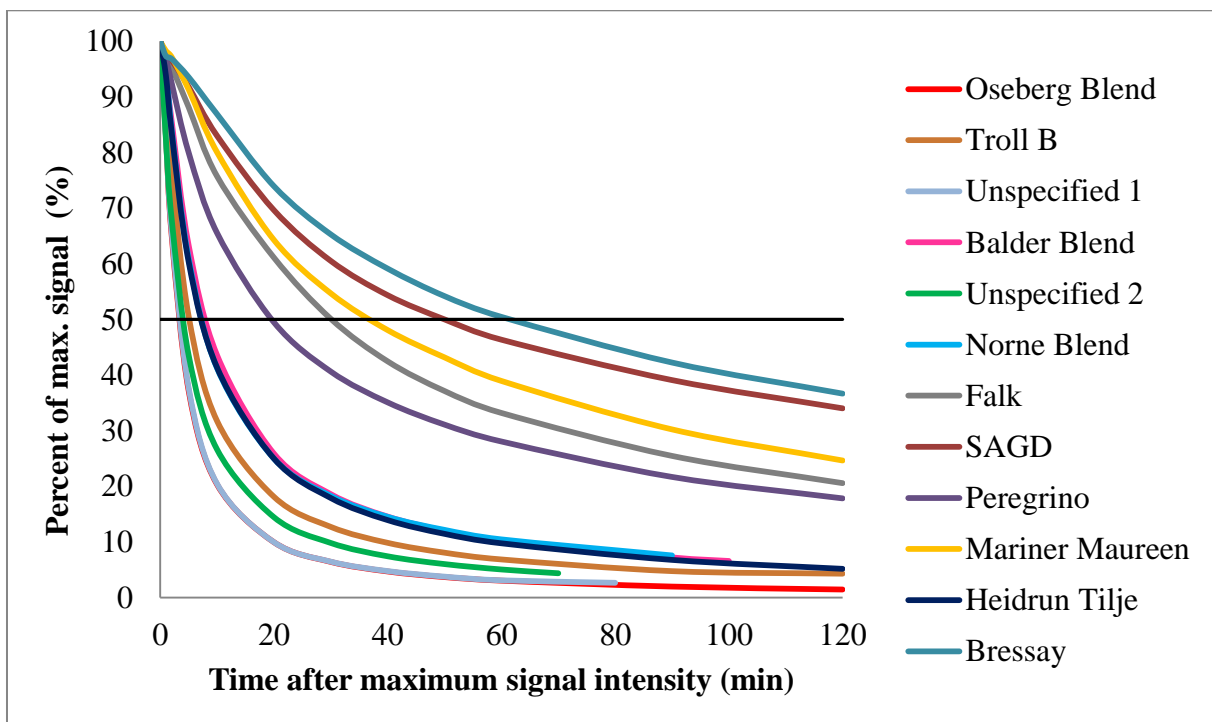
Figure 4.11: Percentual decrement from the maximum signal. Half-times are indicated by the 50 % line. This presentation is based on selected normalized experimental values (converted to percentages of the maximum values), which can be found in appendix F.2. The lines represent a smoothed interpolation of these data points.

59

4.3.2 Repeatability test

Three parallels of Oseberg Blend were analyzed to test the repeatability of the MIFID system. FID signal profiles for these analyses are given in appendix C.5.

As can be seen from Table 4.4 a relative standard deviation (RSD) of 16 % is obtained with calculations based on the maximum signal intensity values. A RSD of 6 % is obtained using values for the area, while a RSD of 8 % is obtained for the response time. The response times have some small variation due to the steep curve calculations are based on. Since the response times are relatively short for Oseberg Blend, small variation will contribute to uncertainties in the repeatability with respect to the response times. Since the values for maximum signal intensities are based on a steep curve, more variations is expected than for values for the area under the whole curve, thus making the last option a more reliable source. A RSD of 6 % still indicates some variations in the analyses, and thus some uncertainties in respect to the repeatability.

To obtain a more reliable result, a larger number of parallels should be analyzed.

Table 4.4: Repeatability test for the MIFID system. Three parallels of Oseberg Blend in air.

	Max. Signal Intensity (µV)	Area	Response time (min)
Oseberg Blend 1	874 000	449 330 000	0.8
Oseberg Blend 2	1 191 000	502 960 000	0.7
Oseberg Blend 3	979 000	492 260 000	0.8
Mean value	1 015 000	481 517 000	0.77
Standard deviation	162 000	28 383 000	0.06
Relative standard deviation (%)	16	6	8

4.4 Oil in air analysis using MIMS

Total ion current (TIC) profiles for the air MIMS analyses, except for Oseberg Blend and SAGD (presented in more detail later), are given in Figure 4.12 and full size versions are presented in appendix D.1.

As for the air MIFID analyses, the air MIMS analyses have relatively short response times. Most of the analyses are not analyzed for a sufficiently long time to enable calculations of half-times. However, for those where these calculations are possible, half-times up to 10 minutes are recorded. Total analysis time for the lighter oils can thus be less than 15 minutes.

From the TIC profiles it can be seen that for the heaviest oils the decrease after maximum signal is relatively slow, even slower than for the air MIFID analyses.

Maximum signal intensities, response times and half-times for the air MIMS analyses are given in Table 4.5.

Table 4.5: Maximum signal intensities, response times and half-times for the oil in air MIMS analyses

	Max. Signal Intensity (a.u. [a])	Response time [b] (min)	Half-time [c] (min)
Oseberg Blend	593 000	1.3	7.6
Troll B	669 000	1.4	10.2
Unspecified 1	1 584 000	1.0	5.6
Balder Blend	348 000	1.7	
Unspecified 2	1 017 000	1.1	6.7
Norne Blend	666 000	1.4	
Falk	168 000	3.4	
SAGD	44 400	5.0	
Peregrino	52 900	3.4	
Mariner Maureen	58 300	5.7	
Heidrun Tilje	581 000	1.8	
Bressay	40 200	7.7	

[a] a.u. = accidental units (referred as Relative Abundance in the software)

[b] Time used for the signal to increase from 10 to 90 % of the maximum signal.

[c] Time used for the signal to decrease from the maximum signal to 50 % of the maximum signal. Only four of the oil samples have been run sufficient to enable these calculations.
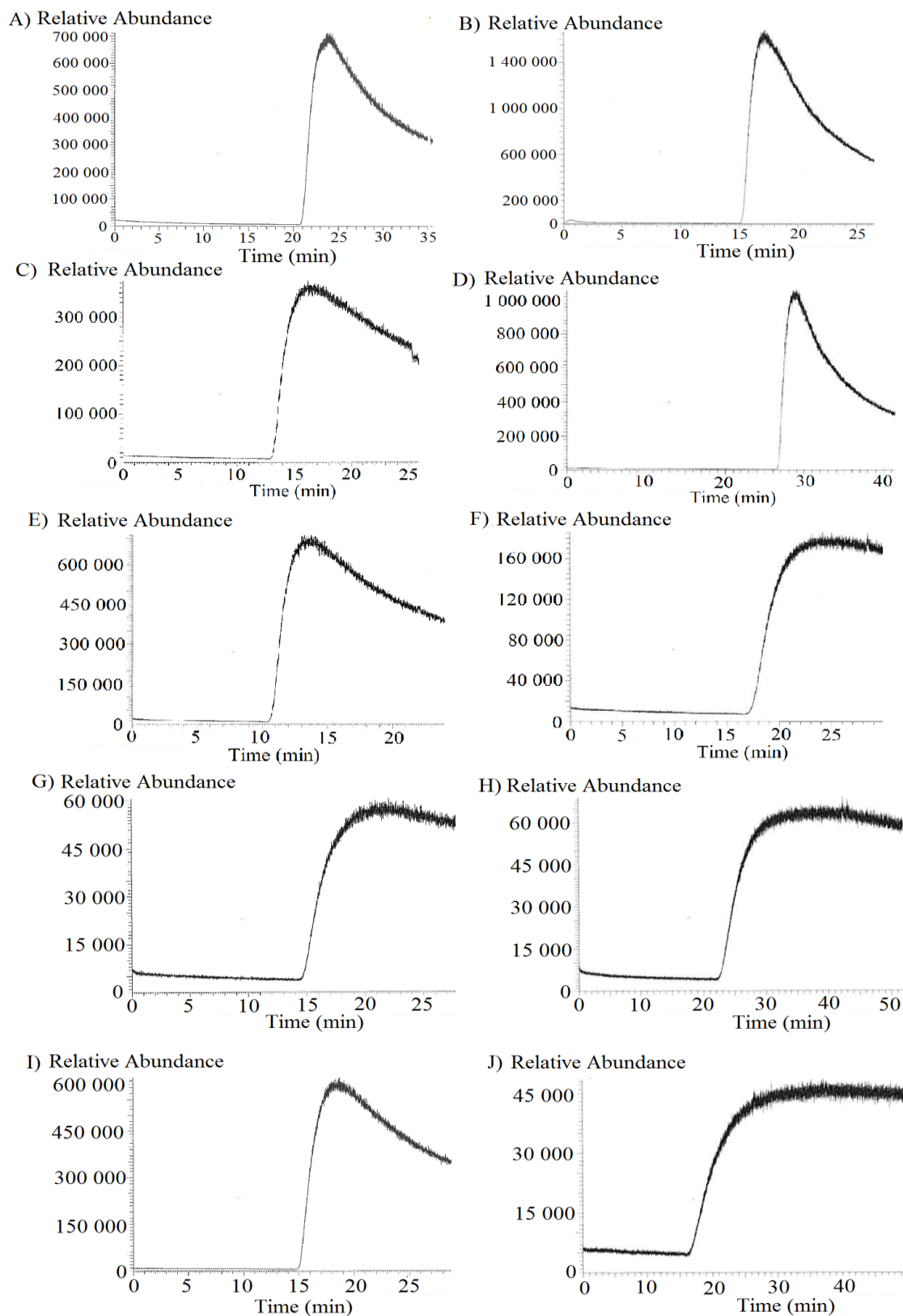
Figure 4.12: Oil in air MIMS analyses. A) Troll B, B) Unspecified 1, C) Balder Blend, D) Unspecified 2, E) Norne Blend, F) Falk Blend, G) Peregrino, H) Mariner Maureen, I) Heidrun Tilje and J) Bressay

TIC signal profile for the Oseberg Blend air analysis is given in Figure 4.13. Mass spectrum from the pre-exposure baseline is given in Figure 4.14. Backgrounds subtracted mass spectra from the beginning of the oil exposure experiment, from the TIC maximum and from the end of the oil exposure experiment are given in Figure 4.15. Uncorrected mass spectra for similar time intervals are given in appendix E.1.
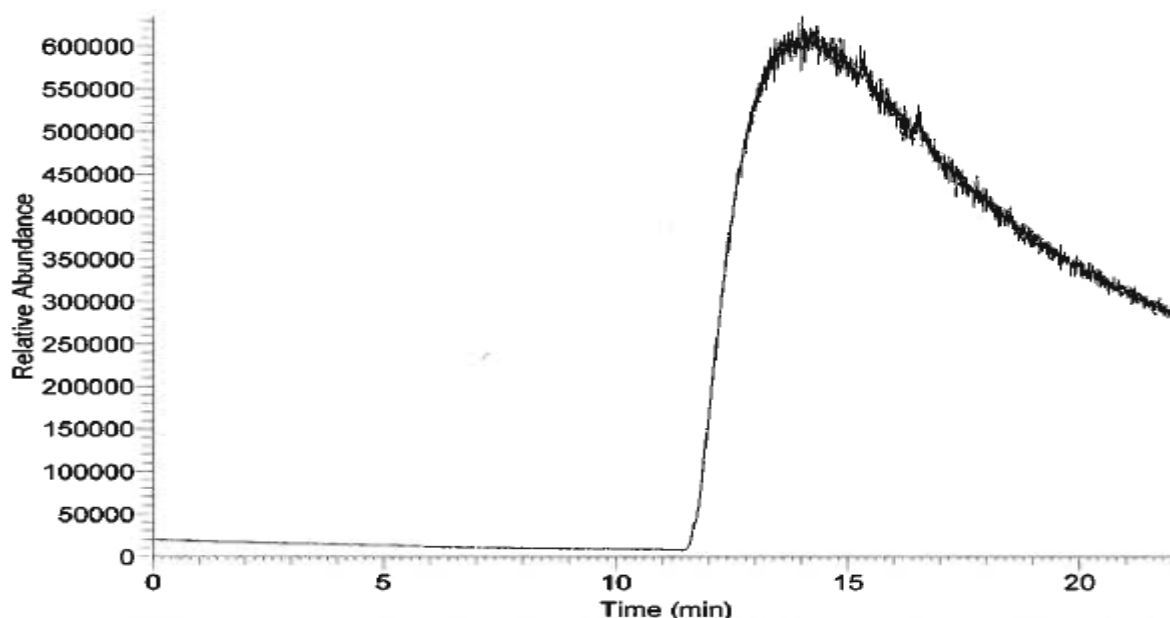
Figure 4.13: Oil in air MIMS analysis: Oseberg Blend (10.0 mg)
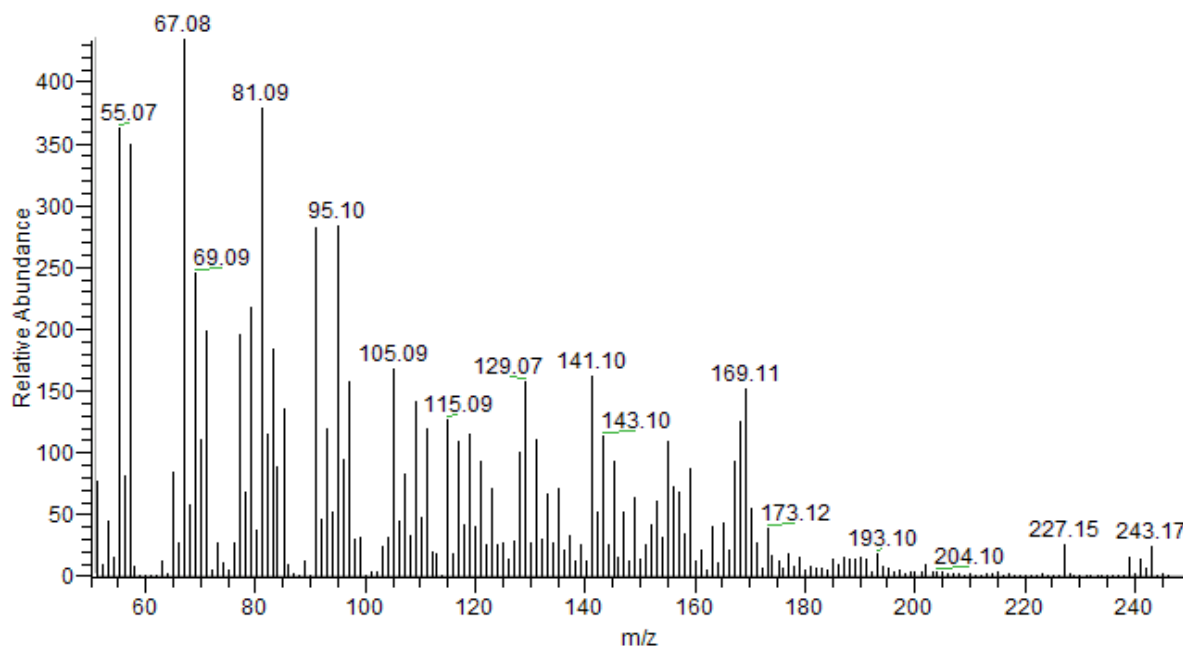
Figure 4.14: System blank: mass spectrum for the Oseberg Blend air analysis, from pre-exposure the baseline (9.66-11.23 min)
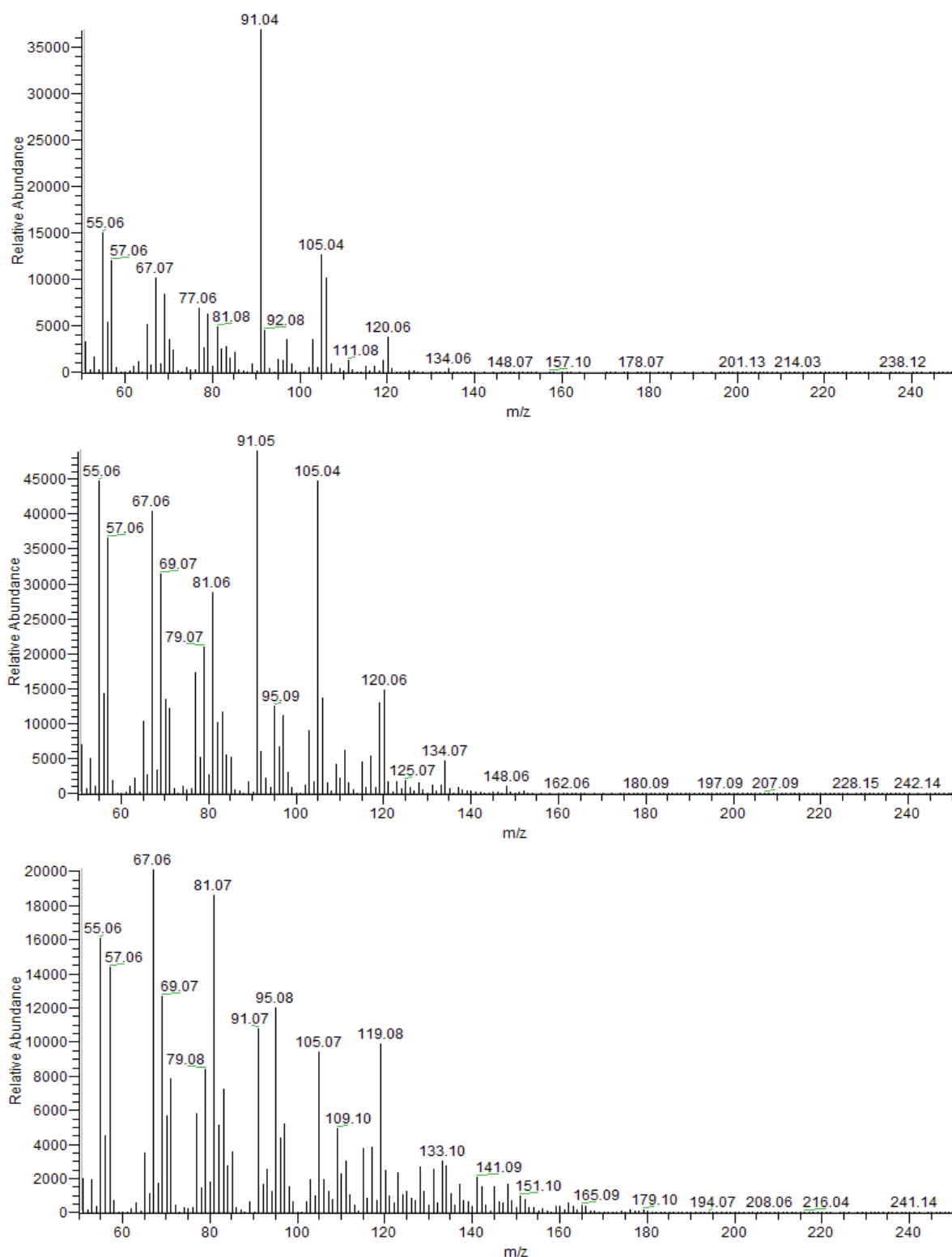
Figure 4.15: Background subtracted spectra for the Oseberg Blend air analysis. A) From the beginning of the oil exposure experiment (11.80-12.35 min). B) From the TIC maximum (13.28-14.61 min). C) From the end of the oil exposure experiment (21.22-22.13 min). For all mass spectra the background at 9.61-11.27 min was subtracted.

From the mass spectra it is shown that *m/z* 91 is the most abundant peak in the beginning of the analysis. Peaks for the masses of 65, 91 and 92 indicates the presence of toluene, see mass spectra for the toluene in water analysis in appendix E.5.

Further along the analysis an increase of especially *m/z* 55, 67 and 105 is observed, and at the end of the analysis *m/z* 67 is the largest peak. A mass of 67 may indicates presence of cyclopentene or pentadiene fragments indicating the presence of naphthene structures (alicydics). Since Oseberg Blend reaches its maximum TIC within the analysis time, the intensities of the peaks decrease at the end of the analysis. The intensity of *m/z* 91 is approximately one quarter of the value in the middle of the analysis (at the peak top) only, while *m/z* 67 is about 50 % of the maximum value at the end.

The presences of even numbered mass numbers are noteworthy. Signals for *m/z* 92, 106, 120, 134 and 148 indicates the presence of C_1-C_5-polyalkyl substituted benzenes.

A general trend for all air MIMS analyses is an increase of the largest m/z-values at the end of the analysis. These mass numbers are from the larger molecules, which are less volatile compared to the smaller compounds with mass numbers in the lower part of the mass spectra. The more volatile samples are depleted over time.

For all MIMS analyses presented it should be noted that peaks at the mass numbers of 167-169 arises from the system (presumably from the silicone tubing).

TIC signal profile for the SAGD air analysis is given in Figure 4.16. Mass spectrum from the pre-exposure baseline is given in Figure 4.17. Backgrounds subtracted mass spectra from the beginning of the oil exposure experiment, from the middle of the oil exposure experiment and from the end of the oil exposure experiment are given in Figure 4.18. Uncorrected mass spectra for similar time intervals are given in appendix E.2.
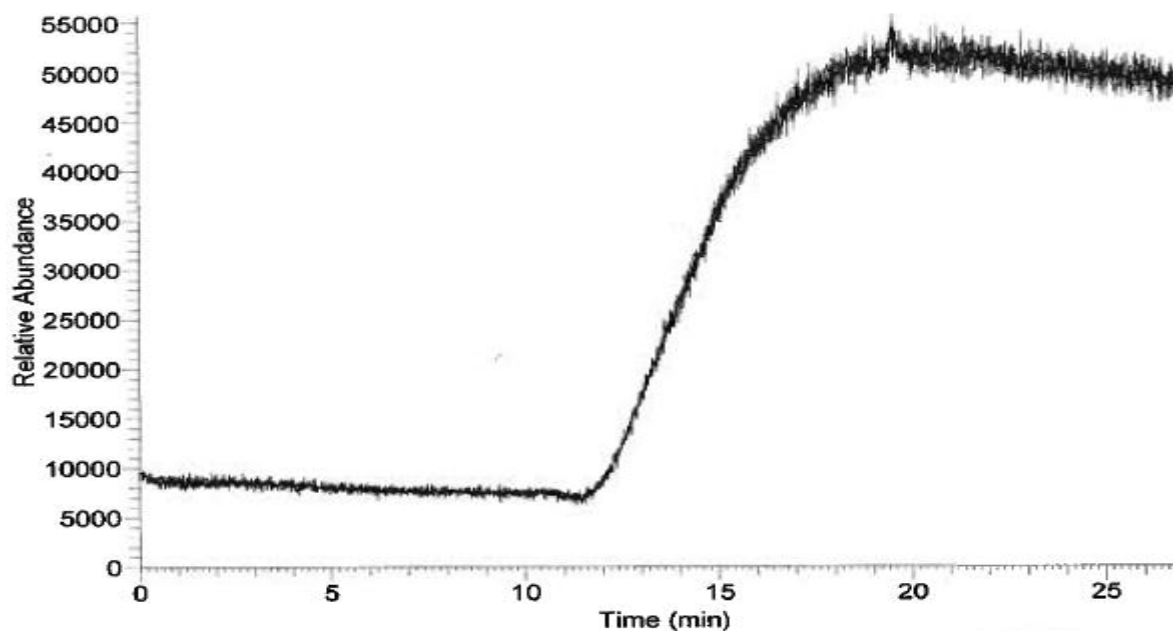
Figure 4.16: Oil in air MIMS analysis: SAGD (9.0 mg)
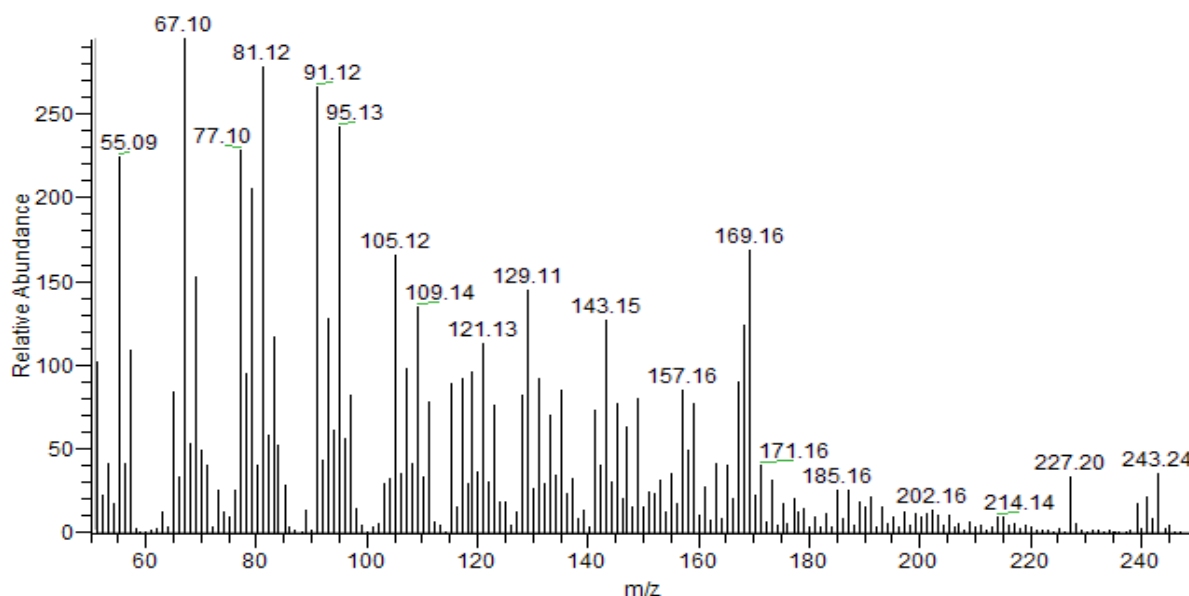
Figure 4.17: System blank: mass spectrum for the SAGD air analysis, from the pre-exposure baseline (8.45-10.75 min)
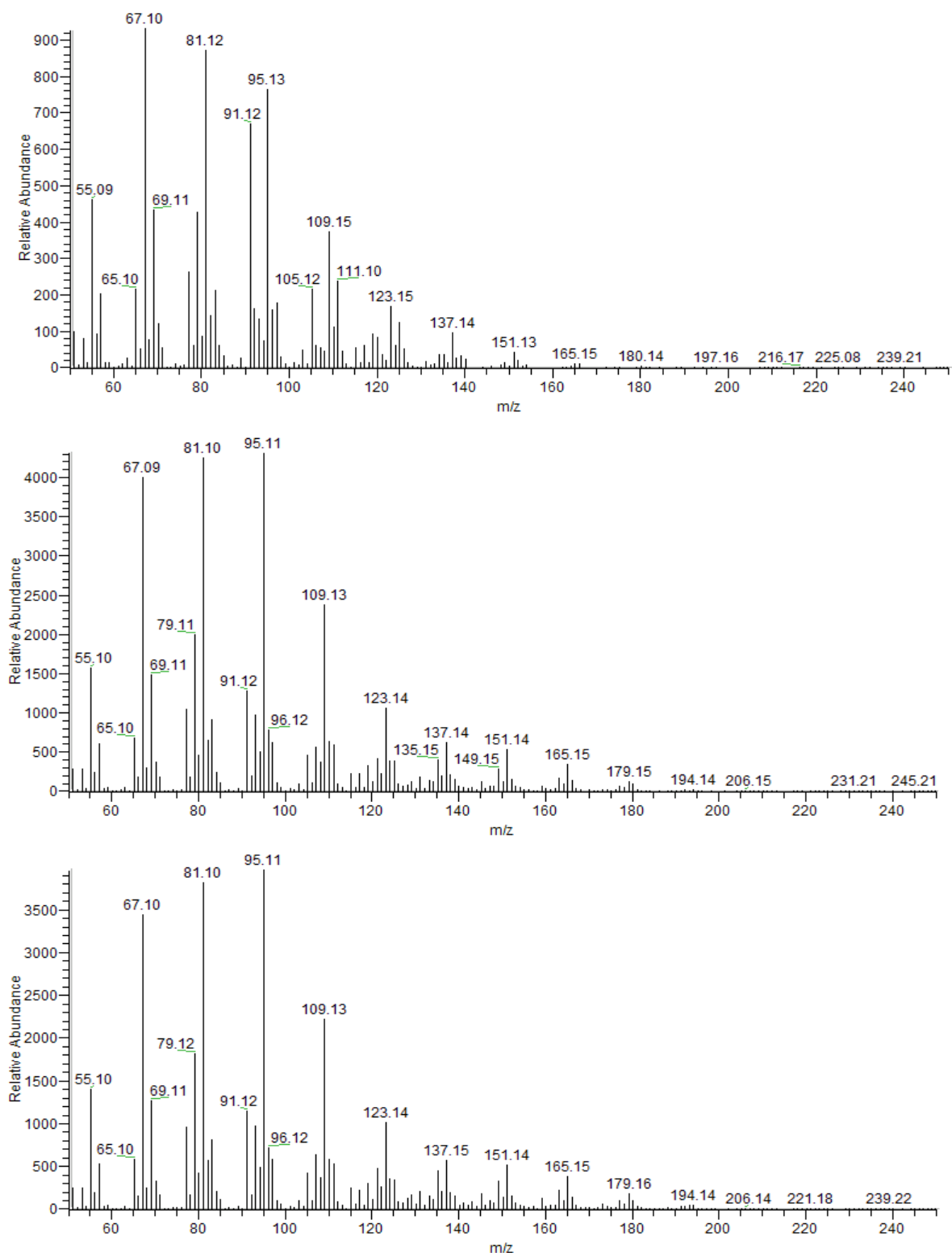
Figure 4.18: Background subtracted spectra for the SAGD air analysis. A) From the beginning of the oil exposure experiment (12.35-13.67 min). B) From the middle of the oil exposure experiment (18.77-20.44 min). C) From the end of the oil exposure experiment (25.74-27.13 min). For all mass spectra the background at 8.88-10.80 min was subtracted.

During the SAGD analysis *m/z* 67, 81 and 95 are the largest peaks throughout the whole oil analysis.

The peaks heights for the SAGD analysis are much smaller than for the Oseberg Blend analysis, due to smaller amounts of the more volatile compounds. Since the SAGD sample lacks small volatile compounds, big changes in the different mass spectrums are not observed.

4.5 Oil in water analysis using MIMS

TIC signal profiles for the water MIMS analyses, except for those presented below, can be found in appendix D.2.

As for the water MIFID analyses, the water MIMS analyses are very time consuming. Slow dissolution from the samples, results in a slow increase of the signal. Oseberg Blend and SAGD were analyzed for 200 minutes only, and at the end of the analyses the signals are still increasing. To enable more efficient measurements of oil samples in water, an equilibration of the samples for several hours before starting the actual MIMS analyses may be done before the TIC signal profiles are recorded. This will bring the oil sample more close to equilibrium, and properties of this state can be measured.

Signal intensities for all water MIMS analyses and response time for toluene are given in Table 4.6

Table 4.6: Signal intensities and response time for the oil in water MIMS analyses

	End signal intensity (a.u. [a])	Response time (min) [b]
Oseberg Blend 1	33 000	
Oseberg Blend 2	81 600	
SAGD	2 900	
Toluene	44 000 [c]	11.8
n-Heptane 1	820	
n-Heptane 2	1 400	

[a]   a.u. = accidental units (referred as Relative Abundance in the software)

[b]   Time used for the signal to increase from 10 to 90 % of the maximum signal.

[c]   Maximum signal intensity (μV)

TIC signal profile for the second Oseberg Blend analysis is given in Figure 4.19, the other Oseberg Blend analysis are presented in Appendix D.2 (due to some complications this sample was exposed to the atmosphere for some period). Mass spectrum from the pre-exposure baseline is given in Figure 4.20. Backgrounds subtracted mass spectra from the beginning of the oil exposure experiment, from the middle of the oil exposure experiment and from the end of the oil exposure experiment are given in Figure 4.21. Uncorrected mass spectra for similar time intervals are given in appendix E.3.
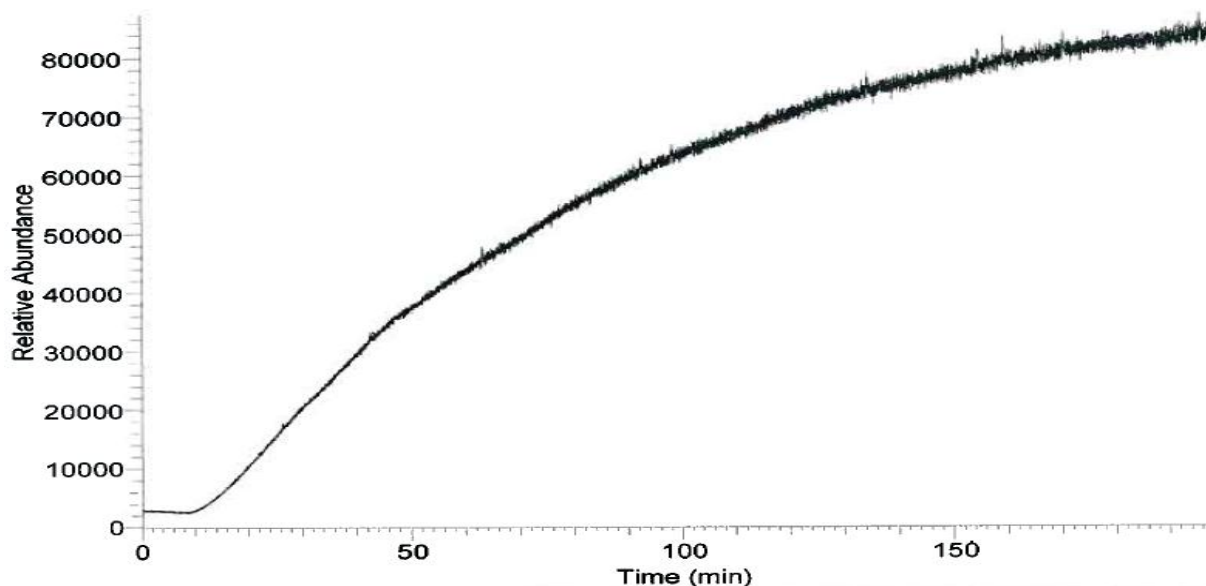
Figure 4.19: Oil in water analysis: Oseberg Blend (8.5 mg)
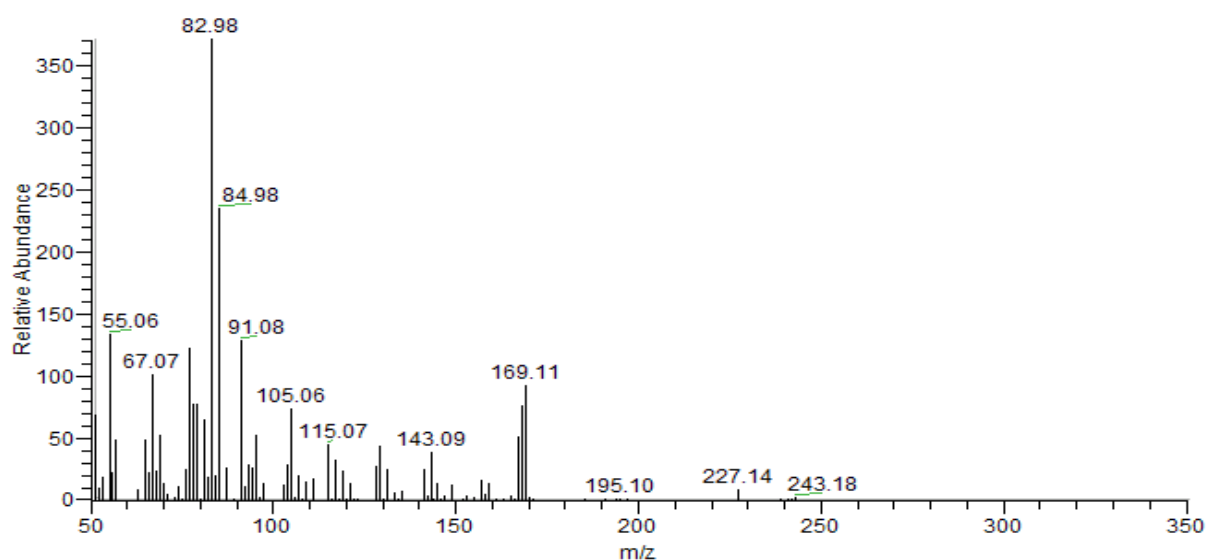
Figure 4.20: System blank: mass spectrum for the Oseberg Blend water analysis, from the pre-exposure baseline (2.64-7.54 min)
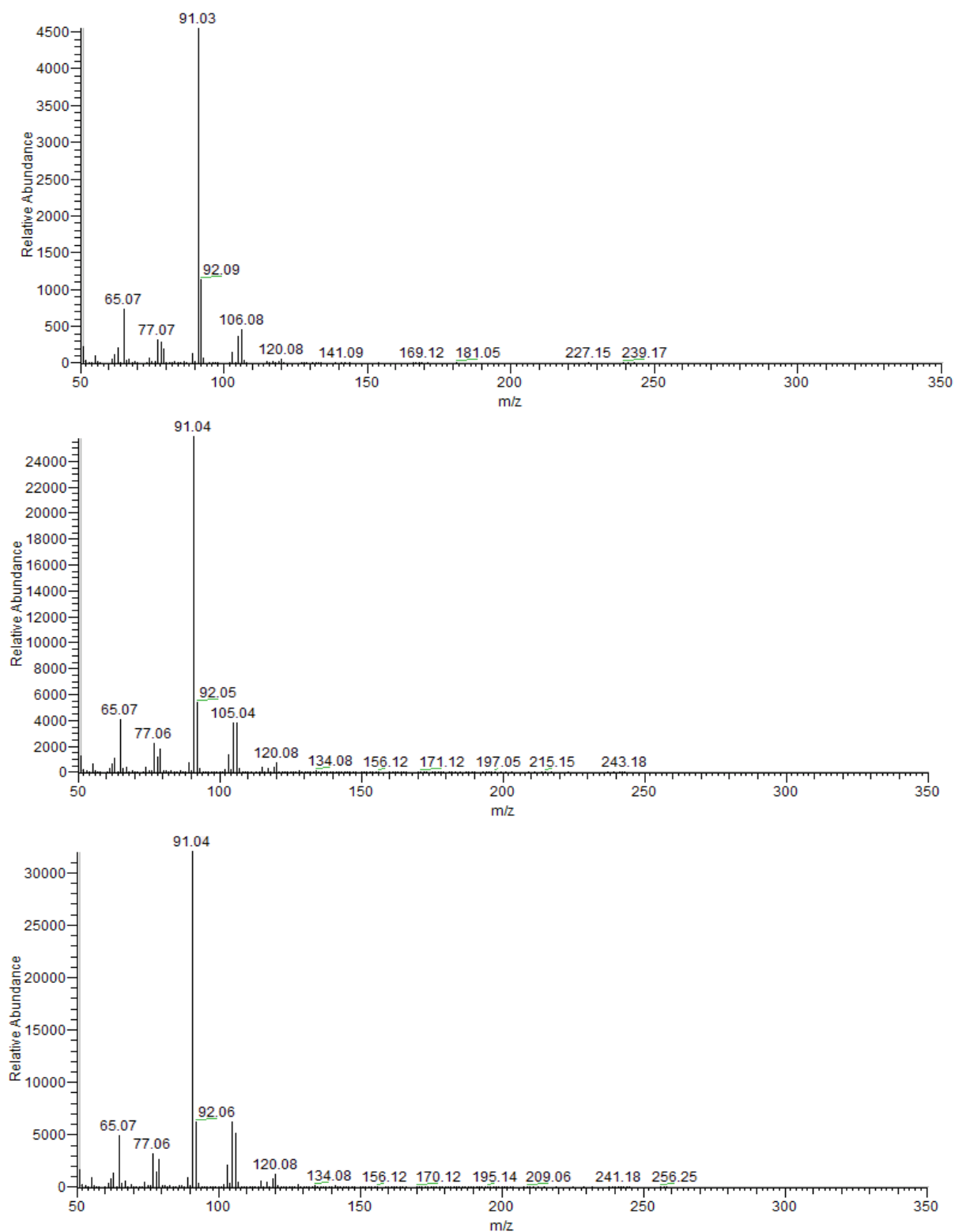
Figure 4.21: Background subtracted spectra for the Oseberg Blend water analysis. A) From the beginning of the oil exposure experiment (17.92-26.14 min). B) From the middle of the oil exposure experiment (98.97-106.31 min). C) From the end of the oil exposure experiment (189.42-199.70 min). For all mass spectra the background at 1.17-8.22 min was subtracted.

The TIC signal for the Oseberg Blend analysis is still increasing at the end of the analysis.

From the mass spectra it can be seen that the largest peak is at *m/z* 91 throughout the whole oil analysis, followed by *m/z* 105, 92, 65, 106, 77 and 79. A indication of the presence of toluene is also the case for this Oseberg Blend analysis, due the presence of the masses 65, 91 and 92.

As for the Oseberg Blend air analysis, even numbered mass numbers are also observed in the water analysis. Mass numbers of 120 and 134 represent C_3- and C_4-polyalkyl substituted benzenes.

For the water MIMS analyses, as for the air MIMS analyses, the higher mass numbers gets more visible towards the end of the analyses. The larger molecules representing these values are less soluble compared to the smaller molecules with lower mass numbers, and thus need longer time to be released from the oil samples.

TIC signal profile for the SAGD analysis is given in Figure 4.22. Mass spectrum from the pre-exposure baseline is given in Figure 4.23. Backgrounds subtracted mass spectra from the beginning of the oil exposure experiment, from the middle of the oil exposure experiment and from the end of the oil exposure experiment are given in Figure 4.24. Uncorrected mass spectra for similar time intervals are given in appendix E.4.
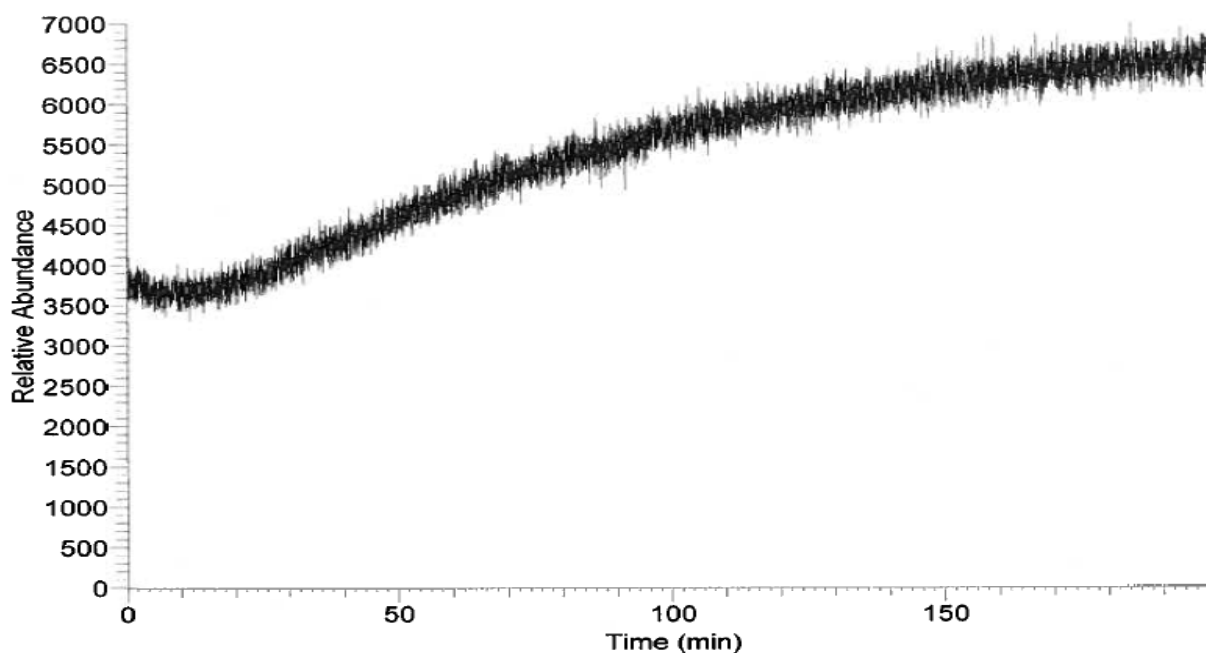
Figure 4.22: Oil in water analysis: SAGD (11.7 mg)
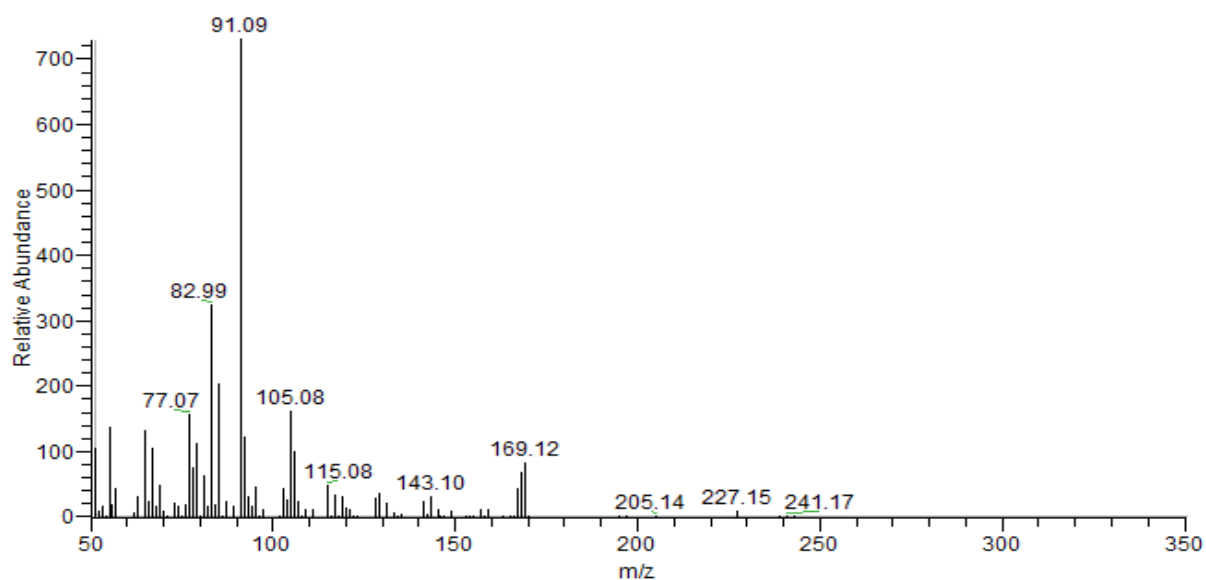
Figure 4.23: System blank: mass spectrum for the SAGD water analysis, from the pre-exposure baseline (4.93-10.58 min)
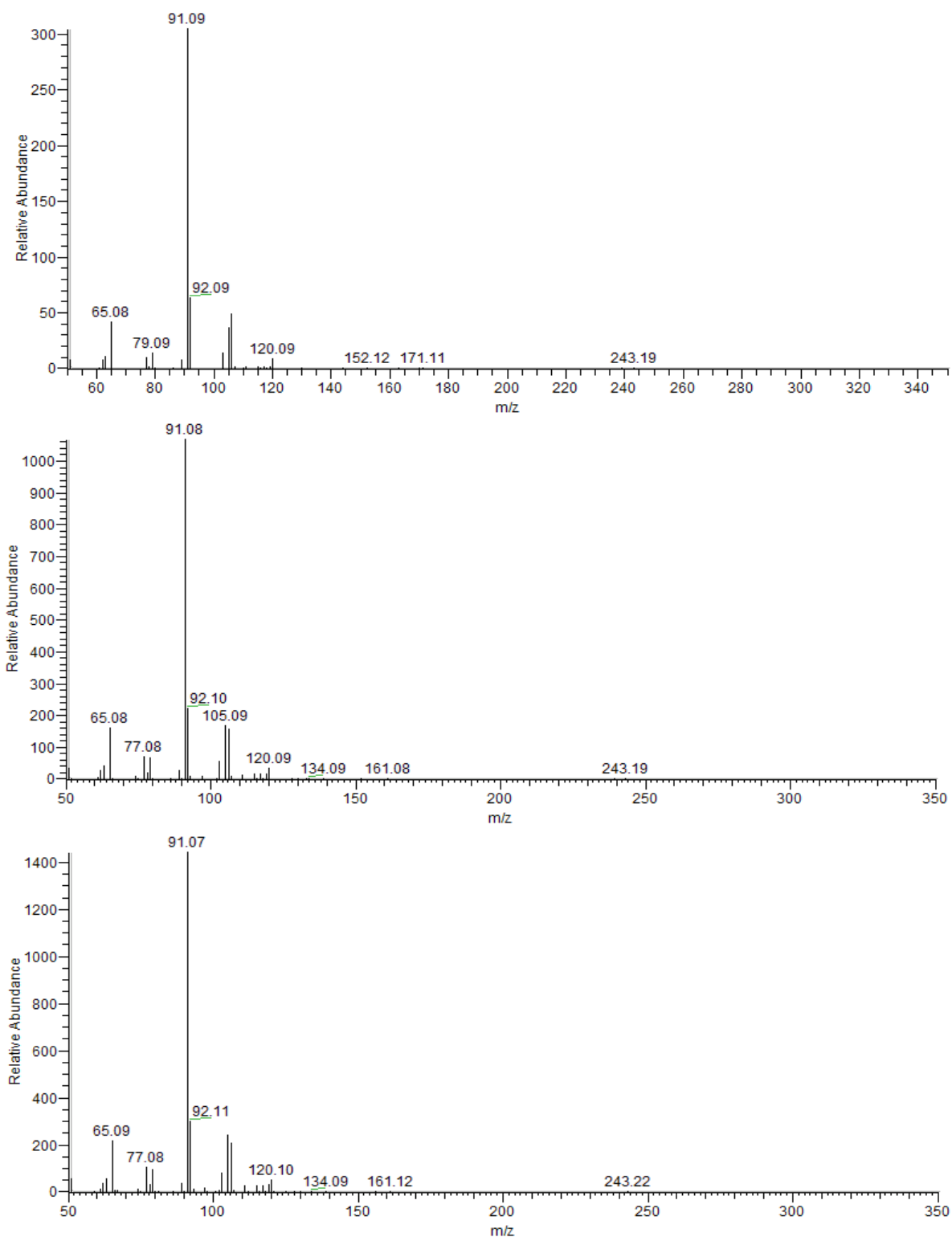
Figure 4.24: Background subtracted spectra for the SAGD water analysis. A) From the beginning of the oil exposure experiment (26.83-34.58 min). B) From the middle of the oil exposure experiment (98.65-106.40 min). C) From the end of the oil exposure experiment (190.74-199.99 min). For all mass spectra the background at 4.76-10.13 min was subtracted.

For the SAGD analysis the TIC signal is also still increasing at the end of the analysis.

The largest peak is at *m/z* 91 throughout the whole oil analysis, as for the Oseberg Blend analysis. The next largest peaks after *m/z* 91 are found at m/z 105, 92, 65, 106, 77, 83, 79 and 85.

The most abundant mass numbers are relatively similar for both the Oseberg Blend and SAGD analyses, except from the masses of 83 and 85 which are visible in the SAGD analysis only. Also, the mass peaks for these analyses follow relatively similar patterns, without respect to the abundance. For both analyses the second largest peaks (*m/z* 105 and 92) are approximately 20 % of the base peak throughout the whole analysis.

4.6 MIFID vs. MIMS

A clear advantage of MIMS, as compared to MIFID, is the achievement of mass spectral information. The presence of different masses gives an indication of the content of the different oil samples. Also, information on how the presence and abundance of the different ions change throughout the analyses is obtained. For overall quantitation of oil samples, air MIFID is well suited, especially for the lightest oil samples. Since quantitation by oil in water analyses is a time consuming process, MIFID analyses would be more beneficial, as compared to MIMS analyses, with respect to the economical aspect.

For both air MIFID and air MIMS good response and generally short response times are obtained. Half-times obtained are also relatively short for the lightest oil, but not so good for the heaviest oils. Summary of maximum signal intensities, response times and half-times for the air analyses are given in Table 4.7, Table 4.8 and Table 4.9, respectively.

Table 4.7: Summary of the maximum signal intensity (listed from highest to lowest) for the oil in air analyses by MIFID and MIMS

MIFID		MIMS	
Oil	**Signal intensity (µV)**	**Oil**	**Signal intensity (a.u. [a])**
Unspecified 1	888 000	Unspecified 1	1 5834 000
Oseberg Blend	808 000	Unspecified 2	1 017 000
Troll B	354 000	Troll B	669 000
Unspecified 2	336 000	Norne Blend	666 000
Heidrun Tilje	231 000	Oseberg Blend	593 000
Norne Blend	188 000	Heidrun Tilje	581 000
Balder Blend	179 000	Balder Blend	348 000
Falk	36 500	Falk	168 000
Peregrino	30 700	Mariner Maureen	58 300
Mariner Maureen	21 100	Peregrino	52 900
Bressay	10 500	SAGD	44 400
SAGD	7 550	Bressay	40 200

[a]   a.u. = accidental units (referred as Relative Abundance in the software)

Table 4.8: Summary of the response times (listed from lowest to highest) for the oil in air analyses by MIFID and MIMS

MIFID		MIMS	
Oil	**Response time (min)**	**Oil**	**Response time (min)**
Unspecified 1	0.7	Unspecified 1	1.0
Unspecified 2	0.8	Unspecified 2	1.1
Norne Blend	0.8	Oseberg Blend	1.3
Heidrun Tilje	0.9	Norne Blend	1.4
Oseberg Blend	1.0	Troll B	1.4
Troll B	1.1	Balder Blend	1.7
Balder Blend	1.4	Heidrun Tilje	1.8
Peregrino	1.4	Peregrino	3.4
SAGD	2.7	Falk	3.4
Mariner Maureen	3.4	SAGD	5.0
Falk	3.7	Mariner Maureen	5.7
Bressay	4.5	Bressay	7.7

Table 4.9: Summary of the half-times (listed from lowest to highest) for the oil in air analyses by MIFID and MIMS

MIFID		MIMS	
Oil	**Half-time (min)**	**Oil**	**Half-time (min)**
Oseberg Blend	3.4	Unspecified 1	5.6
Unspecified 1	3.4	Unspecified 2	6.7
Unspecified 2	4.0	Oseberg Blend	7.6
Troll B	5.0	Troll B	10.0
Heidrun Tilje	7.2		
Norne Blend	7.2		
Balder Blend	7.7		
Peregrino	19.5		
Falk	30.0		
Marine Maureen	36.0		
SAGD	49.5		
Bressay	61.0		

Comparison of the response times and half-times for the air analyses are given in Figure 4.25 and Figure 4.26, respectively. As mentioned before only four of the air MIMS analyses were analyzed sufficiently long to enable calculation of the half-times. However, these figures indicate a general trend for longer analysis times for the MIMS analyses, both considering response times and half-times (only one exception for the response time of Falk).
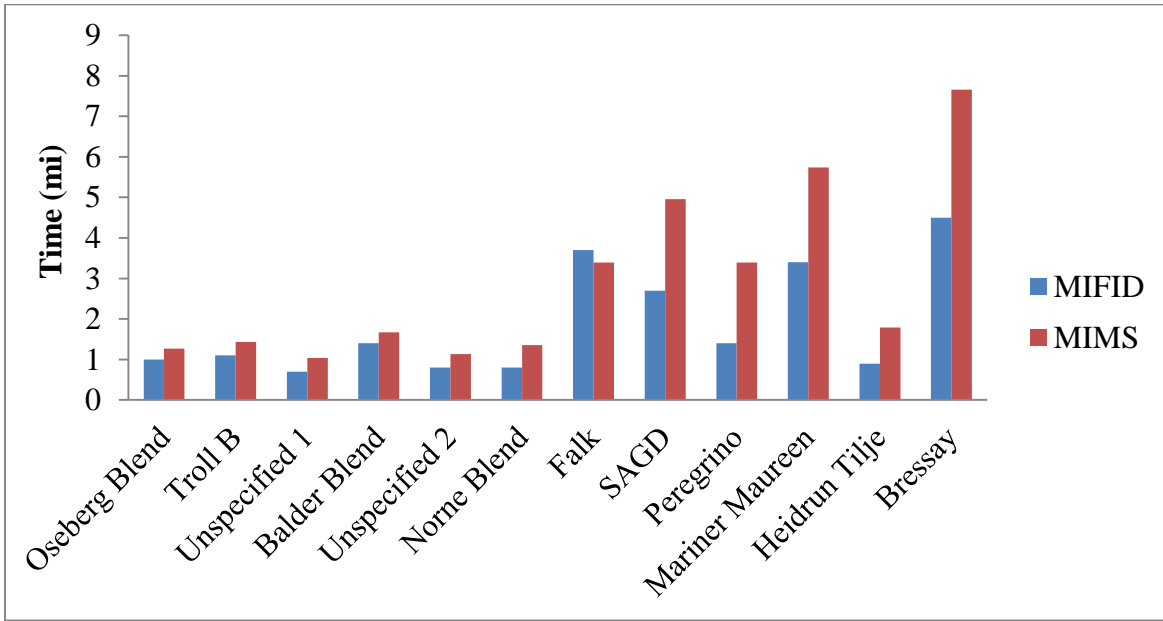
Figure 4.25: Comparison of the response times for the MIFID and MIMS oil in air analyses
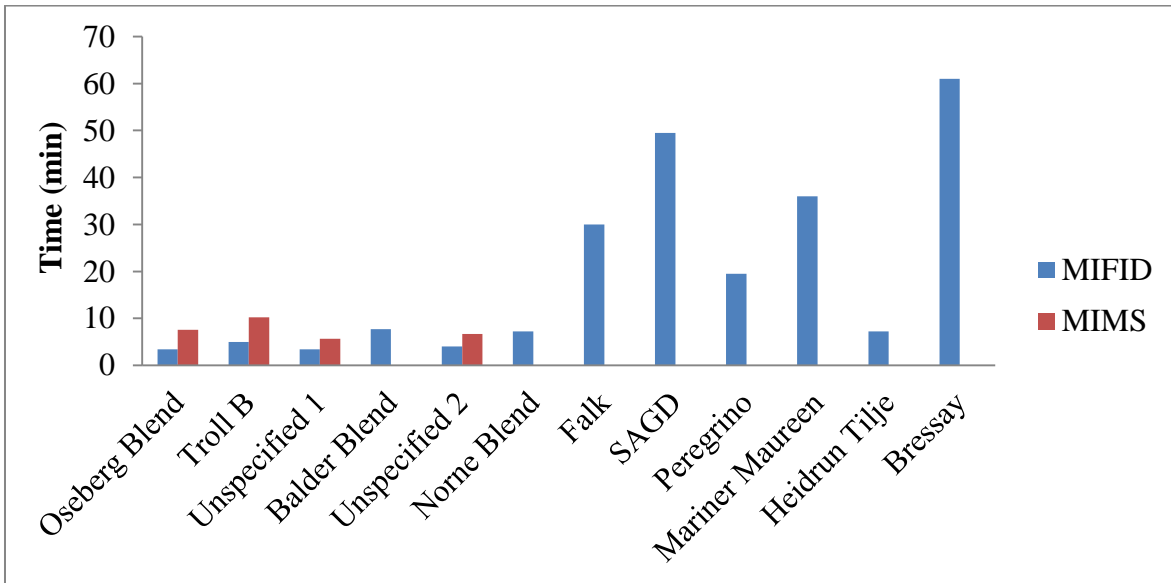
Figure 4.26: Comparison of the half-times for the MIFID and MIMS oil in water analyses

5. Conclusions

Membrane introduction (MI) methods show interesting prospects for analyses of oil samples. However, unsatisfying results were obtained by water MI analyses, due to slow release of weakly water soluble components from the oil samples. It is concluded that improvement of water MI analyses of oils might be obtained by pre-equilibration of the oil samples and relatively long analysis times. For air MI analyses some kinetic information on oil in air weathering can be obtained within reasonable analysis times, and good responses are achieved, for both MIFID and MIMS. For kinetic information, such as response times and half-times, it should be noted that these values are affected by transportation through tubing and the diffusion rates through the membrane.

MIMS provides more informative results compared to MIFID, due to mass spectral information, and especially concerning the possibilities for MS/MS analyses where individual compound identification could be carried out.

It is concluded that for oil analyses MI analyses are best suited for light oil samples, as compared to the heavy oils, especially for water MI analyses, due to shorter analysis times.

For quantitation of oils in air MIFID might be suitable for light and non-weathered samples, but probably has too limited sensitivity for heavy and strongly weathered samples. For oil samples in water, MIFID has limitations due to poor sensitivity and long analysis times. However, with respect to long duration of such water analyses, analyses by MIFID would be more cost effective, as compared to MIMS.

The work and results obtained through this thesis is a foundation for further kinetic studies of oil in air samples by MIMS or MIFID, and has given some indications for how the future work on oil in water analyses could be developed.

6. Further work

6.1 General aspects for membrane introduction analyses

Loss of sample material due to weathering is a concern for membrane introduction analyses, especially with respect to evaporation. The most volatile compounds, which are the most favorable compounds for the membrane interface, will rapidly evaporate from the sample. To reduce evaporation from the samples, preparation of the samples must be carried out close to the MI-system to minimize evaporation by air exposure. Another aspect that may be considered is light exposure. To minimize photo oxidation protection from light exposure of the samples during transportation to the MI-system will minimize this effect. For water MI-analyses covering of the water bath including the glass flask holding the sample will also reduce photo oxidation during analyses.

Other processes that may lead to loss of sample are adsorption or absorption to tubing and valves. Minimizing the length of the tubing system is thus important, and thermostating might be considered.

The analyses carried out in this project show some limitations concerning analyses of heavy oils, especially with respect to water MI-analyses. It may therefore be most reasonable to focus the attention on analyses of light oils.

As mentioned earlier; equilibration of the oil samples prior to the actual MI analyses may reduce the analysis times and improve the analysis quality for water MI-analyses.

6.2 Other possible analyses

To enable more informative analyses with respect to contents of the oil samples, MIMS-analyses with tandem mass spectrometry (MS/MS) should be carried out. MS/MS analyses give the possibility for individual compound identification, despite interfering masses in regular MIMS analyses. E.g., both naphthalene and nonane produces *m/z* 128. Also, the use of chemical ionization (CI) may give additional information.

For MI-analyses in the future it would have been interesting to follow the weathering of oil samples. This could be done with both closed and open systems. In open systems the interaction with the atmosphere will be included. During weathering analyses it would also

been interesting to follow individual masses by the use of MS/MS to see how they change with time.

Stabilization of an MI-system between oil analyses is very time consuming. Thus conditioning of the system may be necessary to speed up this process. Slow stabilization occurs because the different compounds use different amounts of time to diffuse through the membrane. However, it would have been interesting to follow the signal prior to an analysis to measure the amount of time needed to get all the compounds to diffuse from the membrane. This could be done be simply pumping clean air through the system after removal of the oil sample until stable signal is achieved.

Another interesting investigation would be the use of different membranes, and if better analyses could be achieved due to this aspect. E.g., it has been stated that ultra-thin membranes may be suitable for petrochemical online process monitoring (Srinivasan, Johnson et al. 1997).

Due to large amounts of heavy compounds in oil samples, analyses with a heated interface would have been interesting. Better sensitivity is achieved with a heated interface for heavier compounds (Creba, Ferguson et al. 2006), and may thus enable detection of compounds that are not detected with conventional MI-analyses. This could improve both membrane transfer kinetics and the applicability to more heavy oils.

7. References

Alberici, R. M., R. Sparrapan, et al. (2001). "Selective trace level analysis of phenolic compounds in water by flow injection analysis - Membrane introduction mass spectrometry." Environmental Science & Technology **35**(10): 2084-2088.

Bauer, S., J. Amy, et al. (1995). "Direct determination of organic-compounds in water at parts-per-quadrillion levels by membrane introduction mass-spectrometry." Analytical chemistry **67**(8): 1409-1412.

Calvo, K. C., C. R. Weisenberger, et al. (1981). "Permeable membrane-mass spectrometric measurement of reaction kinetics." Analytical chemistry **53**(7): 981-985.

Calvo, K. C., C. R. Weisenberger, et al. (1983). "Permeable membrane/mass spectrometric measurement of an enzymatic kinetic isotope effect: .alpha.-chymotrypsin-catalyzed transesterification." Journal of the American Chemical Society **105**(23): 6935-6941.

Chang, C. C. and G. R. Her (2000). "On-line monitoring trihalomethanes in chlorinated water by membrane introduction-fast gas chromatography mass-spectrometry." Journal of chromatography A **893**(1): 169-175.

Cisper, M. E., C. G. Gill, et al. (1995). "Online Detection of Volatile Organic Compounds in Air at Parts-per-Trillion Levels by Membrane Introduction Mass Spectrometry." Analytical chemistry **67**(8): 1413-1417.

Collin-Hansen, C. (2011). Statoil. Personal communication: oil information.

Creaser, C. S., D. G. Lamarca, et al. (2001). "Reversed-Phase Membrane Inlet Mass Spectrometry Applied to the Real-Time Monitoring of Low Molecular Weight Alcohols in Chloroform." Analytical chemistry **74**(1): 300-304.

Creba, A., R. Ferguson, et al. (2006). "A coaxially heated membrane introduction mass spectrometry interface for the rapid and sensitive on-line measurement of volatile and semi-volatile organic contaminants in air and water at parts-per-trillion levels." Rapid communications in mass spectrometry **20**(13): 2000-2008.

Creba, A., A. Weissfloch, et al. (2007). "An enzyme derivatized polydimethylsiloxane (PDMS) membrane for use in membrane introduction mass spectrometry (MIMS)." Journal of The American Society for Mass Spectrometry **18**(6): 973-979.

References

Daling, P. S. and P. J. Brandvik (2009). Weathering of oil spills at sea and use of numerical oil weathering models. Lecture notes in Marine Organic Environmental Chemistry (KJ3050) 14.09.2010. Trondheim, SINTEF Materials and Chemistry.

Davey, N. G., E. T. Krogh, et al. (2011). "Membrane-introduction mass spectrometry (MIMS)." TrAC Trends in Analytical Chemistry **30**(9): 1477-1485.

Degn, H. and B. Kristensen (1986). "Stopped flow mass spectrometry: applications to the carbonic anhydrase reaction." Journal of Biochemical and Biophysical Methods **12**(5-6): 305-310.

Devlin, J. G. A., J. A. Amaral, et al. (2008). "A membrane introduction flame ionization/electron capture detection (MIFID/ECD) system for the rapid, real-time screening of volatile disinfection byproducts and hydrocarbon contaminants in water." Microchemical journal **88**(1): 74-81.

Dongré, A. R. and M. J. Hayward (1996). "Characterization of a membrane interface designed for analytical scale sample introduction into a mass spectrometer." Analytica Chimica Acta **327**(1): 1-16.

Etzkorn, J. M., N. G. Davey, et al. (2009). "The Use of MIMS-MSMS in Field Locations as an On-Line Quantitative Environmental Monitoring Technique for Trace Contaminants in Air and Water." Journal of Chromatographic Science **47**(1): 57-66.

Greibrokk, T., E. Lundanes, et al. (2005). Kromatografi: separasjon og deteksjon. Oslo, Universitetsforlaget.

Gross, J. H. (2004). Mass spectrometry: a textbook. Berlin, Springer.

Hayward, M. J., D. E. Riederer, et al. (1991). "Bioreactor monitoring using flow injection/membrane introduction mass spectrometry with an ion trap detector." Process Control and Quality **1**(2): 105-116.

Hoch, G. and B. Kok (1963). "A mass spectrometer inlet system for sampling gases dissolved in liquid phases." Archives of Biochemistry and Biophysics **101**(1): 160-170.

Hoffmann, E. d. and V. Stroobant (2007). Mass spectrometry: principles and applications. Chichester, Wiley.

Janfelt, C., H. Frandsen, et al. (2006). "Characterization of a mini membrane inlet mass spectrometer for on-site detection of contaminants in both aqueous and liquid organic samples." Rapid Communications in Mass Spectrometry **20**(9): 1441-1446.

Johnson, R. C., R. G. Cooks, et al. (2000). "Membrane introduction mass spectrometry: Trends and applications." Mass spectrometry reviews **19**(1): 1-37.

Johnson, R. C., K. Koch, et al. (1997). "An evaluation of low vapor pressure liquids for membrane introduction mass spectrometry." Journal of Mass Spectrometry **32**(12): 1299-1304.

Kasthurikrishnan, N., R. G. Cooks, et al. (1996). "Thin Pervaporation Membranes for Improved Performance in On-line Flow Injection Analysis Membrane Introduction Mass Spectrometry." Rapid Communications in Mass Spectrometry **10**(7): 751-756.

Ketola, R. A., J. T. Kiuru, et al. (2003). "Comparison of analytical performances of a micro-array quadrupole instrument and a conventional quadrupole mass spectrometer equipped with membrane inlets." Rapid Communications in Mass Spectrometry **17**(7): 753-756.

Ketola, R. A., T. Mansikka, et al. (1997). "Analysis of Volatile Organic Sulfur Compounds in Air by Membrane Inlet Mass Spectrometry." Analytical chemistry **69**(22): 4536-4539.

Ketola, R. A., M. Ojala, et al. (1999). "A non-linear asymmetric error function-based least mean square approach for the analysis of multicomponent mass spectra measured by membrane inlet mass spectrometry." Rapid Communications in Mass Spectrometry **13**(8): 654-662.

Ketola, R. A., M. Ojala, et al. (1997). "Development of a membrane inlet mass spectrometric method for analysis of air samples." Analytica Chimica Acta **349**(1-3): 359-365.

Ketola, R. A., V. T. Virkki, et al. (1997). "Comparison of different methods for the determination of volatile organic compounds in water samples." Talanta **44**(3): 373-382.

Kostiainen, R., T. Kotiaho, et al. (1998). "Analysis of Volatile Organic Compounds in Water and Soil Samples by Purge-and-Membrane Mass Spectrometry." Analytical chemistry **70**(14): 3028-3032.

Kotiaho, T., M. Cisper, et al. (2002). "Environmental applications of membrane introduction mass spectrometry." Journal of mass spectrometry **37**(5): 457-476.

References

Kotiaho, T. and F. R. Lauritsen (2002). Chapter 16 Membrane inlet mass spectrometry. Comprehensive Analytical Chemistry. J. Pawliszyn, Elsevier. **Volume 37:** 531-557.

Kotiaho, T. D. (1991). "Membrane introduction mass-spectrometry." Analytical chemistry **63**(18): A875.

Lin, C. Y. and R. S. Tjeerdema (2008). Crude Oil, Oil, Gasoline and Petrol. Encyclopedia of Ecology. J. Sven Erik and F. Brian. Oxford, Academic Press**:** 797-805.

Løvås, G. G. (2004). Statistikk for universiteter og høgskoler. Oslo, Universitetsforlaget.

Maden, A. J. and M. J. Hayward (1996). "Sheet Materials for Use as Membranes in Membrane Introduction Mass Spectrometry." Analytical chemistry **68**(10): 1805-1811.

March, R. E. and J. F. J. Todd (2005). Quadrupole ion trap mass spectrometry. Hoboken, N.J., Wiley-Interscience.

McLafferty, F. W. (1980). "Tandem mass spectrometry (MS/MS): a promising new analytical technique for specific component determination in complex mixtures." Accounts of Chemical Research **13**(2): 33-39.

Melbye, A. G. (2011). SINTEF Sealab. Personal communication: oil information.

Mendes, M. A., R. S. Pimpim, et al. (1996). "A Cryotrap Membrane Introduction Mass Spectrometry System for Analysis of Volatile Organic Compounds in Water at the Low Parts-per-Trillion Level." Analytical chemistry **68**(19): 3502-3506.

Ojeda, C., F. Rojas, et al. (2007). "Process analytical chemistry - Application of mass spectrometry in environmental analysis: An overview." Applied spectroscopy reviews **42**(4): 345-367.

Ouyang, Z. and R. G. Cooks (2009). Miniature mass spectrometers. **2:** 187-214.

Reuss, M., H. Piehl, et al. (1975). "Application of mass spectrometry to the measurement of dissolved gases and volatile substances in fermentation." European Journal of Applied Microbiology **1**(4): 323-325.

Riter, L. S., Z. Takáts, et al. (2001). "High surface area membrane introduction mass spectrometry for analysis of volatile and semi-volatile organic compounds in air." Rapid Communications in Mass Spectrometry **15**(17): 1520-1524.

Riter, L. S., Z. Takats, et al. (2001). "Single-sided membrane introduction mass spectrometry for on-line determination of semi-volatile organic compounds in air." Analyst **126**(11): 1980-1984.

Sheppard, S. K., N. Gray, et al. (2005). "The impact of sludge amendment on gas dynamics in an upland soil: monitored by membrane inlet mass spectrometry." Bioresource Technology **96**(10): 1103-1115.

Shukla, A. K. and J. H. Futrell (2000). "Tandem mass spectrometry: dissociation of ions by collisional activation." Journal of Mass Spectrometry **35**(9): 1069-1090.

Silverstein, R. M., F. X. Webster, et al. (2005). Spectrometric identification of organic compounds. Hoboken, N.J., Wiley.

Simanzhenkov, V. and R. Idem (2003). Crude oil chemistry. New York, Marcel Dekker.

Skoog, D. A. (2004). Fundamentals of analytical chemistry. Belmont, Calif., Thomson Brooks/Cole.

Slivon, L. E., M. R. Bauer, et al. (1991). "Helium-purged hollow fiber membrane mass spectrometer interface for continuous measurement of organic compounds in water." Analytical chemistry **63**(13): 1335-1340.

Speight, J. G. (2001). Handbook of petroleum analysis. New York, Wiley-Interscience.

Speight, J. G. (2007). The chemistry and technology of petroleum. Boca Raton, Fla., CRC Press.

Srinivasan, N., R. Johnson, et al. (1997). "Membrane introduction mass spectrometry." Analytica Chimica Acta **350**(3): 257-271.

Srinivasan, N., N. Kasthurikrishnan, et al. (1995). "On-line monitoring with feedback control of bioreactors using a high ethanol tolerance yeast by membrane introduction mass spectrometry." Analytica Chimica Acta **316**(2): 269-276.

Statoil (2011). "Crude oil assays." Retrieved 12.19, 2011, from http://www.statoil.com/en/OurOperations/TradingProducts/CrudeOil/Crudeoilassays/Pages/default.aspx.

Thompson, A., J. Etzkorn, et al. (2008). "Membrane introduction tandem mass spectrometry (MIMS-MS/MS) as a real-time monitor for biogenic volatile organic compound (BVOC) emissions from plants." Canadian journal of analytical sciences and spectroscopy **53**(2): 75-81.

Torkil, H. (1999). "Aspects of the mechanism of the flame ionization detector." Journal of Chromatography A **842**(1-2): 221-227.

Trushina, E. V., N. J. Clarke, et al. (1998). "A miniaturized membrane inlet mass spectrometry interface for analysis of nitric oxide in human plasma." Rapid Communications in Mass Spectrometry **12**(14): 985-987.

Wang, Z. and S. A. Stout (2007). Oil spill environmental forensics: fingerprinting and source identification. Amsterdam, Elsevier/Academic Press.

Wong, P. (1995). "Online, in-situ analysis with membrane introduction MS." Environmental science & technology **29**(5): A215-A218.

Xu, C., J. Patrick, et al. (1995). "Affinity membrane introduction mass spectrometry." Analytical chemistry **67**(4): 724-728.

A. List of figures

B. List of tables

C. FID signal profiles

C.1 Test analyses

Figure A.1: Preliminary tests: MIFID analyses of n-heptane in recirculating water (1.25 L) (non-optimized MIFID). a), b) and c) result from injections of 1.0 µL n-heptane solution (10 % n-heptane in methanol) after 2 minutes. d) result from injection of 2.0 µL n-heptane solution (10 % n-heptane in methanol) after 2 minutes.

C.2 Optimization of the MIFID-system

Figure A.2-Figure A.20: Water analyses. Figure A.21-Figure A.31: Air analyses
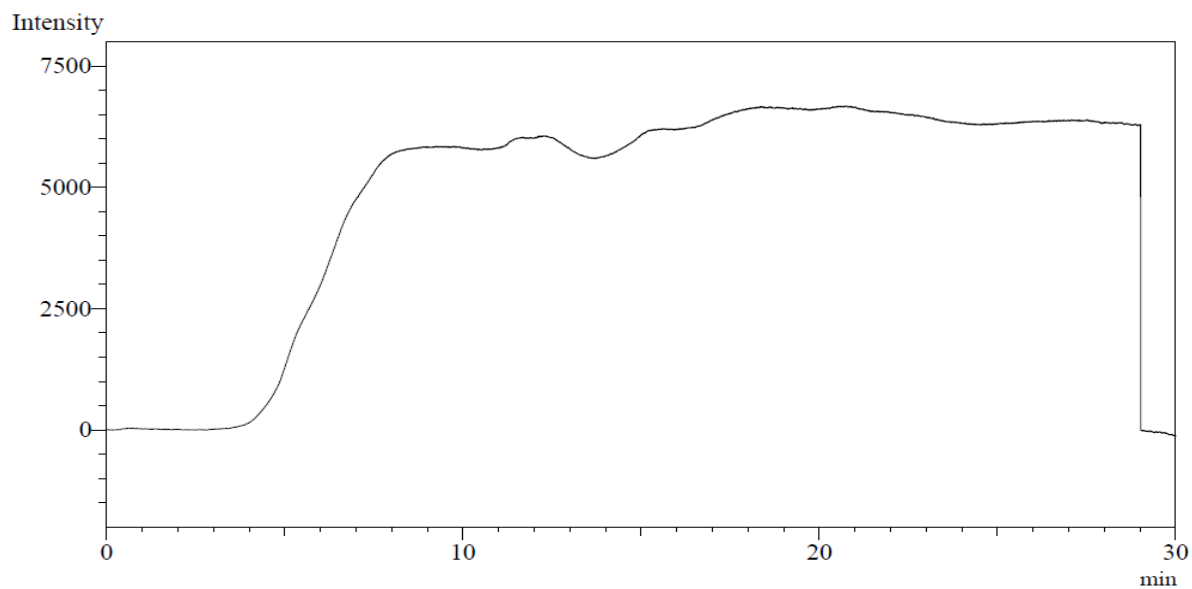
Figure A.2: Water flow optimization: Injection of toluene:methanol 10:90 (1 µL) into 1.25 L of water, closed system with recirculation (Figure A.3-Figure A.6 are based on this injection). Settings: Water flow: 90 mL/min. Interface/water bath: 40 °C. Injector: 40 °C, column flow: 4.74 mL/min (67 kPa). FID: 250 °C, H_2: 30 mL/min, makeup: 30 mL/min, air: 350 mL/min.
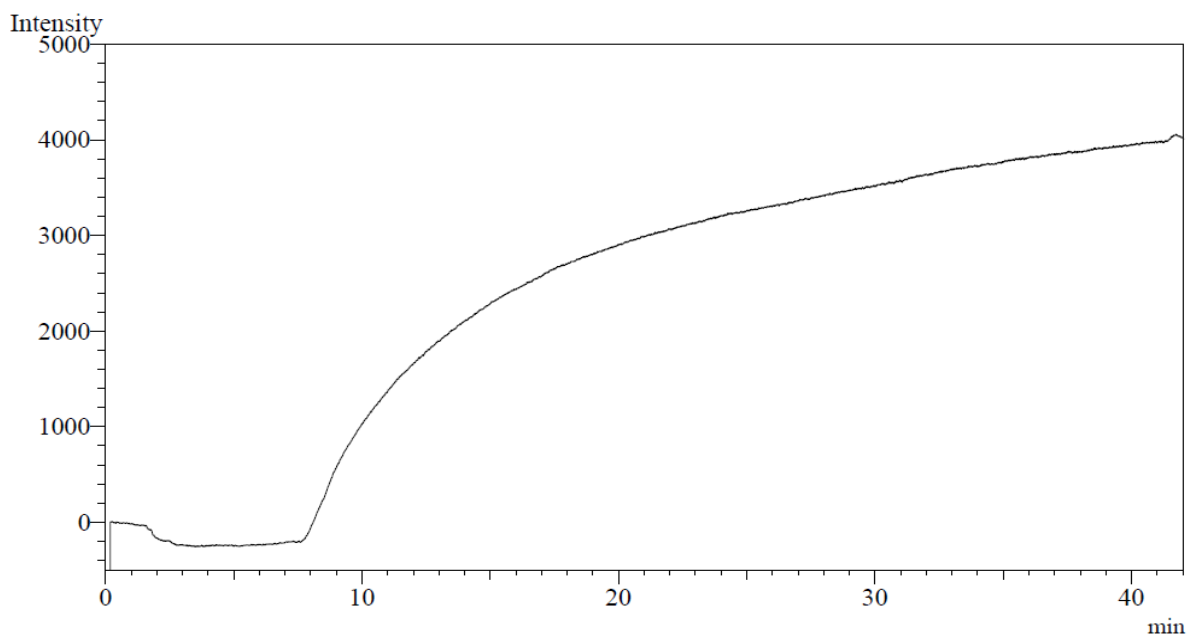
Figure A.3: Water flow optimization: 60 mL/min. Other settings: Interface/water bath: 40 °C. Injector: 40 °C, column flow: 4.74 mL/min (67 kPa). FID: 250 °C, H_2: 30 mL/min, makeup: 30 mL/min, air: 350 mL/min. Test sample: toluene:methanol 10:90 (1 µL) in 1.25 L water.
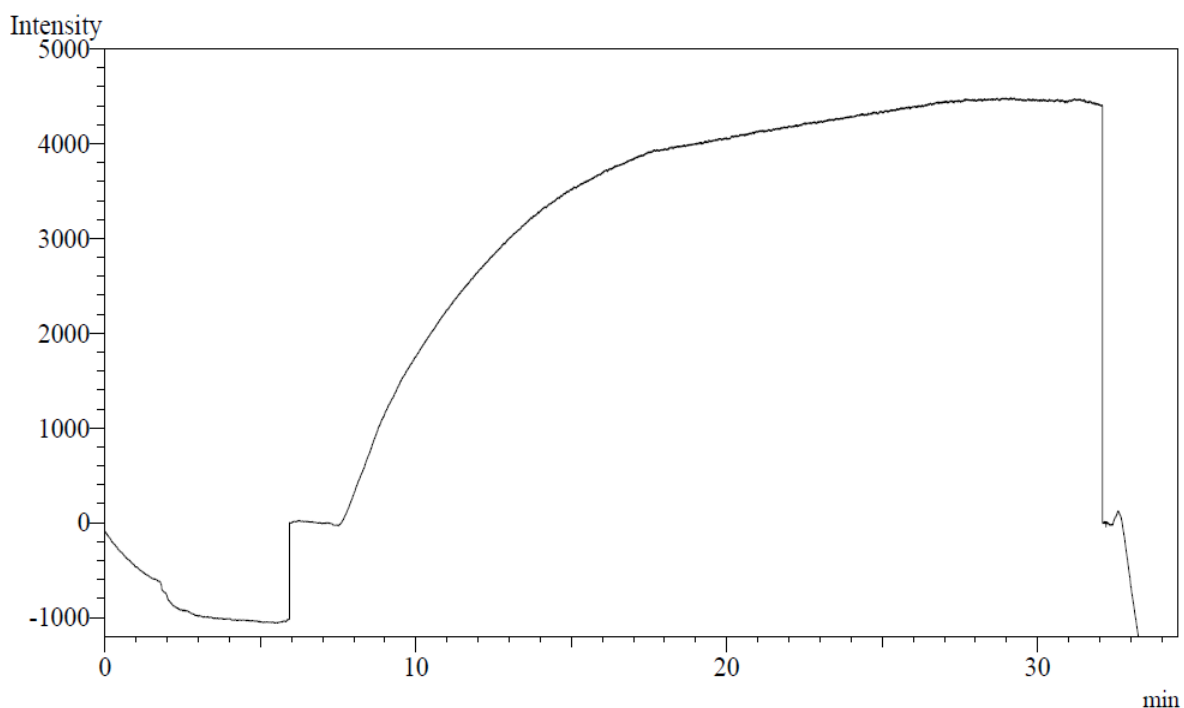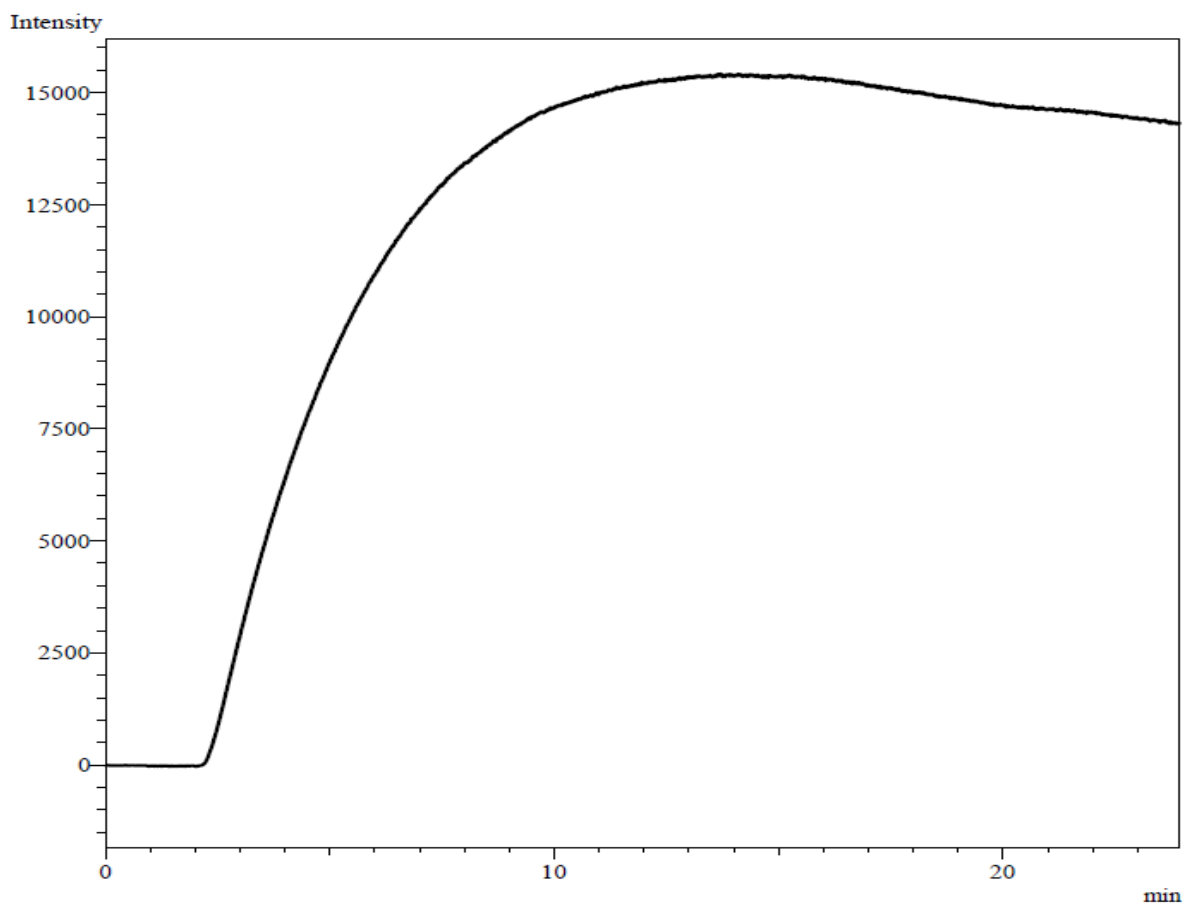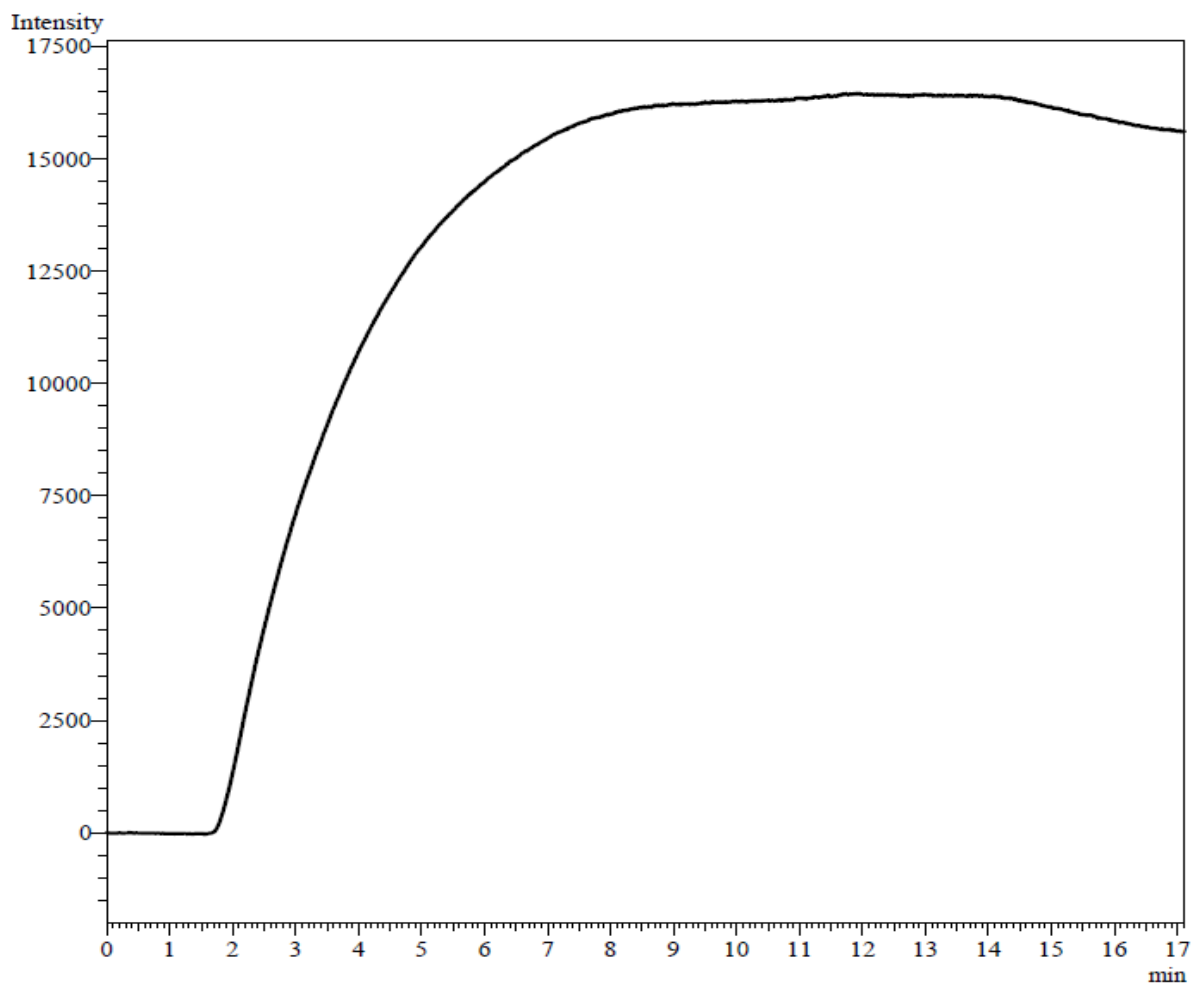

Figure A.4: Water flow optimization: 90 mL/min. Other settings: Interface/water bath: 40 °C. Injector: 40 °C, column flow: 4.74 mL/min (67 kPa). FID: 250 °C, H_2: 30 mL/min, makeup: 30 mL/min, air: 350 mL/min. Test sample: toluene:methanol 10:90 (1 µL) in 1.25 L water.
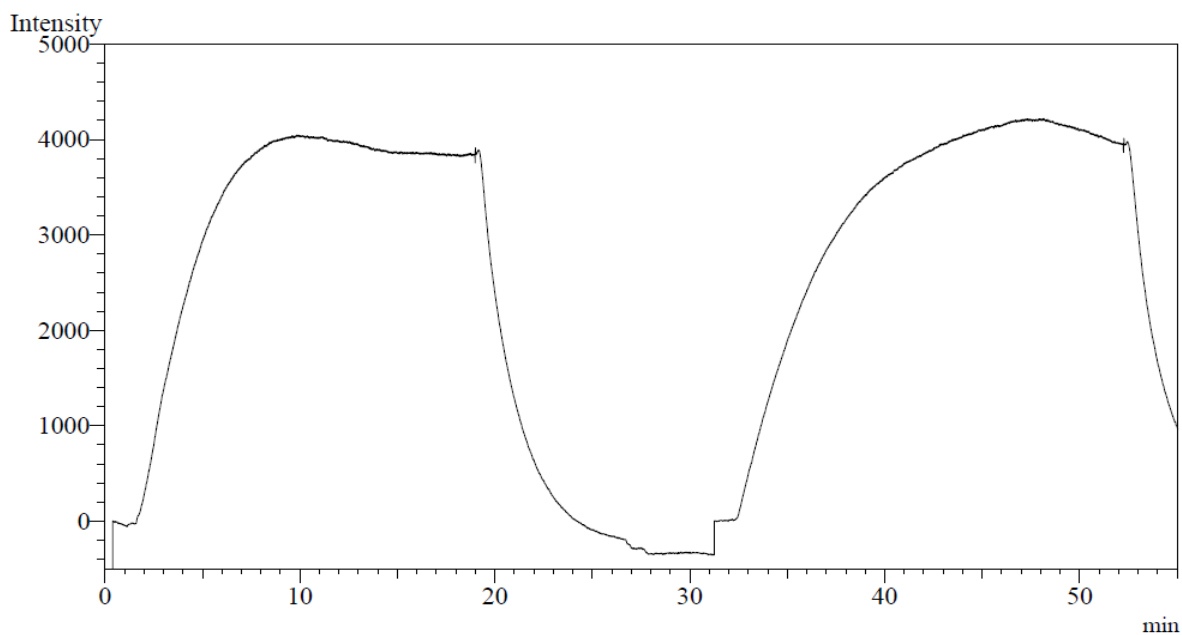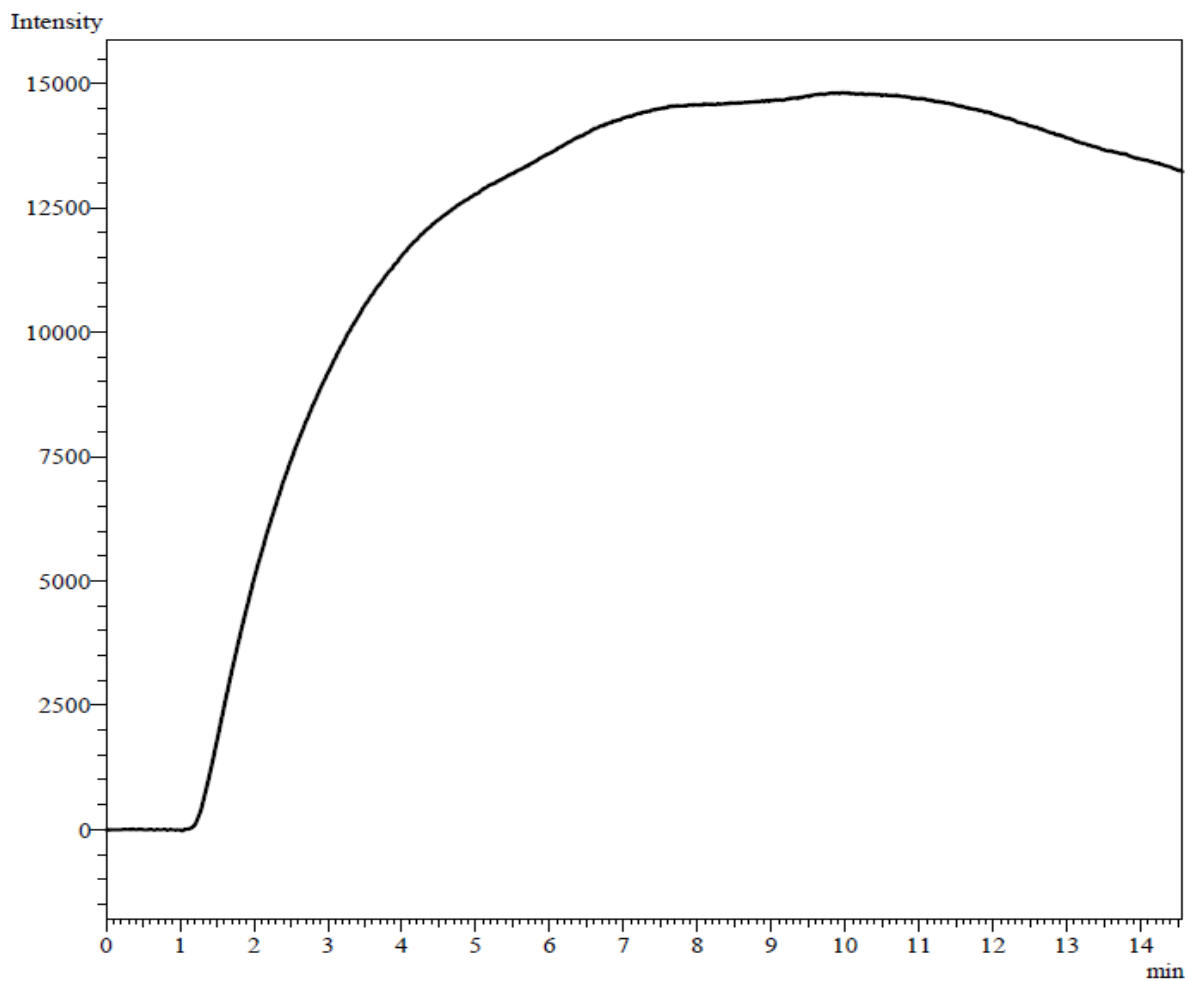
Figure A.5: Water flow optimization: 210 mL/min (0-31 min) and 135 mL/min (31-55 min). Other settings: Interface/water bath: 40 °C. Injector: 40 °C, column flow: 4.74 mL/min (67 kPa). FID: 250 °C, H_2: 30 mL/min, makeup: 30 mL/min, air: 350 mL/min. Test sample: toluene:methanol 10:90 (1 µL) in 1.25 L water.
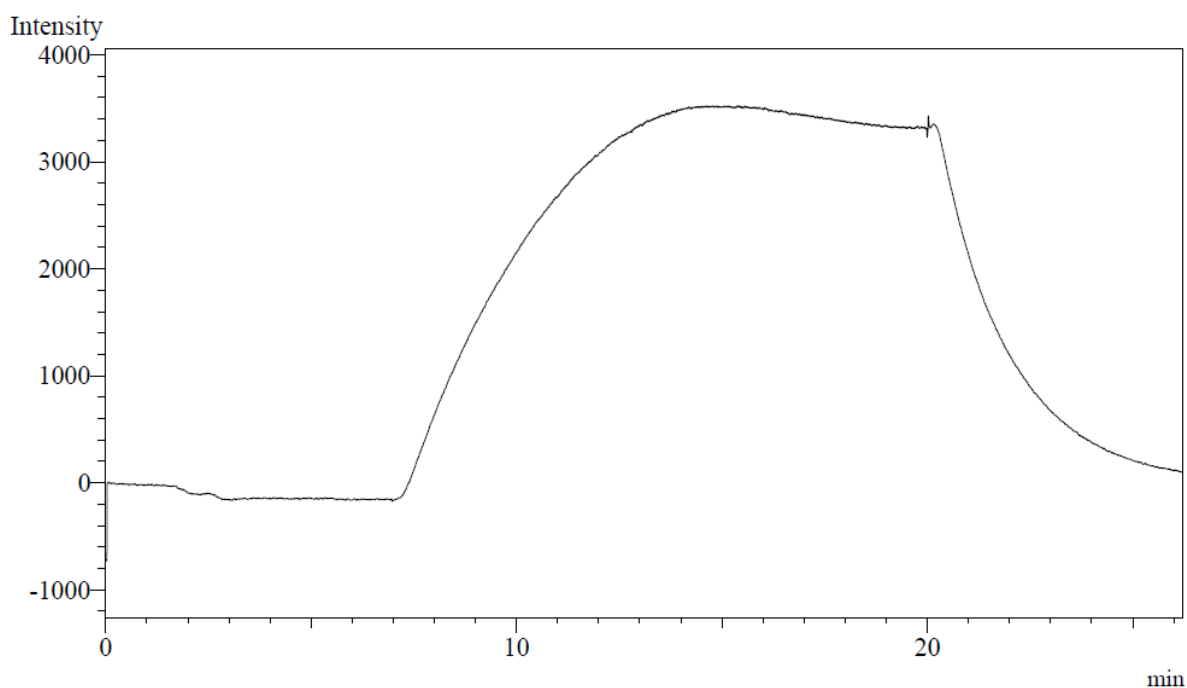
Figure A.6: Water flow optimization: 245 mL/min. Other settings: Interface/water bath: 40 °C. Injector: 40 °C, column flow: 4.74 mL/min (67 kPa). FID: 250 °C, H_2: 30 mL/min, makeup: 30 mL/min, air: 350 mL/min. Test sample: toluene:methanol 10:90 (1 µL) in 1.25 L water.
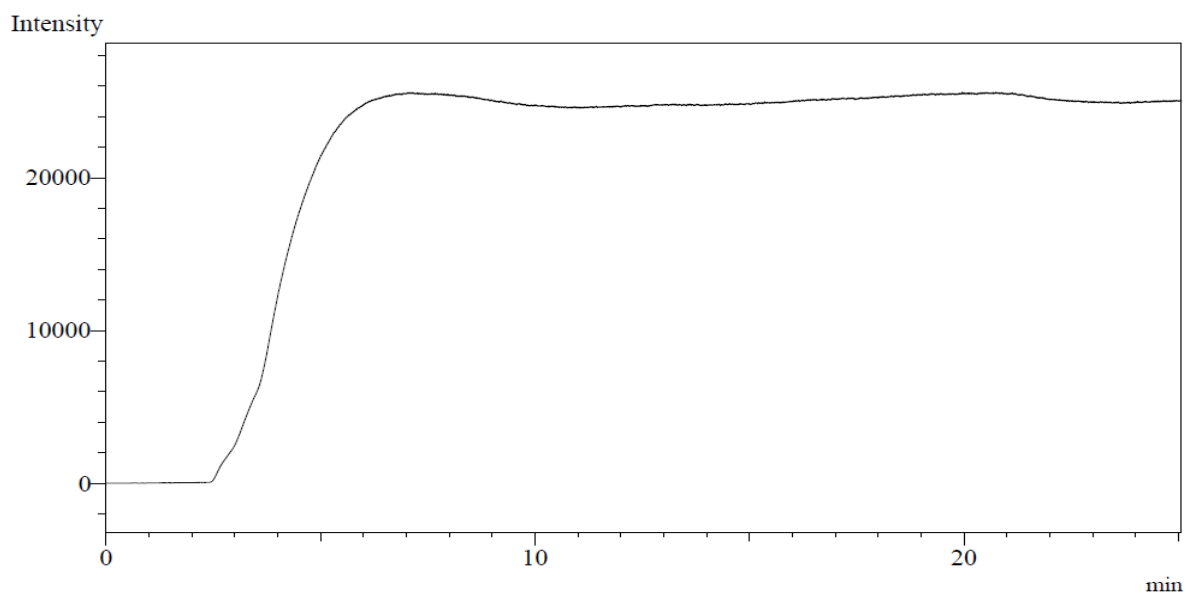
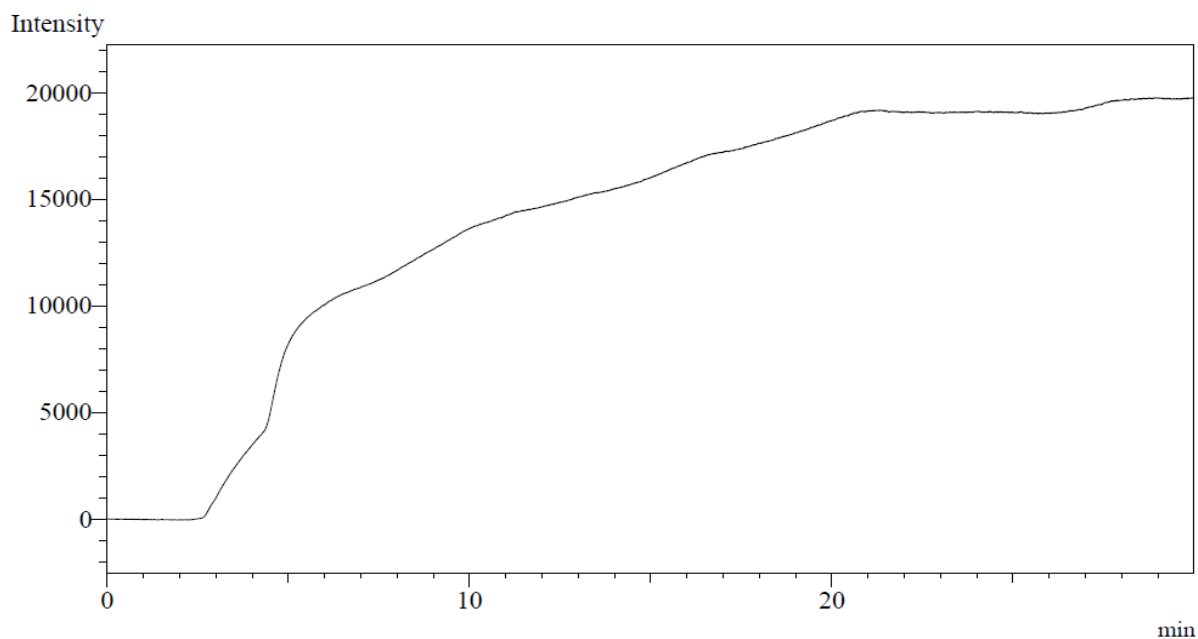**Figure A.7:** Water flow and water bath/interface temperature optimization: Injection of toluene:methanol 10:90 (1 µL) into 1.20 L of water, closed system with recirculation (Figure A.8-Figure A.13 are based on this injection). Settings: Water flow: 210 mL/min. Interface/water bath: 40 °C. Injector: 40 °C, column flow: 4.74 mL/min (67 kPa). FID: 250 °C, H_2: 30 mL/min, makeup: 30 mL/min, air: 350 mL/min.
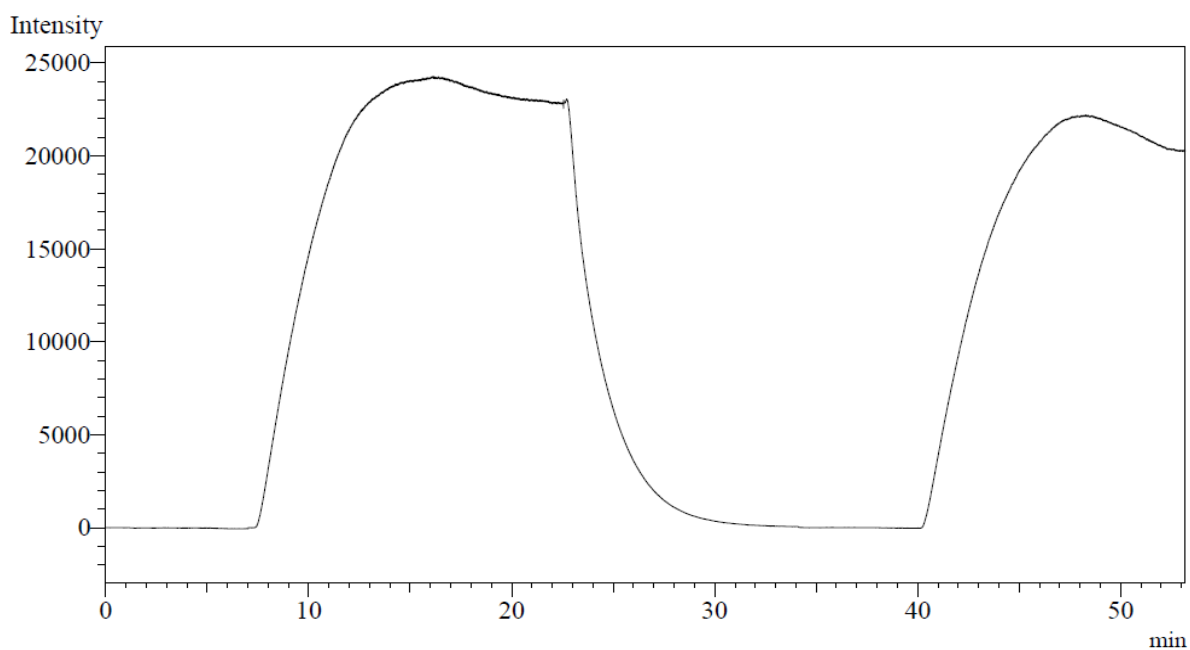

Figure A.8: Water flow optimization: 210 mL/min (0-40 min) and 245 mL/min (40-53 min). Other settings: Interface/water bath: 40 °C. Injector: 40 °C, column flow: 4.74 mL/min (67 kPa). FID: 250 °C, H_2: 30 mL/min, makeup: 30 mL/min, air: 350 mL/min. Test sample: toluene:methanol 10:90 (1 µL) in 1.20 L water.
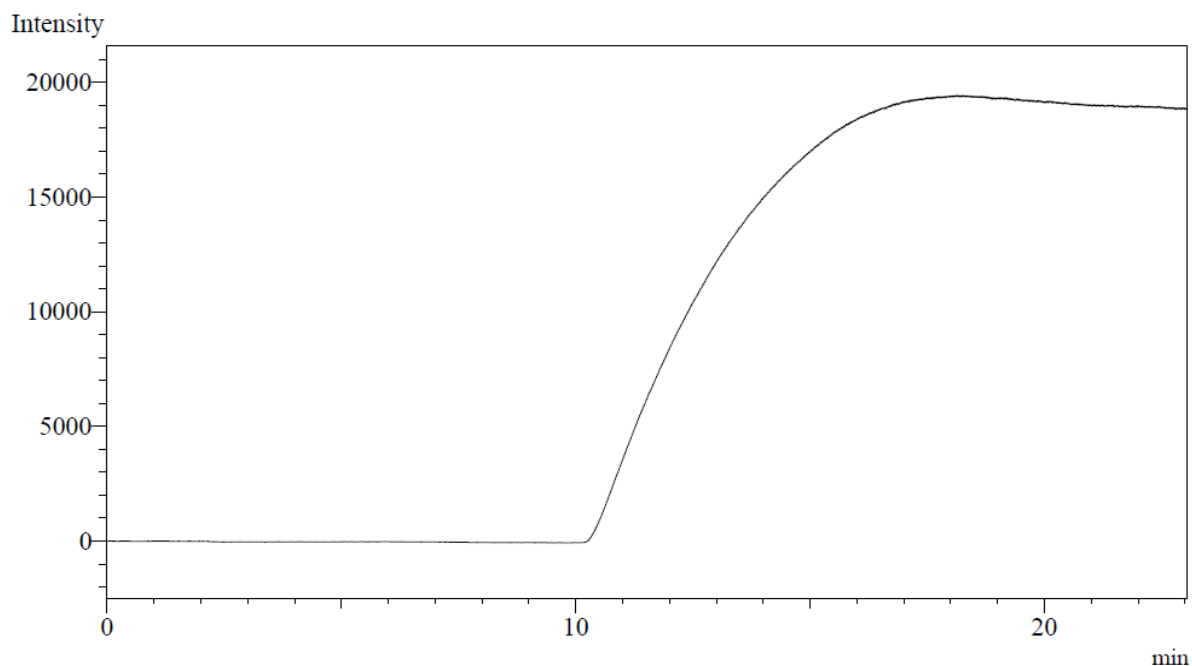
Figure A.9: Water flow optimization: 210 mL/min. Other settings: Interface/water bath: 40 °C. Injector: 40 °C, column flow: 4.74 mL/min (67 kPa). FID: 250 °C, H_2: 30 mL/min, makeup: 30 mL/min, air: 350 mL/min. Test sample: toluene:methanol 10:90 (1 µL) in 1.20 L water.
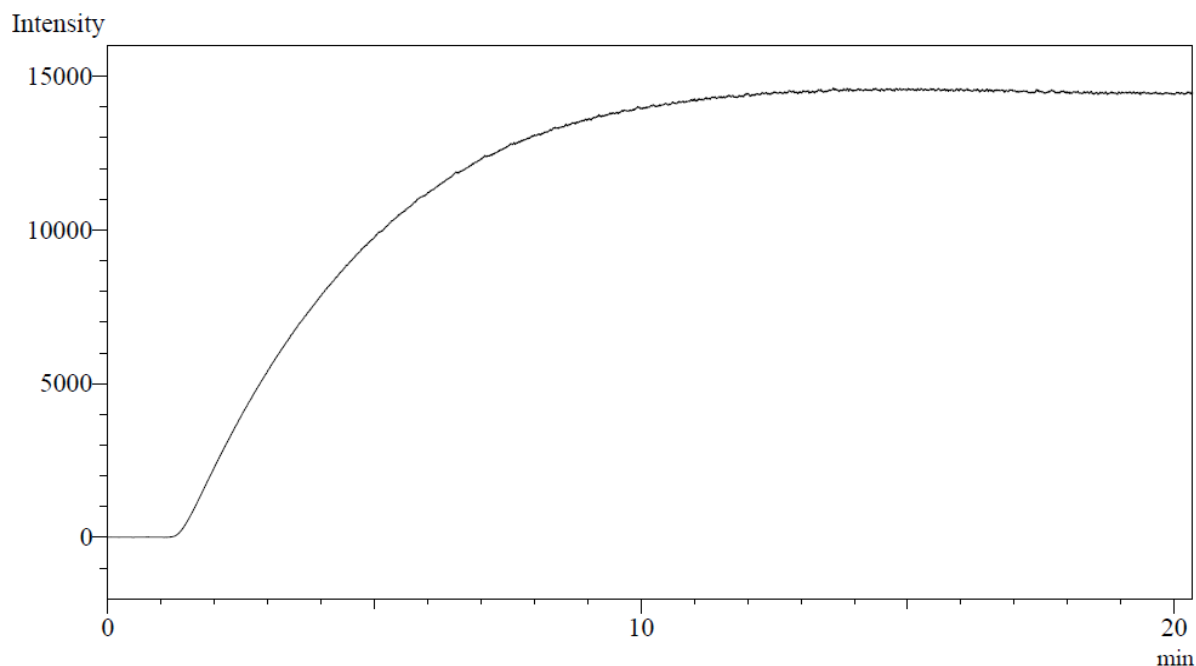
Figure A.10: Water bath/interface temperature optimization: 30 °C. Other settings: Water flow: 245 mL/min. Injector: 40 °C, column flow: 4.74 mL/min (67 kPa). FID: 250 °C, H_2: 30 mL/min, makeup: 30 mL/min, air: 350 mL/min. Test sample: toluene:methanol 10:90 (1 µL) in 1.20 L water.
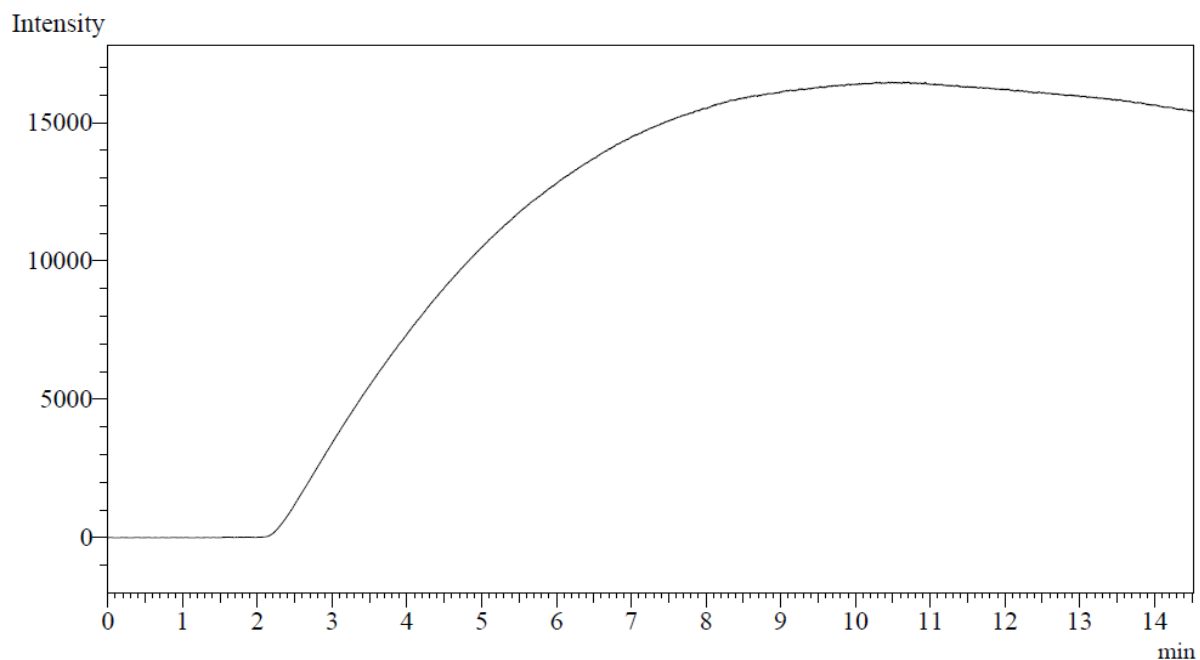
Figure A.11: Water bath/interface temperature optimization: 40 °C. Other settings: Water flow: 245 mL/min. Injector: 40 °C, column flow: 4.74 mL/min (67 kPa). FID: 250 °C, H_2: 30 mL/min, makeup: 30 mL/min, air: 350 mL/min. Test sample: toluene:methanol 10:90 (1 μL) in 1.20 L water.
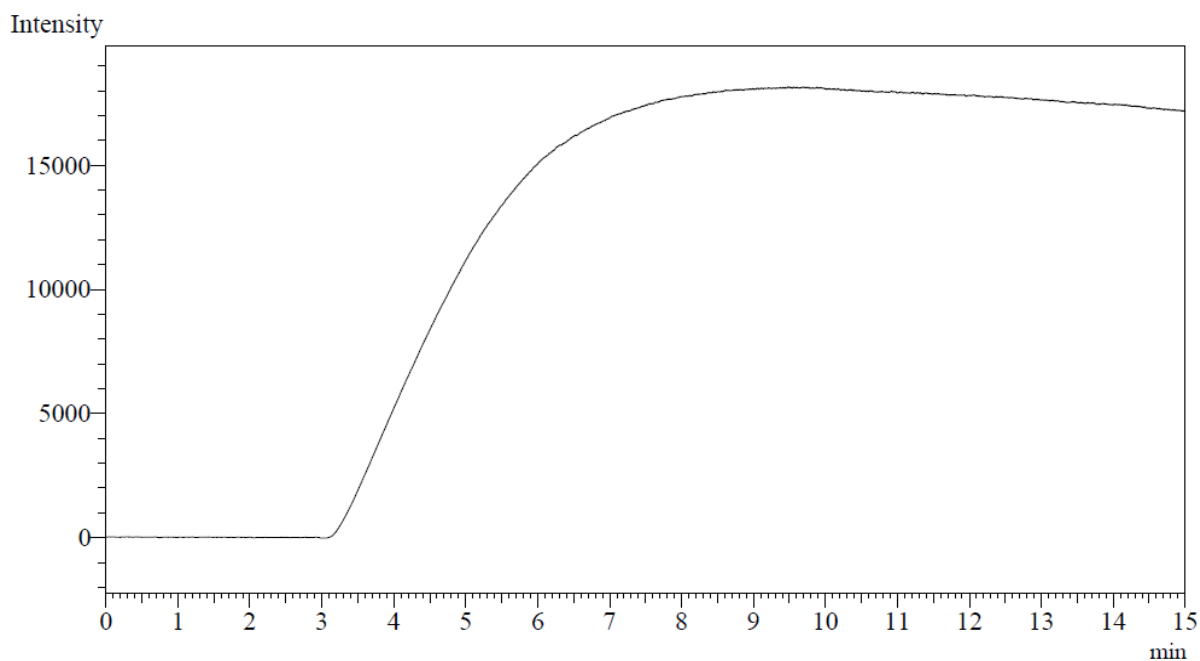
Figure A.12: Water bath/interface temperature optimization: 50 °C. Other settings: Water flow: 245 mL/min. Injector: 40 °C, column flow: 4.74 mL/min (67 kPa). FID: 250 °C, H_2: 30 mL/min, makeup: 30 mL/min, air: 350 mL/min. Test sample: toluene:methanol 10:90 (1 μL) in 1.20 L water.
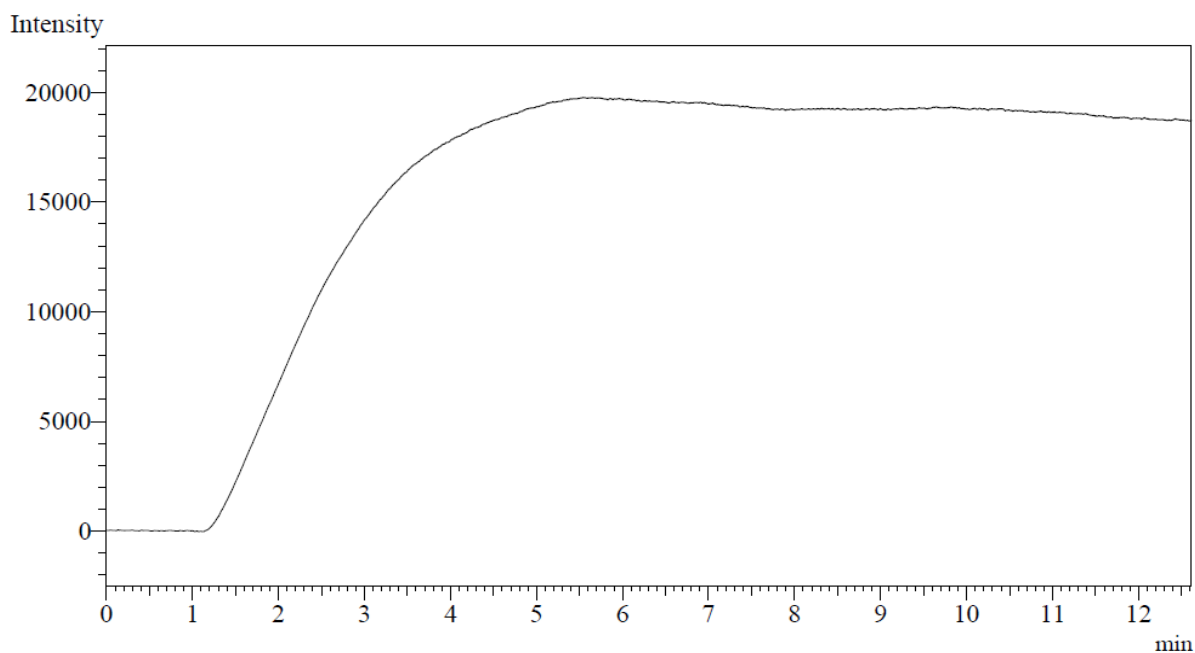
Figure A.13: Water bath/interface temperature optimization: 60 °C. Other settings: Water flow: 245 mL/min. Injector: 40 °C, column flow: 4.74 mL/min (67 kPa). FID: 250 °C, H_2: 30 mL/min, makeup: 30 mL/min, air: 350 mL/min. Test sample: toluene:methanol 10:90 (1 µL) in 1.20 L water.
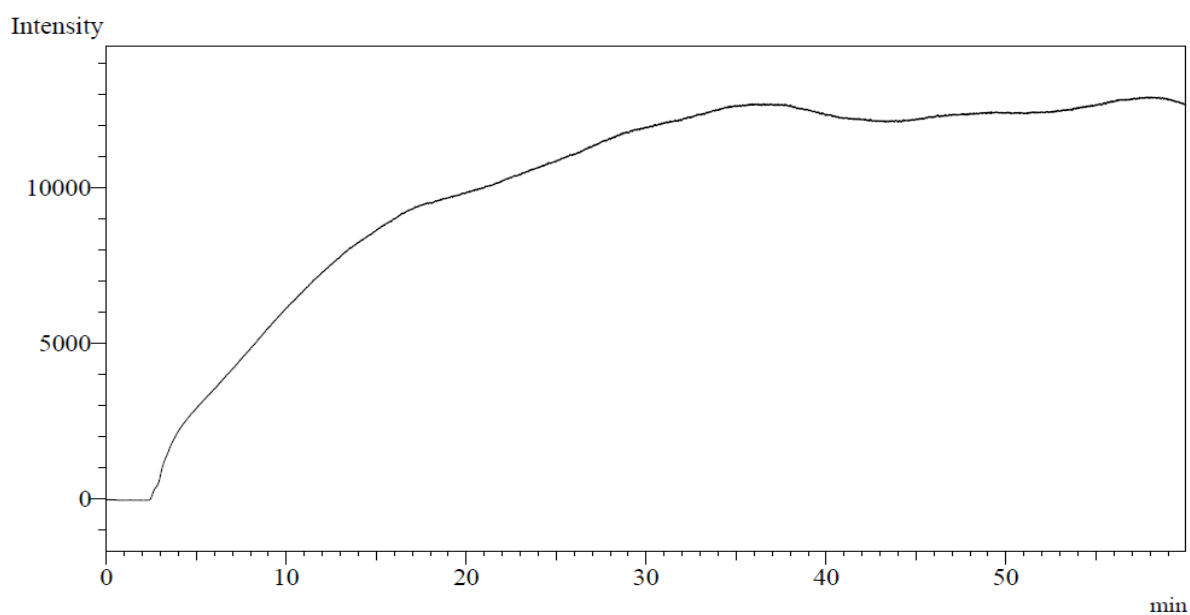
Figure A.14: MI-Hydrogen flow optimization: Injection of toluene:methanol 10:90 (1 µL) into 1.20 L of water, closed system with recirculation (Figure A.15-Figure A.17 are based on this injection). Settings: Water flow: 245 mL/min. Interface/water bath: 40 °C. Injector: 40 °C, "column flow": 4.74 mL/min (67 kPa). FID: 250 °C, H_2: 30 mL/min, makeup: 30 mL/min, air: 350 mL/min. Test sample: toluene:methanol 10:90 (1 µL) in 1.20 L water.

Figure A.15: MI-Hydrogen flow optimization: 5.01 mL/min (70 kPa). Other settings: Water flow: 245 mL/min. Interface/water bath: 40 °C. Injector: 40 °C. FID: 250 °C, H_2: 30 mL/min, makeup: 30 mL/min, air: 350 mL/min. Test sample: toluene:methanol 10:90 (1 µL) in 1.20 L water.

Figure A.16: MI-Hydrogen flow optimization: 10.05 mL/min (119 kPa). Other settings: Water flow: 245 mL/min. Interface/water bath: 40 °C. Injector: 40 °C. FID: 250 °C, H_2: 30 mL/min, makeup: 30 mL/min, air: 350 mL/min. Test sample: toluene:methanol 10:90 (1 μL) in 1.20 L water.

Figure A.17: MI-Hydrogen flow optimization: 20.06 mL/min (193 kPa). Other settings: Water flow: 245 mL/min. Interface/water bath: 40 °C. Injector: 40 °C. FID: 250 °C, H_2: 30 mL/min, makeup: 30 mL/min, air: 350 mL/min. Test sample: toluene:methanol 10:90 (1 μL) in 1.20 L water.

Figure A.18: FID-Makeup gas optimization: Injection of toluene:methanol 10:90 (1 µL) into 1.20 L of water, closed system with recirculation (Figure A.19 and Figure A.20 are based on this injection). Settings: Water flow: 245 mL/min. Interface/water bath: 40 °C. Injector: 40 °C, column flow: 10.05 mL/min (119 kPa). FID: 250 °C, H_2: 30 mL/min, makeup: 30 mL/min, air: 350 mL/min.
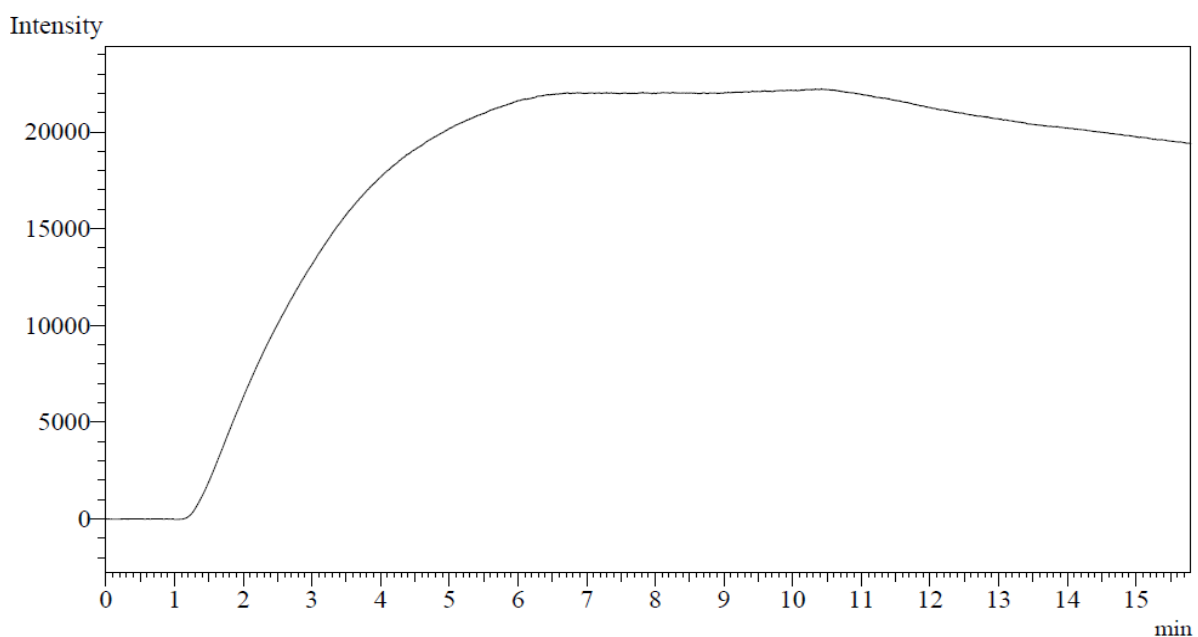
Figure A.19: FID-Makeup gas optimization: With makeup gas, 30 mL/min. Other settings: Water flow: 245 mL/min. Interface/water bath: 40 °C. Injector: 40 °C, column flow: 10.05 mL/min (119 kPa). FID: 250 °C, H_2: 30 mL/min, air: 350 mL/min. Test sample: toluene:methanol 10:90 (1 µL) in 1.20 L water.
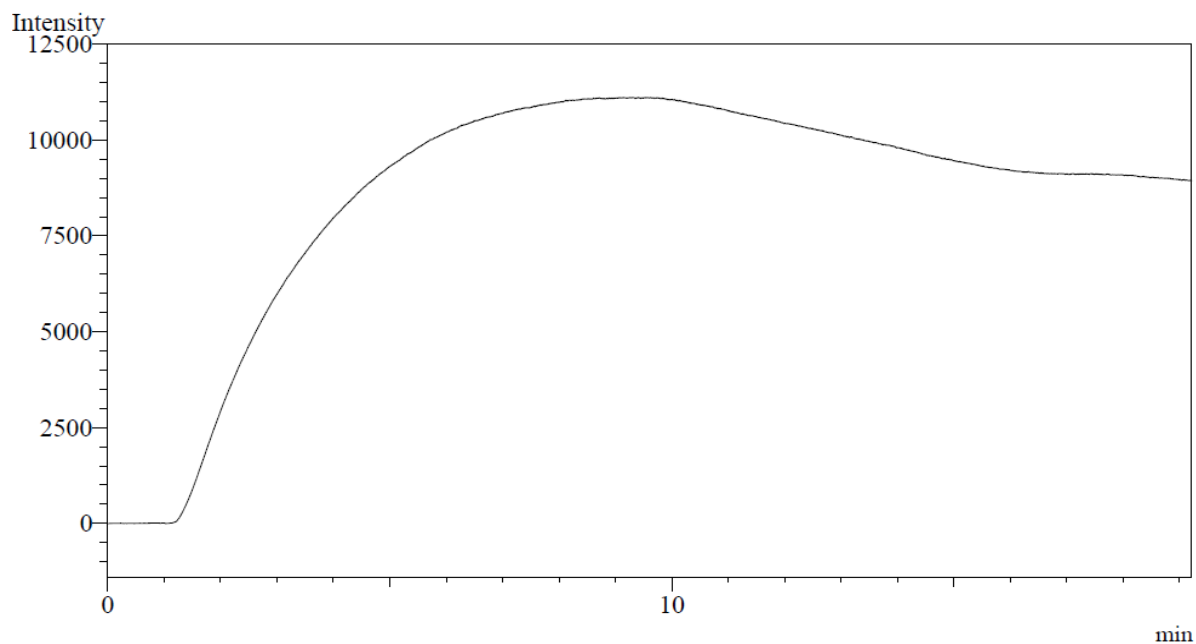
Figure A.20: FID-Makeup gas optimization: Without makeup gas. Other settings: Water flow: 245 mL/min. Interface/water bath: 40 °C. Injector: 40 °C, column flow: 10.05 mL/min (119 kPa). FID: 250 °C, H_2: 30 mL/min, air: 350 mL/min. Test sample: toluene:methanol 10:90 (1 µL) in 1.20 L water.
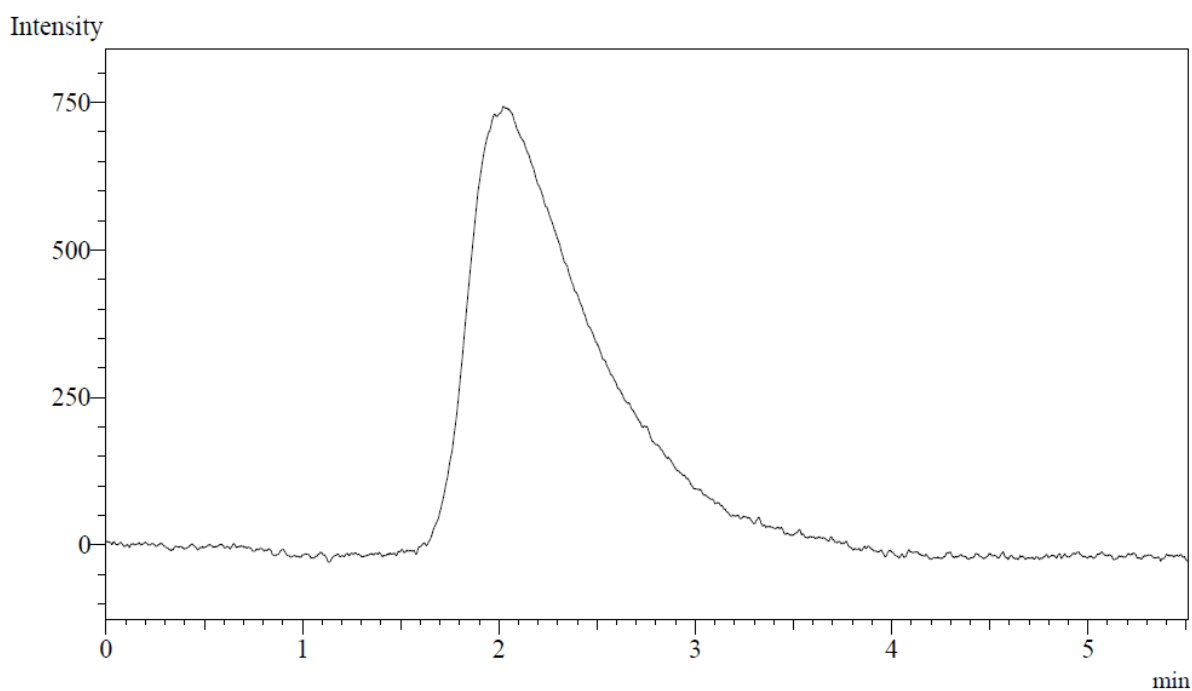
Figure A.21: FID-Hydrogen/air flow optimization: H_2: 30 mL/min, Air: 350 mL/min. Air analysis: Toluene vapor (10 µL). Other settings: Interface: 40 °C. Injector: 40 °C, column flow: 10.05 mL/min (119 kPa). FID: 250 °C, makeup: 30 mL/min air: 350 mL/min.
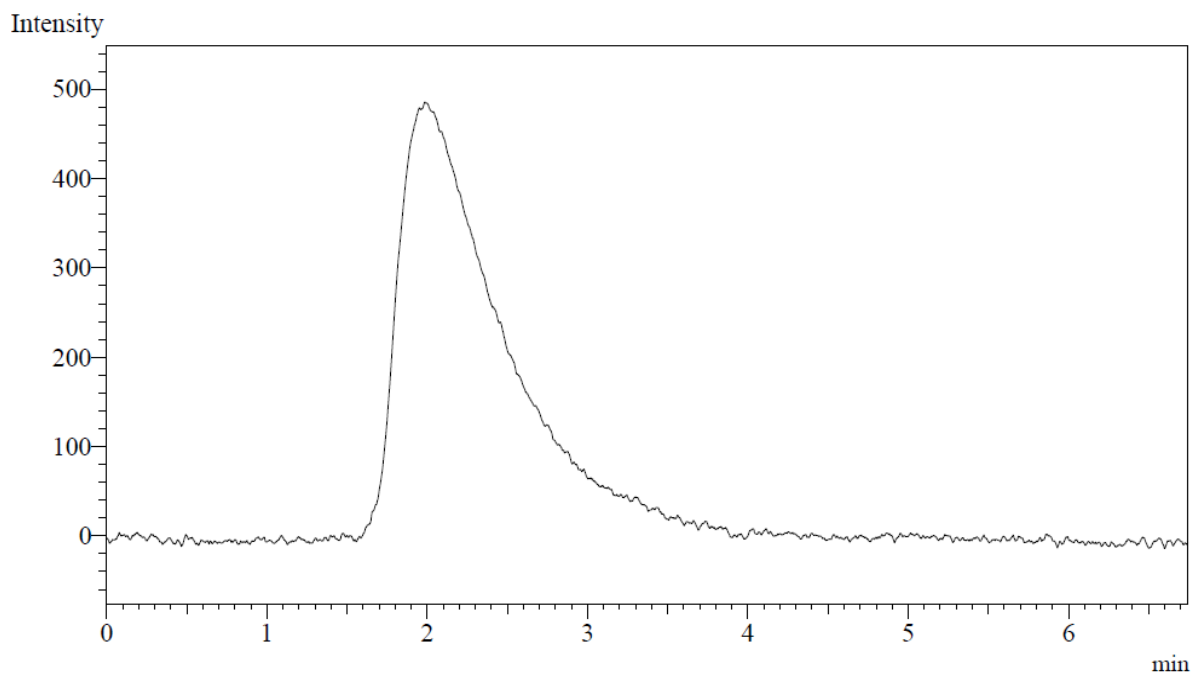
Figure A.22: FID-Hydrogen flow optimization: 20 mL/min. Air analysis: Toluene vapor (10 µL). Other settings: Interface: 40 °C. Injector: 40 °C, column flow: 10.05 mL/min (119 kPa). FID: 250 °C, makeup: 30 mL/min air: 350 mL/min.
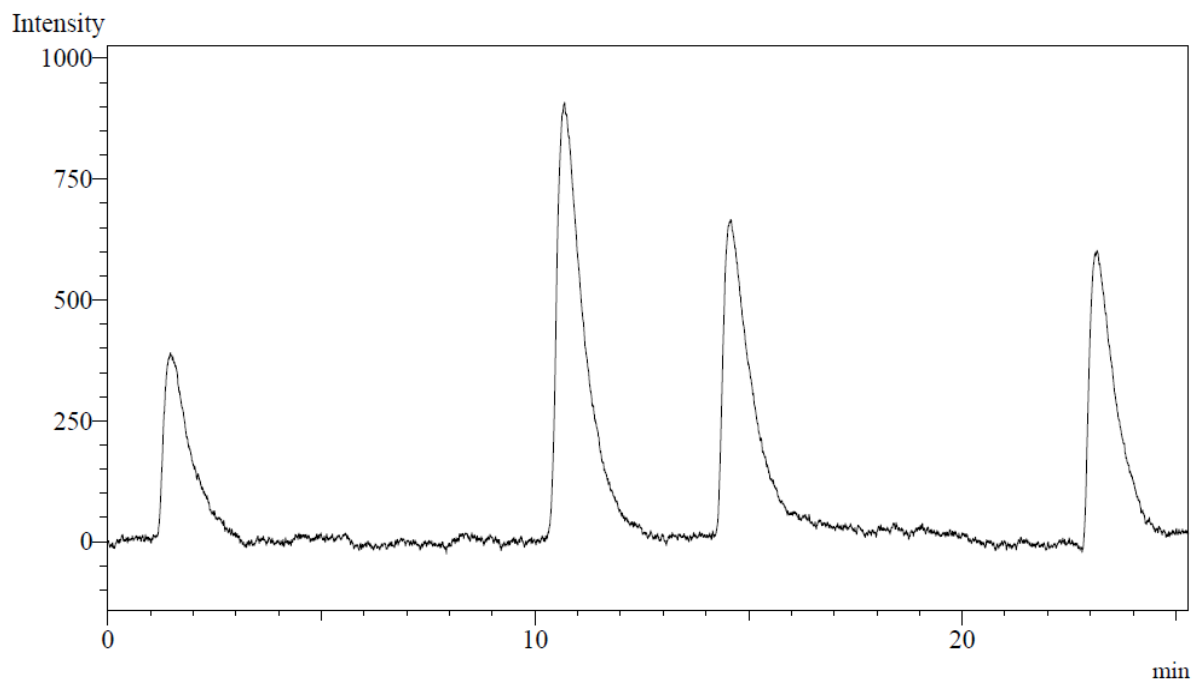
Figure A.23: FID-Hydrogen flow optimization: 40 mL/min. Air analysis: Toluene vapor (10 µL x 4, incorrect injection for the first two). Other settings: Interface: 40 °C. Injector: 40 °C, column flow: 10.05 mL/min (119 kPa). FID: 250 °C, makeup: 30 mL/min air: 350 mL/min.
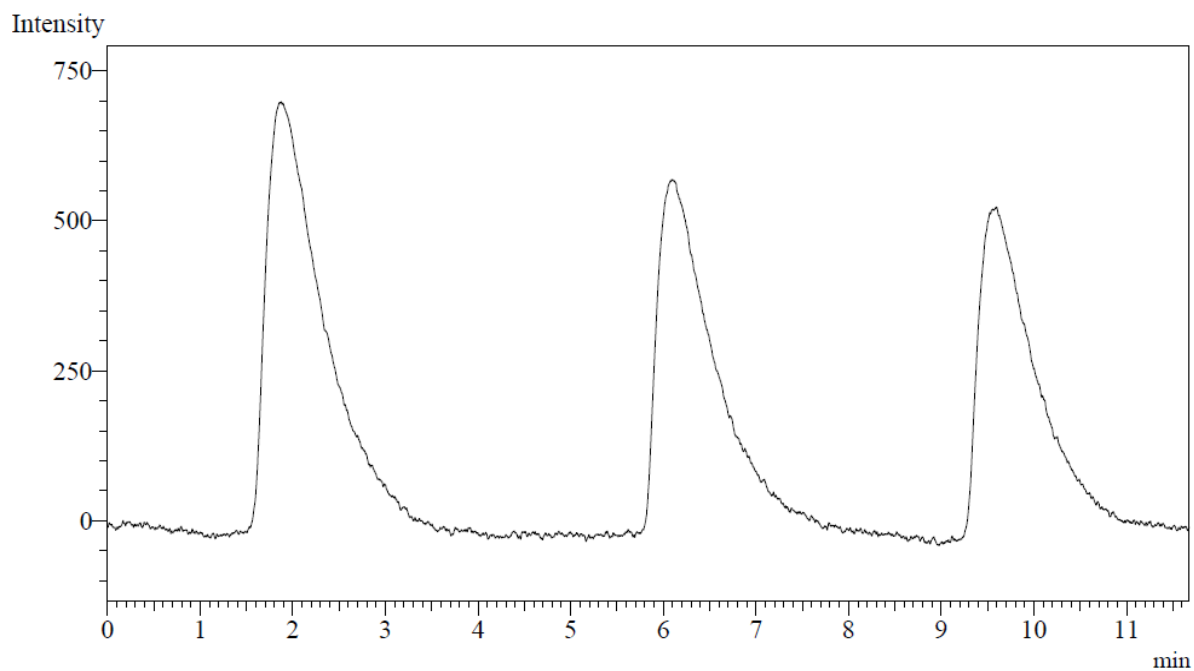
Figure A.24: FID-Air flow optimization: 400 mL/min. Air analysis: Toluene vapor (10 µL x 3). Other settings: Interface: 40 °C. Injector: 40 °C, column flow: 10.05 mL/min (119 kPa). FID: 250 °C, makeup: 30 mL/min.
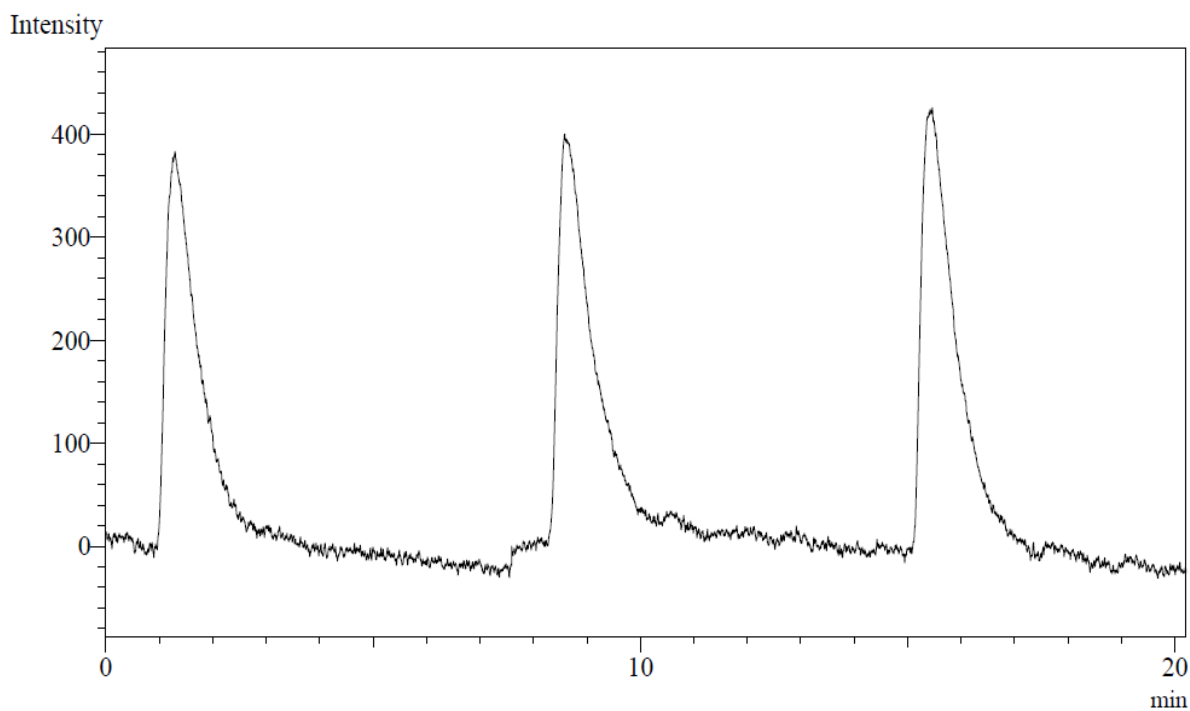
Figure A.25: FID-Make up flow optimization: 30 mL/min. Air analysis: Toluene vapor (10 µL x 3). Other settings: Interface: 40 °C. Injector: 40 °C, column flow: 10.05 mL/min (119 kPa). FID: 250 °C, air: 350 mL/min.
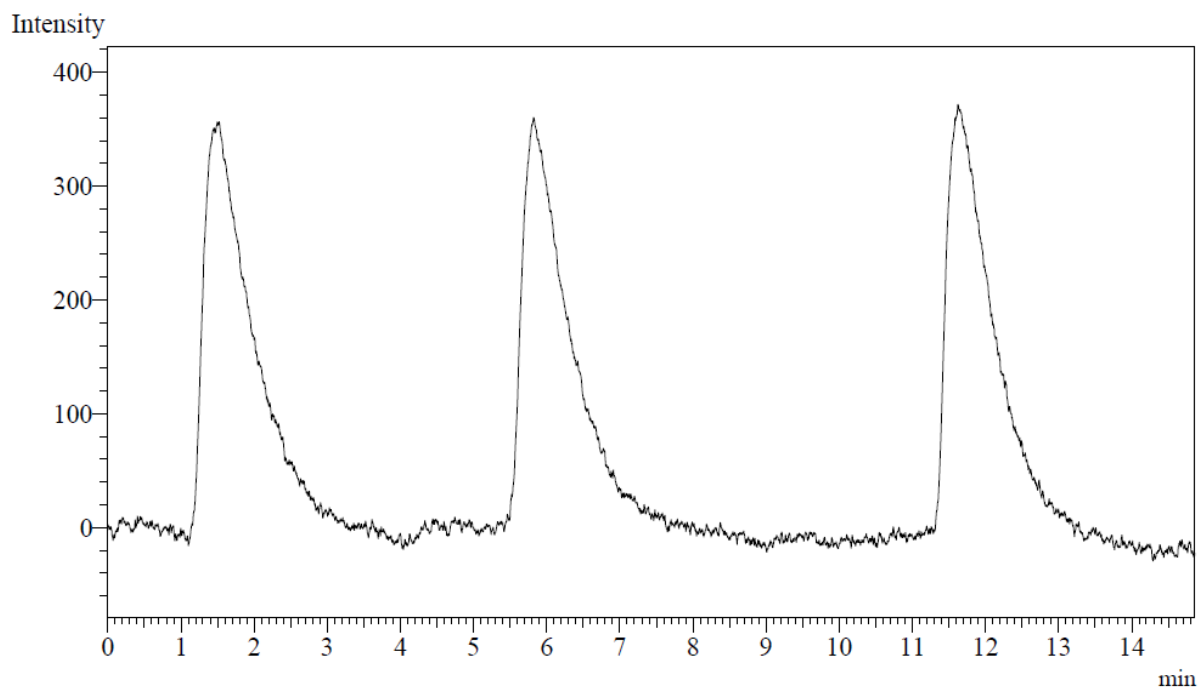
Figure A.26: FID-Make up flow optimization: 20 mL/min. Air analysis: Toluene vapor (10 µL x 3). Other settings: Interface: 40 °C. Injector: 40 °C, column flow: 10.05 mL/min (119 kPa). FID: 250 °C, air: 350 mL/min.
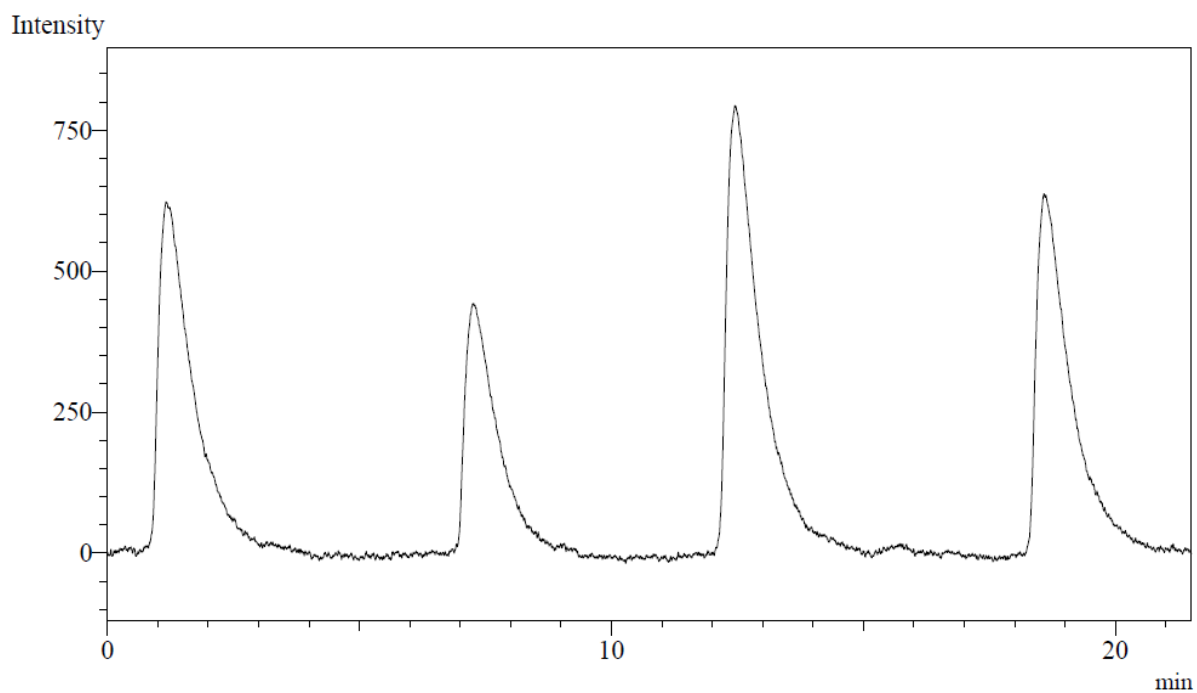
Figure A.27: FID-Make up flow optimization: 40 mL/min. Air analysis: Toluene vapor (10 µL x 4). Other settings: Interface: 40 °C. Injector: 40 °C, column flow: 10.05 mL/min (119 kPa). FID: 250 °C, air: 350 mL/min.
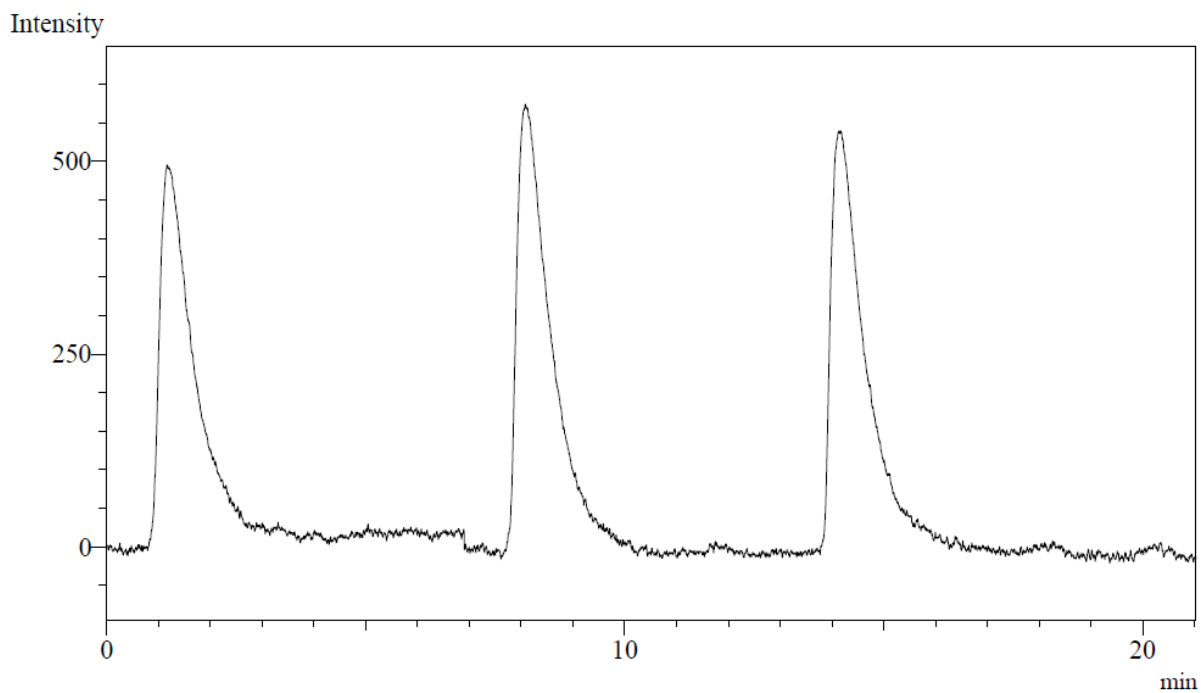
Figure A.28: FID-Make up flow optimization: 40 mL/min. Air analysis: Toluene vapor (10 µL x 3). Other settings: Interface: 40 °C. Injector: 40 °C, column flow: 10.05 mL/min (119 kPa). FID: 250 °C, air: 350 mL/min.
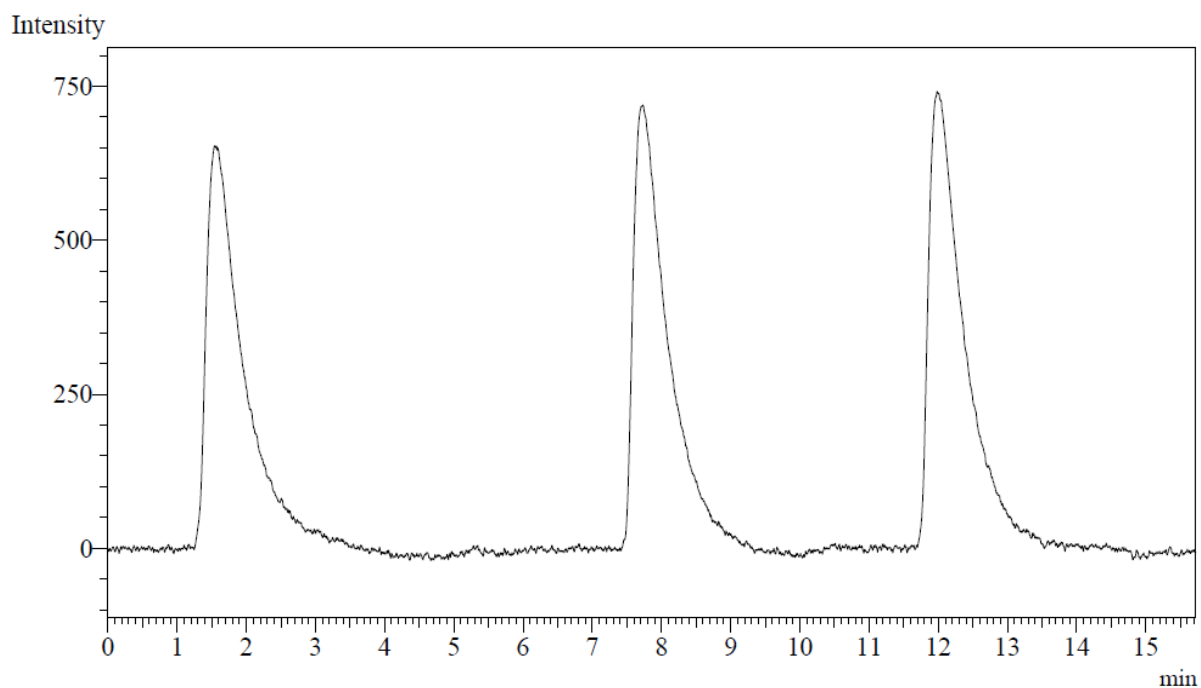
Figure A.29: FID-Make up flow optimization: 40 mL/min. Air analysis: n-heptane vapor (10 µL x 3). Other settings: Interface: 40 °C. Injector: 40 °C, column flow: 10.05 mL/min (119 kPa). FID: 250 °C, air: 350 mL/min.
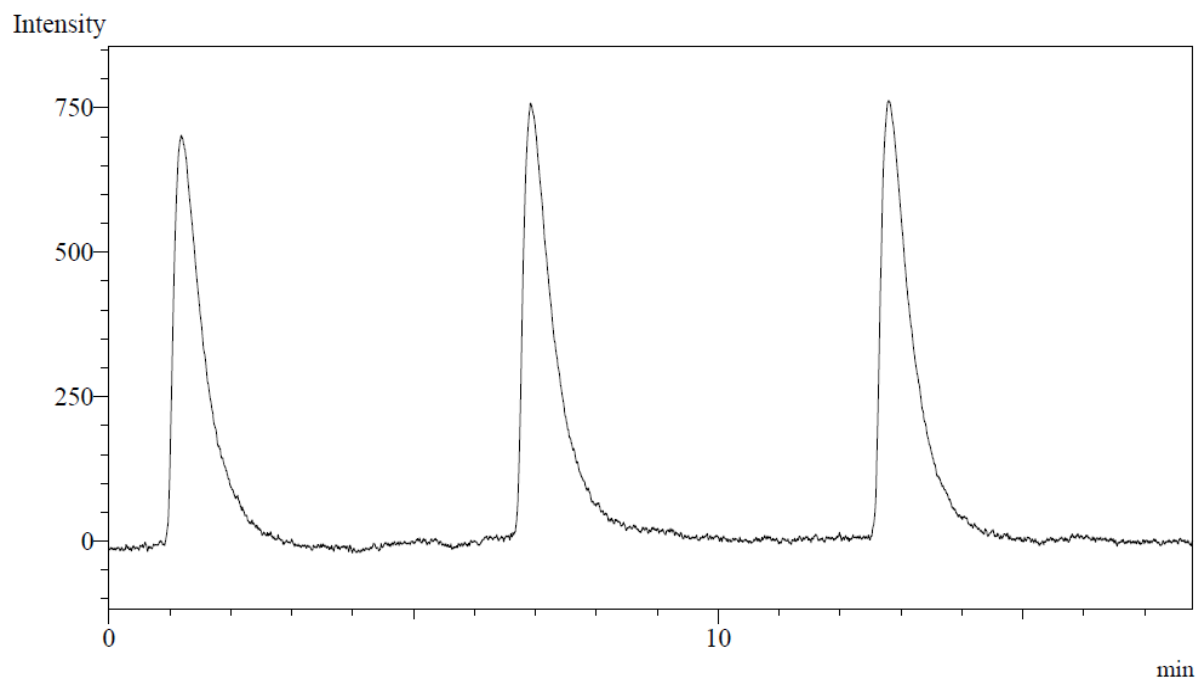
Figure A.30: FID-Make up flow optimization: 50 mL/min. Air analysis: Toluene vapor (10 µL x 3). Other settings: Interface: 40 °C. Injector: 40 °C, column flow: 10.05 mL/min (119 kPa). FID: 250 °C, air: 350 mL/min.
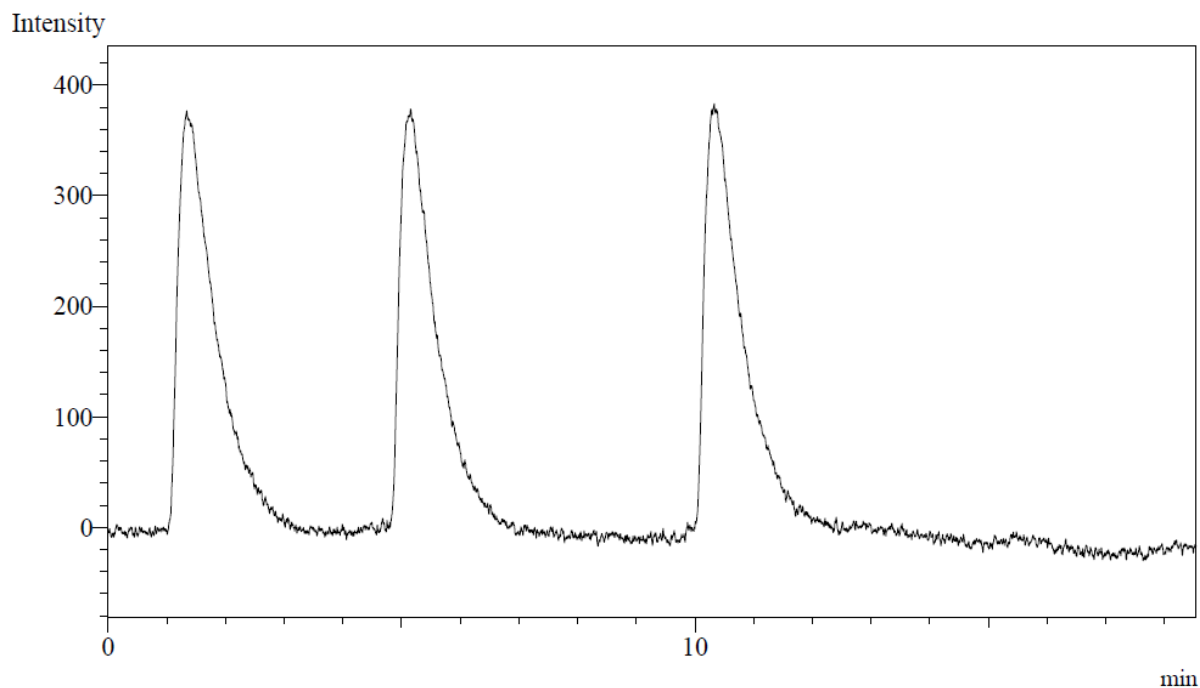
Figure A.31: FID-Make up flow optimization: 50 mL/min. Air analysis: n-heptane vapor (10 µL x 3). Other settings: Interface: 40 °C. Injector: 40 °C, column flow: 10.05 mL/min (119 kPa). FID: 250 °C, air: 350 mL/min.

C.3 MIFID - Oil in water
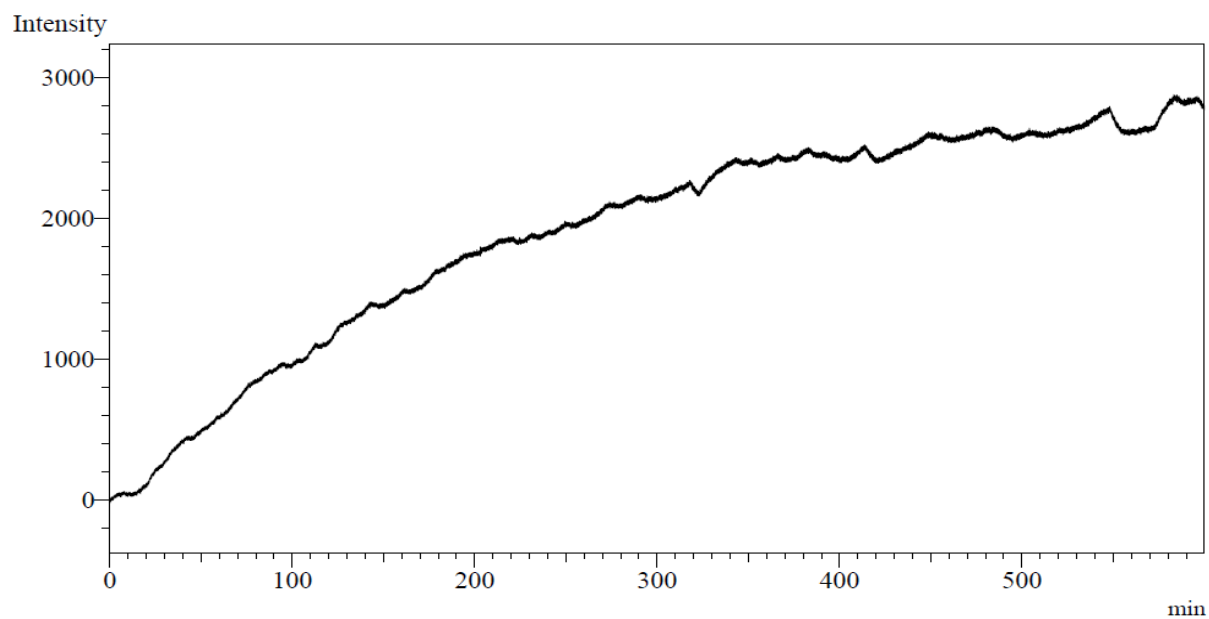
Figure A.32: Oil in water MIFID analysis: Troll B (10.2 mg) in 1.20 L of recirculating water
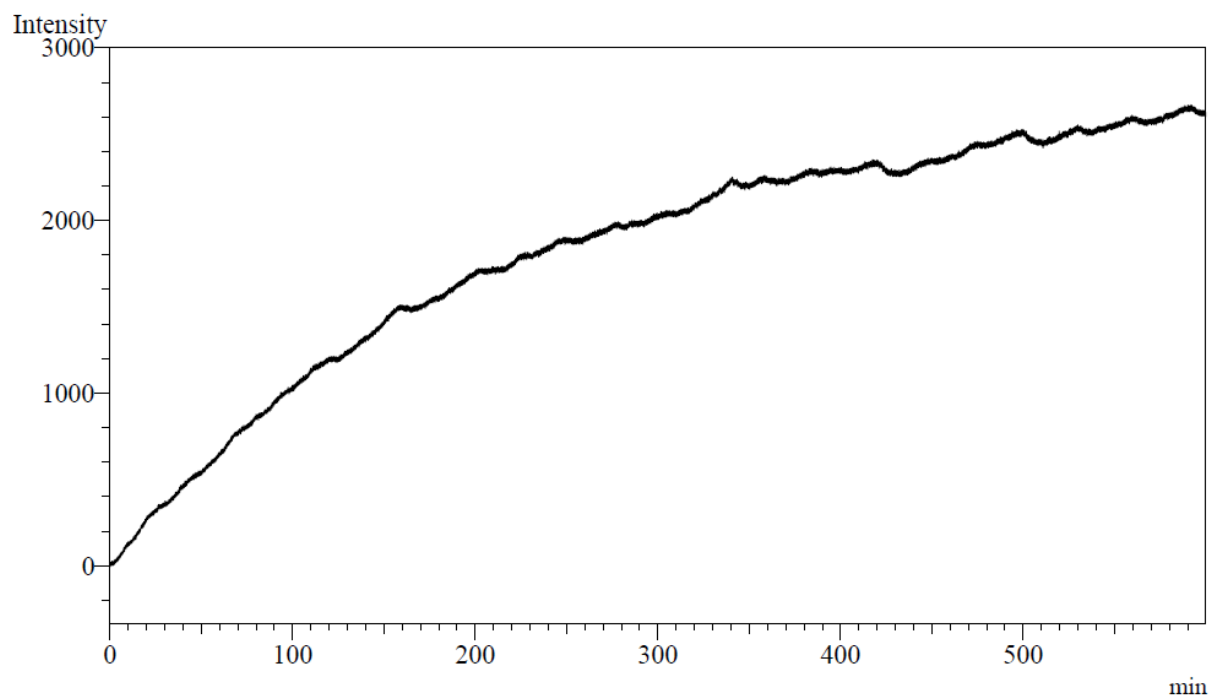
Figure A.33: Oil in water MIFID analysis: Unspecified 1 (10.1 mg) in 1.20 L of recirculating water
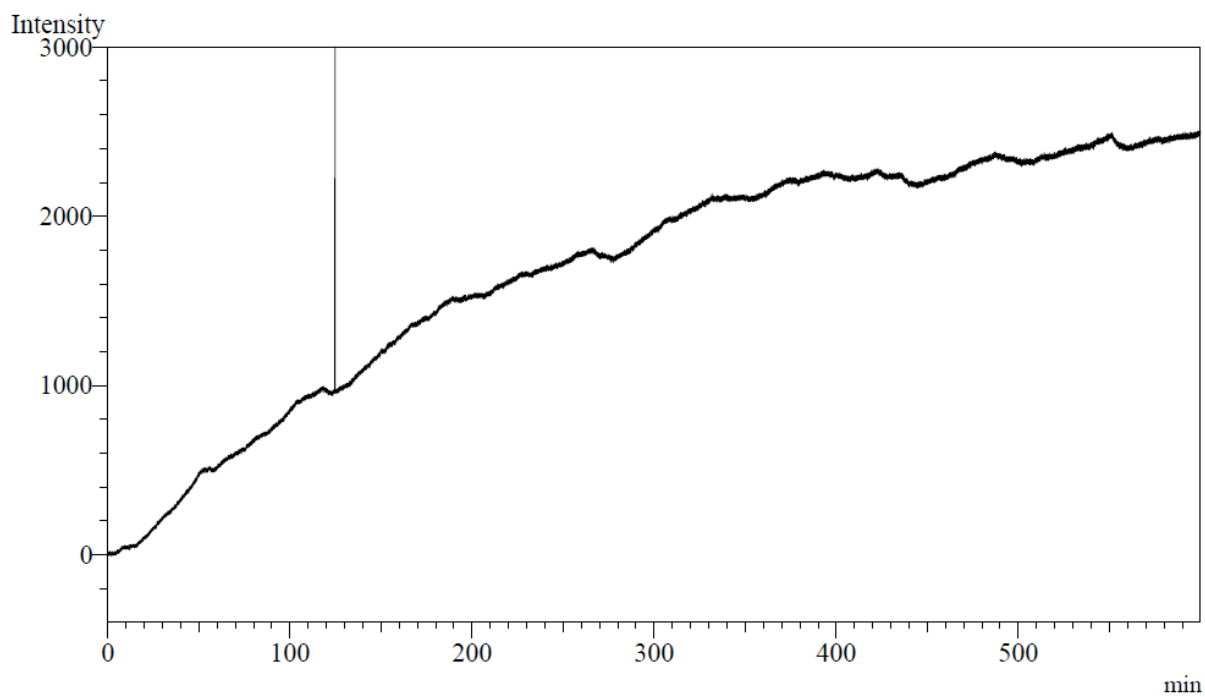
Figure A.34: Oil in water MIFID analysis: Balder Blend (10.3 mg) in 1.20 L of recirculating water
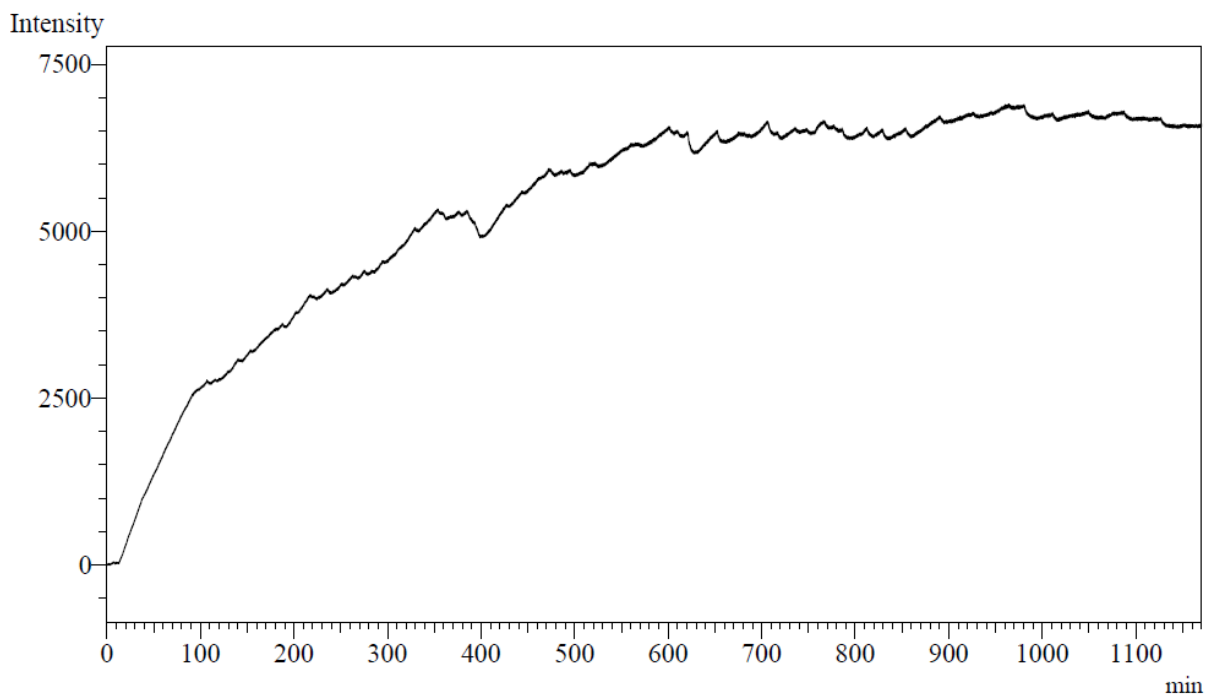
Figure A.35: Oil in water MIFID analysis: Unspecified 2 (10.1 mg) in 1.20 L of recirculating water
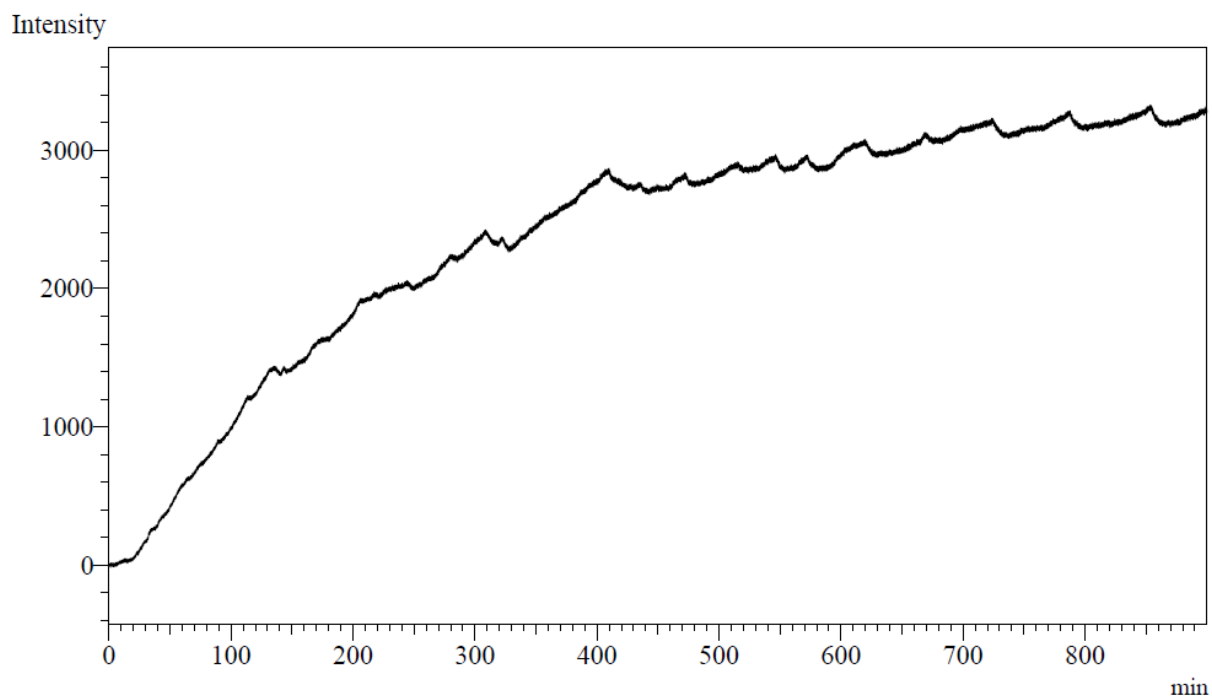
Figure A.36: Oil in water MIFID analysis: Norne Blend (10.9 mg) in 1.20 L of recirculating water
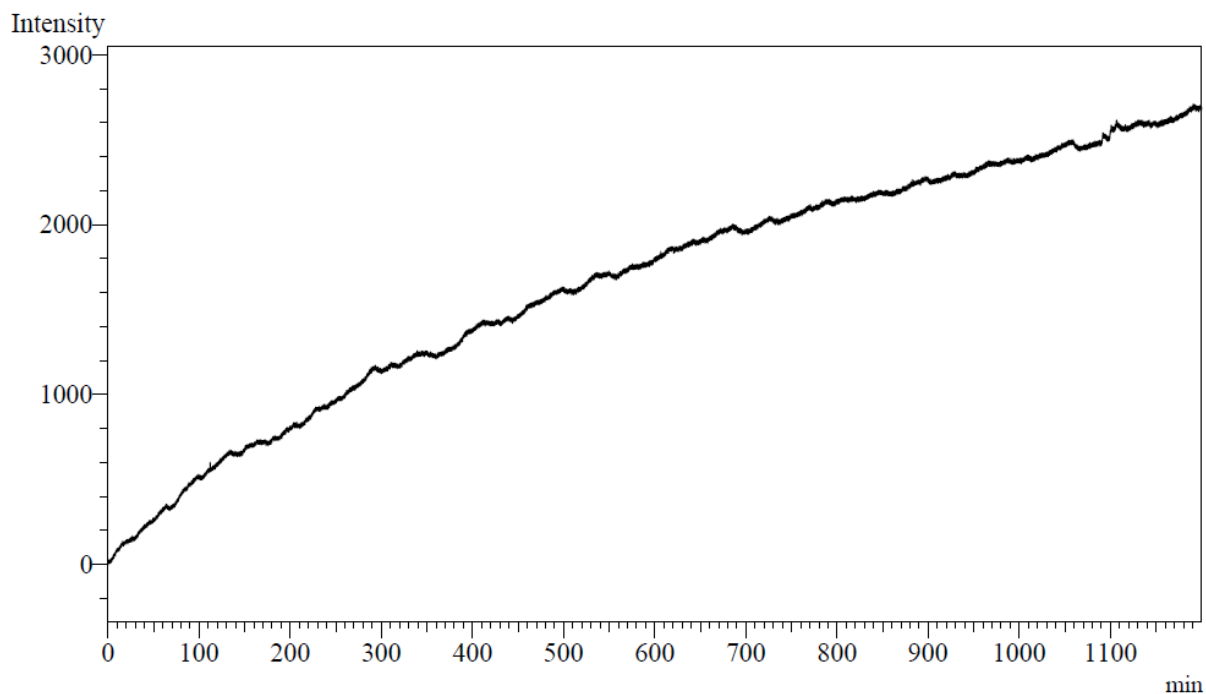
Figure A.37: Oil in water MIFID analysis: Falk (10.5 mg) in 1.20 L of recirculating water
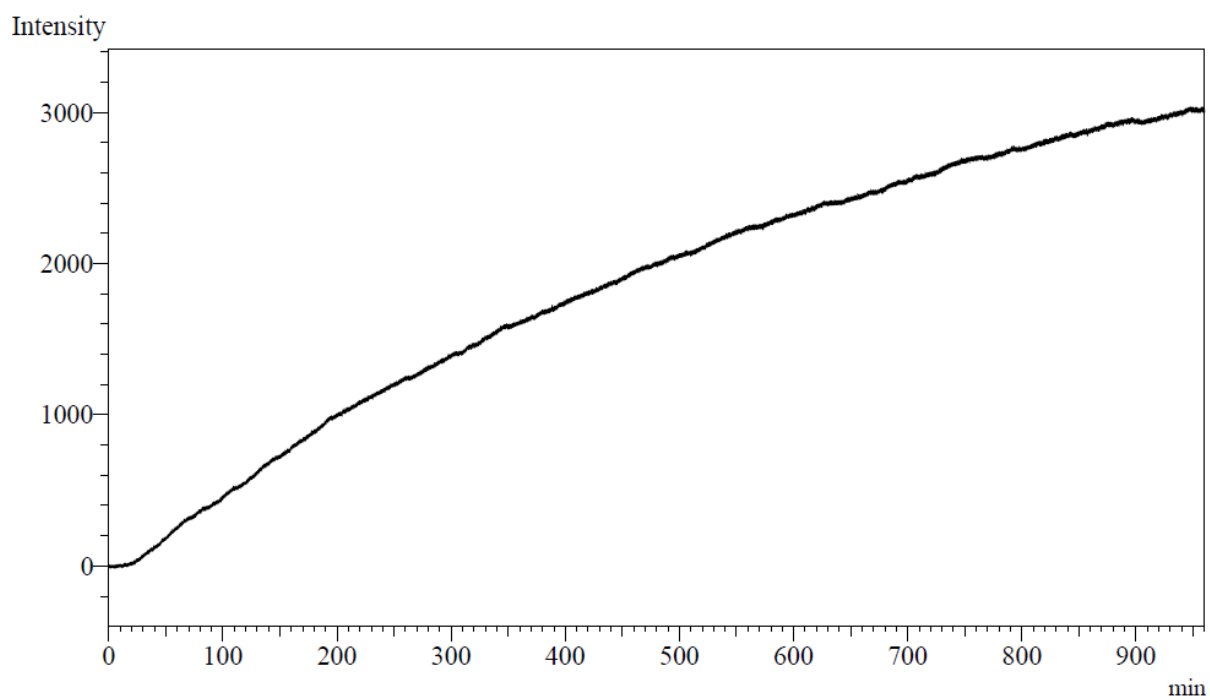
Figure A.38: Oil in water MIFID analysis: Peregrino (9.9 mg) in 1.20 L of recirculating water
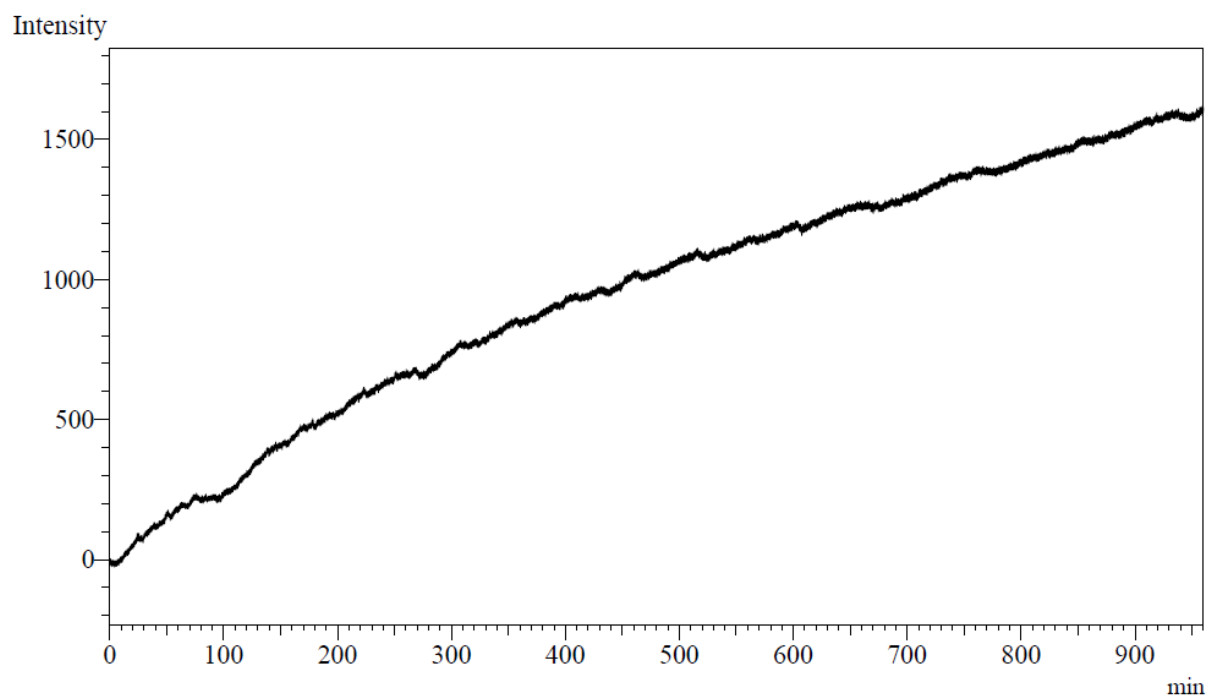
Figure A.39: Oil in water MIFID analysis: Mariner Maureen (9.8 mg) in 1.20 L of recirculating water
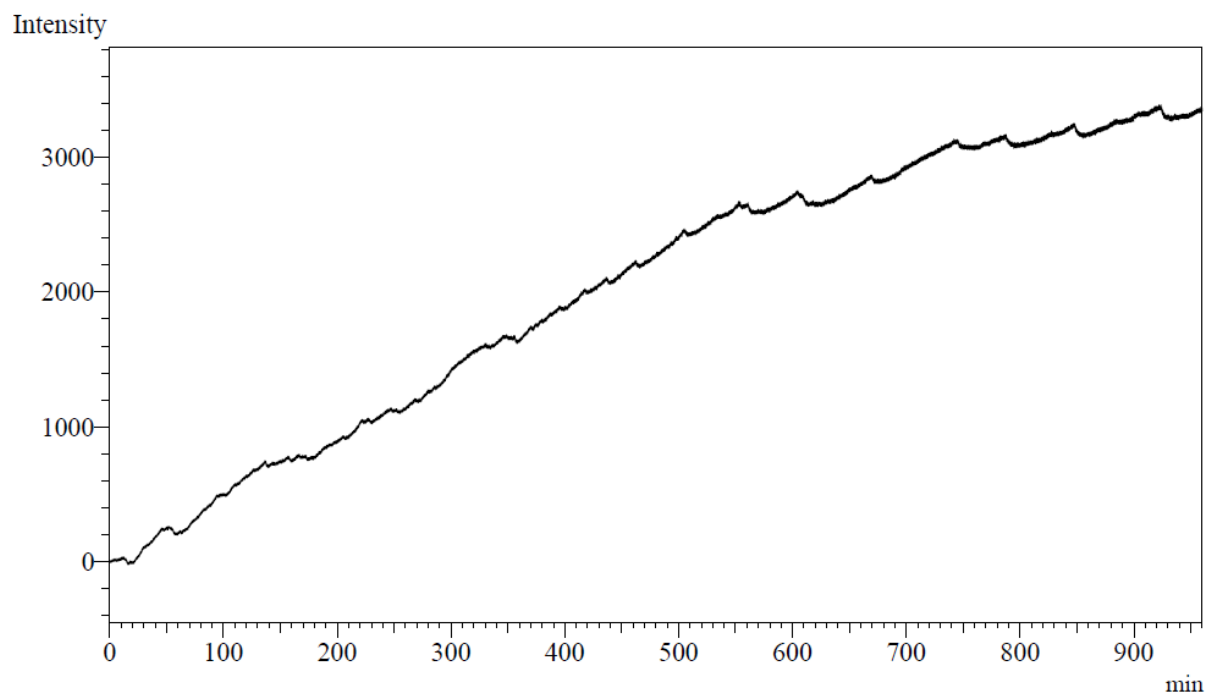
Figure A.40: Oil in water MIFID analysis: Heidrun Tilje (10.0 mg) in 1.20 L of recirculating water
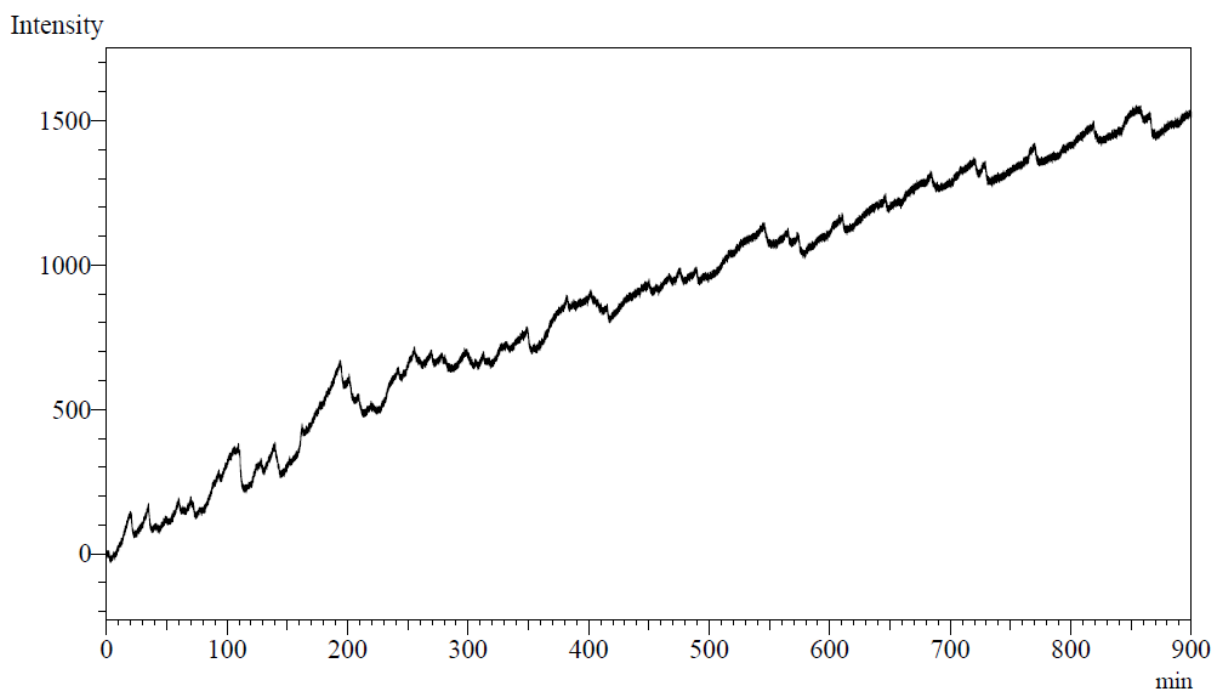
Figure A.41: Oil in water MIFID analysis: Bressay (10.3 mg) in 1.20 L of recirculating water

C.4 MIFID - Oil in air
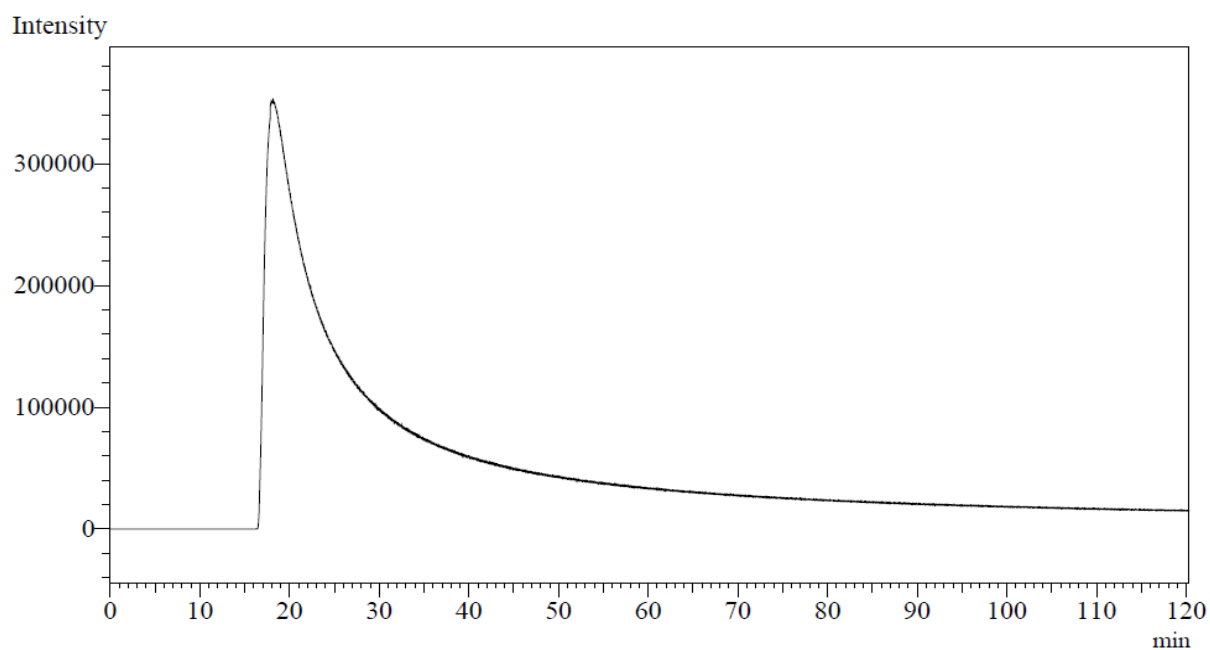
Figure A.42: Oil in air MIFID analysis: Troll B (10.4 mg)
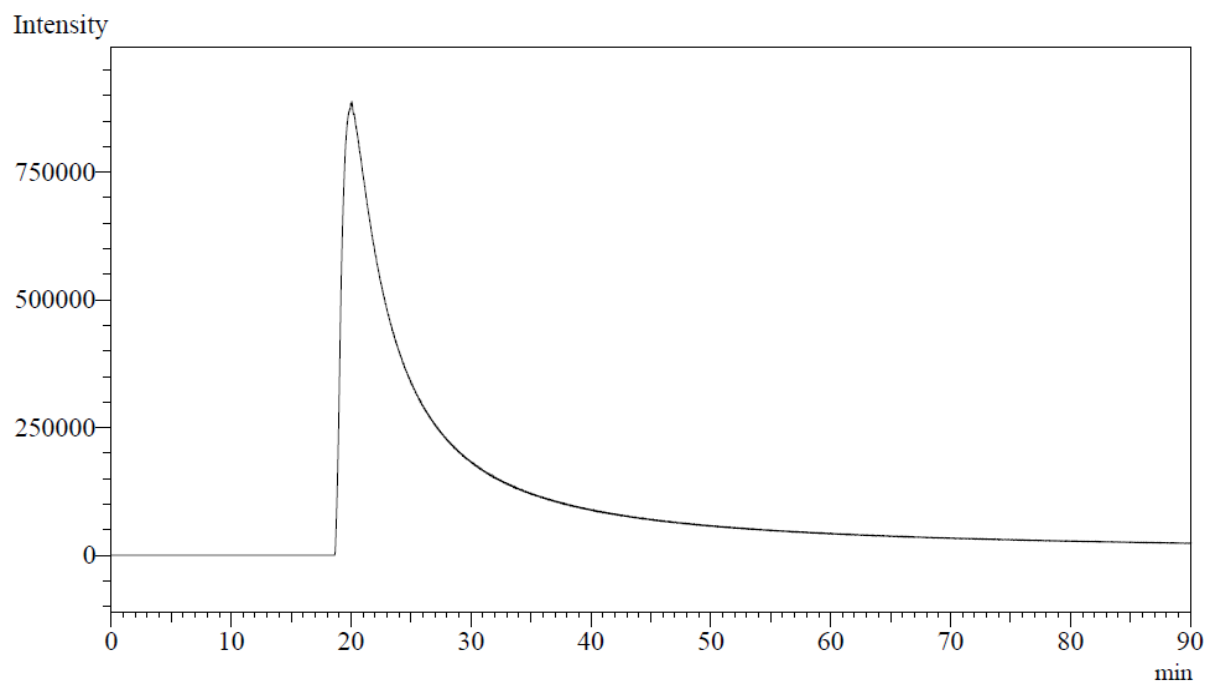
Figure A.43: Oil in air MIFID analysis: Unspecified 1 (9.6 mg)
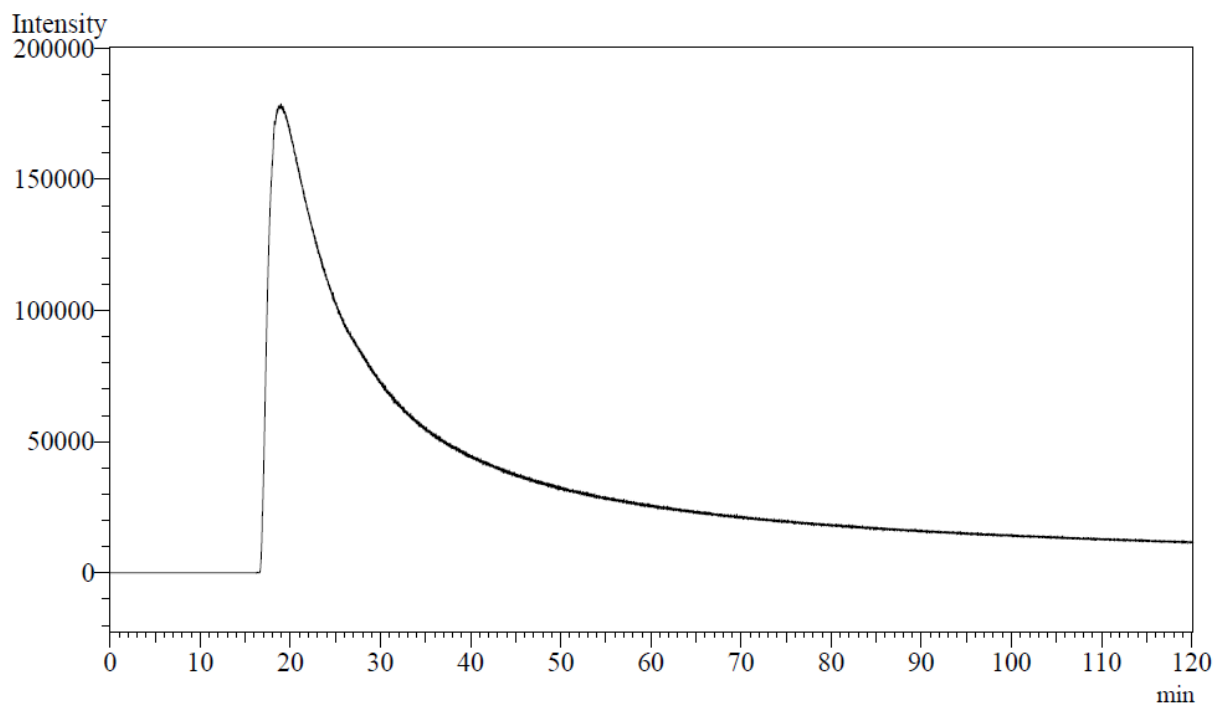
Figure A.44: Oil in air MIFID analysis: Balder Blend (10.4 mg)
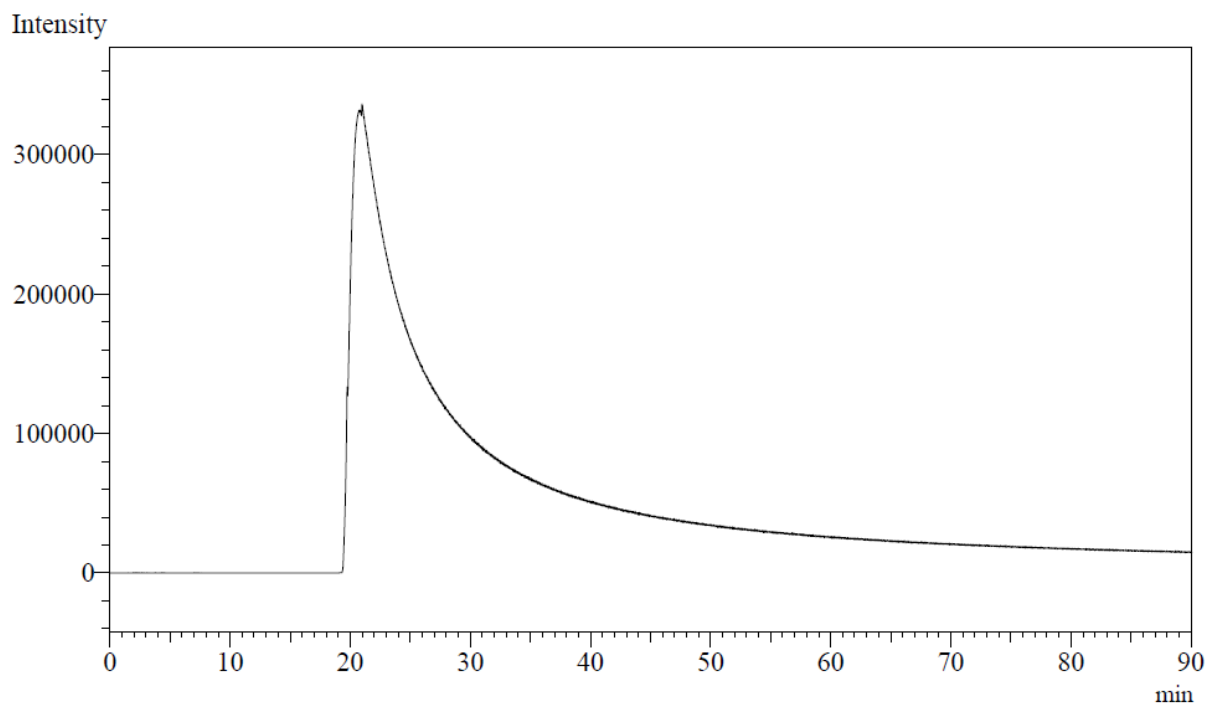
Figure A.45: Oil in air MIFID analysis: Unspecified 2 (10.0 mg)
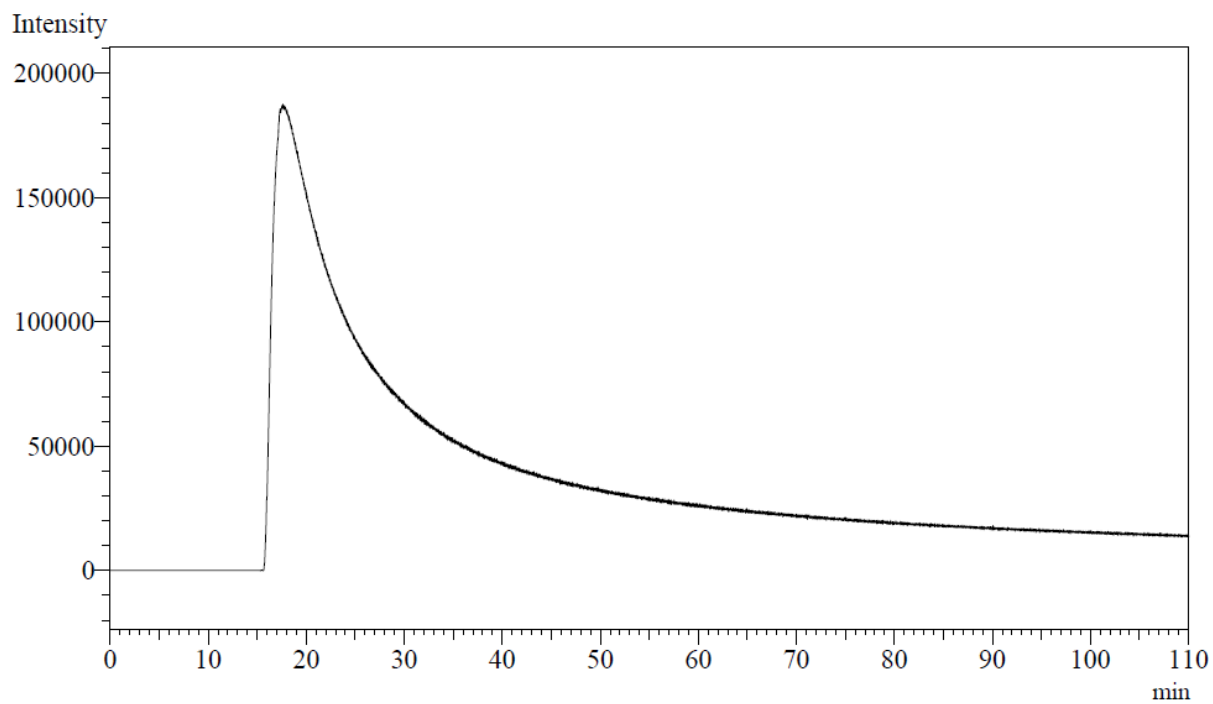
Figure A.46: Oil in air MIFID analysis: Norne Blend (9.9 mg)
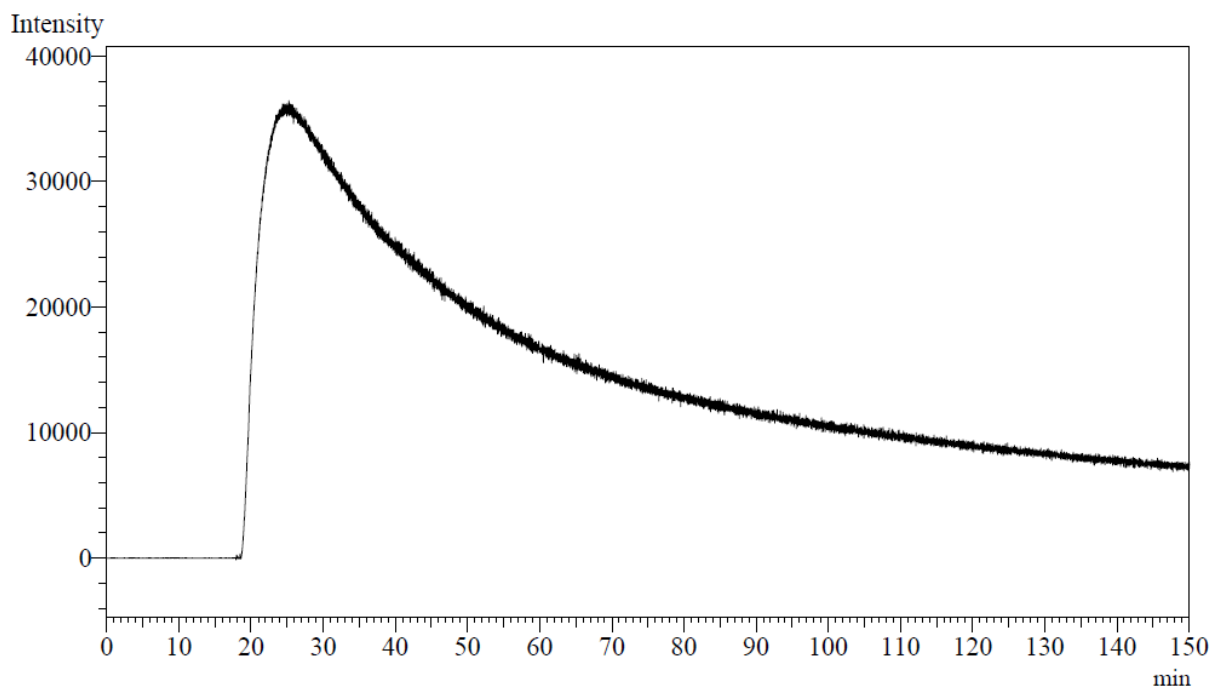
Figure A.47: Oil in air MIFID analysis: Falk (10.1 mg)
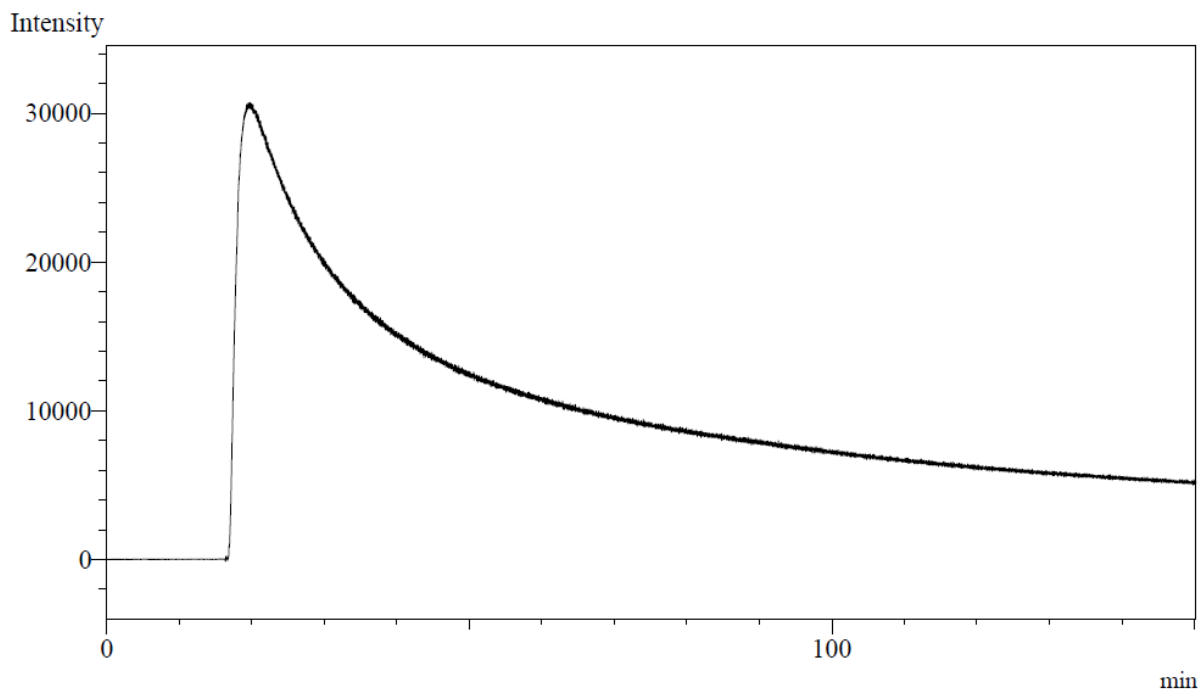
Figure A.48: Oil in air MIFID analysis: Peregrino (10.6 mg)
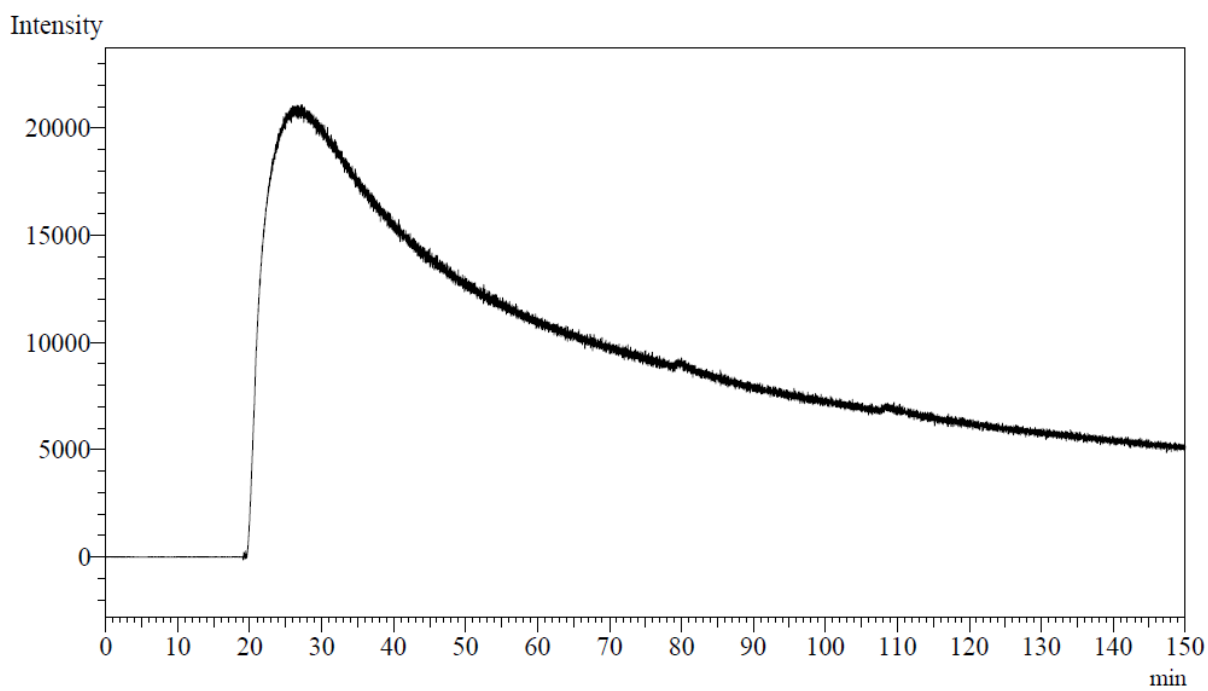
Figure A.49: Oil in air MIFID analysis: Mariner Maureen (10.1 mg)
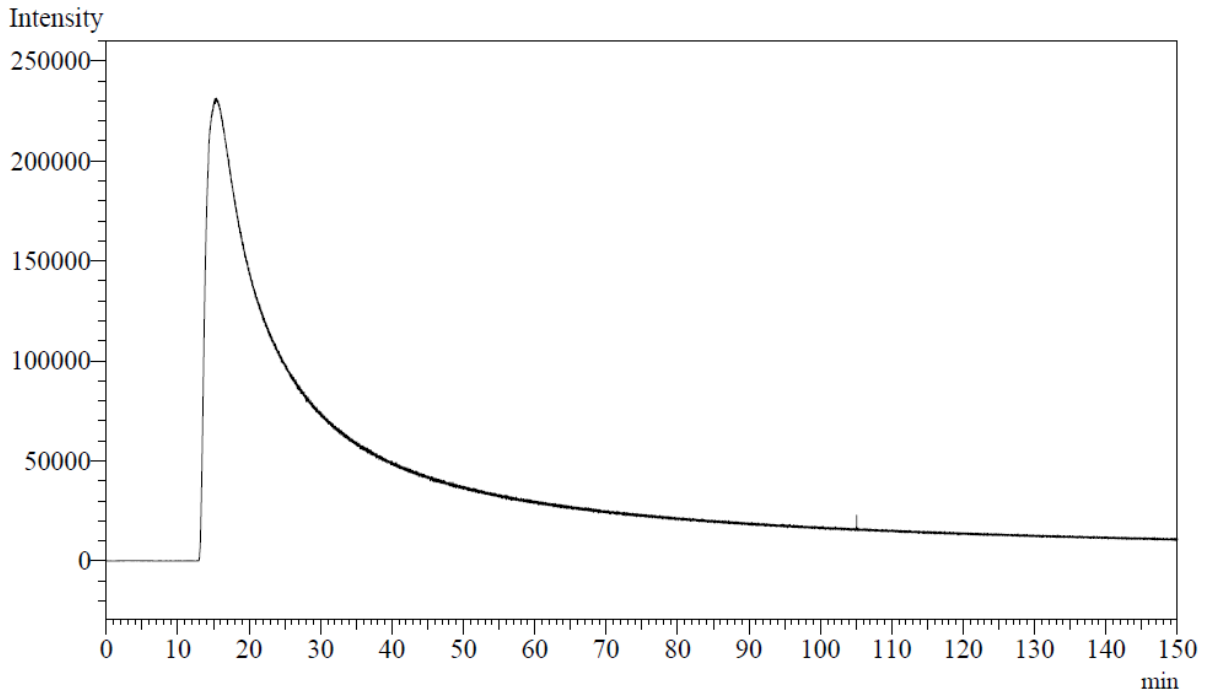
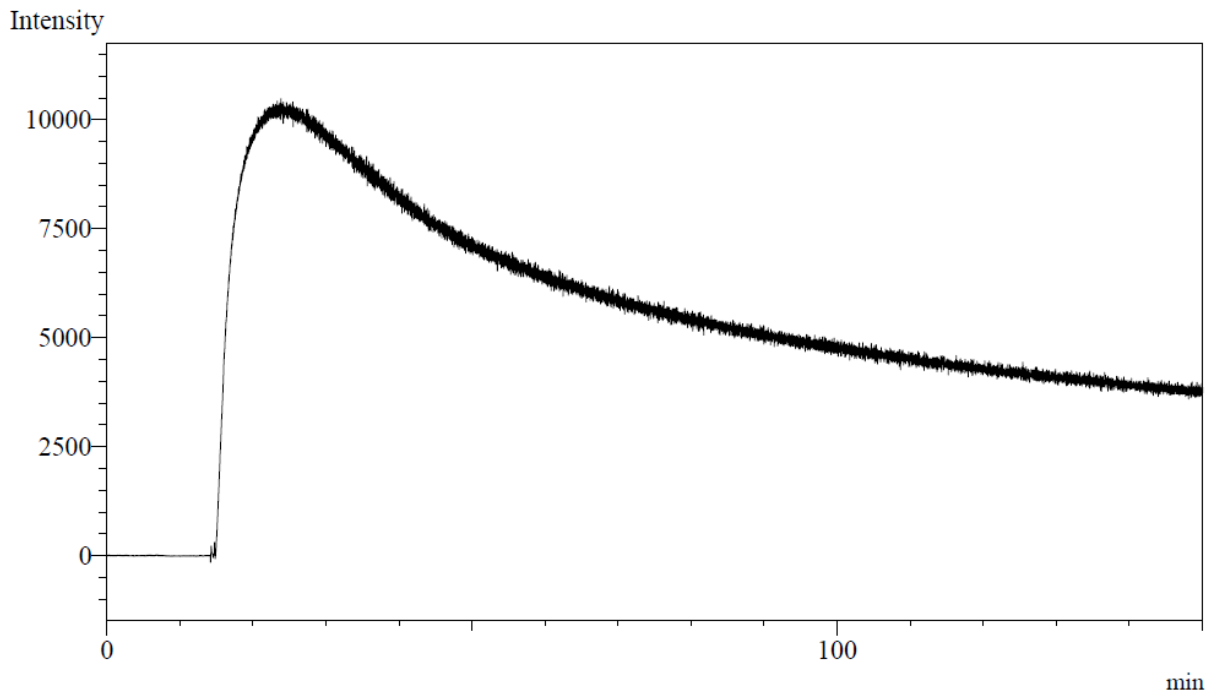**Figure A.50:** Oil in air MIFID analysis: Heidrun Tilje (9.9 mg)

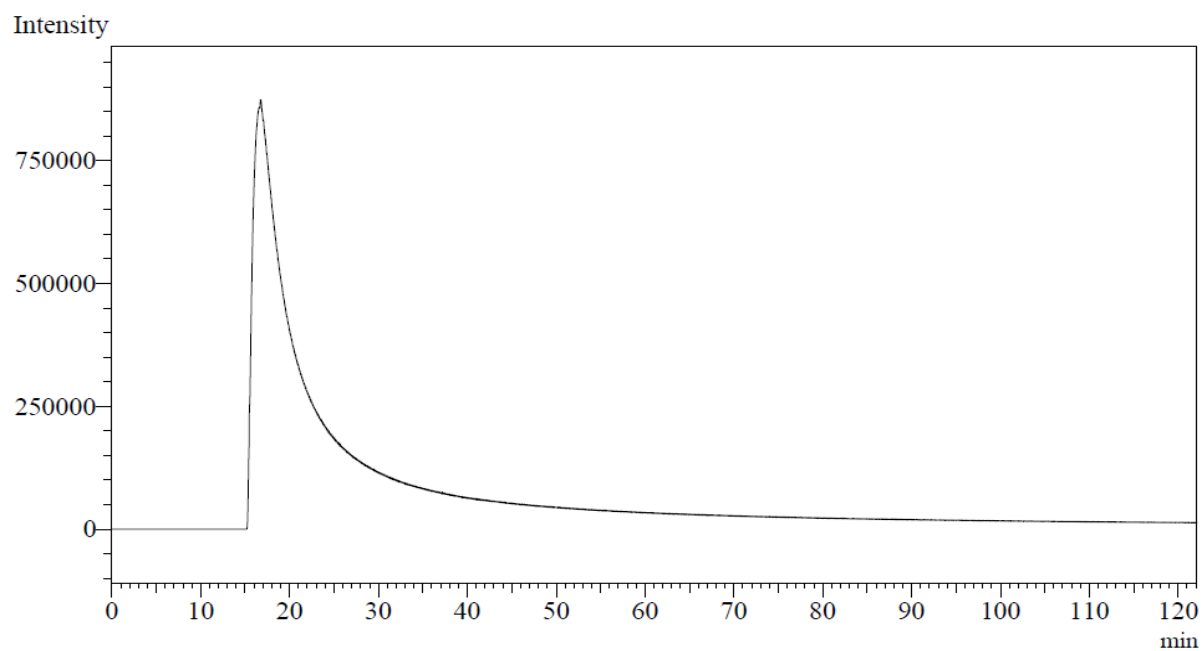**Figure A.51:** Oil in air MIFID analysis: Bressay (10.4 mg)

C.5 Repeatability test

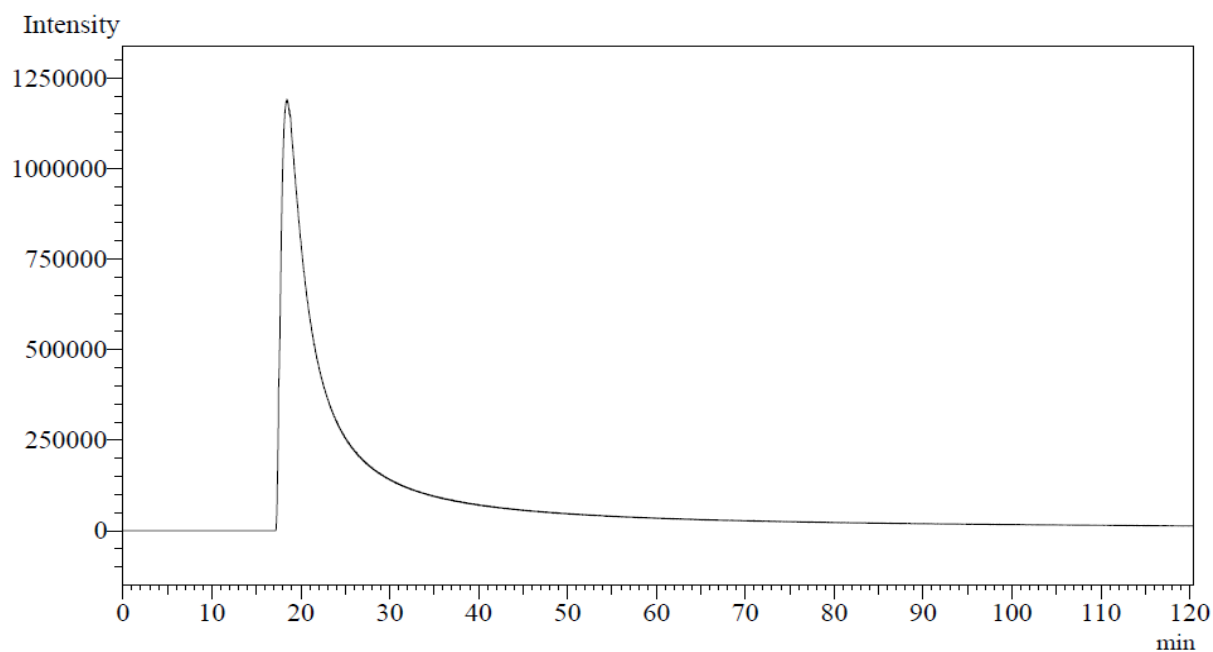**Figure A.52:** Oil in air MIFID analysis: Oseberg (10.0 mg)

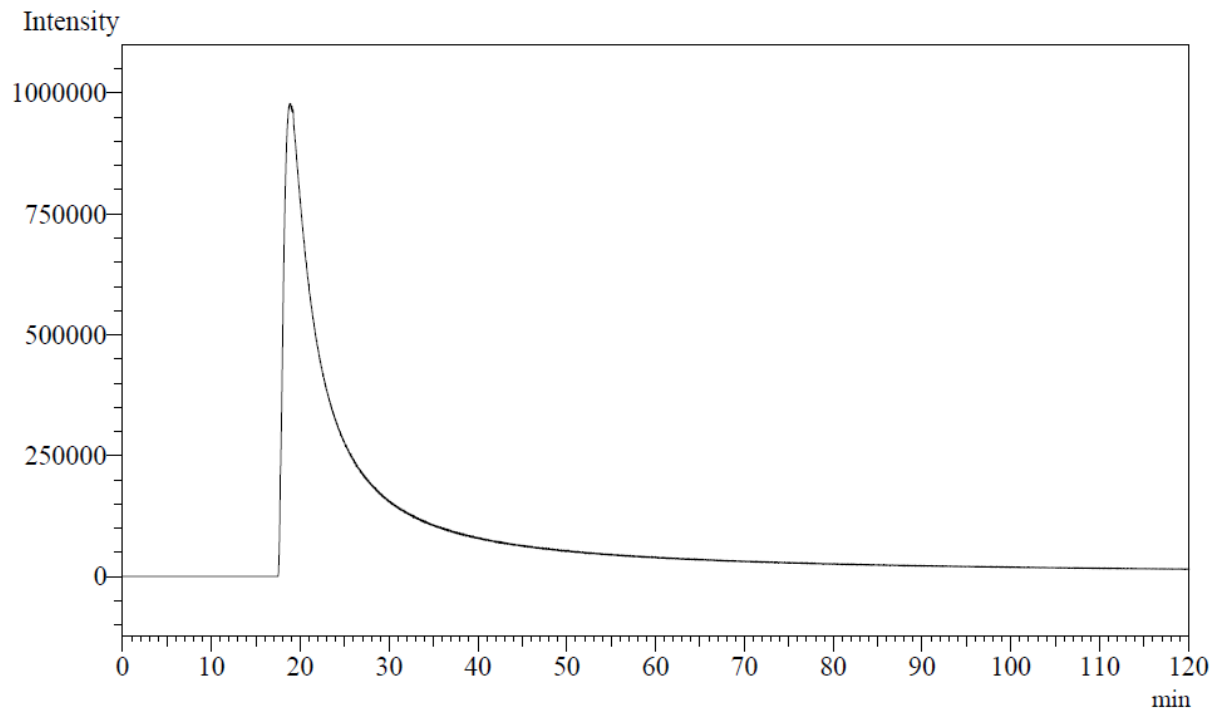**Figure A.53:** Oil in air MIFID analysis: Oseberg (10.2 mg)

Figure A.54: Oil in air MIFID analysis: Oseberg (10.0 mg)

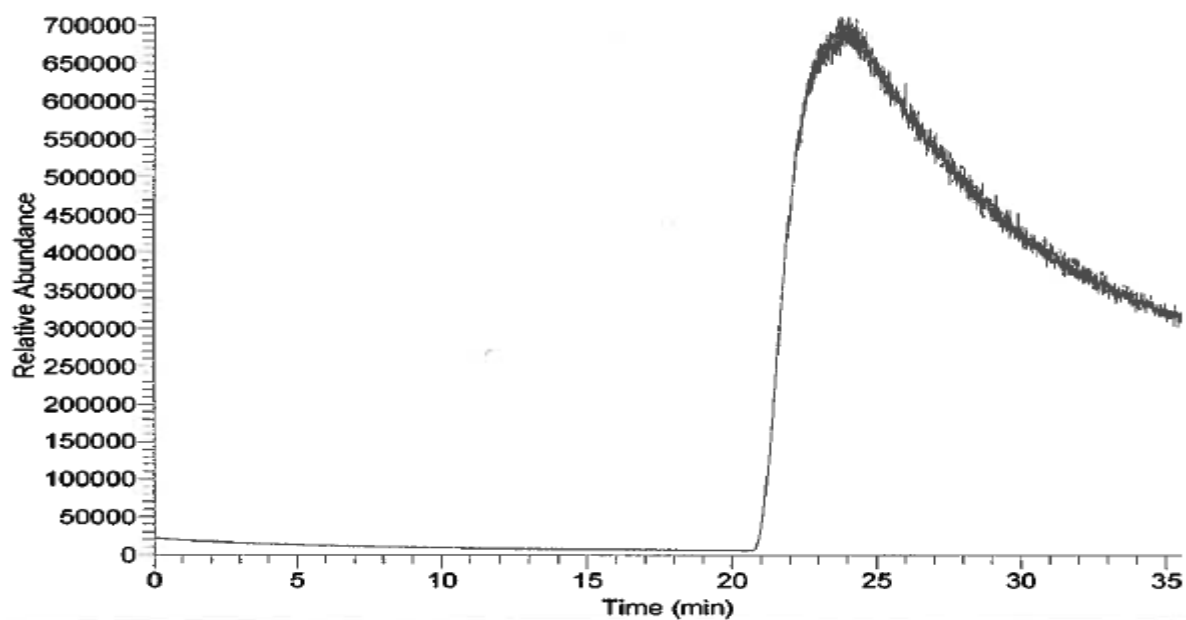# D. TIC signal profiles

D.1 MIMS - Oil in air
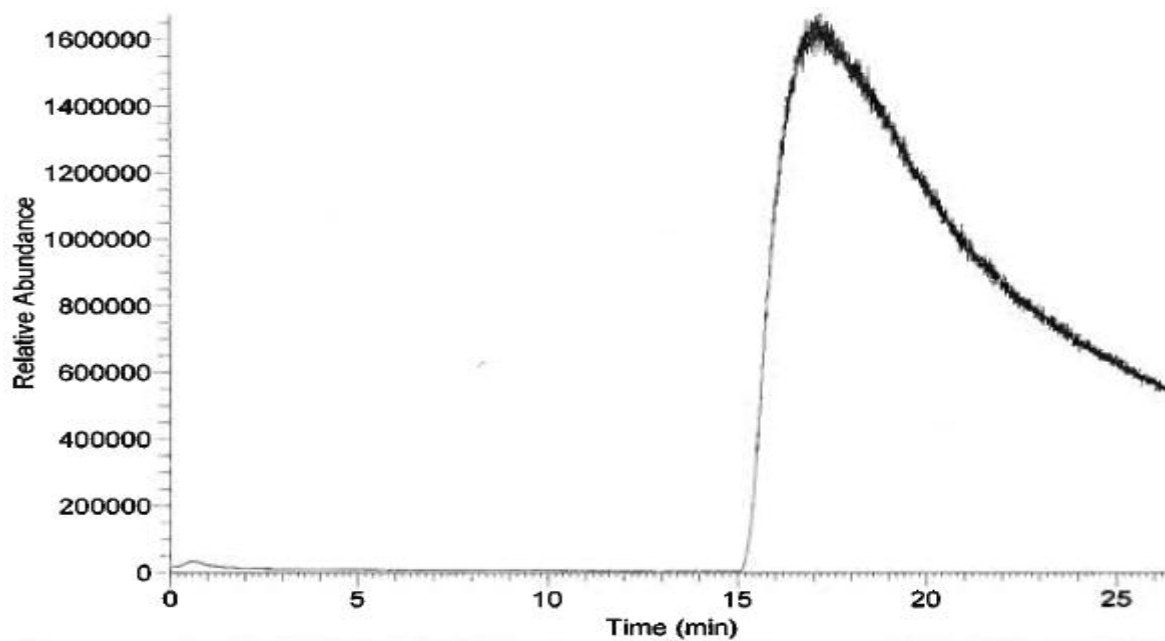

Figure A.55: Oil in air MIMS analysis: Troll B (10.0 mg)

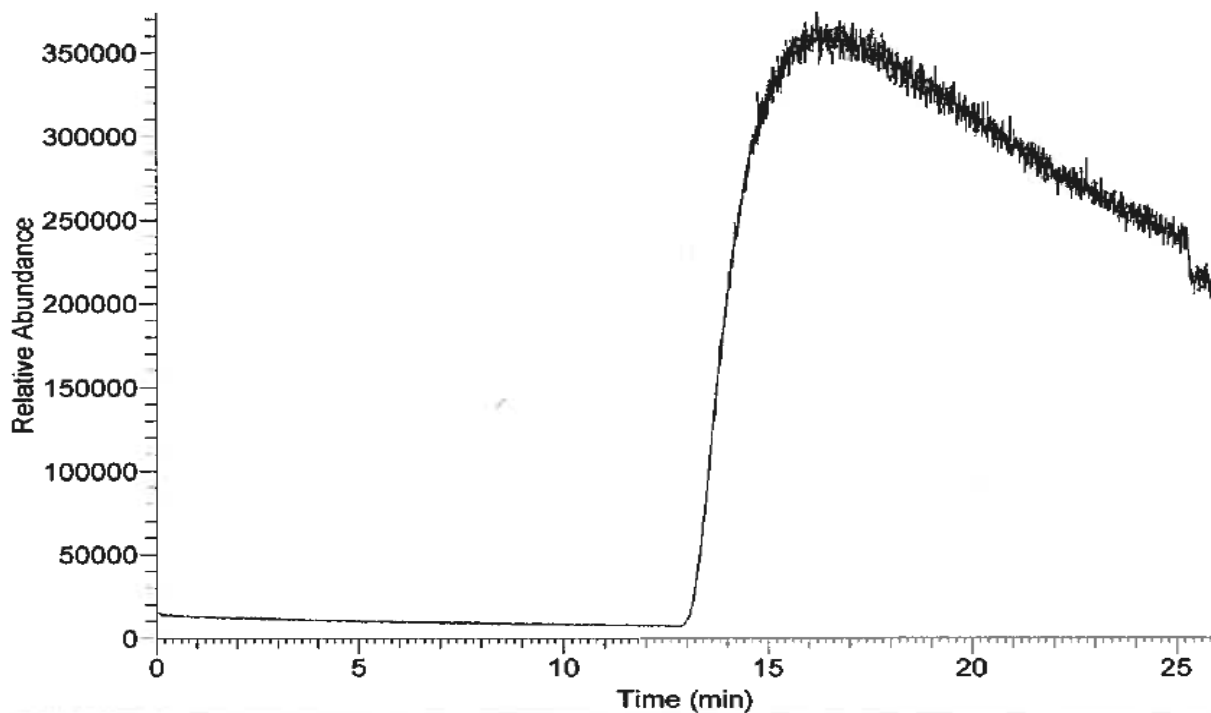**Figure A.56:** Oil in air MIMS analysis: Unspecified 1 (13.5 mg)

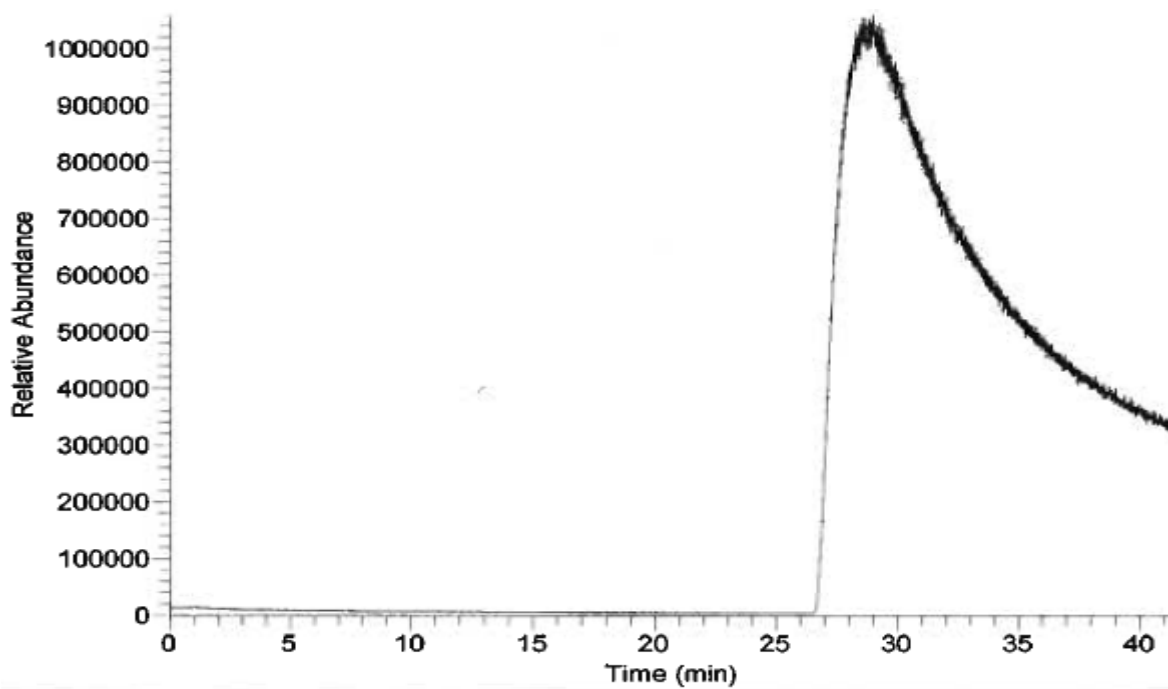**Figure A.57:** Oil in air MIMS analysis: Balder Blend (10.0 mg)

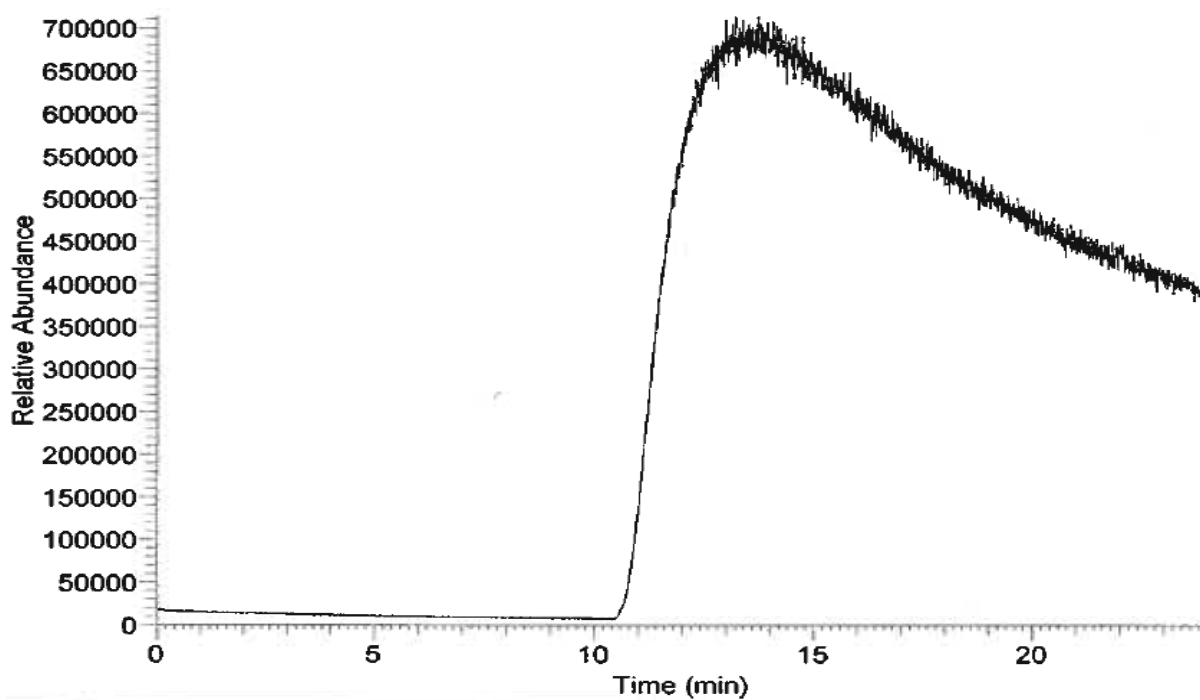**Figure A.58:** Oil in air MIMS analysis: Unspecified 2 (10.0 mg)

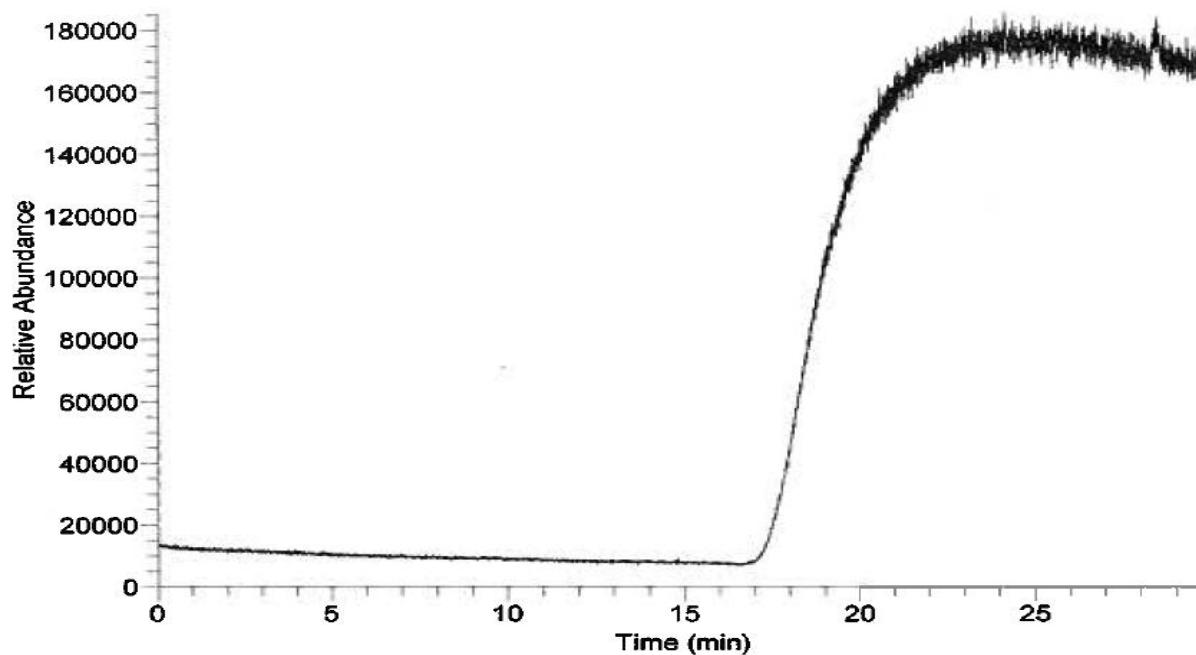**Figure A.59:** Oil in air MIMS analysis: Norne Blend (10.0 mg)

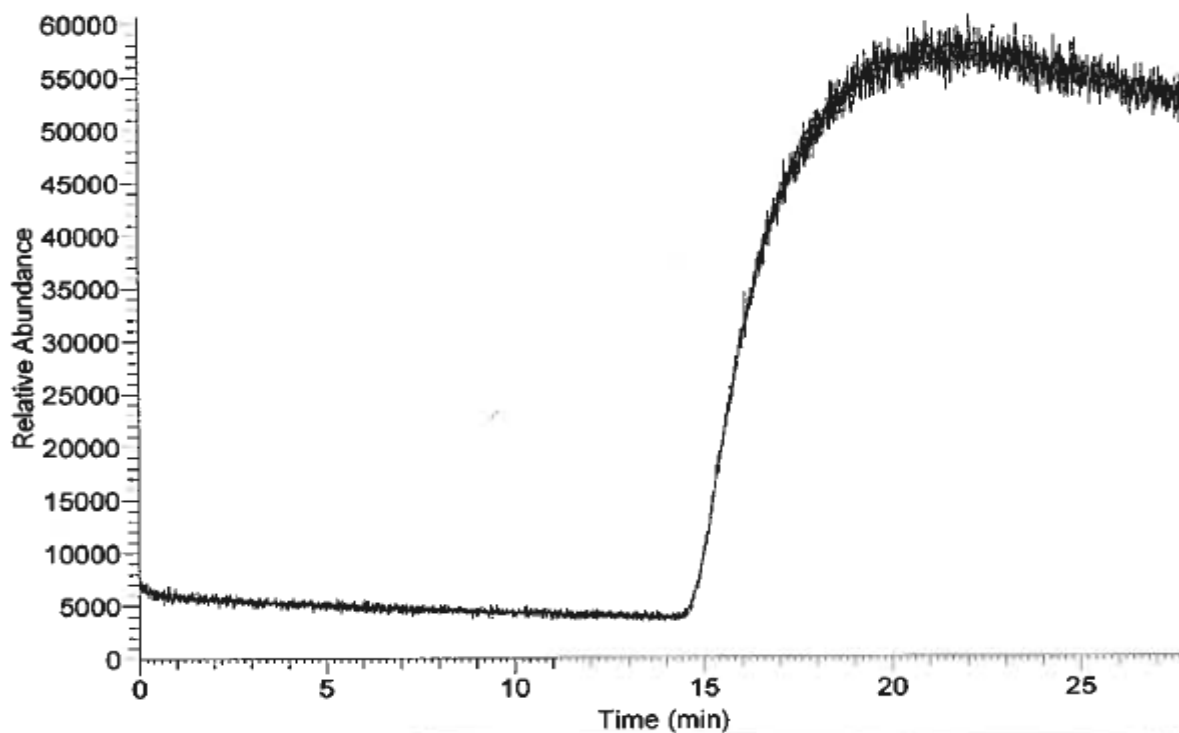**Figure A.60:** Oil in air MIMS analysis: Falk (14.0 mg)

Figure A.61: Oil in air MIMS analysis: Peregrino (13.5 mg)
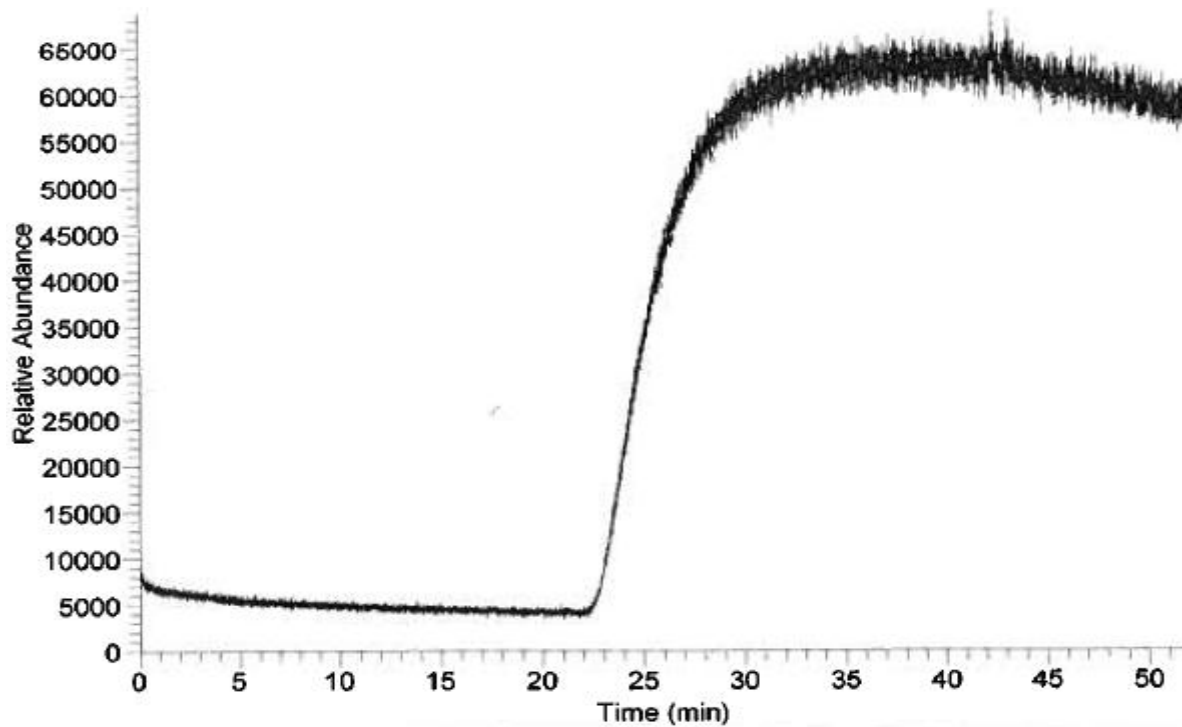
Figure A.62: Oil in air MIMS analysis: Mariner Maureen (10.0 mg)
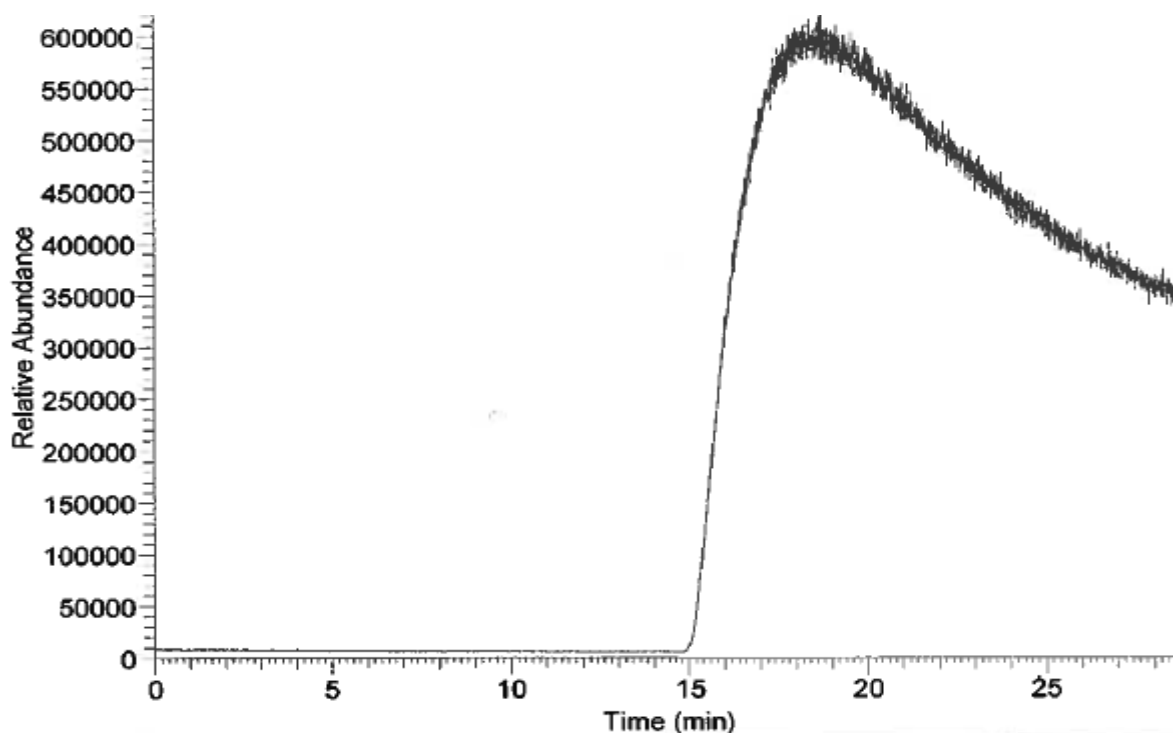
Figure A.63: Oil in air MIMS analysis: Heidrun Tilje (10.0 mg)
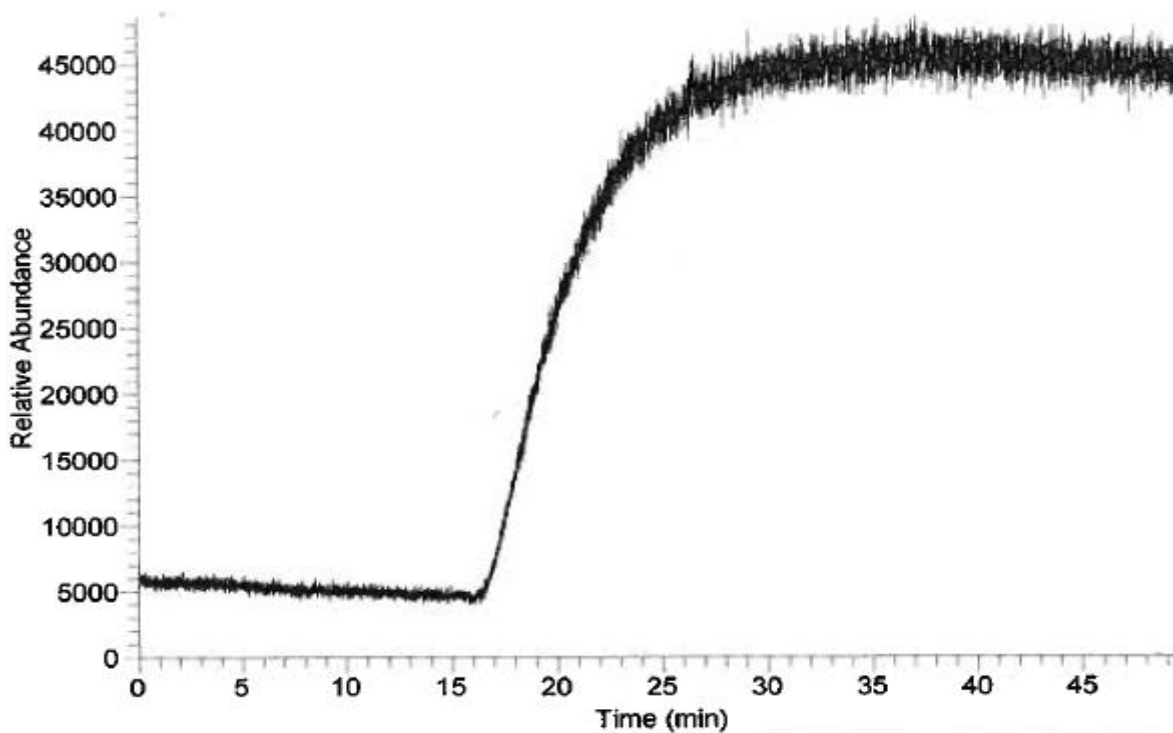
Figure A.64: Oil in air MIMS analysis: Bressay (15.6 mg)

D.2 MIMS – Oil in water
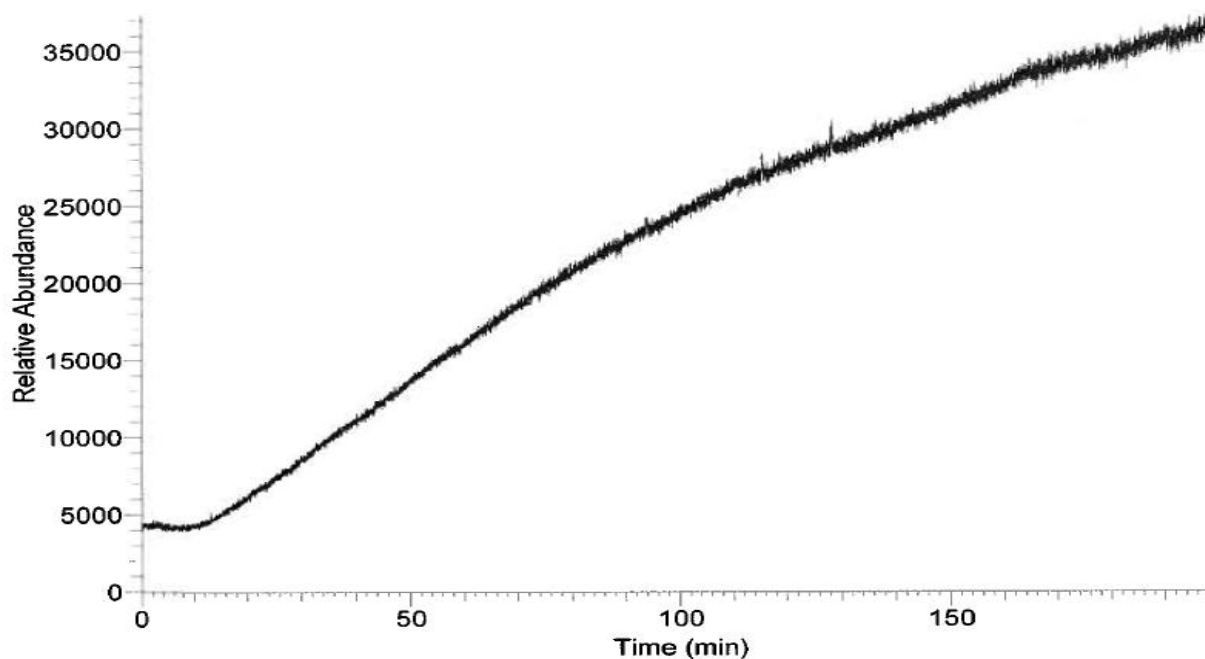
Figure A.65: Oil in water MIMS analysis: Oseberg (8.4 mg) in 1.20 L of recirculating water
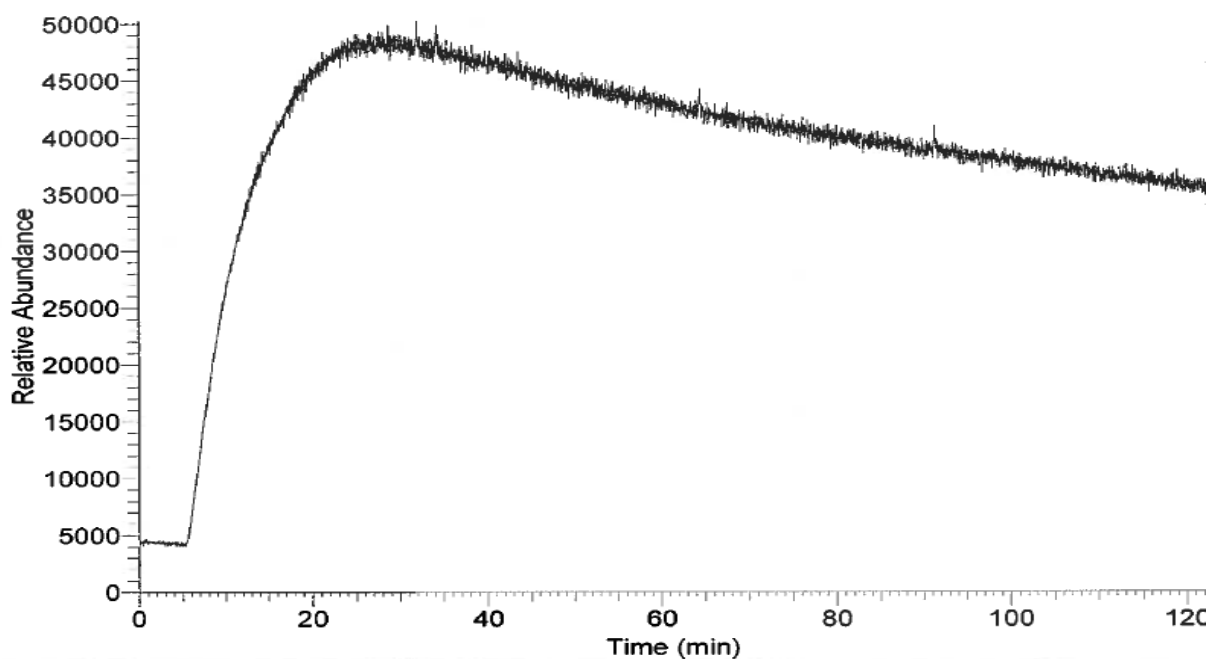
Figure A.66: Water MIMS analysis: Injection of 1.35 µL toluene solution (3 % toluene in methanol) in 1.20 L of recirculating water after 5 minutes
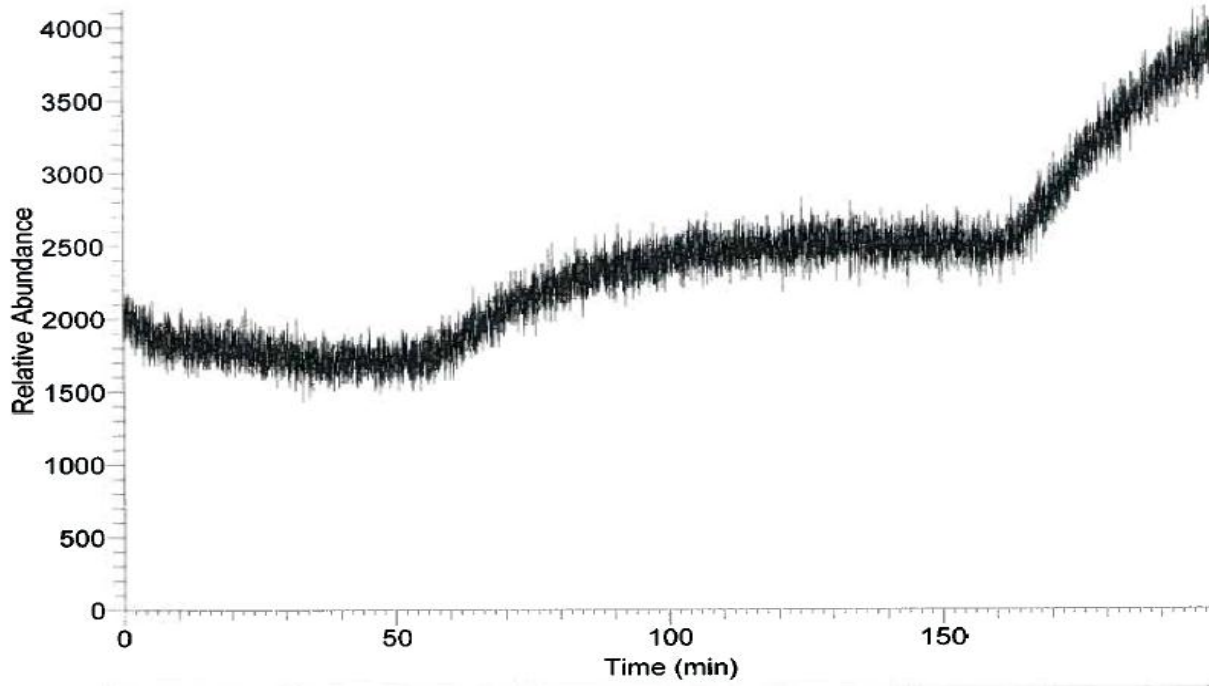
Figure A.67: Water MIMS analysis: 1.3 µL methanol injected after 5 minutes, 0.35 µL n-heptane injected after approximately 50 minutes and 1.0 µL n-heptane injected after approximately 160 minutes in 1.20 L of recirculating water.

E. Mass spectra

E.1 Oseberg Blend – Air

Figure A.68: Uncorrected mass spectrum for the Oseberg Blend air analysis, from the beginning of the oil exposure experiment (11.78-12.38 min)

Figure A.69: Uncorrected mass spectrum for the Oseberg Blend air analysis, from the TIC maximum (13.74-14.59 min)

Figure A.70: Uncorrected mass spectrum for the Oseberg Blend air analysis, from the end of the oil exposure experiment (21.22-22.12 min)

E.2 SAGD – Air

Figure A.71: Uncorrected mass spectrum for the SAGD air analysis, from the beginning of the oil exposure experiment (12.28-13.62 min)
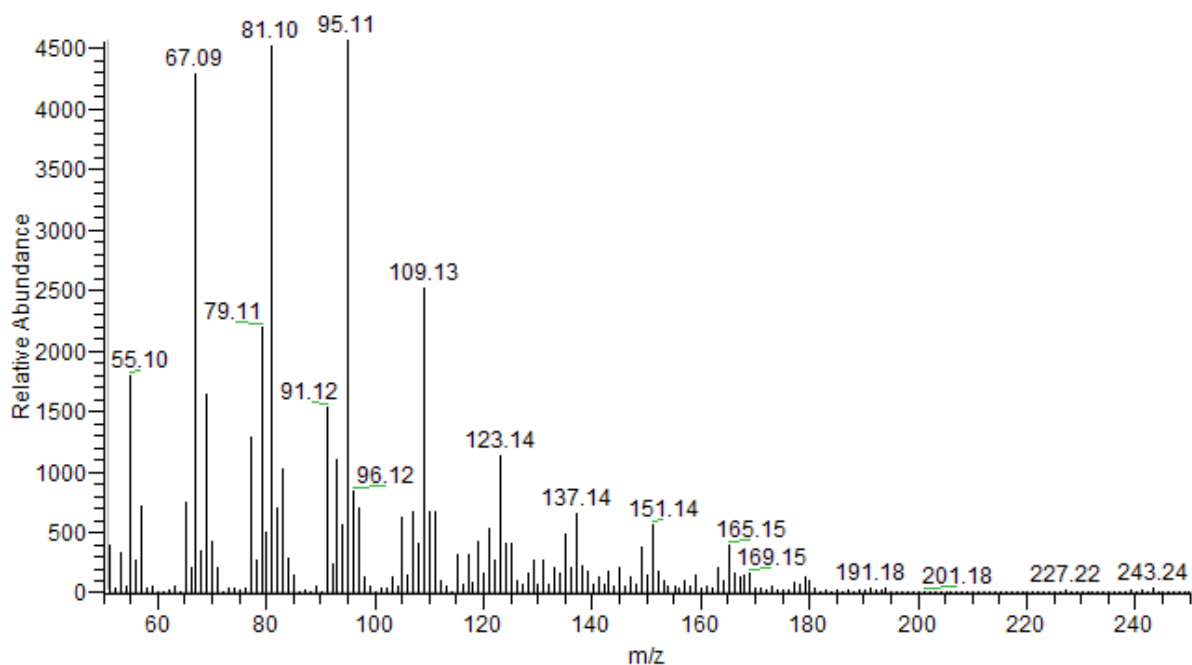
Figure A.72: Uncorrected mass spectrum for the SAGD air analysis, from the middle of the oil exposure experiment (18.74-20.53 min)
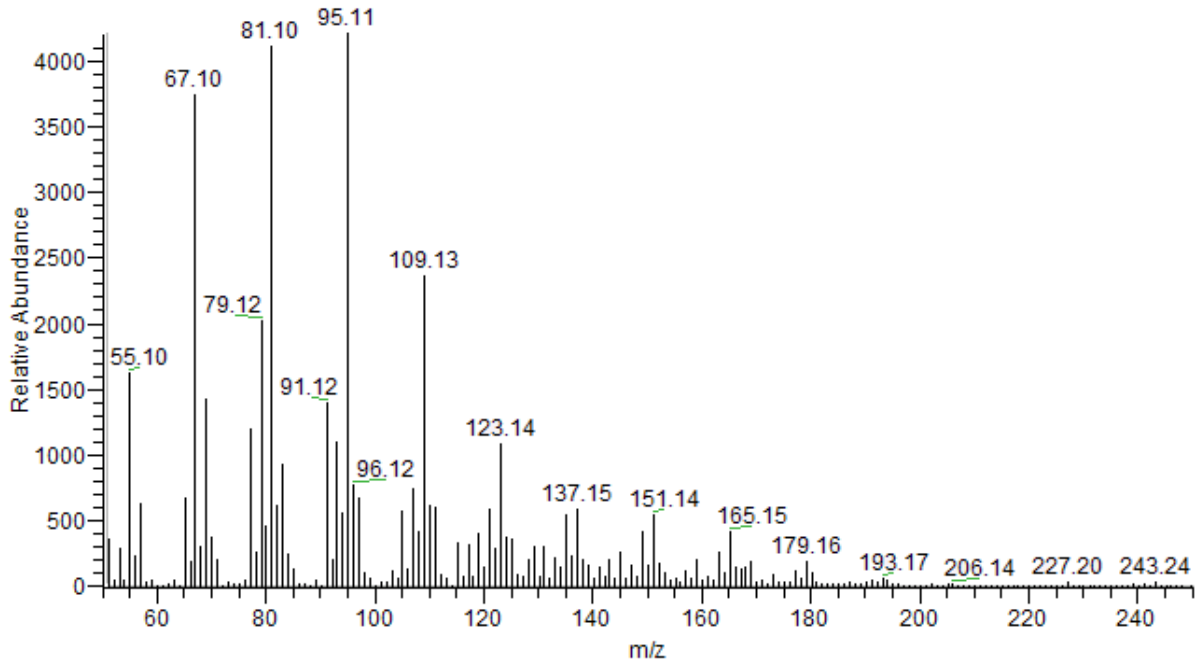
Figure A.73: Uncorrected mass spectrum for the SAGD air analysis, from the end of the oil exposure experiment (25.80-27.03min)

E.3 Oseberg Blend – Water
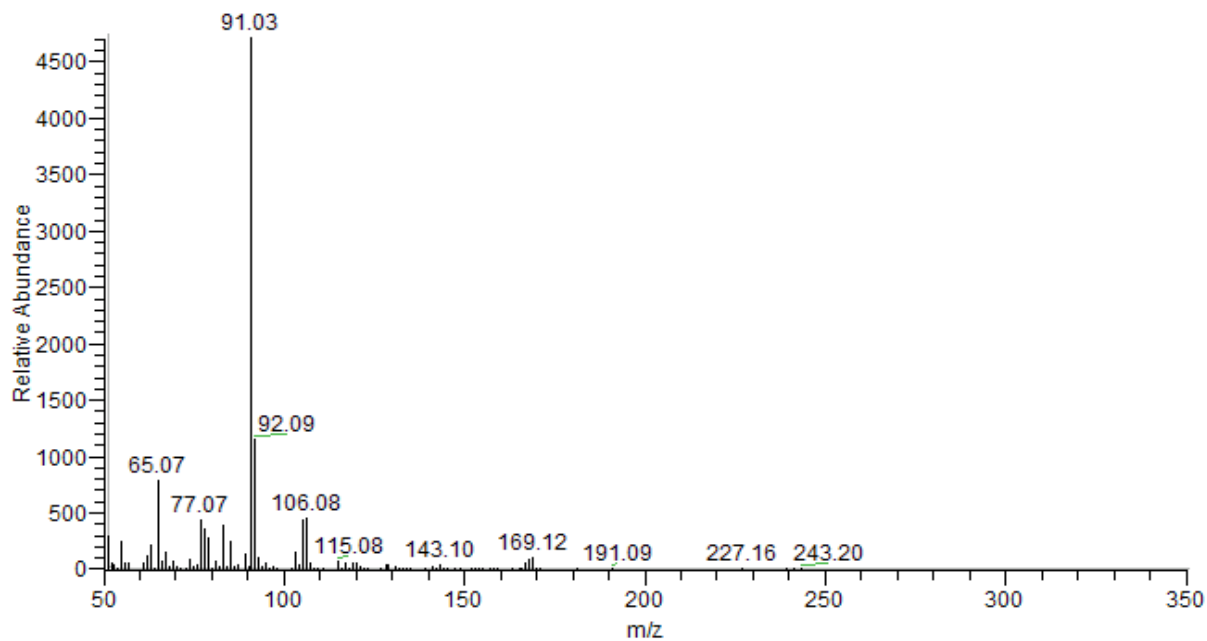
Figure A.74: Uncorrected mass spectrum for the Oseberg Blend water analysis, from the beginning of the oil exposure experiment (18.10-26.04 min)
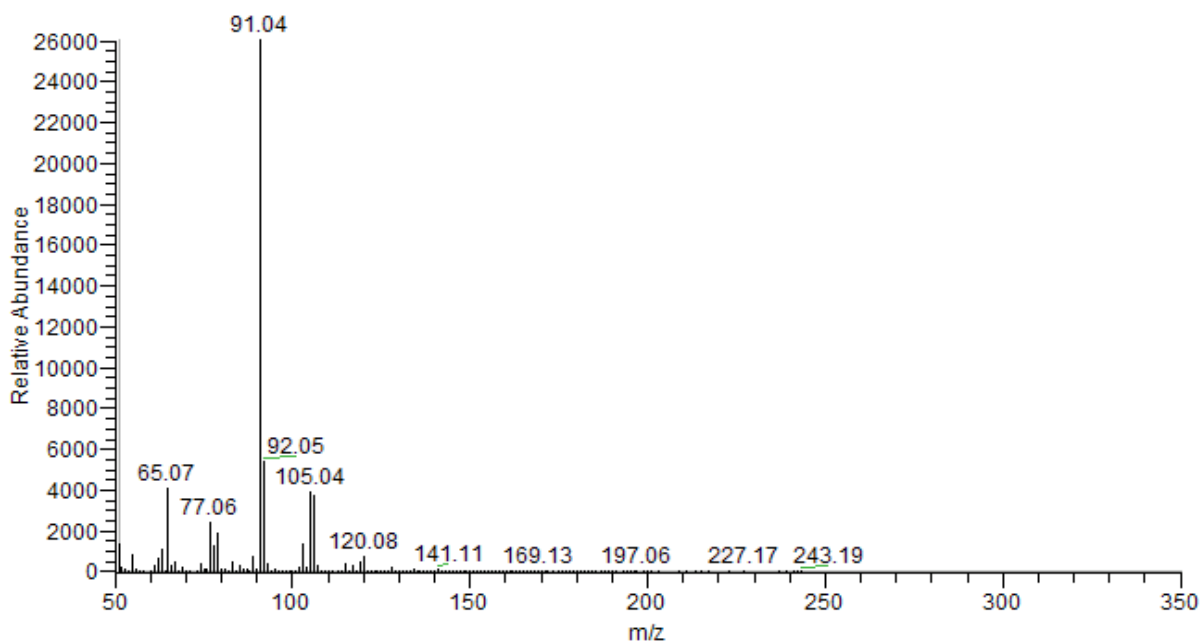
Figure A.75: Uncorrected mass spectrum for the Oseberg Blend water analysis, from the middle of the oil exposure experiment (98.49-106.79 min)
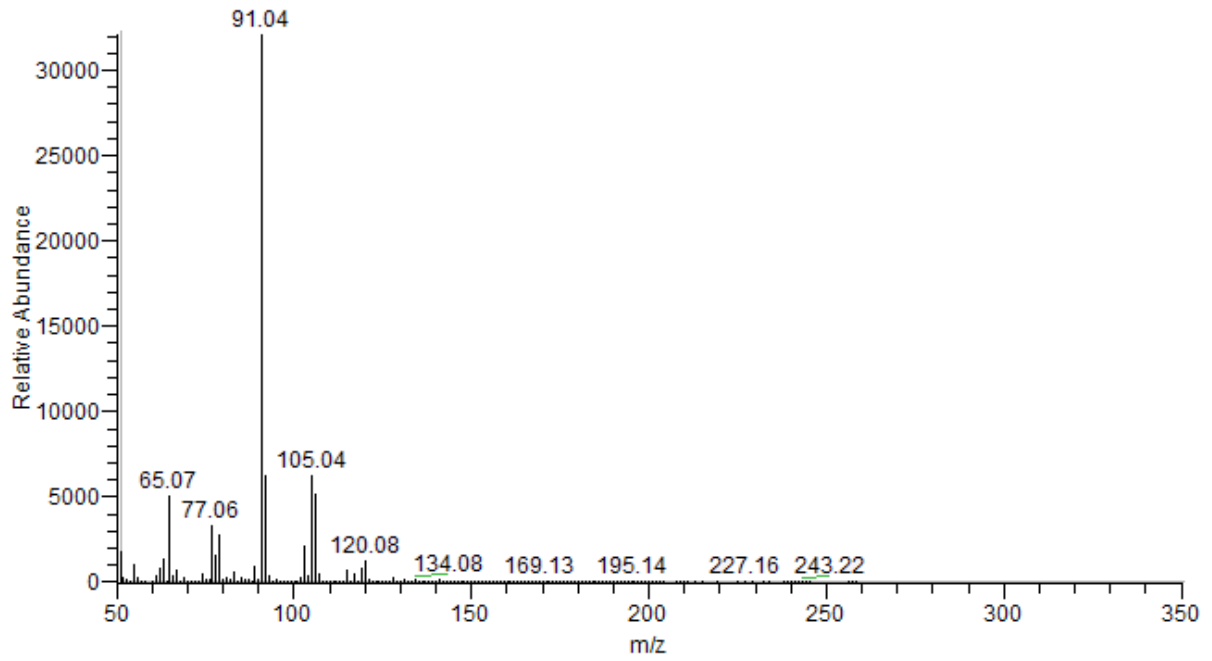
Figure A.76: Uncorrected mass spectrum for the Oseberg Blend water analysis, from the end of the oil exposure experiment (189.42-199.99 min)

E.4 SAGD – Water
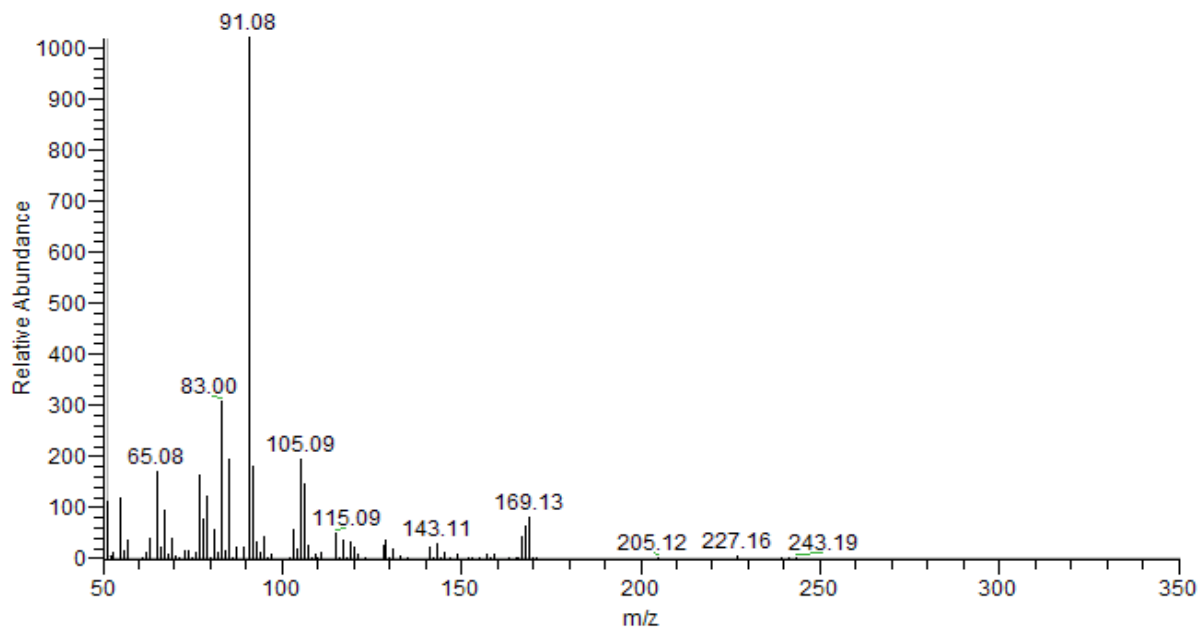
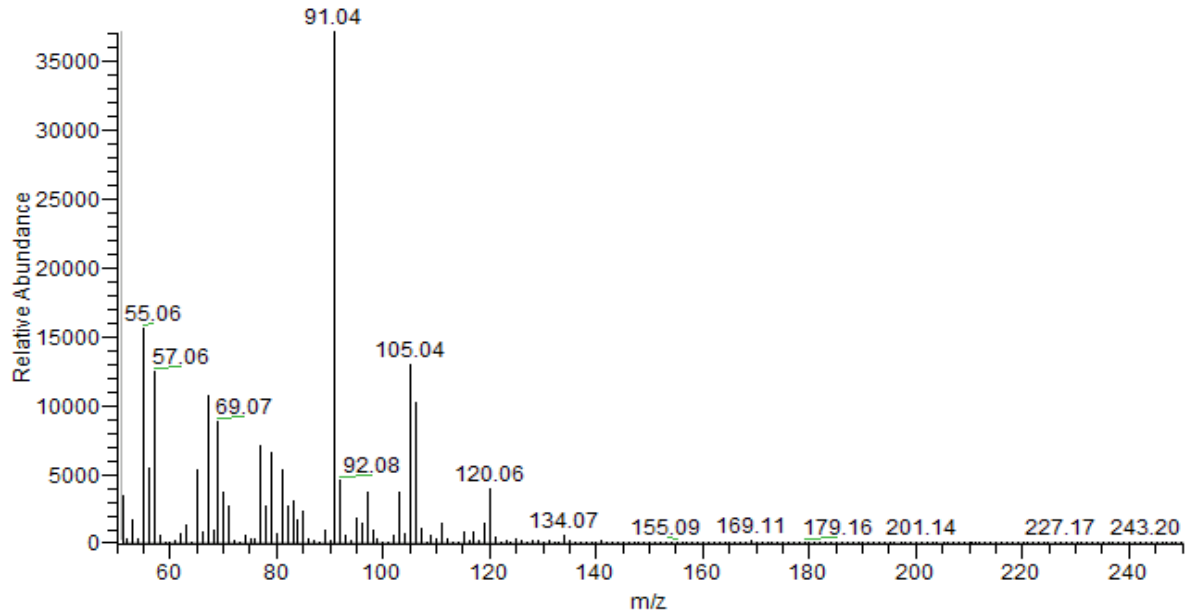**Figure A.77:** Uncorrected mass spectrum for the SAGD water analysis, from the beginning of the oil exposure experiment (26.08.34.02 min)
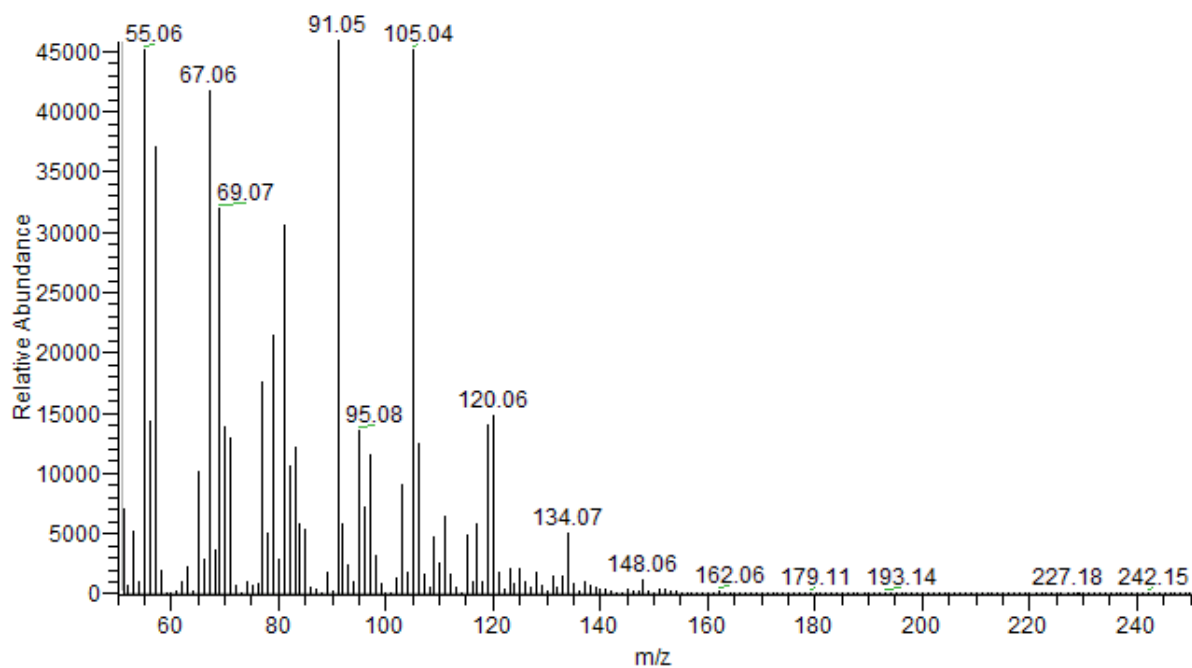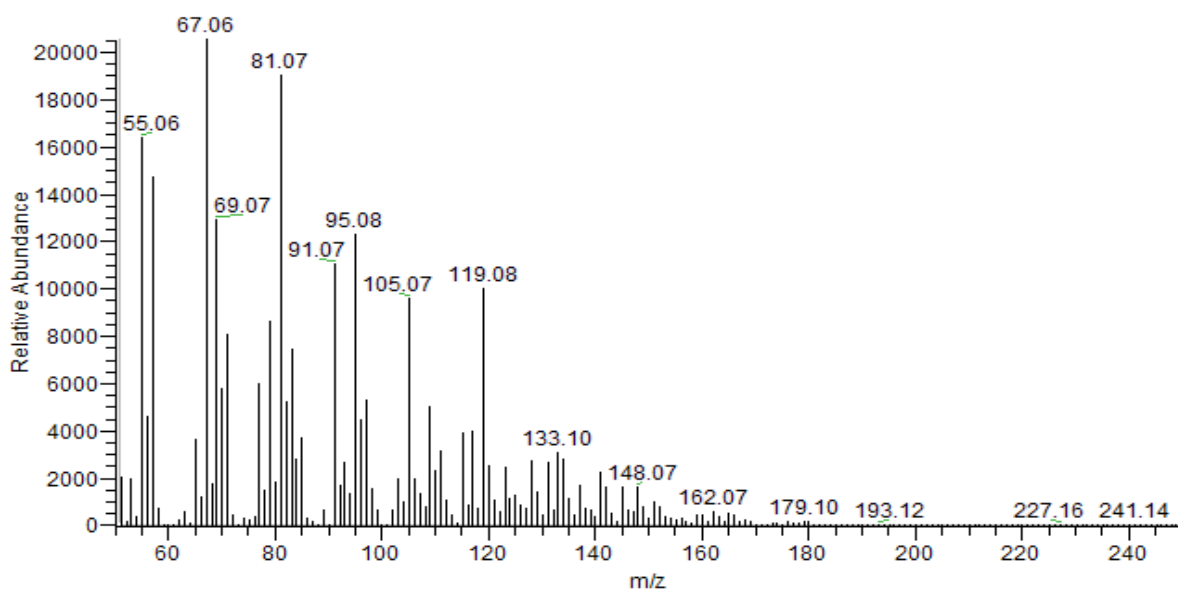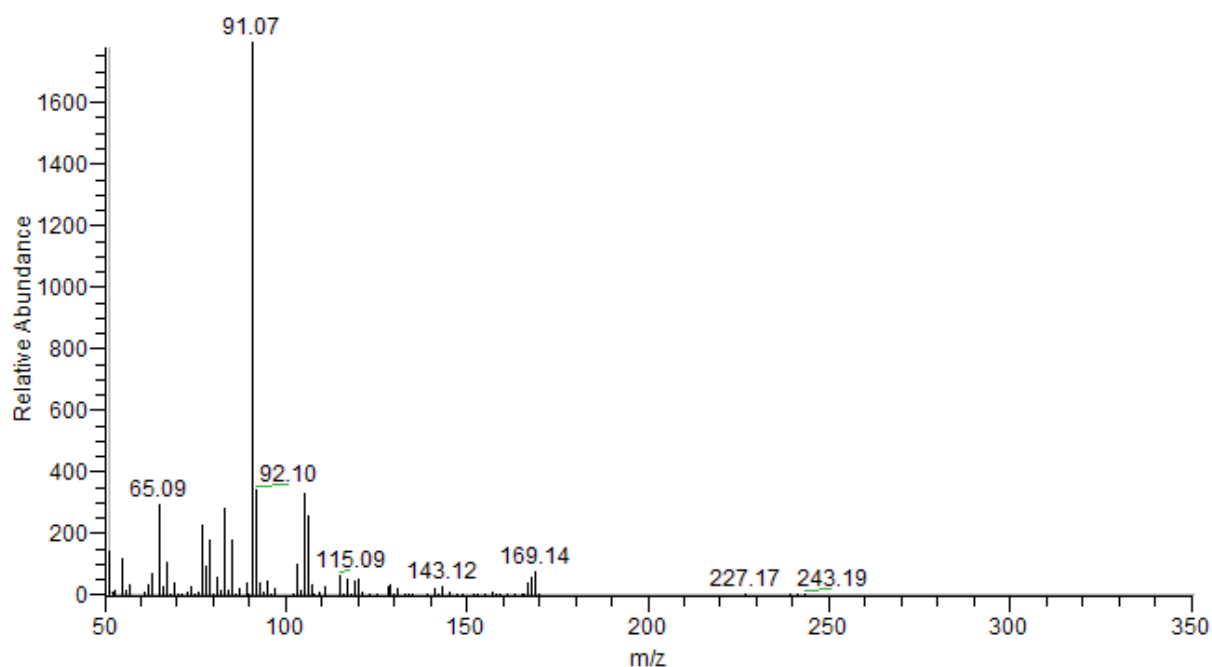

Figure A.78: Uncorrected mass spectrum for the SAGD water analysis, from the middle of the oil exposure experiment (98.30-106.98 min)
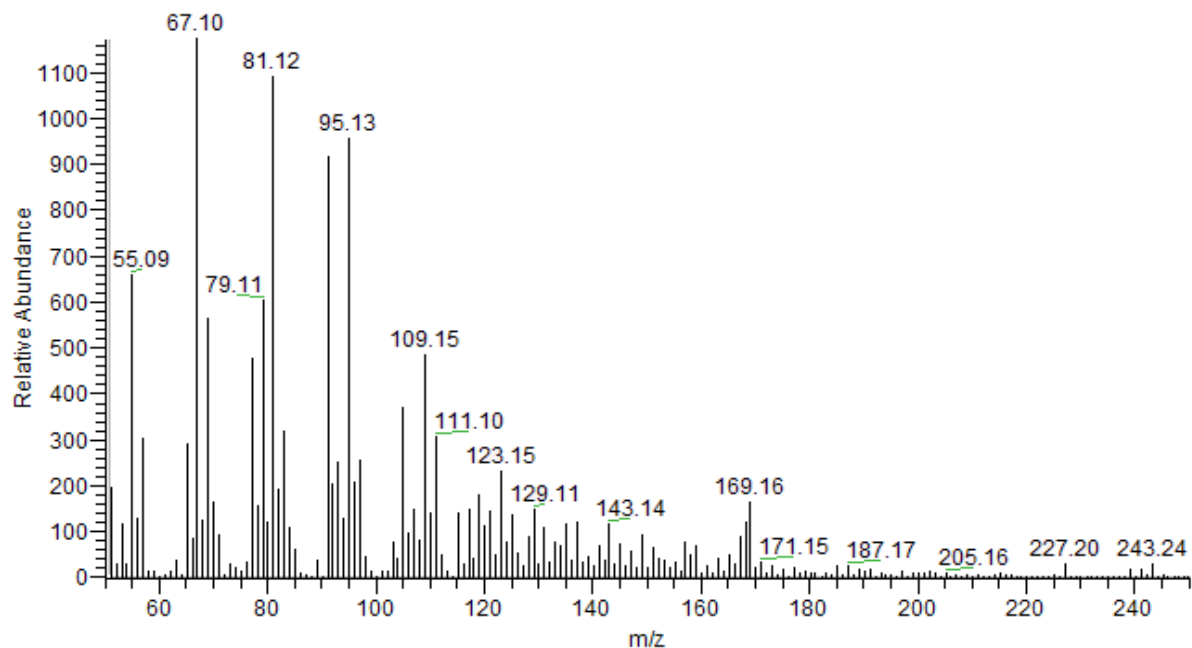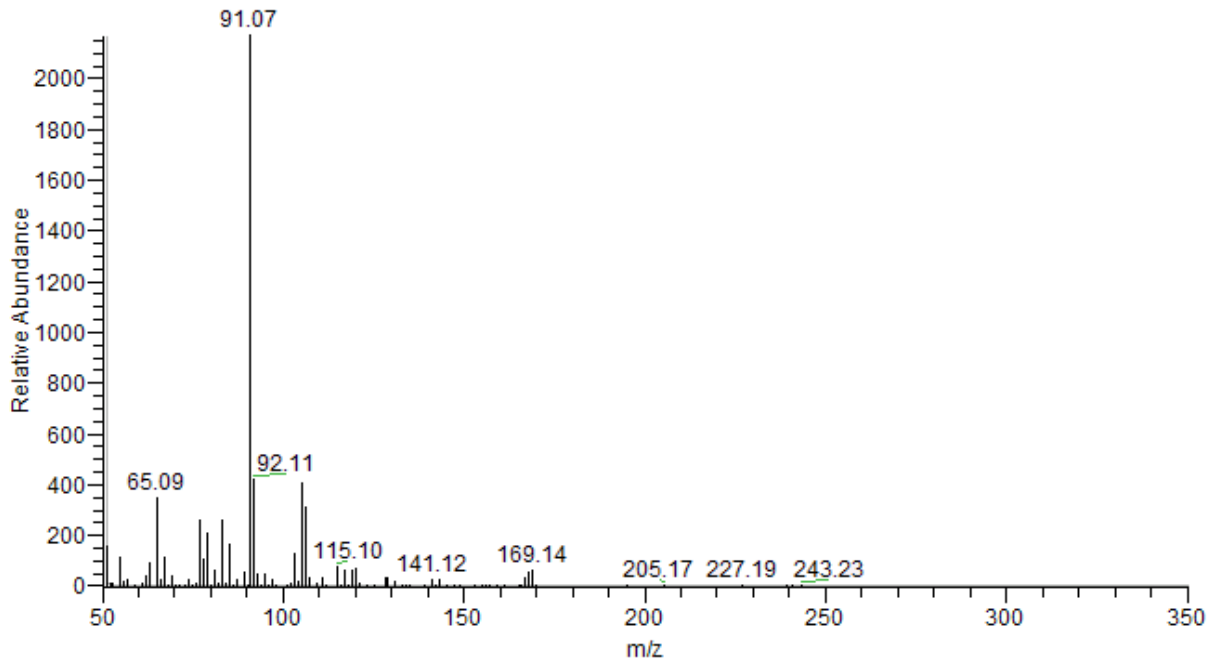
Figure A.79: Uncorrected mass spectrum for the SAGD water analysis, from the end of the oil exposure experiment (191.68-199.62 min)

E.5 Toluene – Water
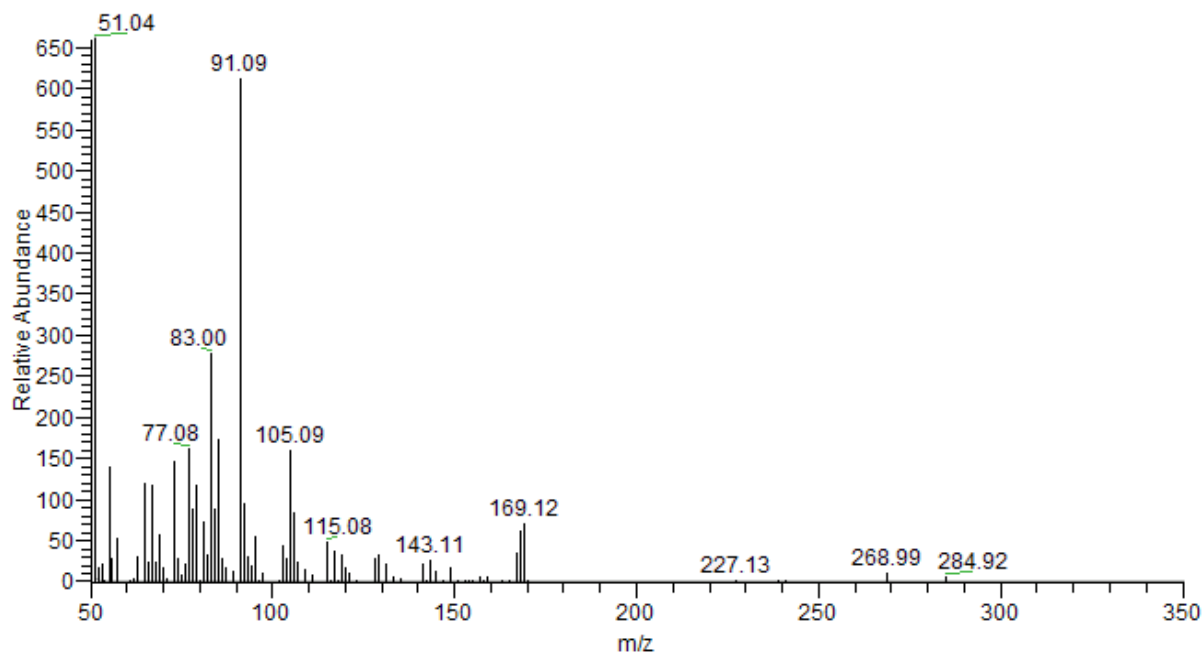
Figure A.80: System blank: mass spectrum for the toluene water analysis, from the baseline (1.38-4.62 min)
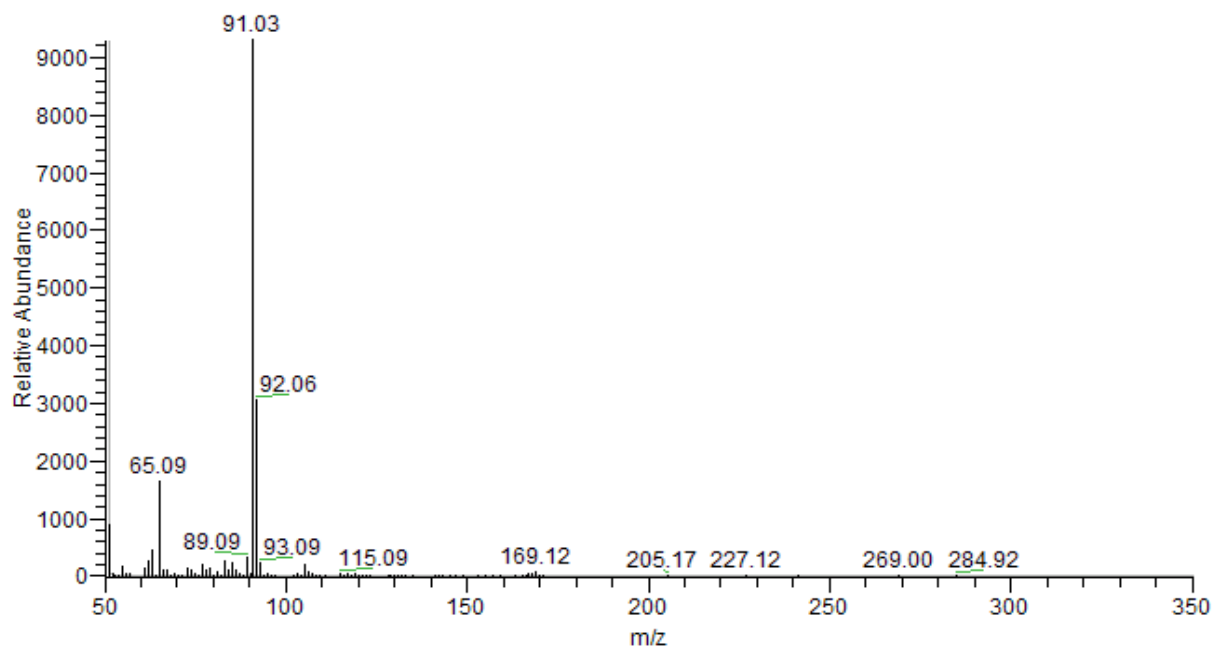
Figure A.81: Uncorrected mass spectrum for the toluene water analysis, from the beginning of the toluene exposure experiment (6.93-9.93 min)
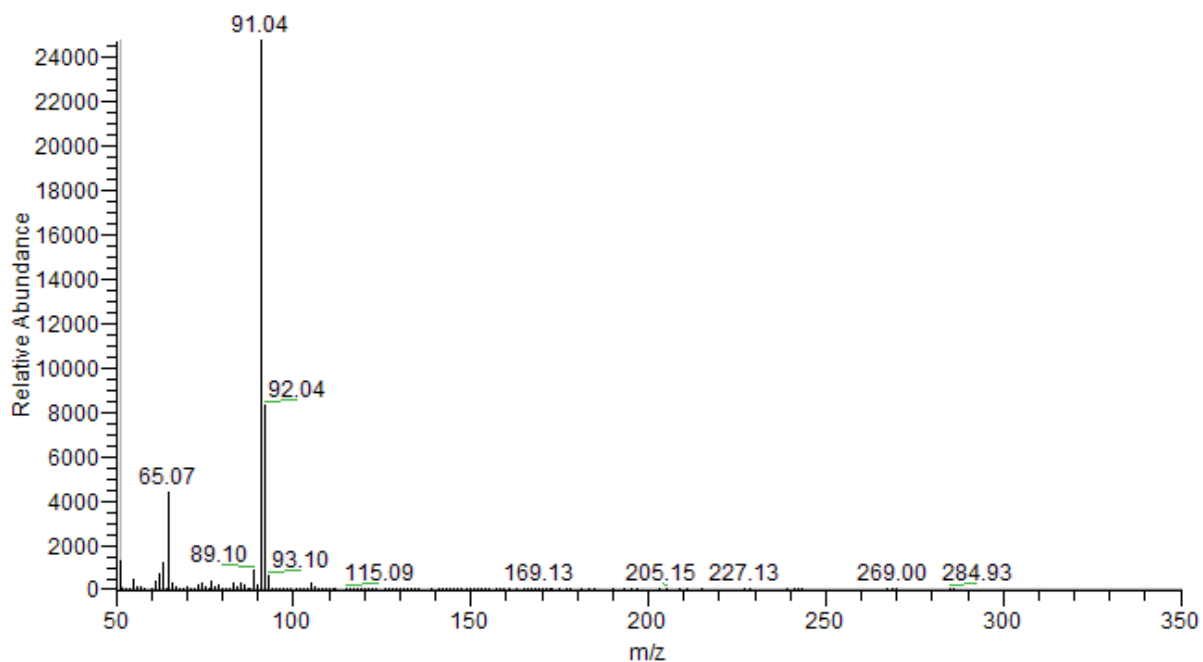
Figure A.82: Uncorrected mass spectrum for the toluene water analysis, from the middle of the toluene exposure experiment (24.95-32.33 min)
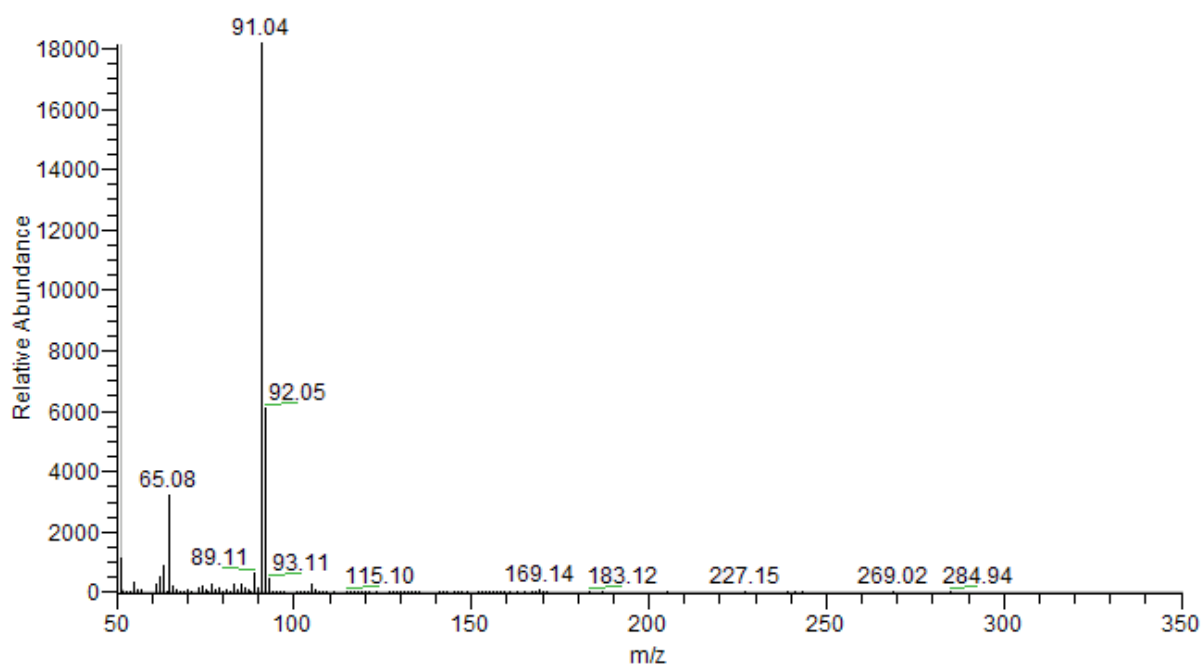
Figure A.83: Uncorrected mass spectrum for the toluene water analysis, from the end of the toluene exposure experiment (114.09-120.80 min)

E.6 Methanol/n-heptane – Water
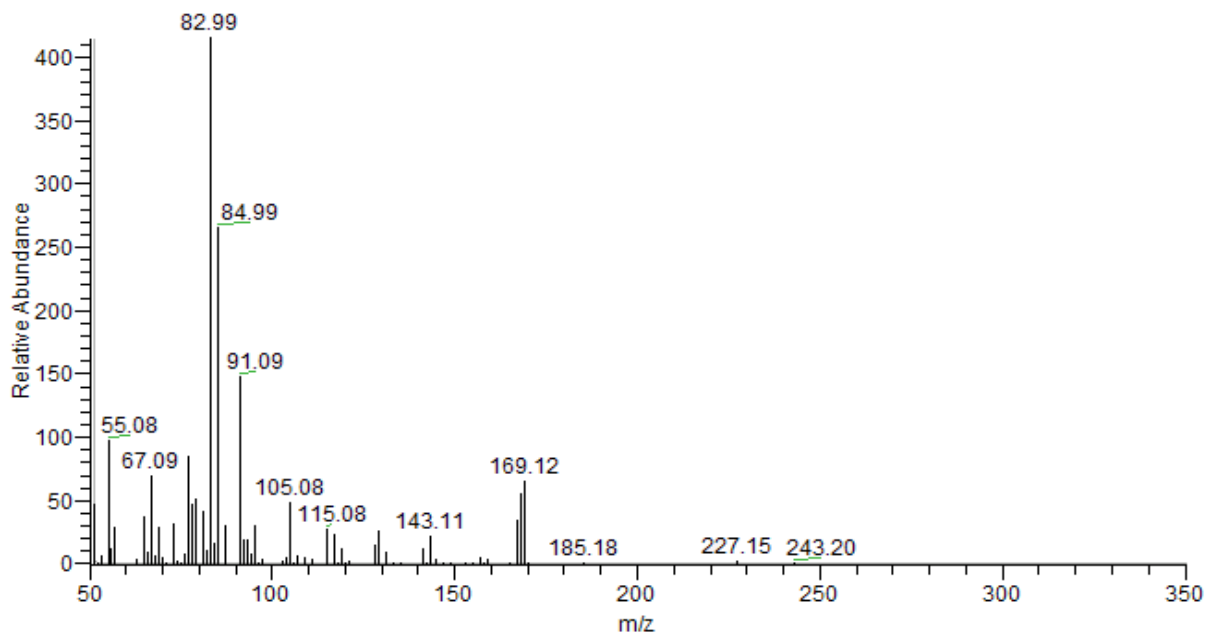
Figure A.84: System blank: mass spectrum for the methanol/n-heptane water analysis, from the baseline (0.04-3.71 min)
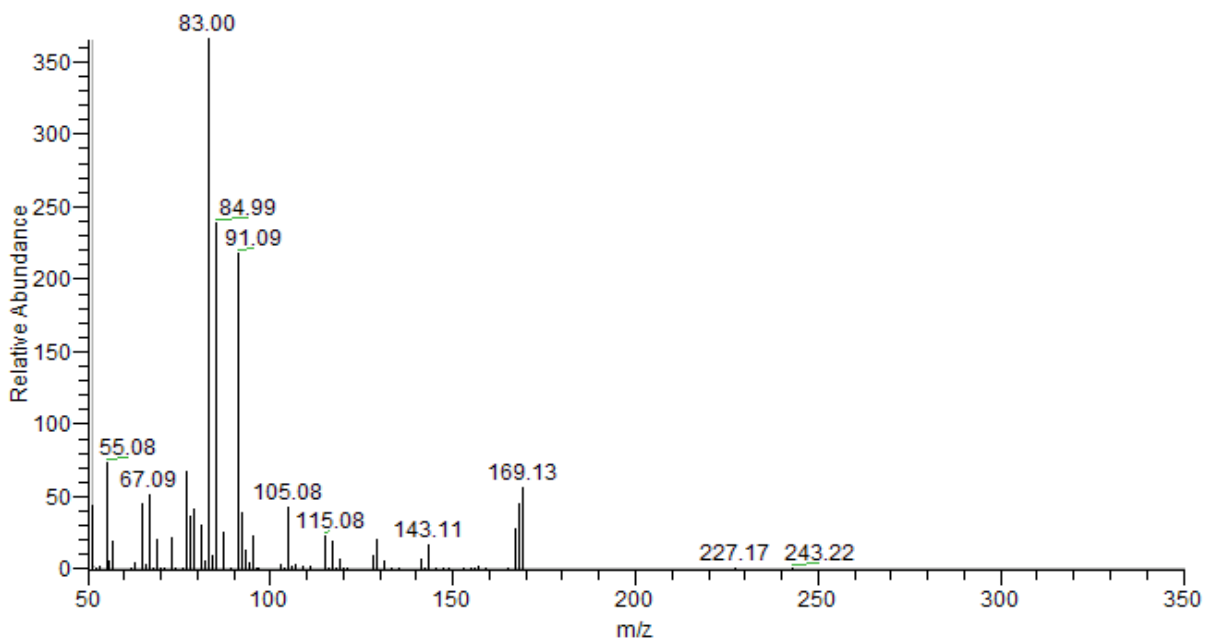
Figure A.85: Uncorrected mass spectrum for the methanol/n-heptane water analysis, from the exposure of methanol (34.50-47.13 min)
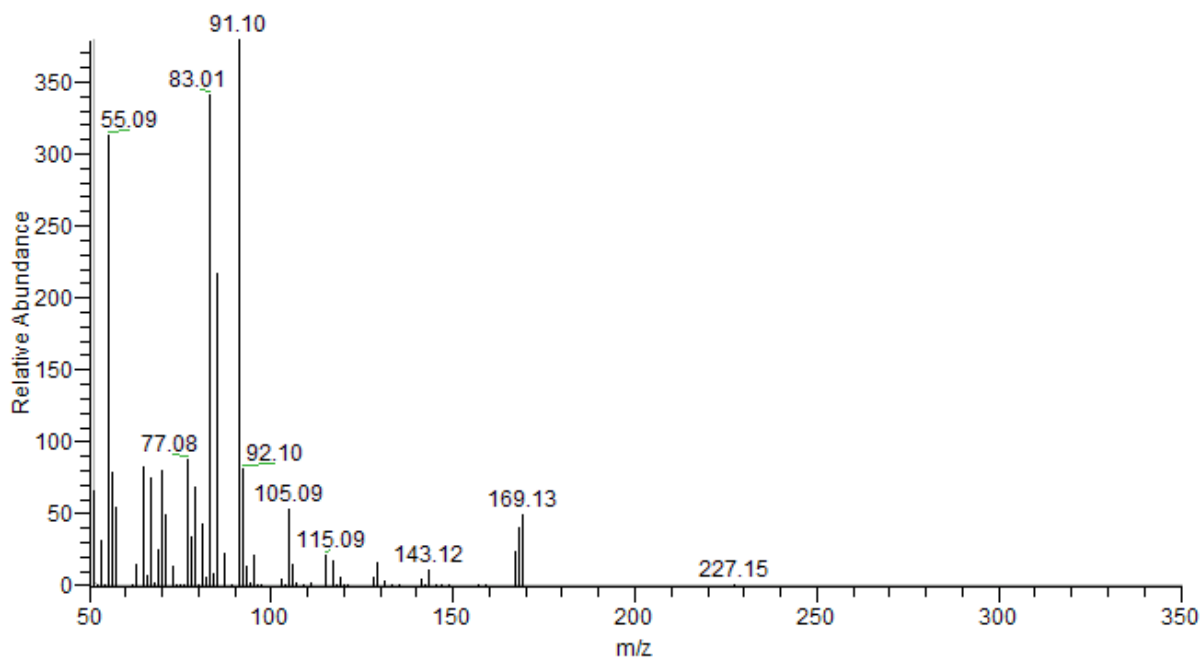
Figure A.86: Uncorrected mass spectrum for the methanol/n-heptane water analysis, from the first exposure of n-heptane (133.57-145.83 min)
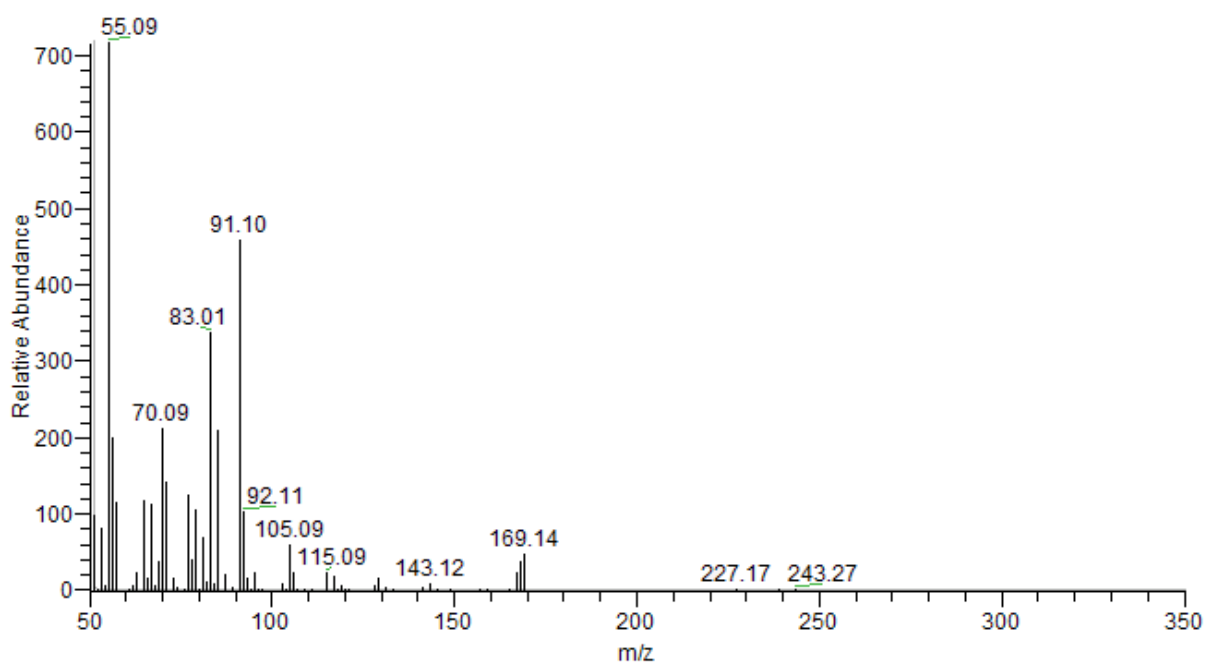
Figure A.87: Uncorrected mass spectrum for the methanol/n-heptane water analysis, from the second exposure of n-heptane (191.10-199.25 min)

F. Data

F.1 Optimization of the MIFID-system

Table A.1: Data from the optimization of the MIFID-system. Analyses are done with toluene if nothing else is specified. Values are not rounded.

	Response time (10-90 %) (min)	Mean value (min)	Max. signal (µV)	Mean value (µV)	Noise (µV)
Water flow (mL/min)					
60	27.449		4246		
90	11.528		4486		
140	8.571		4222		
210	4.440		4043		
250	5.118		3680		
210 [a]	4.191	4.431	24287	21 903	
210 [a]	4.670		19519		
250 [a]	4.790		22252		
Interface temperature (°C) [b]					
30	6.375		14631		5 - 10
40	4.662		16468		10 - 15
50	3.153		18169		20 - 30
60	2.532		19779		20 - 30
MI-hydrogen flow (mL/min)					
5.0	5.884		15420		
10.1	4.238		16454		
20.1	4.208		14821		
FID-Hydrogen flow (mL/min) [c]					
20	0.190		486		
30	0.217		752		
40	0.142	0.142	655	632	
40	0.142		609		
FID-Air flow (mL/min) [c]					
350	0.217		752		
400	0.175		718		
400	0.175	0.182	591	622	
400	0.197		556		
FID-Makeup gas					
With	3.408		22231		
Without	4.145		11117		

Appendix

Table A.1 continues…

FID-Makeup gas flow (mL/min) [c]					
20	0.167		363		
20	0.223	0.195	361	368	
20	0.195		379		
30	0.190		385		
30	0.152	0.177	401	405	
30	0.190		430		
40	0.121		619		
40	0.161	0.161	444	627	
40	0.201		798		
40	0.162		645		
40	0.197		500		
40	0.197	0.197	582	543	
40	0.198		548		
40 [d]	0.147		653		
40 [d]	0.147	0.147	719	705	
40 [d]	0.147		742		
50 [d]	0.133		712		
50 [d]	0.133	0.133	754	741	
50 [d]	0.133		757		
50	0.174		381		
50	0.208	0.185	380	384	
50	0.174		392		

[a] Analyses done another day than the rest of the water flow tests

[b] Water bath and interface holds the same temperature

[c] Analyses done with air samples

[d] Analyses with n-heptane

A60

F.2 MIFID – Oil in air

Table A.2: Decrease signal intensity and percentage decrease at selected points in time after maximum TIC signal. Numbers in parentheses are measurement at other times than the standard ones. Used for construction of Figure 4.11. Values are not rounded.

Time after max. intensity (min)	Signal intensity (µV)					
	Oseberg Blend	Troll B	Unspecified 1	Balder Blend	Unspecified 2	Norne Blend
0	807 997	353 569	888 304	178 762	336 347	187 630
1	669 915	319 968	733 767	168 387	276 612	179 595
2	526 919	270 991	584 693	153 170	229 061	157 901
5	300 116	178 641	334 461	113 099	146 363	114 289
10	164 058	112 118	181 430	77 804	89 458	77 306
20	80 364	64 022	88 394	46 242	48 554	46 862
30	51 780	44 894	57 289	33 212	32 976	34 289
40	37 856	34 752	42 248	26 010	24 942	27 216
50	29 701	28 500	33 401	21 487	20 224	22 821
60	24 529	24 211	27 494	18 410	16 973	19 618
90	15 916	16 780	23 547 (80)	12 893	14 678 (70)	14 197
120	11 679	15 154		11 752 (100)		

Time after max. intensity (min)	Percent of maximum intensity (%)					
	Oseberg Blend	Troll B	Unspecified 1	Balder Blend	Unspecified 2	Norne Blend
0	100.00	100.00	100.00	100.00	100.00	100.00
1	82.91	90.50	82.60	94.20	82.24	95.72
2	65.21	76.64	65.82	85.68	68.10	84.16
5	37.14	50.53	37.65	63.27	43.52	60.91
10	20.30	31.71	20.42	43.52	26.60	41.20
20	9.95	18.11	9.95	25.87	14.44	24.98
30	6.41	12.70	6.45	18.58	9.80	18.27
40	4.69	9.83	4.76	14.55	7.42	14.51
50	3.68	8.06	3.76	12.02	6.01	12.16
60	3.04	6.85	3.10	10.30	5.05	10.46
90	1.97	4.75	2.65 (80)	7.21	4.36 (70)	7.57
120	1.45	4.29		6.57 (100)		

Table A.2 continues…

Time after max. intensity (min)	Signal intensity (µV)					
	Falk	**SAGD**	**Peregrino**	**Mariner Maureen**	**Heidrun Tilje**	**Bressay**
0	36 447	7 545	30 714	21 102	231 457	10 478
1	35 494	7 372	29 762	20 735	217 035	10 197
2	34 761	7 288	28 419	20 505	193 719	10 146
5	32 120	6 926	24 559	19 269	139 604	9 801
10	27 590	6 261	20 120	16 886	95 622	9 103
20	22 267	5 253	15 192	13 562	57 791	7 747
30	18 257	4 565	12 473	11 537	41 400	6 839
40	15 471	4 100	10 773	10 143	32 205	6 195
50	13 529	3 772	9 546	9 108	26 489	5 677
60	12 092	3 497	8 614	8 216	22 560	5 286
90	9 278	2 949	6 658	6 378	15 664	4 426
120	7 495	2 566	5 474	5 198	11 946	3 841
Time after max. intensity (min)	Percent of maximum intensity (%)					
	Falk	**SAGD**	**Peregrino**	**Mariner Maureen**	**Heidrun Tilje**	**Bressay**
0	100.00	100.00	100.00	100.00	100.00	100.00
1	97.39	97.71	96.90	98.26	93.77	97.32
2	95.37	96.59	92.53	97.17	83.70	96.83
5	88.13	91.80	79.96	91.31	60.32	93.54
10	75.70	82.98	65.51	80.02	41.31	86.88
20	61.09	69.62	49.46	64.27	24.97	73.94
30	50.09	60.50	40.61	54.67	17.89	65.27
40	42.45	54.34	35.08	48.07	13.91	59.12
50	37.12	49.99	31.08	43.16	11.44	54.18
60	33.18	46.35	28.05	38.93	9.75	50.45
90	25.46	39.09	21.68	30.22	6.77	42.24
120	20.56	34.01	17.82	24.63	5.16	36.66